THE ALKALINE CONFORMATIONAL TRANSITIONS OF

FERRICYTOCHROME c

by

Federico Ignacio Rosell

B.Sc., The University of British Columbia, 1990

A THESIS SUBMITTED IN PARTIAL FULFILLMENT OF

THE REQUIREMENTS FOR THE DEGREE OF

DOCTOR OF PHILOSOPHY

in

THE FACULTY OF GRADUATE STUDIES

THE DEPARTMENT OF BIOCHEMISTRY AND MOLECULAR BIOLOGY

We accept this thesis as conforming

to the required standard

The University of British Columbia

January 1999

Department of _Biochemistry & Molecular Biology_

The University of British Columbia
Vancouver, Canada

Date _2 March 1999_

ABSTRACT

The alkaline conformational transitions of several yeast *iso*-1-ferricytochrome *c* variants were characterized with a variety of spectroscopic and physical techniques. The first group of variants consists of cytochromes in which selected lysyl residues were replaced by alanine. On the basis of ^{1}H-NMR and EPR spectroscopy, it was shown that Lys73 is one of the residues that replaces Met80 as an axial ligand to the heme iron and results in the alkaline conformer IV_a. Lys79 had been shown previously to coordinate the metal centre in a second alkaline conformer IV_b (Ferrer, J.C., Guillemette, J.G., Bogumil, R., Inglis, S.C., Smith, M. & Mauk, A.G. (1993) *J. Am. Chem. Soc.*, **115**, 7507-7508). The absence of both lysyl residues from the cytochrome sequence (*i.e.*, Lys73Ala/ Lys79Ala double variant) results in the stabilization of the native conformation of the protein which persists at higher pH (pK_a=10.5(3)). However, addition of amino group-containing compounds to solutions of this variant results in a protein adduct with spectroscopic features similar to those of the alkaline isomers. Furthermore, the conformational transition of the wild-type protein (pK_a=8.70(2)) represents a weighted average of the transition of the native Met80-bound conformer to either the Lys73- (pK_a=8.44(1)) or Lys79-bound (pK_a=8.82(2)) conformers. pH-jump kinetics indicate that replacement of Met80 by Lys73 occurs with a greater rate constant (k_f=160(5) s^{-1}) than the replacement by Lys79 (k_f=1.51(5) s^{-1}) despite the more significant structural changes that must take place on the distal side of the protein to accommodate coordination of the heme iron by Lys73. This rearrangement of the molecule, however, does not change significantly the exposure of the heme group to solvent relative to the Lys79-bound isomer. Both alkaline conformers, IV_a and IV_b, have a similar midpoint reduction potential (-190 mV *vs*. SHE, pH ~8.7) suggesting that the dielectric constant of the heme cavity in the two conformers is comparable. The temperature and ionic strength dependence of the conformational equilibria of the Lys73Ala and Lys79Ala variants was studied. The

formation of the Lys73-bound alkaline conformer exhibits a stronger temperature dependence than the isomerization involving Lys79. ^{1}H-NMR shows that salts can significantly affect the distribution of alkaline conformers so that Lys73 ligation to the iron is favoured at low salt concentrations, whereas at higher concentrations, Lys79 coordination is preferred.

The second group of variants includes cytochromes with amino acid replacements at highly conserved sites in the sequence (Thr78Ala, Tyr67Phe, Phe82Gly, Phe82Lys, Phe82Ser, Phe82Asp, Phe82Met, Phe82His, Phe82Trp, and Phe82Ile). In general, the Lys73-bound conformer is the favoured alkaline species in the Phe82Xxx variants, thus accounting in part for the generally decreased pK_{ap} of the transition of these variants. Unconventional cases are the Phe82His variant in which a non-native, bis-histidine ligation is observed that interferes with the normal alkaline transition, and the Phe82Trp variant in which a high-spin species is trapped at mildly alkaline pH. There is no indication at this time that Lys82 coordinates the heme iron. The variant with Phe at position 67 is unique among all the other cytochromes investigated in that the significantly stabilized native conformer appears to undergo the transition to primarily the Lys79- bound conformer.

Finally, the alkaline transition of a cytochrome expressed with a newly developed bacterial expression system was characterized. During bacterial expression, Lys72 is not trimethylated as it is in yeast. The lack of this post-translational modification results in a third alkaline conformer in which this lysyl residue replaces Met80 as a heme ligand. Although this isomerization occurs more readily than that involving Lys73 or Lys79, the absence of the methionyl ligand in Tml72Lys/Met80Ala variant does not facilitate the formation of any of the three alkaline conformers. In this variant, the lysyl residues must compete with water and hydroxide for the axial heme iron coordination site, and the Lys72-bound conformer appears to be preferred alkaline species.

TABLE OF CONTENTS

2. EXPERIMENTAL PROCEDURES

3. RESULTS

4. DISCUSSION

LIST OF TABLES

LIST OF FIGURES

ABBREVIATIONS

ATP	adenosyl triphosphate
CAPS	3-(cyclohexylamine)-1-propane sulfonic acid
Cb_5	cytochrome b_5
CcO	cytochrome c oxidase
CcP	cytochrome c peroxidase
CcR	cytochrome c reductase
CD	circular dichroism
CHES	2-(N-cyclohexylamino)ethane sulfonic acid
CT	charge transfer
dipic	dipicolinic acid
DNA	deoxyribonucleic acid
DNase	deoxyribonuclease
DTT	dithiothreitol
DSS	2,2-dimethyl-2-silapentane-5-sulfonate
dut	dUTpase activity deficient
EPR	electron paramagnetic resonance
e.u.	entropy unit
FID	free induction decay
flavo-Cb_2	flavocytochrome b_2
IR	infrared
kpoint	kilopoint
MCD	magnetic circular dichroism

MES	2-(*N*-morpholino)ethane sulfonic acid
MRW	mean residue molecular weight
NMR	nuclear magnetic resonance
NOE	nuclear Overhausser effect
pge	pyrolytic graphite electrode
PMSF	phenyl methyl sulfonic acid
RNA	ribonucleic acid
RNase	ribonuclease
SCE	standard calomel electrode
seq	sequencing
SHE	standard hydrogen electrode
T_m	melting temperature
TAPS	*N*-tris(hydroxymethyl)methyl-3-aminopropane sulfonic acid
Tml	trimethyllysine
TOC	total overall correlation
Tris	Tris (hydroxymethyl) amino methane
UAS	upstream activating sequence
ung⁻	uracyl *N*-glycosylase activity deficient
UV	ultraviolet
Vis	visible
YP	yeast/peptone

ACKNOWLEDGMENTS

1 Introduction

1.1 Overview

Regulatory responsiveness is an important feature of proteins which allows them to react appropriately to changes in solution conditions (Somero, 1986). pH, for example, can have significant effects on the function of a protein, and in many instances, the influence of pH on rates of enzymatic activity can be explained readily in terms of acid/base catalysis. However, examples of proteins which exhibit distinct pH-dependent conformational states (Guss *et al.*, 1986; Holzman *et al.*, 1990; Dewan *et al.*, 1993; Evans & Chan, 1994; Chaine & Pakdaman, 1995; Tatulian & Tamm, 1996) indicate that pH can also exert a significant influence over enzymatic activity by modulating protein structure. Although such a relationship is not surprising, our understanding regarding pH-linked conformational equilibria of proteins is far from complete.

Mitochondrial cytochrome *c* has been used extensively to model important chemical and biological processes, most notably electron transfer reactions. Because this heme protein also exhibits not one, but rather five spectroscopically distinct forms depending on pH (Theorell & Åkesson, 1941), cytochrome *c* serves also as a valuable model of the intricate relationship between pH and protein structure. Thus, the alkaline conformational transition has been the focus of many studies involving novel chemical and spectroscopic techniques (see for *e.g.*, Moore & Pettigrew, 1990; Wilson & Greenwood, 1995 and references therein). Many of these approaches are used in concert with site-directed mutagenesis in the present study to define important aspects about the alkaline isomerization of ferricytochrome *c* that remain to be elucidated even after close to sixty years after the discovery of this phenomenon (Theorell & Åkesson, 1941).

1.2   Mitochondrial Cytochromes c

1.2.1   The Native Structure of Cytochrome c

Mitochondrial cytochromes c are soluble, globular proteins that consist of a single heme prosthetic group and 103-113 amino acids (108 amino acids in yeast; Figure 1). During protein assembly, apo-cytochrome c attaches to the outer mitochondrial membrane, and the N- terminus of the polypeptide is spontaneously inserted across to the intermembranal space (Nicholson *et al.*, 1988; Stuart *et al.*, 1990). Here, cytochrome c heme lyase (sometimes also called cytochrome c synthetase; Taniuchi *et al.*, 1983) catalyzes the covalent attachment of a ferrous heme to the incoming apo-cytochrome c chain (Nicholson & Neupert, 1989). The newly incorporated prosthetic group then serves as the core around which the polypeptide chain folds (Dumont *et al.*, 1994) to enclose the heme within a hydrophobic environment. This folding of the polypeptide is believed to drive the translocation of the apo-protein across the mitochondrial outer membrane (Stuart *et al.*, 1990). Some cytochromes c undergo further post-translational modification such as specific trimethylation of lysyl residues (*e.g.*, Lys72 in yeast cytochrome c) and N-terminal acetylation (*e.g.*, equine cytochrome c).

Recently, Thöny-Meyer presented an in-depth review on the biogenesis of respiratory cytochromes in bacteria (Thöny-Meyer, 1997). Although some steps for the assembly of c-type cytochromes in bacteria are similar to those outlined above, it appears that threading of the apo-cytochrome across a membrane is not an essential requirement. Mauk and coworkers have successfully expressed holo-cytochrome c in the cytoplasm of *E. coli* by co-expressing cytochrome c heme lyase (*CYC3*) and mitochondrial cytochrome c from yeast (*CYC1*) (Pollock *et al.*, 1998).
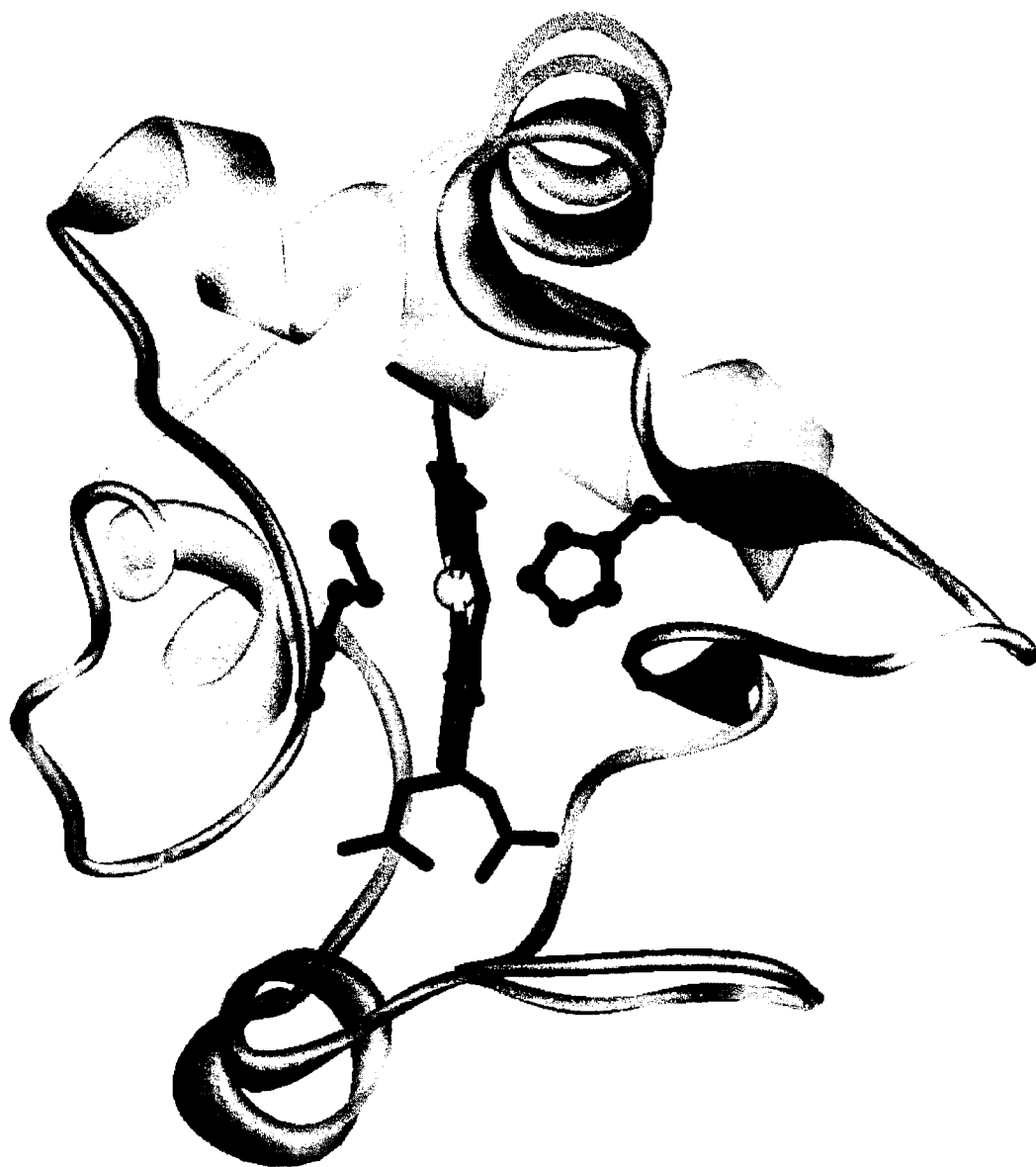
Figure 1. Ribbon representation of yeast *iso*-1-cytochrome *c* in the classical orientation of Takano and Dickerson (1980) (coordinate data set: 2ycc; Berghuis & Brayer, 1992). The heme group, illustrated in red with the iron in yellow, is at the center of the molecule and is viewed edge-on with Met80 (green) and His18 (blue) on the distal (left) and proximal (right) sides respectively.

The amino acid sequences of more than one hundred cytochromes c have been published (Moore & Pettigrew, 1990 and references therein) and are available in a number of databases (*e.g.*, Brookhaven Protein Data Bank; GenBank; PROMISE, Degtyarenko *et al.*, 1997, 1998). Sequence comparison analysis of 96 mitochondrial cytochromes c reveals striking similarities between these proteins (Cutler *et al.* 1987; Moore & Pettigrew, 1990; Louie, 1990; Brayer & Murphy, 1995). Many of these analogies, and presumably the most significant, persist if the sequences of some bacterial cytochromes and those of more recently published mitochondrial proteins are included. Comparison of yeast *iso*-1-cytochrome c (reference sequence) to 137 other sequences reveals at least five regions bearing a high degree of conservation (residues 14-18, 29-38, 45-49, 70-80, and 84-87; Figure 2). From a structural standpoint, the most significant region is the consensus sequence Cys-Xxx-Zzz-Cys-His which is generally regarded as a requirement for lyase-catalyzed heme attachment to the apoprotein (Hampsey *et al.*, 1988). A covalently-bound heme prosthetic group is, after all, the principal criterion for classifying a heme protein as a c-type cytochrome. Moreover, His18 is an axial ligand to the heme iron and is essential for the function of cytochrome c (Fumo *et al.*, 1995). Notably, the majority of mitochondrial cytochrome c sequences can include as many as 19 lysyl, 4 arginyl, and 4 histidyl residues distributed throughout the polypeptide chain. The abundance of these residues reflects the unusual basicity of these proteins (pI 9.7-10.5) and makes them well-suited to interact electrostatically with a variety of acidic electron transfer proteins (*vide infra*).

With the elucidation of the X-ray crystal structures of horse (Dickerson *et al.*, 1971; Bushnell *et al.*, 1990; Sanishvili *et al.*, 1995), tuna (Takano *et al.*, 1973, 1977; Swanson *et al.*, 1977), bonito (Ashida *et al.*, 1973; Tanaka, *et al.*, 1975), rice (Ochi *et al.*, 1983), and yeast (Louie *et al.*, 1988; Louie & Brayer, 1990; Berghuis & Brayer, 1992) cytochromes c, it was found that in addition to high sequence conservation, these mitochondrial cytochromes c also exhibit a high degree of structural
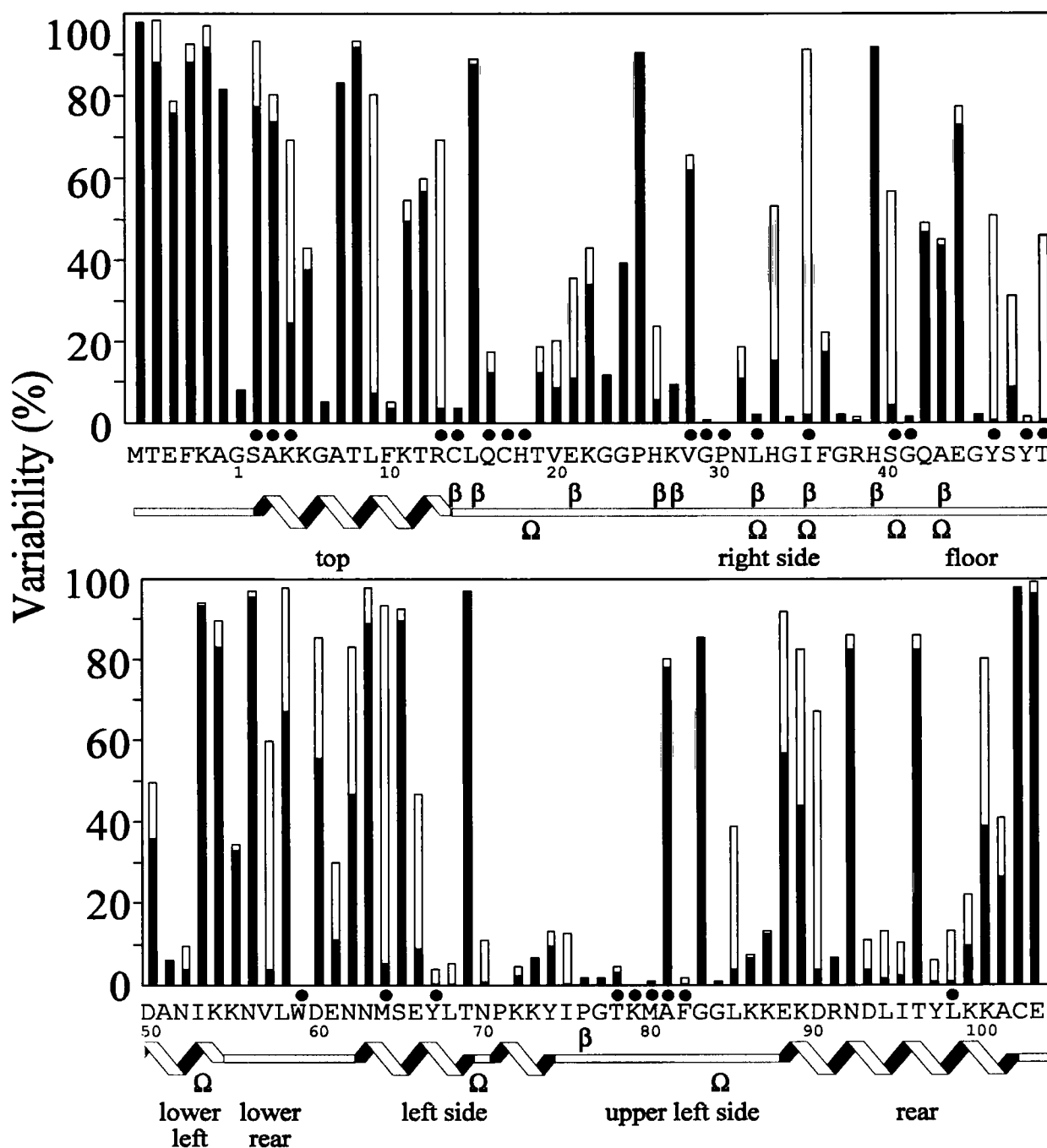
Figure 2. Comparison of the primary structure of yeast *iso*-1-cytochrome *c* to 137 known *c*-type cytochromes (GenBank). Variability at each position is defined as the percentage of sequences that bear a residue other than the one found in the sequence of yeast *iso*-1-cytochrome *c*. Conservative mutations are depicted with a white bar, and non-conservative mutations are depicted in black. The green dots emphasize residues that line the heme cavity of the protein. The secondary structure elements of the protein are illustrated beneath the sequence where β and Ω label the residues that form β-turns and Ω-loops. The approximate location of these structural elements in the fully folded protein is quoted in relation to the perspective shown in Figure 1.

homology. Approximately 40% of the cytochrome polypeptide chain is organized into five α-helices: 2-14 (top), 49-55 (lower left), 60-70 and 70-75 (left face), and 87-102 (rear) (perspective according to Figure 1; Takano & Dickerson, 1980). The remainder of the protein is arranged primarily into type II β-turns (21-24, 32-35, 35-38, 39-42, 43-46, and 75-78), located mainly on the floor and right face of the protein, and Ω-loops (18-32, 34-43, 40-54, and 70-84) on both sides of the cytochrome. Mapping the most highly conserved lysyl (27, 72, 73, 79, 86, 87, and 89), arginyl (13, 38, and 91) and histidyl (26) residues on the protein surface reveals that they cluster asymmetrically with the majority arranged around the periphery of the exposed heme edge (Figure 3). This observation has been interpreted by many authors to suggest that this region is the preferred docking surface for the interaction of cytochrome c with its electron transfer partners (*vide infra*).

The X-ray crystal structures also confirm that the cysteine residues in the consensus sequence are the sites of heme attachment in mitochondrial cytochromes c. Cys14 and 17 form thioether bonds with the α-ethylene carbon atoms of the heme pyrrole rings B and C, respectively (Figure 4). These linkages and other constraints within the heme cavity force the porphyrin ring to ruffle such that it is saddle-shaped with the top and bottom edges bending towards the proximal side, and the rear and front edges bending towards the distal side. Furthermore, it is clear that the ε2 nitrogen atom of the His18 imidazole ring coordinates the heme iron from the proximal side of the protein while the δ-sulfur atom of Met80 binds to the iron on the opposite side (Figure 1).

An issue of long standing interest has been the identification of the structural properties that influence the electron transfer function of cytochrome c (Margoliash & Schejter, 1995). Therefore, significant efforts have been made to define structural differences between the ferrous (Fe^{2+}) and the ferric (Fe^{3+}) states of the protein. From their X-ray crystallographic analysis conducted on yeast *iso*-1-cytochrome c, Berghuis and Brayer (1992) noted that only minor changes in the general protein fold
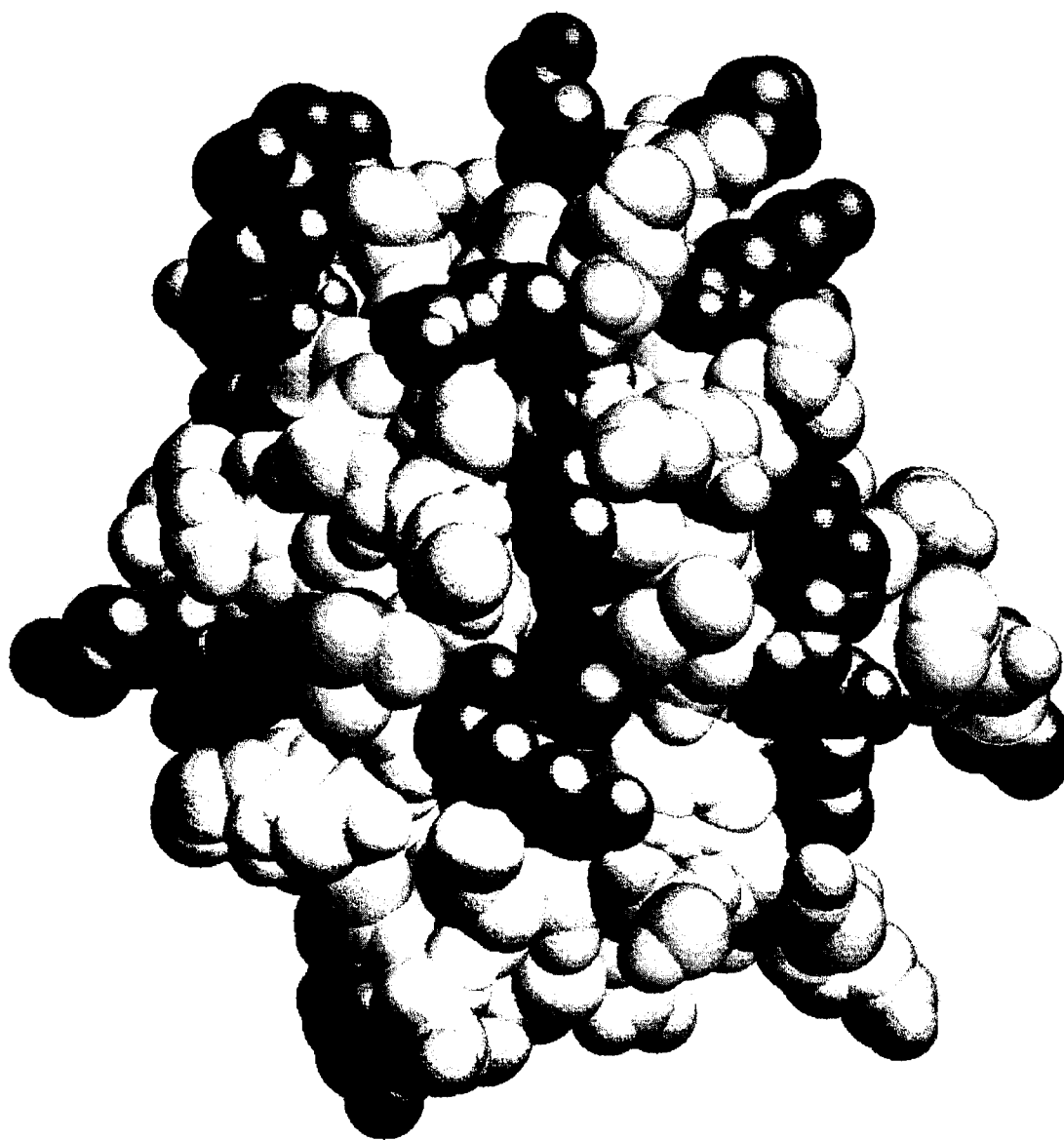
Figure 3. Spacefilling Model of wild-type, yeast *iso*-1-ferricytochrome *c*. The exposed edge of the heme is illustrated in red, and the highly conserved lysyl residues are shown in blue. Arginyl and histidyl residues are shown in green and cyan respectively.
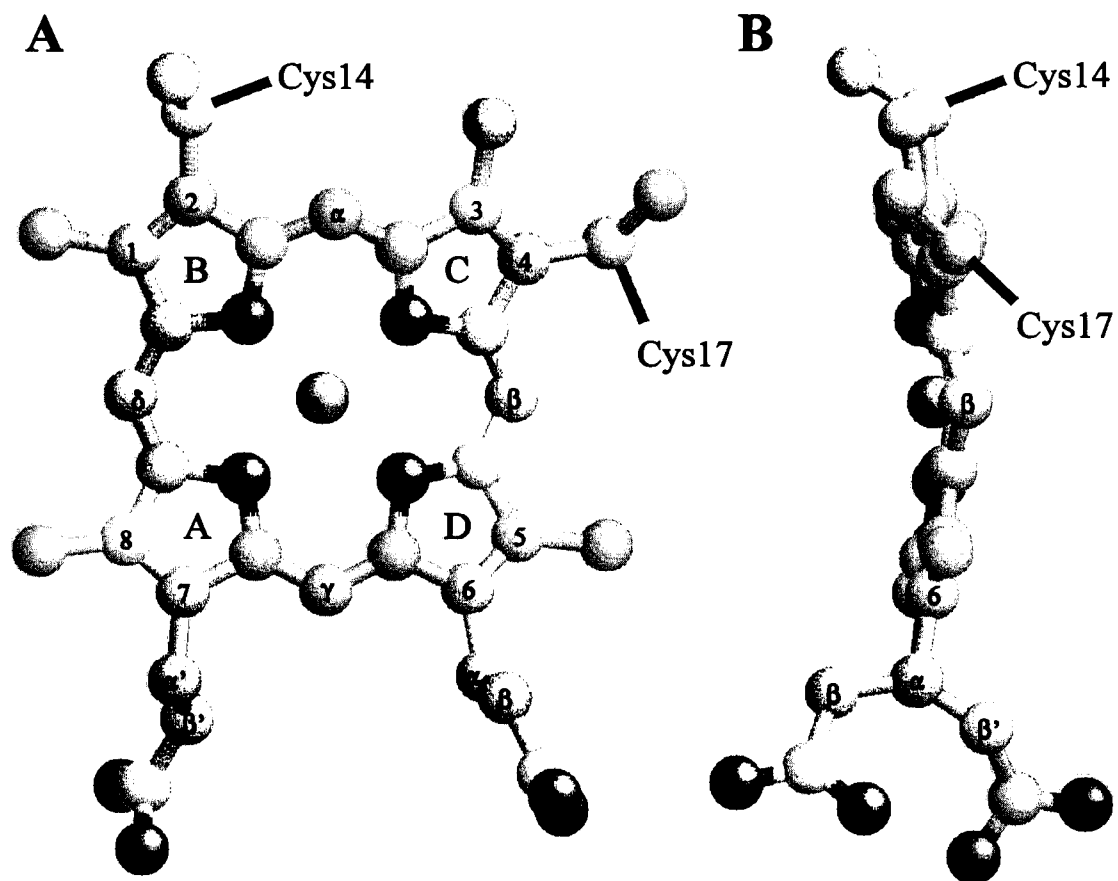
Figure 4. Diagram of the heme prosthetic group of cytochrome c and the Fischer nomenclature used in the text. The axial ligands His18 and Met80 are located below and above the plane of the page, respectively, in view (A), and to the right and left in view (B).

occur upon oxidation. Interestingly, these authors identified subtle structural changes in the area of the heme. The hydrogen bond formed between the hydroxyl group of Tyr67 and the sulfur atom of Met80 is severed, thus reducing the electron withdrawing ability of the axial ligand and weakening its bond strength to the iron atom. The increased mobility of Met80, as well as the mobilities of its preceding and succeeding polypeptide segments, is reflected in their greater thermal factor parameters. At the same time, the ruffling of the heme becomes more pronounced, and the plane of the imidazole ring of the axial His18 ligand rotates slightly about the normal to the heme plane. Finally, the most significant structural change reported by Berghuis and Brayer (1992) involves an internal water molecule (H_2O 166) which moves ~1.7 Å closer to the heme iron to break the hydrogen bond between this water molecule and Asn52. This migration is accompanied by a rotation of the water molecule such that the oxygen atom is closest to the heme iron.

The structural analysis described above was recently extended to yeast cytochrome c in solution. Using ^{1}H-NMR, Baistrocchi *et al.* (1996) and Banci *et al.* (1997) confirmed many of the observations by Berghuis and Brayer (1992) and emphasized that two segments of the protein (residues 14-26 and 75-82, inclusive) experience greater dynamic freedom in the oxidized protein. Increased mobility was not an entirely unexpected result considering that oxidation state-linked structural differences were known from previous observations such as an increased susceptibility to proteases (Nozaki *et al.*, 1958; Yamanaka *et al.*, 1959), denaturing agents (Butt & Keilin, 1962; Dickerson & Timkovich, 1975), thermal denaturation (Pfeil, 1981; Moore & Pettigrew, 1991 and references therein; Nall, 1995), and earlier NMR experiments (Moore, 1983; Williams *et al.*, 1985). The increased ruffling of the porphyrin ring upon oxidation could not be confirmed by the ^{1}H-NMR studies because the heme was defined as a planar molecule in the computational determination of the solution structures. However, detection of structural changes about the heme, including the formation

9

of a hydrogen bond between heme 7-propionate and the amide nitrogen of Gly41, may indirectly confirm the enhancement of the porphyrin ruffling observed in the crystal structure.

It is tempting to assume that because a high degree of sequence identity and structural homology exists among mitochondrial cytochromes c, the oxidation state-dependent structural differences observed in the yeast protein also occur in cytochromes from other species. Indeed, similar structural differences were observed previously in crystallographic studies conducted on tuna cytochrome c (Takano & Dickerson, 1980). However, comparison of reduced and oxidized horse heart cytochrome c by ^{1}H-NMR spectroscopy indicates that upon oxidation, this protein undergoes more significant structural changes than does the yeast protein (Qi et al., 1994, 1996). Whereas the secondary structure of the yeast protein is relatively unaffected by a change in oxidation state, Qi et al. report several significant differences in hydrogen-bond networks of the backbone of the equine cytochrome. Helices (3_{10}-helix: 60-63; α-helix: 49-54) that are detectable in the structure of the ferrous protein are not detectable in the oxidized protein. Furthermore, the highly conserved Phe82 is found to be further from the heme iron in the oxidized protein than in the reduced protein (ζ-C: ~2.5 Å; γ-C: ~1 Å).

More recently, Dong and coworkers (Calvert et al., 1997) compared the effect of oxidation state on the structures of yeast, tuna, and some mammalian cytochromes c. In the amide I band region, the FT-IR spectra of these cytochromes c exhibit similar structural changes (in α-helix, β-turns, extended β, and disordered structure content) upon oxidation, but the magnitude of these differences is not the same for all species. Not surprisingly, Dong and coworkers found that the extent to which the structure of these proteins changes upon oxidation increases as the sequence identity between these proteins decreases.

1.2.2 The Physiology of Cytochrome c

The primary function of cytochrome c is to transfer electrons between a variety of electron transfer partners. Cycling between the ferrous (Fe^{2+}) and ferric (Fe^{3+}) oxidation states, cytochrome c promotes a multitude of metabolically significant reactions. This heme protein resides primarily in the intermembranal space of mitochondria where it is most closely associated with ubiquinol-cytochrome c oxidoreductase (complex III, CcR) and cytochrome c oxidase (complex IV, CcO) as part of the electron transport chain (Figure 5). However, cytochromes c also interact with other proteins, including cytochrome b_5, liver sulfite oxidase (SOx), and yeast flavocytochrome b_2 (flavo-Cb_2) (Pettigrew & Moore, 1987) (Figure 6). Although all of these electron transfer reactions may ultimately result in the production of ATP by regenerating cytochrome c oxidase, the latter two also regenerate the electron donating enzymes for the breakdown of sulfur-containing amino acids (SOx) and the conversion of lactic acid to pyruvate (flavo-Cb_2). A third detoxifying reaction that occurs in yeast includes cytochrome c as an electron donor to cytochrome c peroxidase (CcP) for the breakdown of potentially harmful peroxides.

More recently, the involvement of cytochrome c in apoptosis (programmed cell death) has become evident to the extent that this heme protein is regarded as an apoptosis-triggering factor (Kluck *et al.*, 1997; Yang *et al.*, 1997; Skulachev, 1998). The exact role of cytochrome c in the complex chain of events leading to nucleo- and cytoplasmic condensation, cytoplasmic membrane blebbing, and cellular fragmentation is not known. However, it has been established that cytochrome c is a required component for the activation of some caspases (CPP32 and CPP32-like cysteine proteases) (Liu *et al.*, 1996; Kluck *et al.*, 1997; Yang *et al.*, 1997). Antibody-mediated sequestration of cytochrome c from cell-free extract assays blocks the apoptotic response. Conversely, addition of exogenous cytochrome c to these cell-free extracts and micro-injection of the heme protein into live

11
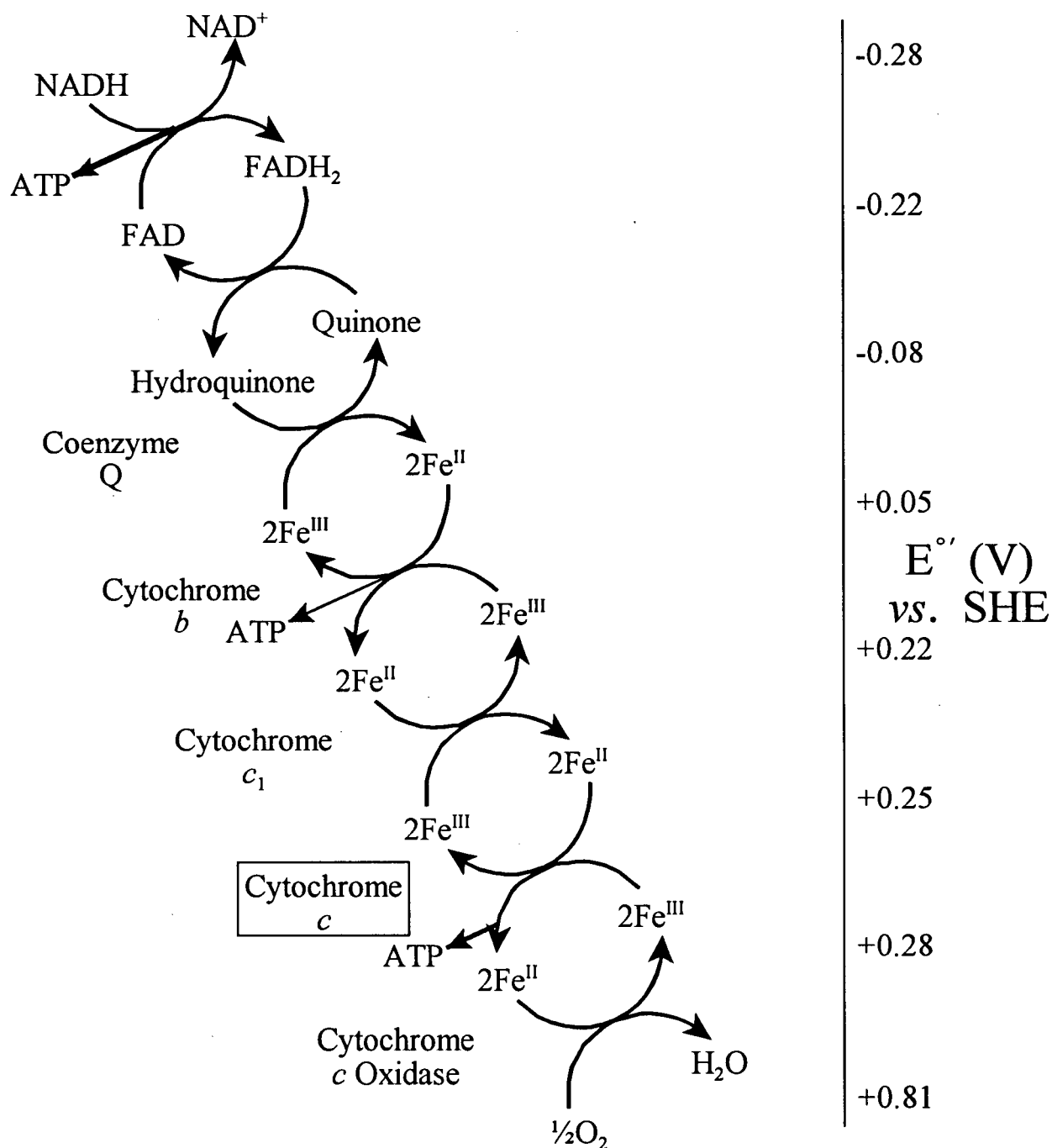
Figure 5. Schematic Diagram of the energy transducing pathway of oxidative phosphorylation showing the path of electrons to the terminal oxidase where oxygen is reduced to form water. The curved arrows indicate the cycle between the redox species at each step, while the straight arrows denote the reactions that result in the phosphorylation of ADP to ATP. The scale on the right denotes the reduction potential involved in the electron transfer at each couple.
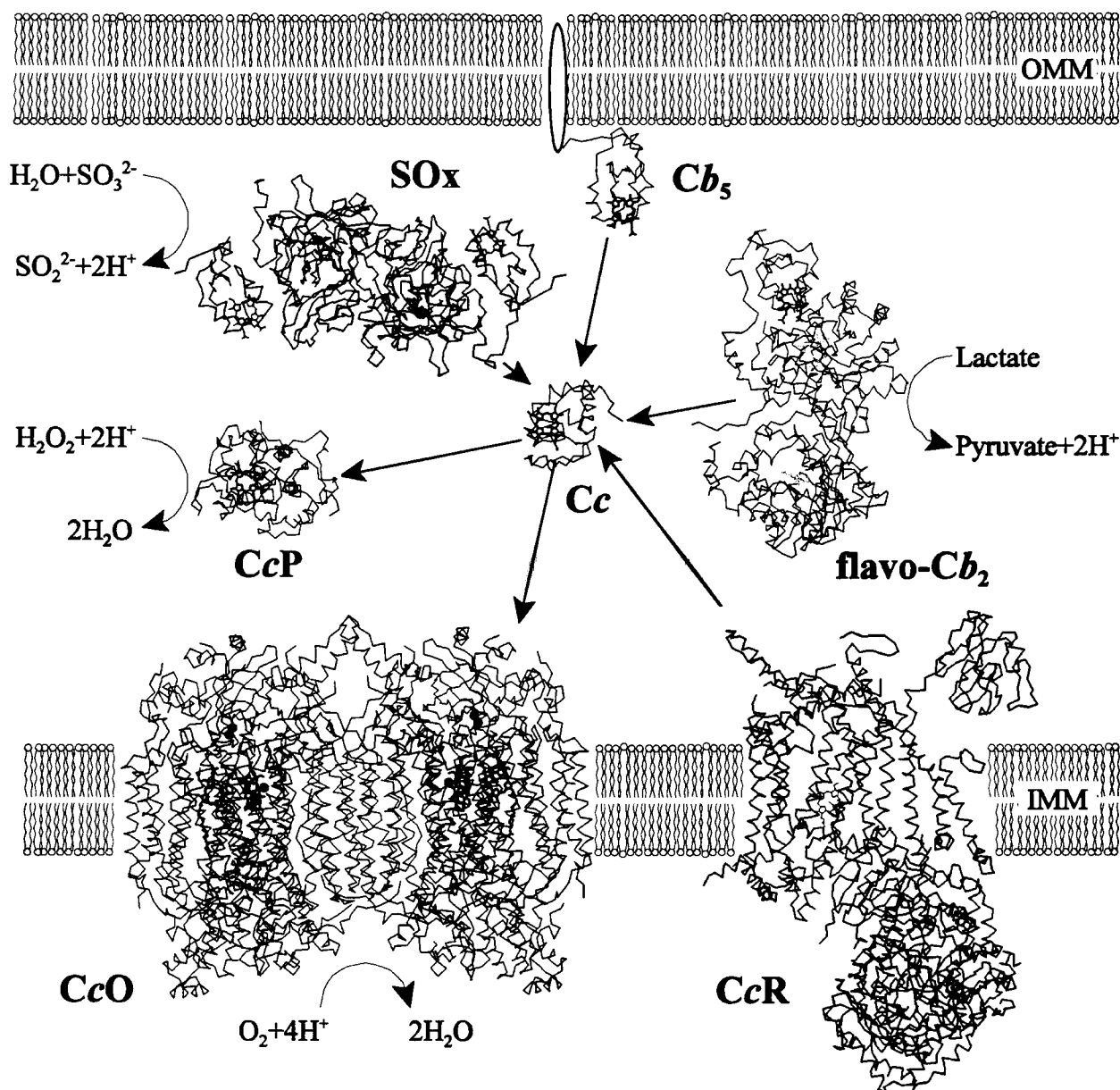
Figure 6. The cellular organization of cytochrome c (Cc; 2YCC) and its electron transfer partners cytochrome c reductase (CcR; 1QCR), cytochrome c oxidase (CcO; 1OCC), cytochrome b_5 (Cb_5; 1CYO), liver sulfite oxidase (SOx; 1SOX), yeast flavocytochrome b_2 (flavo-Cb_2; 1LDC), and yeast cytochrome c peroxidase (CcP; 2PCC). Each structure is illustrated approximately to scale, and these were obtained from the Brookhaven Protein Data Bank (PDB). CcR and SOx are shown as monomers (as opposed to the whole complex) to reflect the data contained within the PDB files. Similarly, additional cofactors that do not appear in the PDB file are not included in this Figure. The arrows indicate the flow of electrons while IMM and OMM denote the inner and the outer mitochondrial membranes respectively. The heme, flavin, and molybdopterin prosthetic groups are illustrated in red, yellow, and cyan respectively, while copper and molybdenum atoms are shown in green and magenta respectively.

cells induces events associated with cell death (Liu *et al.*, 1996; Li *et al.*, 1997; Zhivotovsky *et al.*, 1998). Cytochrome *c*-mediated caspase activation is specifically triggered only by the holoprotein. Related heme proteins are ineffective. Furthermore, caspase activation appears to involve electrostatically stabilized protein complexes because high salt concentrations interfere with the process (Hampton *et al.*, 1998). Initial results also suggest that cytochrome *c*-mediated initiation of cell death occurs independently of the oxidation state of the heme protein (Kluck *et al.*, 1997; Hampton *et al.*, 1998). Newmeyer and coworkers note that although agents added to apoptosis assays to maintain cytochrome *c* oxidized (*e.g.*, $K_3[Fe(CN)_6]$) also perturb downstream effectors to account for a reduced apoptosis triggering efficiency, it is likely that some step(s) in the activation of caspases by cytochrome *c* requires reducing conditions (Kluck *et al.*, 1997).

1.3 The Alkaline Transition of Ferricytochrome *c*

1.3.1 pH-Linkage in Brief

In 1936, eleven years after the rediscovery of cytochrome *c* by Keilin (1925), Theorell and Åkesson reported the pH-linkage of the spectrophotometric characteristics of the protein (Åkesson, 1936; Theorell & Åkesson, 1939, 1941; Theorell, 1941). In the reduced state, cytochrome *c* exists in one of three spectroscopically distinct forms. The spectroscopic changes associated with the interconversion of the acidic (state I) and alkaline (III) forms to the intermediate, neutral state (II) are a consequence of specific amino acid ionizations which are coupled to structural changes. The equilibria are described as :

$$\underset{\text{p}K_{ap} < 4}{} \qquad \underset{\text{p}K_{ap} > 12}{}$$
$$\text{I} \quad \rightleftarrows \quad \text{II} \quad \rightleftarrows \quad \text{III} \qquad (1)$$
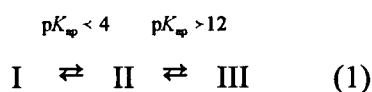
Note that the pK_{ap} values associated with these equilibria are only approximations because their exact

14

values depend on the species of the protein as well as other factors such as ionic strength and temperature.

State II is the isomer of ferrocytochrome c that is functionally relevant, at least in terms of energy transduction. This species has been thoroughly characterized by a myriad of techniques because of its important physiological role. The structure and properties of state II, therefore, are well defined (see section 1.2.1) unlike those of states I or III which are largely unfolded.

Ferricytochrome c exhibits at least five pH-dependent isomers and, therefore, four conformational changes (Moore and Pettigrew, 1990) :

$$
\begin{array}{ccccccccc}
 & pK_{sp} \sim 0.4 & & pK_{sp} \sim 2.5 & & pK_{sp} \sim 9.3 & & pK_{sp} \sim 12.8 & \\
\text{I} & \rightleftharpoons & \text{II} & \rightleftharpoons & \text{III} & \rightleftharpoons & \text{IV} & \rightleftharpoons & \text{V}
\end{array}
\qquad (2)
$$
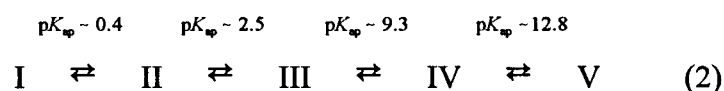
As in the case of ferrocytochrome $c,$ the exact values of these equilibrium constants are species-dependent and subject to the conditions of measurement. Of the five conformers, the functionally relevant isomer for oxidative phosphorylation is state III. This conformer is also very well characterized, especially because the paramagnetic nature of the oxidized heme centre makes this group an informative reporter group in the active site of the molecule (*vide infra*). EPR spectroscopy parameters, for example, are perturbed only by environmental changes in the immediate vicinity of the heme as are the hyperfine shifted regions in ^{1}H-NMR spectra.

States I and II of ferricytochrome c are the acid-denatured forms of the protein. Under some circumstances, His33 and His26 can replace Met80 as a heme ligand (Elöve *et al.*, 1994; Colon *et al.*, 1997). With increasing proton concentrations, the neutralization of Glu and Asp residues results in a net increase of the positive character of the protein. In the absence of electrolytes to shield these positive charges, electrostatic repulsions induce the protein to adopt an extended conformation. Although the tertiary structure of the protein is lost under these conditions, localized regions of

secondary structure elements may remain in a moderately stable form (Jeng & Englander, 1991). It follows that the charge-shielding effect of salt results in a stabilized, molten-globule-like conformation of the protein that retains the secondary structure elements of the native form but only a range of dynamic tertiary interactions (Goto *et al.*, 1990). The molten-globule forms of various proteins are generally regarded as models of protein folding intermediates. As such, cytochrome *c* at low pH (~2) and in the presence of salt (*e.g.*, ≥20 mM NaCl) has been the focus of much interest insofar as it a useful model for our understanding of structural determinants in cytochrome *c* and other proteins.

State IV is generally known as the alkaline conformer of cytochrome *c*, and the interconversion between the native form and this isomer has been the focus of much interest. A pivotal characteristic of this structural reorganization is the loss of the absorbance band centered at 695 nm from the electronic spectrum of the protein (Theorell & Åkesson, 1941). Because this band arises from ligation of Met80 to the heme iron, the loss of this absorbance reflects the disruption of this bond (Harbury *et al.*, 1965; Schechter & Saludjian, 1967; Eaton & Hochstrasser, 1967; Smith & Williams 1970). State IV also possesses a low-spin heme iron which suggests that the native Met ligand is replaced by another strong field ligand. At even higher pH, this new ligand is also removed from the coordination sphere of the iron to yield state V of ferricytochrome *c*. A species with spectroscopic characteristics similar to those of state V are observed when ferricytochrome *c* binds to cytochrome *c* oxidase (Döpner *et al*, submitted). Although this possibility had been proposed earlier (Weber *et al.*, 1987; Alleyne & Wilson, 1987), there is a conflicting report in which no changes in the CD spectrum of the cytochrome were encountered that would confirm the proposal (Michel *et al.*, 1989).

1.3.2   Identity of the Axial Ligand in Ferricytochrome c, State IV

A heme prosthetic group coordinated axially by at least one histidyl residue is a common structural element in many of the known heme protein structures. Despite this common characteristic, heme proteins can execute a wide variety of functions and display a range of spectroscopic properties. Although the immediate environment around the heme can exert considerable influence, the physicochemical characteristics of the heme protein are determined in large part by the second axial ligand to the heme iron (Loew, 1982; Wallace & Clark-Lewis, 1992). Therefore, it is important in characterizing a heme protein and its various conformers to identify the axial ligands. This information about the heme core is an essential first step in understanding the structure/function relationships of the protein.

Sulphur, nitrogen, and oxygen atoms are endogenous components of a polypeptide chain that can coordinate to a metal centre. With the exception of the amino terminus in cytochrome f (Martinez et al., 1994), examples in which the backbone carbonyl or amide groups coordinate the heme iron are not known. Consequently, only a handful of the twenty naturally occurring amino acids are considered here as potential ligand replacements for Met80 in the alkaline conformer of cytochrome c. Furthermore, consideration of the protein fold limits the list of potential residues to those that are located in the upper left side of the molecule (i.e., residues 60-90; Figure 1). This observation is consistent with chemical modification studies conducted on cytochromes c in which various lysyl residues were derivatized with a variety of functional groups (Tables 1a & 1b) (Moore & Pettigrew, 1990; Wilson & Greenwood, 1996; Rosell et al., 1998). In general, modification of all lysyl residues resulted in altered alkaline transitions and non-native cytochromes of mixed-spin state. Specifically, these anomalous properties were observed when lysines between residue 65 and the C-terminus of the polypeptide were modified. As modification and purification techniques became

Table 1a. Chemical modification of surface lysyl residues used in the study of cytochrome *c*.
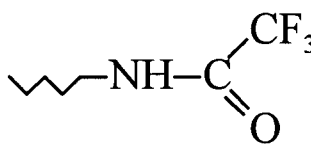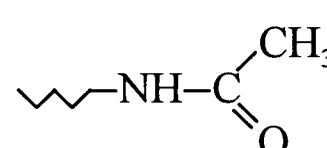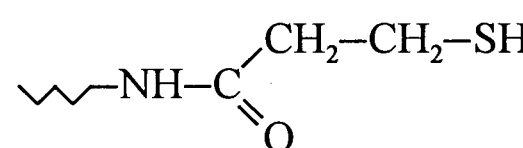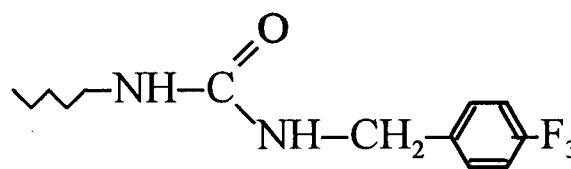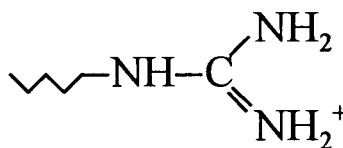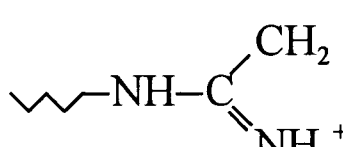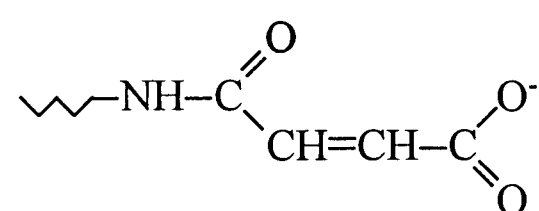
Trifluoroacetyl-Lys	$\sim\!\!\!\sim\!\!-NH-C\stackrel{CF_3}{\underset{O}{\diagdown}}$
Acetyl-Lys	$\sim\!\!\!\sim\!\!-NH-C\stackrel{CH_3}{\underset{O}{\diagdown}}$
β-Thipropionyl-Lys	$\sim\!\!\!\sim\!\!-NH-C\stackrel{CH_2-CH_2-SH}{\underset{O}{\diagdown}}$
Trifluoro(phenyl) carbamyl-Lys	$\sim\!\!\!\sim\!\!-NH-C\stackrel{O}{\underset{NH-CH_2-\langle\ \rangle-F_3}{\diagup}}$
Guanidyl-Lys	$\sim\!\!\!\sim\!\!-NH-C\stackrel{NH_2}{\underset{NH_2^+}{\diagdown}}$
Acetimidyl-Lys (amidyl-Lys)	$\sim\!\!\!\sim\!\!-NH-C\stackrel{CH_2}{\underset{NH_2^+}{\diagdown}}$
Maleyl-Lys	$\sim\!\!\!\sim\!\!-NH-C\stackrel{O}{\underset{CH=CH-C\stackrel{O^-}{\underset{O}{}}}{\diagdown}}$

18

Table 1b. Effect of Chemical Modification of Surface Lysyl Residues on the Alkaline Transition of Horse Heart Cytochrome c.

Modification		Protein[a]	pK_{ap} [μ (M)]	method[b]	spin state[c]	Conclusions/Comments	Ref[e]
Tryptic digest/complexation		1-38/39-104 T	7.1[0.05]	EAS	low		1
		1-65/66-104 T	8.9[0.05]	EAS	low		2
Acetimidylation[d]							
	Complete	holoprotein	9.2-9.9	EAS	low		3
	Partial	1-38*/39-104	7.0	EAS		Lys is not an axial ligand in alkaline ferricytochrome c	1
		1-38/39-104*	8.3	EAS			1
		1-38*/39-104*	8.15	EAS			1
		1-65*/66-104	9.98	EAS			1
		1-65/66-104*	9.67	EAS			1
		1-65*/66-104*	9.18	EAS			1
	Selective	holoprotein vs 66-80	-	differential chemical modification	-	no difference detected in the susceptibility of Lys72, 73 or 79 to acetic anhydride	4
Maleylation		holoprotein	> 9[0.15]	EAS	low	not 100% modified, denaturation occurs with reaction of >15Lys/cytc	3, 5
(Trifluoro)phenylcarbamylation							
	Selective	Lys13	8.9[0.05]	EAS	low	Lys79,and possibly Lys72 may be axial ligands of alkaline ferricytochrome c	6
		Lys72	9.3[0.05]	EAS	equil		6
		Lys79	8.9[0.05]	EAS	low		6
Trifluoroacetylation							
	Complete	holoprotein	9.9[0.2]-10.3[0.5]	EAS, FTIR	equil	unstable OH- bound at pH>11	7-10
	Selective	Lys72	9.6[0.05]	EAS	low		6
		Lys79	8.9[0.05]	EAS	low		6

19

Table IIb. Effect of Chemical Modification of Surface Lysyl Residues on the Alkaline Transition of Horse Heart Cytochrome c. (Continued)

Modification		Protein[a]	pK_ap [μ (M)]	method[b]	spin state[c]	Conclusions/Comments	Ref[e]
Guanidination							
	Complete	holoprotein	8.8-9.4	EAS	equil		8, 9 11-13
	Selective	1-65*/66-104	8.9[0.05]	EPR	low		2
		1-65/66-104*	8.8[0.05]		equil		2
Acetylation							
	Selective	holoprotein vs 66-80	-	differential chemical modification	-	Lys72, 73 and 79 are equally modified by acetic anhydride	4
β-Thiopropionylation							
	Selective	Lys72		EAS, EPR, NMR, & ESEEM	equil	non-native ligation	14
		Lys73			low	dimerizes easily, otherwise native characteristics	14
		Lys79			low	similar to Lys72 modified HH but slowly dimerizes like Lys73	14

a Sequence numbers refer to peptides derived from tryptic hydrolysis or CNBr treatment of cytochrome c that form cytochrome-like complexes when mixed with complementary peptides (interacting peptides are separated by "/"). The asterisk denotes chemical modification of a peptide by the method indicated.

b Abreviations: EAS, electronic absorption spectroscopy; ESEEM, electron spin echo envelope modulation.

c None of the cytochrome derivatives referred to here occurs in a purely high-spin ferric form; therefore, "equil" refers to a spin equilibrium.

d Also referred to as amidination in the older literature.

e References: (1) Wallace, 1984; (2) Wilgus & Stellwagen, 1974; (3) Pettigrew et al., 1976; (4) Bosshard, 1981; (5) Aviram et al., 1981; (6) Smith & Millet, 1980; (7) Morton, 1973a; (8) Stellwagen et al., 1975; (9) Fanger & Harbury, 1965; (10) Tonge et al., 1989; (11) Hettinger & Harbury (1965); (12) Brittain & Greenwood 1975; (13) Uno et al., 1984; (14) Theodorakis et al., 1995.

available to generate and isolate singly modified cytochromes c, a variety of lysyl residues within the C-terminal region of the protein were targeted for scrutiny (Morton, 1973; Wilgus & Stellwagen, 1974; Smith & Millet, 1980; Bosshard, 1981; Wallace, 1984; Theodorakis $et\,al.$, 1995). The results from trifluorophenyl-carbamylation and β-thiopropionylation of these amino acids suggested that Lys72 and perhaps Lys79 are the residues that replace Met80 in the alkaline transition of horse heart ferricytochrome c (Smith & Millet, 1980; Theodorakis $et\,al.$, 1995). However, in differential chemical modification experiments, these residues were as susceptible to modification in the native and alkaline states as in the free amino acid form (Bosshard, 1981). It was concluded, therefore, that the alkaline conformer ligand can not be a lysyl residue because a heme-bound amino group is protected and should not be susceptible to attack.

The apparently contradictory conclusions from the different chemical modification strategies can be reconciled considering the NMR results of Hong and Dixon (1984). At alkaline pH, horse heart ferricytochrome c, and presumably other eukaryotic and bacterial cytochromes, undergoes two independent alkaline conformational transitions rather than one. These two structural isomerizations result in different alkaline species that originate from one of two lysyl residues binding to the heme. In yeast iso-1-cytochrome c one of these lysyl residues is located at position 79 (Ferrer $et\,al.$, 1993). Because these ligand exchanges are dynamic processes, one residue is susceptible to modification while the second is protected by coordination to the heme. When this interaction is severed, the second ligand also becomes susceptible to modification.

1.3.3 The Mechanistic Features of the Isomerization

The alkaline isomerization of ferricytochrome c is typically quantified by a pK_{ap} value determined under equilibrium conditions (see Appendix 1). However, the process consists of a

combination of events that is more complex than the simple ionization of a titratable group. The simplest model that more accurately takes into account an ionization-linked structural reorganization was described by Davis *et al.* (1974). Based on pH-jump kinetics experiments, these authors postulated Relation 3, where N–H and N denote, respectively, the protonated and deprotonated species that possess native structure and absorbance at 695 nm, and A is the alkaline species.

$$\text{N–H} \underset{pK_H=11}{\overset{H^+}{\rightleftharpoons}} \text{N} \underset{k_b=.05s^{-1}}{\overset{k_f=6s^{-1}}{\rightleftharpoons}} \text{A} \qquad (3)$$
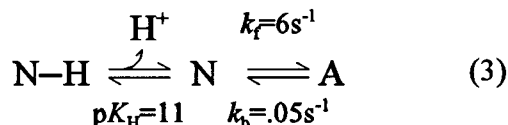
K_H is the equilibrium constant for the deprotonation, and k_f and k_b are the forward and reverse rate constants for the conformational reorganization. The entire process thus consists of two components (pK_H and $p[k_f/k_b]$) that together comprise the pK_{ap} that is measured under equilibrium conditions. This analysis has also been applied to various species of cytochrome *c* and to variants of the yeast protein (Pearce *et al.*, 1989; Nall *et al.*, 1989; Saigo, 1981; Rafferty, 1992). In some of these proteins, the pK_{ap} for the transition was altered by changes in the dynamic properties ($p[k_f/k_b]$), the deprotonation component, or a combination of both.

Although the model described above can account for the data collected in pH-jump experiments below pH 10, it does not explain a second kinetic phase observed at higher pH and at wavelengths other than in the region around 695 nm band. This additional level of complexity was addressed with Relation 4 (Kihara *et al.*, 1976; Hasumi, 1980). It was proposed that below pH 10, the alkaline transition progresses essentially as first outlined by Davis *et al.* (1974), resulting in the alkaline species A–H. Above pH 11, however, an alternate path via the transient T is favoured. At a pH between these limits, the alkaline transition occurs via both pathways.

A simpler alternative to the mechanism described by Davis *et al.* (3; 1974) incorporates a

$$
\begin{array}{c}
\text{A--H} \xrightleftharpoons[\quad]{pK=11.4} \text{A} \\[6pt]
k_{-2}=.05s^{-1} \quad k_2=6.7s^{-1} \quad H^+ \\[4pt]
N\text{--}H_2 \xrightleftharpoons{H^+} N\text{--}H \qquad k_3=7.8s^{-1} \quad k_{-3}=.25s^{-1} \qquad (4) \\[4pt]
pK=11.4 \quad k_1=31s^{-1} \\
k_{-1}=58s^{-1} \quad H^+ \\[4pt]
\text{T--H} \xrightleftharpoons[pK=10.4]{\quad} \text{T}
\end{array}
$$
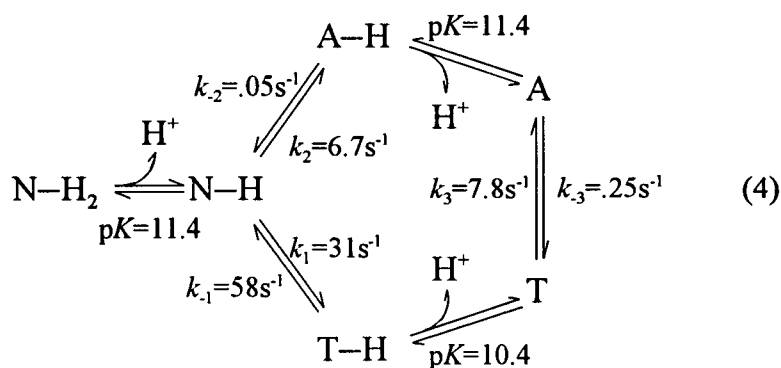
transient intermediate into the pathway from the native cytochrome to its alkaline conformer (Mechanism 5; Saigo, 1981 a, b):

$$
N\text{--}H \underset{pK_H=11}{\overset{H^+}{\rightleftharpoons}} N \rightleftharpoons I \rightleftharpoons A \qquad (5)
$$
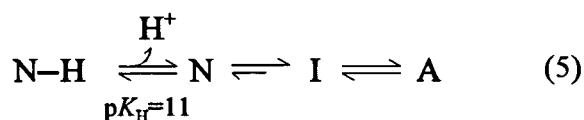
The fast phase that results in pH-jump experiments to pH above 10 reflects the rapid formation of this intermediate which then decays to the stable alkaline conformer. Presumably, at lower pH this intermediate still forms; however, its concentration under these conditions is too low for detection. In theory, the ligand exchange could result in an S_N1 fashion: (1) coordination of the incoming lysyl residue as (2) the Met80-Fe^{3+} bond is broken. The formation of a transient, 5-coordinate intermediate upon breaking the Met80 bond and before coordination of the incoming lysyl residue is likely included in this mechanism (Palmer, 1977). This 5-coordinate intermediate would be a common transient for the formation of both alkaline conformers discovered by Hong and Dixon (1989).

It is noteworthy that a native or native-like species precedes a transient in experiments where guanidine-denatured yeast *iso*-2-ferricytochrome *c* is renatured at alkaline pH (Nall, 1986). This result suggests that the alkaline conformational transition of ferricytochrome *c* is an ordered event, and that native tertiary structure elements are required to direct the structural reorganization.

1.3.4 The Trigger Group

In parallel to the search for the sixth axial ligand in the alkaline conformer of cytochrome c, the identity of the titratable or "trigger" group which, upon ionization, initiates the alkaline transition has been sought (Moore & Pettigrew, 1990; Wilson & Greenwood, 1996). Close examination of the available crystal and NMR structures of cytochrome c reveals a multitude of hydrogen bonds (main chain: main chain = 49; main chain–side chain = 38; side chain–side chain = 10; Louie, 1990). The perturbation of many of these structure-stabilizing interactions could, in principle, trigger at least a local structural collapse with the ensuing reorganizations of the polypeptide. The titration of this group occurs with a pK_H of ~11 in equine cytochrome c as determined by pH-jump experiments (Davis *et al.*, 1974). Therefore, amino acids that have been considered to fulfill the trigger role include the lysyl residue that also acts as a heme ligand, Tyr67, an internal water molecule (H_2O166), His18, and the heme 6-propionate group.

A lysyl residue that replaces Met80 cannot be protonated if the ϵ-amino group is to coordinate the heme iron. Therefore, the ionization of this group, followed by the ligand exchange, is consistent with the kinetic mechanisms noted above. Moreover, the high pK_a value associated with a primary amine is compatible with the pK_H values determined by pH-jump experiments. However, chemical modification of all lysyl residues in cytochrome c does not stabilize the Met80-Fe^{3+} bond, suggesting that ionization of the true trigger group is still initiating an alkaline conformational transition (Fanger & Harbury, 1965; Hettinger & Harbury, 1965; Morton, 1973; Stellwagen *et al.*, 1975).

Nitration (Skow *et al.*, 1969; Schejter *et al.*, 1970; Pal *et al.*, 1975) and iodination (Morton, 1973b; Pal *et al.*, 1975) of Tyr67 in horse heart cytochrome c results in a significantly less stable protein with a pK_{ap} for the alkaline conformational transition of ~6. Replacement of this residue with

phenylalanine, on the other hand, increases the pK_{ap} of the rat ferricytochrome by ~1.1 pH units (Luntz *et al.*, 1989). These observations suggest that ionization of the hydroxyl group of Tyr67 perturbs the local environment on the distal side of the heme to trigger the alkaline transition. This assumption is consistent with the known structures of ferrocytochrome *c*, which does not exhibit a stable alkaline conformation and in which Tyr67 hydrogen bonds the δ-sulfur atom of Met80. However, in a double variant where the Tyr67Phe mutation was combined with Pro30Ala (located on the proximal side of the heme), the pK_{ap} value was restored to ~9.5 (Schejter *et al.*, 1992). Therefore, it would appear that Tyr67 does participate in the alkaline conformational transition of cytochrome *c* but not in the capacity of the trigger group that initiates the process.

Takano and Dickerson (1981) favour the ionization of an internal water molecule as the trigger of the structural reorganization. This water molecule is located close to the iron on the distal side of the heme where it forms hydrogen bonds a number of amino acids, including Tyr67. The migration of the water molecule away from the iron in the more stable ferrocytochrome, the absence of an equivalent water molecule in cytochrome c_{551} from *Pseudomonas aeruginosa* (pK_{ap}~11), and the perturbation of the alkaline pK_{ap} upon modification or replacement of Tyr67 have been interpreted to support this assignment. Moreover, Takano and Dickerson proposed that, upon ionization, the resulting hydroxide coordinates the iron to form an intermediate. This intermediate is the product when all lysyl residues in the protein are chemically modified and, therefore, incapable of coordinating the iron (Table 1b). However, no unequivocal evidence is yet available to confirm whether or not this water molecule potentiates the alkaline transition.

Ionization of His18 has also been suspected to trigger the alkaline isomerization of cytochrome *c* (Gadsby *et al.*, 1987). A pH titration of the methylimidazole complex of the protein, monitored by EPR, showed that the His⇌His⁻ interconversion (pK_{ap}~11.6) is consistent with the high

pK_H values reported in the mechanism of Davis *et al.* (1974). Based on these observations Thomson and coworkers proposed that (1) His18 ionizes to histidinate, thus (2) causing the rupture of the Met80-Fe^{3+} bond. (3) Upon ligation of a deprotonated lysyl residue to the iron, (4) the pK_{ap} of His18 increases, and (5) the histidinate reprotonates. The principal attraction of this scheme is the apparent consistency of the pK values and the net change of one protonation state.

Finally, the heme 6-propionate group has also been identified as the functional group that induces the alkaline transition (Hartshorne & Moore, 1989; Tonge *et al.*, 1989). This proposal is based on the abnormally high pK_a (~10.4) value of the carboxyl group as monitored by the asymmetric carbonyl stretch at 1571 cm^{-1} in the FTIR spectrum of the protein. Like all of the other proposed trigger groups, the involvement of the heme 6-propionate group in the initiation of the alkaline transition remains to be established unambiguously.

1.3.5 Functional Considerations

Discussion of the alkaline conformational transition of ferricytochromes c inevitably concerns the metabolic role(s) that states IV or V of the protein may fulfill. Considering that the alkaline transition is highly reversible and widespread among cytochromes c, it could be argued that the phenomenon does not occur without a useful purpose. On the other hand, it is possible that the alkaline isomers of the protein were metabolically relevant in the distant past, and their occurrence today is simply an evolutionary vestige. Generally, the pH required for the alkaline conformational reorganization of most cytochromes c *in vitro* is greater than the upper limit of what is normally accepted to be of physiological significance or even attainable. However, the occurrence of this phenomenon is very sensitive to conditions such as temperature (Taler *et al.*, 1995) and ionic strength (Osheroff *et al.*, 1988; Rosell *et al.*, 1998). Therefore, it is conceivable that during various metabolic

states, regions within the intermembranal space of mitochondria provide a suitable microenvironment in which the transition may take place more readily. Heavy physical exertion, for example, can raise the core temperature of a horse to 45 °C (Hodgson *et al.*, 1995). At this temperature, the pK_{ap} decreases as much as one pK unit from the value that is normally observed *in vitro*: 9.3 at 25 °C (Davis *et al.*, 1974; Taler *et al.*, 1995). Moreover, the interaction of cytochrome *c* with other proteins and membrane surfaces may also exert a destabilizing influence on the structure of the native protein thereby reducing the effective pK_{ap} of the alkaline transition. For example, Aviram and Schejter showed that removal of water from cytochrome *c* through lyophilization results in the disruption of the Met80-Fe^{3+} bond (1972). Although the environment within the intermembranal space of mitochondria is not severe as lyophilization, the reduced water content within this compartment, which may be comparable to that of the cytoplasm (~70% water; Alberts, 1994), may also exert some influence on the conformational equilibria of the protein.

Barker and Mauk (1992) demonstrated that the midpoint reduction potential of state IV is almost 0.5 V lower than that of the native protein. This property of alkaline cytochrome *c* would ensure that the electron flow is unidirectional during the interaction of the protein with its oxidizing electron transfer partners. If, through this interaction, cytochrome *c* reorganizes to its alkaline conformation immediately after donating the electron, the markedly lowered midpoint reduction potential would make it unlikely for the electron to return to the donor. In the most extreme of cases, the drop in potential essentially blocks oxidative phosphorylation.

The heme edge that is partially exposed to solvent on the surface of cytochrome *c* is generally considered to be the optimum site for electron transfer. Here, the heme comes closest to the protein surface where the sulfur atom of Cys17, which is also partially exposed, can act as an electron conduit by coupling to the π-electron system of the heme group (Tollin *et al.*, 1986). Forming a docking site

around this exposed heme are highly conserved, basic residues which can direct and stabilize the formation of protein:protein complexes (Salemme, *et al.*, 1973; Meyer *et al.*, 1994; Figure 3). Results from chemical modification experiments (Fergusson-Miller *et al.*, 1978; Moore *et al.*, 1998), Brownian dynamics simulations (Northrup *et al.*, 1988), and X-ray diffraction studies of the cytochrome *c*:cytochrome *c* peroxidase complex (Pelletier & Kraut, 1992) suggest that Lys13, 27, 72, 73, 79, and 87 are involved in establishing the protein:protein interface. Similarly, Lys13, 72, 79, 86, 87, and probably 73, also appear to be involved in the complexation of cytochrome *c* to cytochrome b_5 (Salemme, 1976; Rodgers *et al.*, 1988; Burch *et al.*, 1990; Northrup *et al.*, 1993; Guillemette *et al.*, 1994), and to cytochrome *c* oxidase (Döpner *et al.*, submitted). The alkaline conformational transitions of ferricytochrome *c* essentially remove Lys79 (Ferrer *et al.*, 1993) and a second lysyl residue from the surface of the protein. Like chemical modification, or replacement of these amino acids by an aliphatic side-chain, the alkaline structural reorganization reduces the ability of the cytochrome to interact properly with its electron transfer partners. The level of oxidative phosphorylation would also be reduced as a result of the decreased affinity for cytochrome *c* in the alkaline state.

The view expressed by Moore and Pettigrew is that non-native conformations of cytochrome *c in vivo*, including the alkaline conformers, constitute too small a percentage of the protein to be of physiological significance (1990). Moreover, these authors cite the slow isomerization of the protein to its native structure, and the acidic nature of the intermembranal space of mitochondria, as further indications that the alkaline conformers are not functionally significant. Wilson and Greenwood (1995), on the other hand, do not dismiss the possibility that the alkaline transition is a "design feature selected through evolution" rather than "a chance byproduct of molecular architecture." Indeed, the participation of cytochrome *c* in apoptosis would not have been considered 2-3 years ago, but

cytochrome c is now regarded as an integral part of programmed cell death (Kroemer *et al.*, 1998; Mignotte & Vayssiere, 1998; Skulachev, 1998). In a similar way, our present inability to assign a function to the alkaline conformers of cytochrome c does not, by itself, constitute irrefutable evidence that these structures are physiologically inactive.

1.4   Spectroscopic Characteristics of Cytochromes c

The iron porphyrin in heme proteins can provide valuable information about the active site of cytochrome c through the use of a wide variety of spectroscopic techniques. Spectroscopic characterization of heme-containing proteins typically includes electronic absorption spectroscopy, nuclear magnetic and electron paramagnetic resonance spectroscopies, conventional and magnetically-induced circular dichroism spectroscopy, and resonance Raman spectroscopy (Moore & Pettigrew, 1990; Scott & Mauk, 1996 and references therein). These techniques probe various aspects of the interaction between the protein matrix and the prosthetic group. Therefore, a multidisciplinary approach is often implemented in the thorough characterization of heme proteins.

The most common oxidation states of the heme iron are the ferrous (Fe^{2+}: [Ar] $3d^6 4s^0$) and the ferric (Fe^{3+}: [Ar] $3d^5 4s^0$) states, although examples of the ferryl form (Fe^{4+}: [Ar] $3d^4 4s^0$) are also encountered in the form of Fe^{4+}=O (for *e.g.*, compounds I and II in peroxidases). As noted earlier, the electronic configuration of the metal centre depends in large part on the nature of the axial ligands. The heme iron of both ferri- and ferrocytochromes c is in a tetragonally distorted ligand field generated by the equatorial heme and the axial Met80 and His18 ligands. Under these conditions, the d-orbitals of the iron are split as shown in Figure 7a, and the iron has low-spin electronic configurations in both oxidation states (Fe^{3+}: S=1/2; Fe^{2+}: S=0). High-spin hemoproteins are also common in nature (for *e.g.*, S=5/2: 5-coordinate cytochrome c peroxidase in the resting state; S=2:

A

$d_{x^2-y^2}$

d_{z^2} $d_{x^2-y^2}$

$\uparrow$ $\uparrow$ $\uparrow$ $\uparrow$ $\uparrow$
d_{xy} d_{xz} d_{yz} d_{z^2} $d_{x^2-y^2}$

$\uparrow\downarrow$ $\uparrow\downarrow$ $\uparrow$
d_{xy} d_{xz} d_{yz}

$\uparrow\downarrow$ $\uparrow$
d_{xz} d_{yz}

$\uparrow\downarrow$
d_{xy}

Free Ion   Octahedral   Tetragonal
                  Field   Field

B

$e_g \pi^*$

$d_{x^2-y^2}$
d_{z^2}

d_{xz} $\uparrow\downarrow$ $\uparrow$ d_{yz}

$\uparrow\downarrow$ d_{xy}

$a_{2u}\pi$

$a_{1u}\pi$

π^*

$\uparrow\downarrow$ π

$\uparrow\downarrow$ σ

Porphyrin   Metal   Ligand
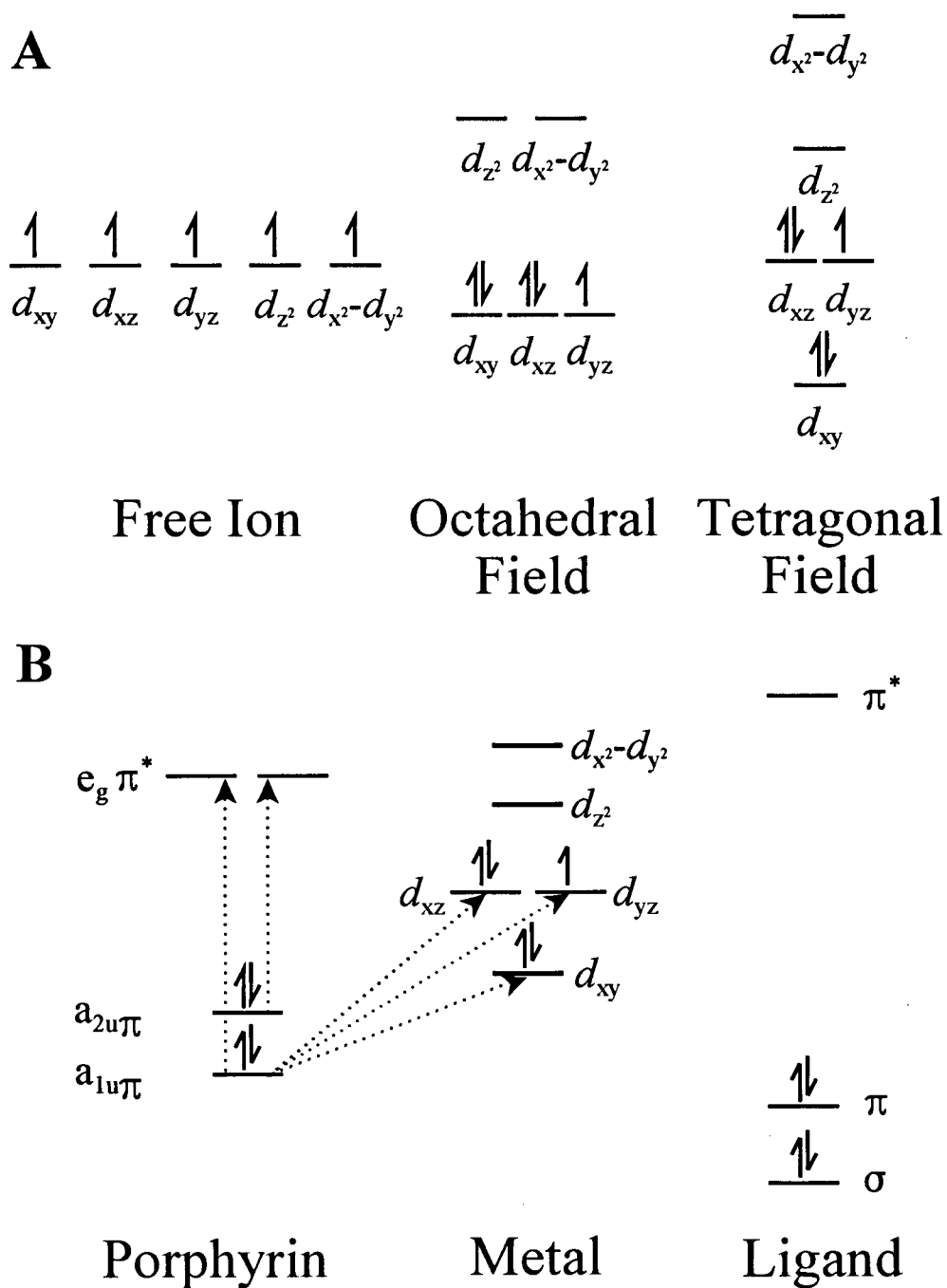
Figure 7. (A) Schematic Diagram illustrating the effect of octahedral and tetragonal field distortions on the d-orbital splitting of a low-spin ferric heme. (B) Schematic Diagram illustrating the commonly accepted electronic transitions between porphyrin and metal electronic orbitals that are detectable by electronic absorption spectroscopy.

5-coordinate deoxymyoglobin), and while an example of a quantum mechanically admixed spin state (QMAIS) has been described (S=3/2, 5/2 : 5-coordinate cytochrome c') (Maltempo *et al.*, 1974; Maltempo, 1976 a and b), naturally occurring hemoproteins with intermediate-spin states (S=3/2) have not. In mitochondrial cytochromes c, however, high-spin states and admixtures are often evidence of gross structural perturbations (for *e.g.*, acid or chaotropic denaturation) and require more thorough characterization to define the cause and consequences of the perturbation with some precision.

Although resonance Raman spectroscopy has been used successfully in the characterization of heme proteins including cytochrome c (Spiro, 1985; Desbois, 1994), the bulk of this dissertation consists of data collected with CD, electronic absorption, EPR, MCD, and ^{1}H-NMR spectroscopy. Therefore, only the latter techniques are considered briefly in the following sections. Much of this material is applicable to heme proteins in general, but the emphasis here is on the relevance of these techniques to the study of mitochondrial cytochromes c or on the issues that are relevant to this work.

1.4.1 Electronic Absorption Spectroscopy

The UV-vis spectrum of cytochrome c is dominated by the Soret (γ or B) band centred at ~410 (Fe^{3+}) or 416 nm (Fe^{2+}). This intense absorbance (ϵ ~106100 M^{-1} cm^{-1} oxidized and ϵ ~129100 M^{-1} cm^{-1} reduced) arises from strongly allowed electronic transitions between bonding and antibonding molecular orbitals of the porphyrin ($\pi \rightarrow \pi^*$) (Figure 7b). At longer wavelengths, two less intense features (α and β, or Q_o and Q_v, respectively) appear in the visible region (~530 nm) and are minor components of the same excitations. According to the four-orbital model of Gouterman (1959), $\pi \rightarrow \pi^*$ transitions interact unfavourably and mix, thus separating otherwise degenerate excited states. The Soret band and the α-β system are manifestations of the higher and the lower excited states,

respectively (Smith & Williams, 1970). Vibrational processes contribute further to split the transition of the lower excited state into the two bands that are labeled α and β. Additional absorption bands attributable to porphyrin $\pi \rightarrow \pi^*$ orbital transitions can appear between 215 and 325 nm, but these features are weak and often masked by absorbances from peptide bonds (~190-230 nm) and aromatic groups (~280 nm) (Moore & Pettigrew, 1990).

In general, displacement of electronic distribution to the periphery of the porphyrin ring causes the Soret and α-β bands to shift to lower energy. Reduction of the metal centre, for example, exhibits this spectroscopic result as does replacement of the iron by a metal that is less electronegative and the introduction of stronger electron withdrawing substituents to the porphyrin ring system. Concomitantly, these absorbances shift to higher energy as the electron withdrawing strength of the axial ligands increases. The spectroscopic influence of axial ligands is demonstrated by the alkaline conformer of ferricytochrome c which displays a blue-shifted Soret band as a result of the replacement of Met80 for a nitrogenous base (Theorell & Åkesson, 1941).

Figure 7b illustrates electronic transitions from the porphyrin π- to the lower available metal d-orbitals. These charge transfer (CT) bands are associated with absorbances of ferricytochromes c in high- (~600 nm) and low-spin (1200-1500 nm) electronic configurations (Smith & Williams, 1970; Gouterman, 1978; Makinen & Churg, 1983; Spiro, 1983). CTs from the axial ligand $\pi \rightarrow$ metal d-orbitals are allowed for some ligand types but these bands are difficult to assign and predict. The present consensus is that the weak 695 nm band (ϵ ~ 1 mM^{-1}cm^{-1}) arises from just such a CT (Smith & Williams, 1970; Makinen & Churg, 1983) based on the similar characteristics of this band and those observed in the spectra of the OH$^-$ and N$_3^-$ adducts of metmyoglobin. This band is of particular interest because it is diagnostic of the Met80-Fe^{3+} bond (Harbury $et\,al.$, 1965; Schechter & Saludjian, 1967; Eaton & Hochstrasser, 1967; Smith & Williams 1970) and its strength. Consequently, this

feature is often used in spectroscopic studies to assess the structural integrity of the heme cavity. Metal $d \rightarrow d$ transitions are generally forbidden. Therefore, if such transitions occur, they are nearly undetectable in visible spectra where they are largely obscured by the more intense porphyrin $\pi \rightarrow$ metal d-orbital CTs.

1.4.2 Electron Paramagnetic Resonance Spectroscopy

One of the earlier applications of EPR spectroscopy to the study of heme proteins, was the elucidation of axial ligands of low-spin, ferrihemoproteins (Blumberg & Peisach, 1971). This technique is sensitive to structural perturbations that change the geometry of the iron core, and in particular, to ligand exchanges. These perturbations invariably affect the axial (Δ) and rhombic (V) symmetry elements that define the ligand field of the iron. These parameters reflect the energy separation between the metal t_{2g} orbitals. Whereas axial distortions destabilize the d_{xz} and d_{yz} orbitals relative to d_{xy}, rhombic distortions lift the degeneracy of the former pair (Palmer, 1977). Furthermore, the t_{2g} orbitals mix through spin-orbit coupling (λ) so that three resonance conditions exist (Equation 1):

$$h\upsilon = g\beta B_0 \qquad (1)$$

where $h\upsilon$ is the energy of the excitation radiation (microwave region), g a proportionality factor, β is the Bohr magneton, and B_0 is the applied magnetic field, and. Each of these conditions is associated with a g-factor which is read from the EPR spectrum and which corresponds to each of the coordinate axes (g_x, g_y, g_z) where the iron ion is at the origin.

Mathematical relationships have been derived to determine the tetragonality and rhombicity normalized with respect to the spin-orbit coupling (Palmer, 1977) :

$$\frac{V}{\lambda} = \frac{g_x}{g_z + g_y} + \frac{g_y}{g_z - g_x} \qquad (2)$$

$$\frac{\Delta}{\lambda} = \frac{g_x}{g_z + g_y} + \frac{g_z}{g_y + g_x} - \frac{1}{2}\frac{V}{\lambda} \qquad (3)$$

With these coordinates in hand, proteins of unknown coordination environment have been compared to structurally-characterized standards which are compiled in so-called "truth diagrams" (Figure 8) (Blumberg & Peisach, 1971). Proteins with equivalent axial ligation cluster into well-defined regions, so ligand assignment is often possible based largely on the similarity of these ligand field parameters.

In the native state, cytochromes c correspond to group C in the truth diagrams and are characterized by the lowest tetragonal fields (Figure 8). At higher pH, the EPR spectra of the protein reveal the presence of at least two additional low-spin species (Morton, 1972; Brautigan *et al*, 1977; Gadsby *et al.*, 1987; Gadsby & Thomson, 1990; Ferrer *et al.*, 1993) with ligand field parameters similar to those of group H members. According to these EPR data, the alkaline forms of ferricytochrome c are similar to the N-butylamine adduct of leghemoglobin (Gadsby *et al.*, 1987) and to cytochrome f (Rigby *et al.*, 1988; Gadsby & Thomson, 1990). In the former example, the amino group of the exogenous ligand acts as the ligand, while in the latter protein, the N-terminus of the polypeptide chain fulfills this role (Martinez *et al*, 1994).

At first sight, the use of EPR spectroscopy in the identification of residues that are coordinated to the heme is a convenient approach because of the relative simplicity of the measurement. However, this method is not always accurate or precise. Group B in the truth diagrams, for example, is composed of heme proteins with bis-histidine ligation such as cytochrome b_5. Member proteins of this family exhibit a large variation in g-values (*i.e.*, $g_{max} \sim 3.0$-3.6) depending on the orientation of the histidine ring planes in relation to each other and to the porphyrin ring (Gadsby and
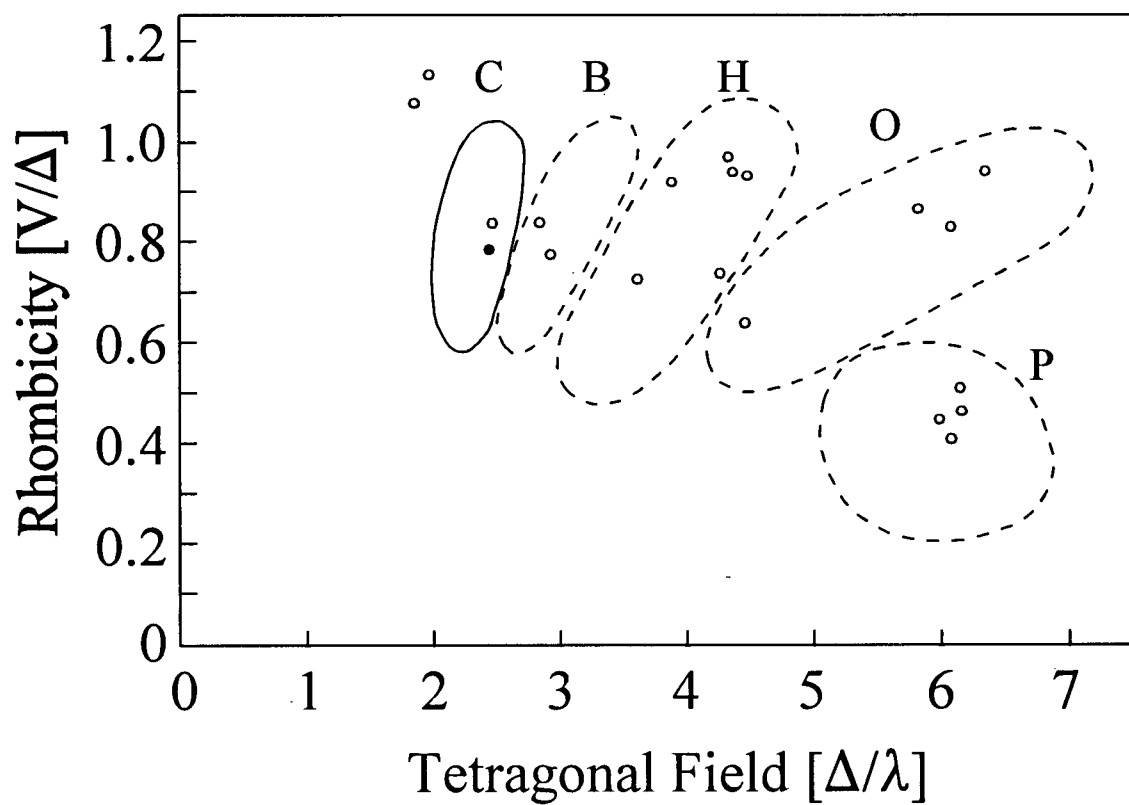
Figure 8. Crystal-field correlation diagram denoting the five common families of low-spin ferric hemoproteins as defined by Blumberg and Peisach (1971). Rhombicity values of 0 and 0.66 corresponds to purely axial and purely rhombic systems, respectively. Cytochromes c (solid circle) reside in zone C (solid line).

Thomson, 1990). In many of these spectra, it is difficult to determine g_{mid} and g_{min} values experimentally when g_{max} is greater than ~3.4 (Salerno, 1984). In the worst of cases, the truth diagram approach of ligand identification can lead to the incorrect assignments in cytochromes (Gasby & Thomson, 1990; Teixeira *et al.*, 1993; Arciero *et al.*, 1994) exhibiting HALS (highly axial, low-spin)-type EPR spectra (Migita & Iwaizumi, 1981; Walker *et al.*, 1986).

As noted earlier, weak manifestations of CT bands from the porphyrin π (a_{1u} and a_{2u} symmetry) to an available metal t_{2g} orbital appear in the near-IR region (700-3000 nm) of ferric, low-spin hemoproteins (Figure 7b). These transitions are diagnostic of heme coordination because when the axial ligands affect the axial and rhombic symmetry elements of the iron (as detected by EPR spectroscopy), they also affect the resonant frequency v for the CT (Gadsby &Thomson, 1990 and references therein). Although, under ordinary conditions vibrational bands from C–H, O–H, and N–H bonds overlap and obscure these CT transitions, application of a magnetic field considerably enhances the CT bands. This enhancement is a consequence of the stronger magnetic moment associated with electrons relative to nuclei. Optionally, freezing samples to cryogenic temperatures further enhances the CT bands because nuclear vibrations are discouraged. Thomson and coworkers (1990) have thus compiled an extensive database of near-IR MCD spectral parameters of well characterized heme proteins and model porphyrin compounds. Therefore, the presently accepted criteria for the spectroscopic identification of heme axial ligation in low-spin, ferrihemoproteins combines EPR and near-IR MCD spectroscopy (Gadsby & Thomson, 1990; Arciero *et al.*, 1994; Hawkins *et al.*, 1994).

1.4.3 Nuclear Magnetic Resonance Spectroscopy

The value of NMR spectroscopy for the investigation of macromolecules such as cytochromes *c* is well established (see for *e.g.*, Wüthrich, 1996; Roberst, 1993; Pielak *et al.*, 1995 and references

therein). As early as 1971, NMR was used to solve important questions about this protein. Redfield and Gupta, for example, demonstrated that Met80 is the sixth axial ligand in native ferricytochrome *c* (1971). Previous to this report it was commonly believed that the axial ligand was a histidyl residue or even a lysine. More recently, high resolution NMR spectrometers, and the increasing availability to obtain isotopically-enriched protein samples (^{13}C and ^{15}N) have facilitated the assignment of chemical shifts in the spectra of proteins of ~120 amino acids, though the upper limit is ~250 residues. Concurrently, innovative strategies for data acquisition and analysis frequently permit the elucidation of protein three-dimensional structures.

NMR-active nuclei in paramagnetic proteins are subject to the same forces that affect nuclei in diamagnetic molecules (for *e.g.*,, ring current shifts, nuclear Overhausser effect, etc.). However, in the proximity of transition metal ions, the large magnetic moment associated with unpaired electrons of the metal ion exerts a significant influence over the chemical shift of nuclei (Equation 4a and b).

$$\delta_{observed} = \delta_{diamagnetic} + \delta_{paramagnetic} \qquad (4a)$$

$$\delta_{paramagnetic} = \delta_{dipolar} + \delta_{contact} \qquad (4b)$$

This physical influence has dipolar (or pseudocontact) and contact (or Fermi) components. As the names imply, the dipolar shift results from through-space, dipolar coupling of the magnetic moments of the unpaired electron(s) and the nuclei. The contact shift, on the other hand, is a consequence of direct delocalization of the electron spin density through chemical bonds. Therefore, this influence affects primarily the nuclei that are directly bound to the paramagnetic centre. In the case of heme proteins, electronic spin density can be delocalized throughout the heme macrocycle and into the axial ligands (La Mar & Walker, 1979). Therefore, protons that are located relatively far away from the

iron centre (*e.g.*, heme methyl groups and propionate groups) are susceptible to the effects of the unpaired electron(s) of the metal mainly through contact interactions.

In ^{1}H-NMR spectra of ferricytochromes *c*, resonance frequencies of heme substituent groups are shifted considerably outside of the diamagnetic envelope. Heme methyl group protons, for example, exhibit chemical shifts between 0 and 40 ppm. Because of the near-C_2 symmetry of the electronic distribution on the heme plane, these heme methyl groups cluster in pairs with the most deshielded pair (~20-40 ppm) reflecting the residence of high spin density in the corresponding pyrrole rings. The pattern of these heme group chemical shifts have been correlated with the stereochemistry of the axial ligands with respect to the heme plane (Satterlee, 1986; Marion, 1994). When the *sp*^{3} lone-pair orbital of the Met80 δ-sulfur atom points towards the nitrogen of pyrrole ring A (as it does in yeast *iso*-1-ferricytochrome *c*), heme 8- and 3-methyl group protons are the most deshielded. In cytochrome *c* from *Pseudomonas aeruginosa*, it is heme 5- and 1- methyl group protons that are most deshielded reflecting the orientation of the sulfur lone-pair orbital towards the nitrogen of pyrrole ring B (Marion, 1994). The relative orientation of the axial histidyl imidazole with respect to the heme plane is also known to steer electronic spin density in other heme proteins (*e.g.*, myoglobin and cytochrome *c* peroxidase; Satterlee, 1986). However, the orientation of this side chain is constant in the known structures of cytochromes *c* so that it is not a significant factor in this case.

The chemical shifts of axial ligand protons in low-spin cytochromes *c* are also influenced considerably by the paramagnetism of the iron. For example, the ϵ-CH_3 protons of Met80 resonate between -9 and -24 ppm while the His18 ϵ1-CH appears typically at ~25 ppm. Although the paramagnetically-induced shift is not as marked for protons of residues not directly attached to the heme, the protons near the prosthetic group are affected through dipolar interactions. Examples of this behaviour are protons of Leu48 and Pro30 which exhibit signals as low as ~-5 ppm. However,

the dipolar influence of the unpaired electron(s) on the chemical shift of nuclei falls off in proportion to the inverse cube of the distance that separates the paramagnetic center and the nuclei so that only residues in the immediate vicinity of the porphyrin are affected.

In addition to being susceptible to the paramagnetism of the metal center, proton chemical shifts in heme proteins exhibit a considerable temperature dependence. Most resonances in cytochromes *c* obey Curie Law behaviour (*i.e.*, the chemical shift of resonances decrease with increasing temperature), except for heme 5-methyl group protons and those of the Met80 ϵ-CH_3 group (Ångström *et al.*, 1982).

The longitudinal and transverse relaxation rates (T_1^{-1}, T_2^{-1}) of nuclei are also affected significantly by the influence of the magnetic moment of unpaired electron(s). This influence, through pseudocontact and contact contributions, enhances the rates of nuclear relaxation to broaden resonances. Complex formulae (see reviews by La Mar and Walker, 1977, Satterlee, 1986, and Bertini *et al.*, 1989) reveal that the rates of relaxation are a function of the distance separating the nuclei and the paramagnetic center (r^{-6}), the spin transition frequencies of the nuclei/electron(s) involved, and the correlation time that modulates the dipole-dipole interaction. In cytochromes *c*, the electronic relaxation is fast in low- and high-spin species ($\tau_s \sim 10^{-11}$-10^{-12} and 10^{-13} respectively) so that these formulae can be approximated by Equation 5 (Marion, 1994):

$$T_1^{-1} \approx T_2^{-1} \approx (\frac{\mu_0}{4\pi})^2 \cdot \frac{\hbar^2 \gamma_I^2 \gamma_S^2}{r^6} \cdot \tau_S \quad (5)$$

Line broadening caused by increasing relaxation rates is often an indication of changes in the environment of the nucleus and, therefore, reflects structural heterogeneity or chemical exchange. This phenomenon is not exclusive to paramagnetic molecules, but the large chemical shifts induced

by the unpaired electrons in such systems helps to resolve the magnetically non-equivalent environments when the rate of the chemical exchange is comparable to the difference in chemical shift between the species undergoing the exchange (La Mar & Walker, 1979).

1.5 Thesis Objectives

The primary goal of the work presented in this dissertation was to identify the second lysyl residue in yeast *iso*-1-ferricytochrome *c* that replaces Met80 as an axial ligand to the heme iron at elevated pH (Hong & Dixon, 1989; Ferrer *et al.*, 1993). Based on chemical modification results obtained using the horse heart cytochrome (Wilgus & Stellwagen, 1974), the search for this second ligand was narrowed to six out of eight lysyl residues that are located toward the *C*-terminus of residue 65 and which can potentially take part in the isomerization (Figure 9). Yeast cytochrome *c* is amenable to site-directed mutagenesis (Pielak *et al.*, 1985). This genetic technique was used instead of chemical modification to eliminate one alkaline conformer and thus isolate the other in a homogenous form. The second part of this work deals with the factors that influence the alkaline conformational equilibria of the protein. In particular, the influence of ionic strength, temperature, and protein structural elements were investigated to define the determinants of each transition at a molecular level. Finally, the determination of the three-dimensional structure of one of these alkaline conformers was initiated.

Excerpts of this work were published prior to the completion of this dissertation (Ferrer *et al.*, 1993; Pollock *et al*, 1998; Rosell *et al.*, 1998), and others are in preparation.
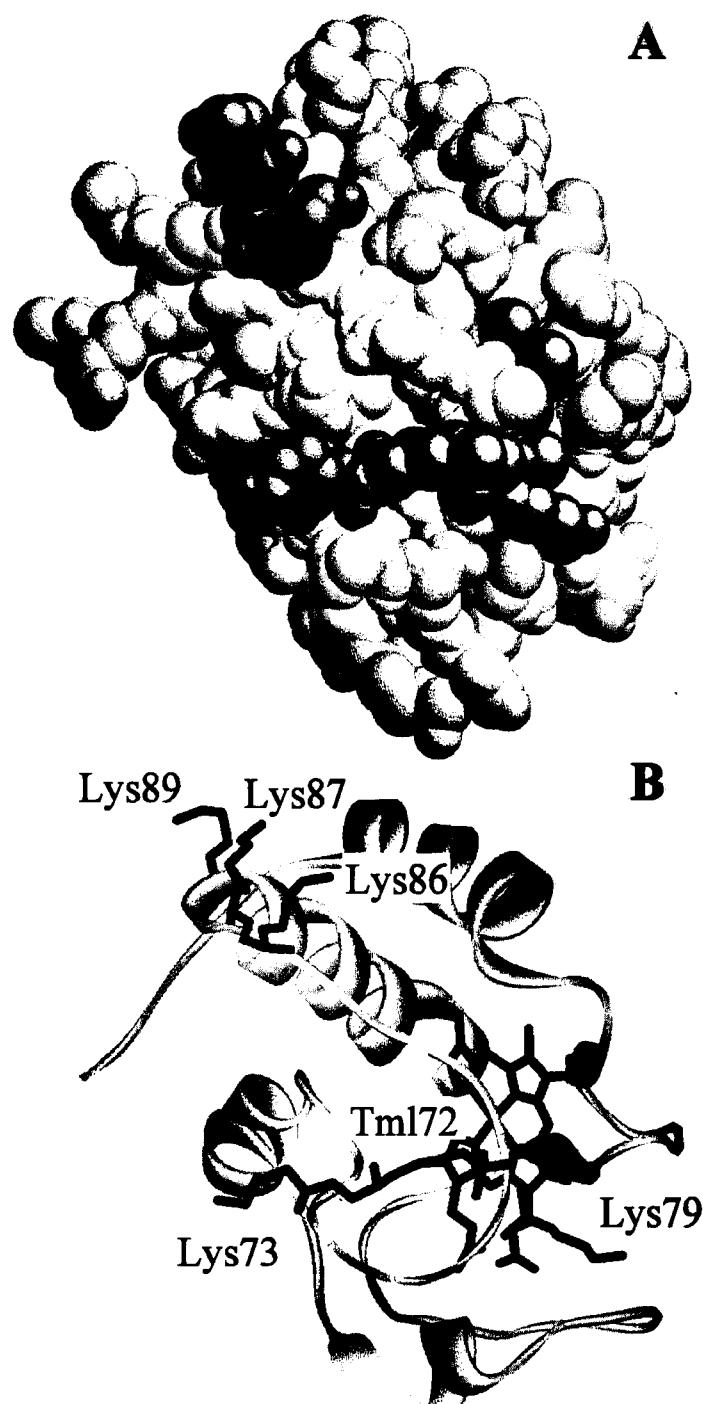
Figure 9. Models of yeast *iso*-1-ferricytochrome *c* illustrating six of the eight lysyl residues (shown in green) that are located towards the *C*-terminus from residue Met65. Lys99 and Lys100 are located at the back. The porphyrin ring is illustrated in red. The spacefilling model (A) and the ribbon representation (B) are rotated ~45° relative to the perspective shown in Figure 1.

2.   Experimental Procedures

2.1   Production of Yeast *iso*-1-Cytochrome *c* Variants

All the yeast *iso*-1-cytochromes *c* used in this work were expressed in either yeast or bacteria. Regardless of the expression host, all the proteins were encoded by the gene *CYC*1 (Figure 10a; Smith *et al.*, 1979) cloned in the vector pING4 (Figure 10b) (Inglis *et al.*, 1991). In this gene the codon for the wild-type Cys residue at position 102 (vertebrate numbering scheme) was mutated to encode for Thr to avoid protein autoreduction and dimerization (Cutler *et al.*, 1987). Therefore, the variant Cys102Thr is referred to as the wild-type protein, and this replacement is included in all other proteins even though it is not specifically listed in the text.

In general, molecular biology techniques were carried out according to Sambrook and coworkers (1989) or as outlined in **Current Methods in Molecular Biology on CD-ROM** (Ausubel, 1993). All enzymes were obtained from Sigma-Aldrich, Promega, Gibco BRL, New England Biolabs, or Pharmacia Biotech. The entire open reading frame of all new mutants was sequenced with a Sequenase version 2.0 kit (Amersham) and α-[^{35}S]-dATP (Dupont) prior to protein expression to ensure that only the desired mutations were present. The mutagenic and sequencing oligonucleotide primers (Table 2) were complementary to the coding strand and were synthesized with an Applied Biosystems 380A DNA synthesizer by the Nucleic Acid and Protein Synthesis Laboratory of the University of British Columbia.

2.1.1   Cytochrome *c* Expression in Yeast

The mutants Lys79Ala and Phe82Xxx (where Xxx is Gly, Lys, Ser, Asp, His, Met, Trp, and Ile) were constructed in the phagemid pING4 by Dr. Stephen Inglis in the laboratory of Professor Michael Smith (Pielak *et al.*, 1985; Inglis *et al.*, 1991). Site-directed mutagenesis was performed by

```
SmaI                                                    UAS 1
CCCGGGAGCAAGATCAAGATGTTTTCACCGATCTTTCCGGTCTCTTTGGCCGGGGTTTACGGACGATGACCGA
GGGCCCTCGTTCTAGTTCTACAAAAGTGGCTAGAAAGGCCAGAGAAACCGGCCCCAAATGCCTGCTACTGGCT
    -380        *             *           *          *         *        *
                    UAS 2
AGACCAAAGCGCCAGCTCATTTGGCGAGCGTTGGTTGGTGGATCAAGCCCACGCGTAGGCAATCCTCGAGCA
TCTGGTTTCGCGGTCGAGTAAACCGCTCGCAACCAACCACCTAGTTCGGGTGCGCATCCGTTAGGAGCTCGT
    *           *         *         *         *         *          *

GATCCGCCAGGCGTGTATATAGCGTGGATGGCCAGGCAACTTTAGTGCTGACACATACAGGCATATATATAT
CTAGGCGGTCCGCACATATATCGCACCTACCGGTCCGTTGAAATCACGACTGTGTATGTCCGTATATATATA
*            *         *          *        *          *         *        *

GTGTGCGACGACACATGATCATATGGCATGCATGTGCTCTGTATGTATATAAAACTCTTGTTTTCTTCTTTT
CACACGCTGCTGTGTACTAGTATACCGTACGTACACGAGACATACATATATTTTGAGAACAAAAGAAGAAAA
           *         *         *          *          *          *       *

CTCTAAATATTCTTTCCTTATACATTAGGTCCTTTGTAGCATAAATTACTATACTTCTATAGACACGCAAAC
GAGATTTATAAGAAAGGAATATGTAATCCAGGAAACATCGTATTTAATGATATGAAGATATCTGTGCGTTTG
        *          *          *          *          *          *        *

                            -5                                         10
                        M   T   E   F   K   A   G   S   A   K   K   G   A   T   L   F
ACAAATACACACACTAAATTAATAATGACTGAATTCAAGGCCGGTTCTGCTAAGAAAGGTGCTACACTTTTC
TGTTTATGTGTGTGATTTAATTATTACTGACTTAAGTTCCGGCCAAGACGATTCTTTCCACGATGTGAAAAG
        *             *       1       *        20        *        40
                    20                              30
    K   T   R   C   L   Q   C   H   T   V   E   K   G   G   P   H   K   V   G   P   N   L   H   G
AAGACTAGATGTCTACAATGCCACACCGTGGAAAAGGGTGGCCCACATAAGGTTGGTCCAAACTTGCATGGT
TTCTGATCTACAGATGTTACGGTGTGGCACCTTTTCCCACCGGGTGTATTCCAACCAGGTTTGAACGTACCA
*            60        *          80        *          100       *       120
            40                              50
    I   F   G   R   H   S   G   Q   A   E   G   Y   S   Y   T   D   A   N   I   K   K   N   V   L
ATCTTTGGCAGACACTCTGGTCAAGCTGAAGGGTATTCGTACACAGATGCCAATATCAAGAAAAACGTGTTG
TAGAAACCGTCTGTGAGACCAGTTCGACTTCCCATAAGCATGTGTCTACGGTTATAGTTCTTTTTGCACAAC
            *         140       *          160       *          180       *
    60                              70                              80
    W   D   E   N   N   M   S   E   Y   L   T   N   P   K   K   Y   I   P   G   T   K   M   A   F
TGGGACGAAAATAACATGTCAGAGTACTTGACTAACCCAAAGAAATATATTCCTGGTACCAAGATGGCCTTT
ACCCTGCTTTTATTGTACAGTCTCATGAACTGATTGGGTTTCTTTATATAAGGACCATGGTTCTACCGGAAA
            200       *         220       *          240       *        260
                    90                              100
    G   G   L   K   K   E   K   D   R   N   D   L   I   T   Y   L   K   K   A   T   E   O
GGTGGGTTGAAGAAGGAAAAAGACAGAAACGACTTAATTACCTACTTGAAAAAAGCCACTGAGTAAACAGGC
CCACCCAACTTCTTCCTTTTTCTGTCTTTGCTGAATTAATGGATGAACTTTTTTCGGTGACTCATTTGTCCG
            *         280       *          300       *          320       *

CCCTTTTCCTTTGTCGATATCATGTAATTAGTTATGTCACGCTTACATTCACGCCCTCCCCCCACATCCGCT
GGGAAAAGGAAACAGCTATAGTACATTAATCAATACAGTGCGAATGTAAGTGCGGGAGGGGGGTGTAGGCGA
        *          *          *          *          *          *         *

CTAACCGAAAAGGAAGGAGTTAGACAACCTGAAGTCTAGGTCCCTATTTATTTTTTTATAGTTATGTTAGTA
GATTGGCTTTTCCTTCCTCAATCTGTTGGACTTCAGATCCAGGGATAAATAAAAAAATATCAATACAATCAT
*            *          *         *         *          *          *       *

TTAAGAACGTTATTTATATTTCAAATTTTTCTTTTTTTTTCTGTACAGACGCGTGTACGCATGTAACATTATA
AATTCTTGCAATAAATATAAAGTTTAAAAAGAAAAAAAAGACATGTCTGCGCACATGCGTACATTGTAATAT
        *          *          *         *          *          *         *

                                                        HindIII
CTGAAAACCTTGCTTGAGAAGGTTTTGGGACGCTCGAAGGCTTTAATTTGCAAGCTT
GACTTTTGGAACGAACTCTTCCAAAACCCTGCGAGCTTCCGAAATTAAACGTTCGAA
        *          *          *         *          600
```

Figure 10a. DNA sequence of the *Sma*I-*Hind*III fragment of pING4 (Inglis *et al.*, 1992). The *CYC1* gene (1-330) encodes the expression of yeast *iso*-1-cytochrome *c* (one-letter code symbol for amino acids and sequence number in italics; *Sma*I and *Hind*III restriction sites and the upstream activating sequences (UAS) are indicated). This figure is reproduced from Inglis *et al.*, 1992.
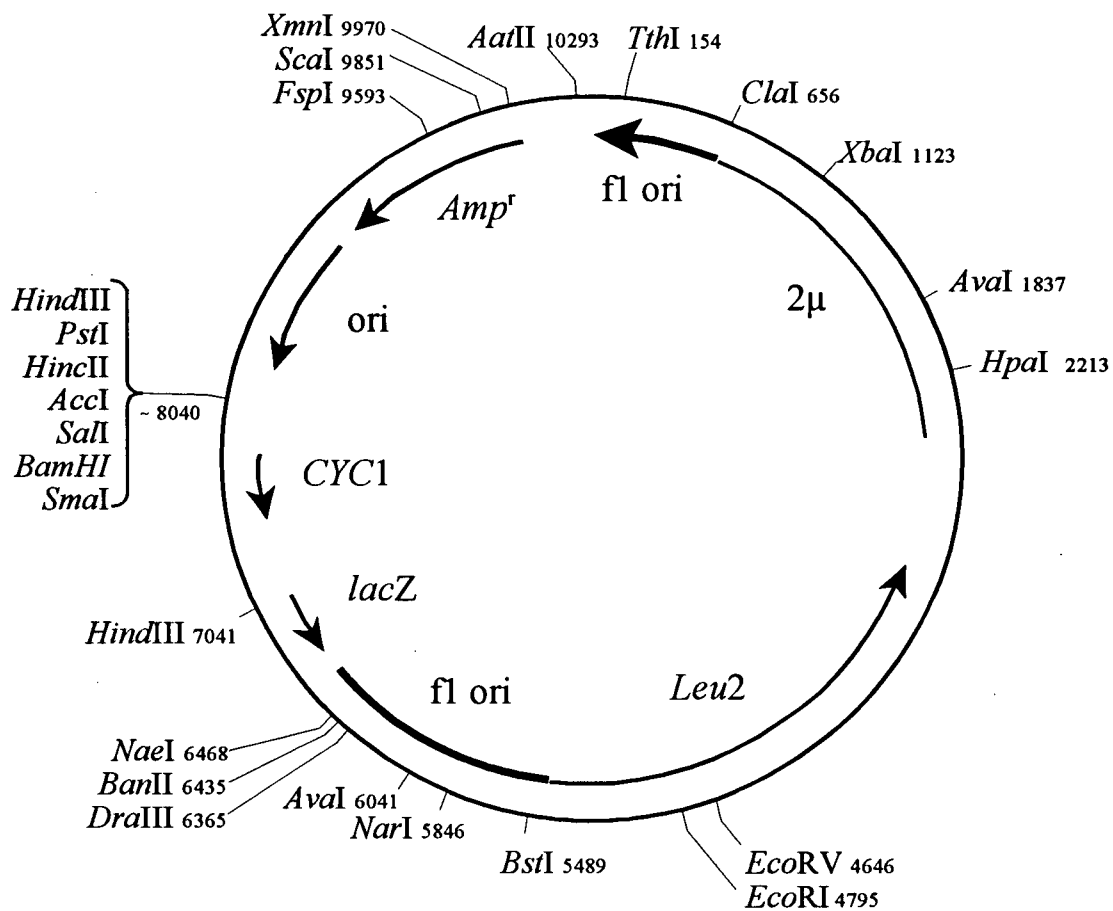
Figure 10b. Functional map of the 10.5 kbp phagemid pING4. Selected restriction sites are shown as are the genes of the β-lactamase (*Amp*^r), yeast *iso*-1-cytochrome *c* (*CYC*1), the yeast (2μ), bacterial (ori), and phage (f1 ori) origins of replication, and the β-isopropylmalate dehydrogenase gene (*Leu*2) (Satyanarayana, 1968; Mortimer, 1980). The size of the genes and the distance between restriction sites are drawn approximately to scale.

the method of Zoller and Smith (1982 a and b, 1984) as adapted by Kunkel and coworkers for high efficiency (1985, 1987). Single-stranded, uracil-containing DNA was obtained using *E. coli* strain RZ1032 (*dut,⁻ ung⁻*) and helper phage R408 (Russel *et al.*, 1986). The mutants Lys73Ala, Lys86Ala, Lys87Ala, and Lys73Ala/Lys79Ala were prepared in the same manner. However, for the latter set of mutants, the protocol of Inglis and coworkers (1991) was modified in that transfection of mutated phagemid into *S. cerevisiæ* strain GM3C-2 was achieved by enzymatic digestion (Glusulase, Dupont) of the cell wall prior to transfection by heat shock (Ausubel, 1993). The phagemid was then rescued from this host and transfected into *E. coli* Sure® cells (Stratagene) by electroporation (25 μF, 2.5 kV, 200 Ω) for sequencing with a Sequenase version 2.0 sequencing kit.

Table 2. Synthetic mutagenic and sequencing (seq) oligonucleotide primers used in the preparation of yeast *iso*-1-cytochrome *c* variants. The underlined bases are those that introduce the mutation.

Primer	Mutation	Nucleotide Sequence
FRA73	Lys73Ala	5'-P-AGG•AAT•ATA•<u>GGC</u>•CTT•TGG•GTT•AGT-3
FRA86	Lys86Ala	5'-P-T•TTC•CTT•C<u>GG</u>•CAA•CCC•ACC•AAA-3'
FRA87	Lys87Ala	5'-P-GTC•TTT•TTC•C<u>GG</u>•CTT•CAA•CCC•ACC-3'
BTR-5A	Ala-5Thr	5'-P-C•CTT•GAA•TTC•AG<u>T</u>•CAT•GGATATATCT-3'
SCI33	Tml72Ala	5'-P-C•AGG•AAT•ATA•TTT•C<u>GC</u>•TGG•GTT•AG-3'
JB1	seq	5'-GGGGAGGGCGTGAATGTAAG-3'
CYC1X	seq	5'-GAATTCGAGCTCGGTACCCG-3'
BTR-SA	seq	5'-AGCTAGCTTACTAAAAAGAT-3'

Expression of variant cytochromes *c* with the *S. cerevisiæ* GM3C-2::pING-4 expression system entailed fermentation of the yeast in 50 L batches as described previously (Cutler *et al.*, 1987), except that the duration of the incubation period after lactate addition was prolonged to a total of 72 h. The YP medium consisted of peptone (2% w/v), yeast extract (1% w/v), glycerol (3 % v/v), and sodium lactate (1 % v/v) pH ~5.5. In addition, the cultures were supplemented with ~40 ml Antifoam

45

C, and one dose of 2 g streptomycin sulphate and 0.5 g tetracycline hydrochloride at the time of inoculation and again at the time of the lactate boost. The resulting yeast were harvested using a CEPA Z41 continuous flow centrifuge (Carl Padberg Zentrifugenbau) operating at room temperature and ~20000 rpm.

2.1.2   Cytochrome *c* Expression in *E. coli*

pBPCYC1/3 (*vide infra*, Figure 13) is a vector that harbours both *CYC*1 and *CYC*3 for the co-expression in *E. coli* of yeast *iso*-1-cytochrome *c* and cytochrome *c* heme-lyase. pBPCYC1/3 and the mutant that encodes the variant Tml72Lys/Met80Ala were constructed by Dr. Brent Pollock, and this work is described in detail elsewhere (Pollock *et al.*, 1998). Briefly, a DNA cassette was constructed which contains the *CYC*1 gene. This cassette is amenable to mutagenesis in M13 phage and can be incorporated into the pUC18-based plasmid pBPCYC1(wt)/3 directly upstream from *CYC*3 by gene exchange using the unique *Sac*I and *Bam*HI restriction sites.

A second vector was constructed for the expression of cytochrome *c* in bacteria to facilitate mutagenesis by a variety of methods and to improve protein yields. This phagemid, pBTR1, was constructed by isolating the 1.6 kbp *Hind* III—*Nco*I, *CYC*1- and *CYC*3-containing fragment from pBPCYC1(T-5A)/3. The fragment was purified by agarose gel electrophoresis and ligated to the 4 kbp *Nco* I—*Hind* III fragment of pGYM (Guillemette *et al.*, 1991). The resulting phagemid was analyzed by restriction mapping with *Cla*I and *Sca*I. pBTR1 was mutated to encode the Lys72Ala variant of cytochrome *c* using the unique site elimination approach of Deng and Nickoloff (1992) whereby the *Nco*I site was eliminated while at the same time the Thr-5Ala mutation was reverted. Because this vector is a phagemid, it is also possible to isolate the single-stranded form for mutagenesis by the method of Zoller and Smith (1982 a and b, 1984).

Expression of recombinant cytochromes *c* in *E. coli* using either pBPCYC1/3 or pBTR was carried out essentially in the same manner as for other heme proteins (Guillemette *et al.*, 1991; Lloyd *et al.*, 1994). Large batch cultures consisted of 8-12 2 L Erlenmeyer flasks containing 1-1.5 L Luria broth (Sambrook *et al.*, 1989) that was supplemented with 100 mg/L ampicillin (di-sodium salt) and 0.1% v/v glycerol. A notable exception was the expression of the Tml72Lys/Met80Ala variant for which 25 mM sodium nitrate was substituted for sodium chloride. The bacteria were harvested 36-48 hours after culture initiation by pooling the contents of every flask in a 50 L fermentor which acted as a reservoir to chill the culture and for centrifugation using the continuous flow centrifuge (*vide supra*).

2.1.3 Purification of Cytochromes *c*

The cytochromes *c* used in this work were isolated in one of three ways depending on the expression host and cytochrome *c* variant. Yeast pellets were treated overnight with ethyl acetate and sodium chloride to extract the cytochrome from the cells (Sherman *et al.*, 1968; Rafferty *et al.*, 1990). Reducing agents such as DTT or mercaptoethanol were excluded from all buffers. For proteins that were unstable in the presence of the organic solvent, the yeast cake was suspended in sodium phosphate buffer [460 mM, pH 7.2, 4 °C] to a concentration of 15-20 % w/v. This suspension was processed twice at 4 °C with a Dyno-Mill Type KDL bead mill (Willy A. Bachofen AG Maschinenfabrik) equipped with a water-jacketed 600 ml steel vessel and 0.5 mm acid-washed, lead-free, glass beads. Cell debris was removed by filtration through a bed of wet, shredded filter paper (Whatman BioSystems Ltd.) followed by centrifugation [Sorvall GS3 rotor, 8000 rpm, 4 °C, 30 min]. The protein in the resulting solutions of ethyl acetate treatment or bead mill grinding was extracted with cellulose CM52 (Whatman BioSystems Ltd.) in batch-wise fashion with approximately 150 ml

wet resin *per* 30 L of diluted protein (resistivity < 7000 $\Omega^{-1}cm^{-1}$). The resin was transferred to a 10 cm diameter sintered glass funnel where it was washed with two column volumes of Buffer A [46 mM sodium phosphate buffer, pH 7.2, 4 °C] before elution [Buffer A plus 1 M sodium chloride]. The resulting eluate was dialyzed against cold, distilled water to a resistivity < 7000 $\mu\Omega^{-1}cm^{-1}$ and the pH was adjusted to < 7 when necessary.

E. coli suspended in a minimum volume of sodium phosphate buffer [460 mM, pH 7.2] supplemented with PMSF [0.1 mM] were treated with lysozyme, frozen in liquid nitrogen and thawed to lyse the cells. DNase I and RNase A [~20 mg and ~5 mg, respectively] were added together with ~2 mL of a 2 M solution of magnesium chloride to break down the DNA and RNA. Cell debris was removed by centrifugation (*vide supra*). Ammonium sulphate was added slowly to the supernatant fluid on ice to a concentration of 320 g/L, and the solution was stirred thoroughly. Debris was removed by centrifugation, and the supernatant fluid was dialyzed as above.

After dialysis the protein solutions were centrifuged, and the protein in the supernatant fluid was oxidized with a small excess of [Co(dipic)$_2$]NH$_4$ (Mauk *et al.*, 1979) prior to further purification by cation exchange chromatography on CM-Sepharose CL-6B (Pharmacia Biotech) equilibrated in Buffer A. The proteins were eluted with a linear salt gradient (0-125 mM sodium chloride) in a total volume of 300-400 ml Buffer A. The final purification step consisted of Fast Protein Liquid Chromatography using a MonoS HR 10/10 column (Pharmacia Biotech) equilibrated with sodium phosphate buffer [20 mM, pH 7.2, 25 °C]. The proteins were again developed with a linear sodium chloride gradient of 1.0 mM/mL typically above 300 mM salt. Fractions with purity index ratios ($A_{409.5}/A_{280}$, pH 7.2) above 4.5 were pooled, concentrated by centrifugal ultrafiltration (Centriprep 10 and Centricon 10 units, Amicon), flash-frozen in liquid nitrogen, and stored at −80°C until needed for experimentation.

Protein concentrations were determined spectrophotometrically at 410 nm assuming that the extinction coefficient of the variants at this wavelength is the same as that of horse heart ferricytochrome c (ϵ_{410} 106.1 mM^{-1}cm^{-1}, pH 7.0) (Margoliash & Frohwirt, 1959). The concentration of the Tml72Lys/ Met80Ala variant of cytochrome c was estimated from the reported ϵ_{406} of 115 mM^{-1}cm^{-1} (Bren, 1996).

2.2   Spectroscopic Techniques

2.2.1 ^{1}H-NMR Spectroscopy

One dimensional ^{1}H-NMR spectra were recorded with a Bruker MSL-200 spectrometer operating in quadrature detection mode at 200 MHz. Some of these spectra were collected in close collaboration with Dr. Juan Ferrer. Also, a Varian Unity spectrometer operating at 500 MHz was used with the assistance of Prof. Lawrence McIntosh, Dr. Greg Connelly, or Dr. Logan Donaldson. Protein samples (2-3 mM, 400 µL) were prepared in deuterated water and either sodium phosphate buffer (50 mM) or a solution of sodium phosphate and sodium borate buffers (25 mM each). The pH was adjusted to the desired value (6-11) by titration with ~1 M deuterated sodium hydroxide or deuterated phosphoric acid, and it was measured with a micro-combination electrode (Aldrich #Z 11,343-3). The pH values are direct meter readings and are, therefore, denoted as pH* (Glasoe & Long, 1960; Kalinichenko, 1976). Spectra were obtained using a superWeft pulse sequence (Inubushi & Becker, 1983) (Figure 11a) with a recycle delay of 220 ms and consisted of at least 2000 transients. The spectral resolution was enhanced by multiplication of the FID with a 90° phase shifted sine curve prior to Fourier transform, and baselines were corrected with an interactive polynomial function. In cases where spectra were integrated to estimate relative concentrations of a particular species within a sample, no window functions were implemented. Curve-fitting was
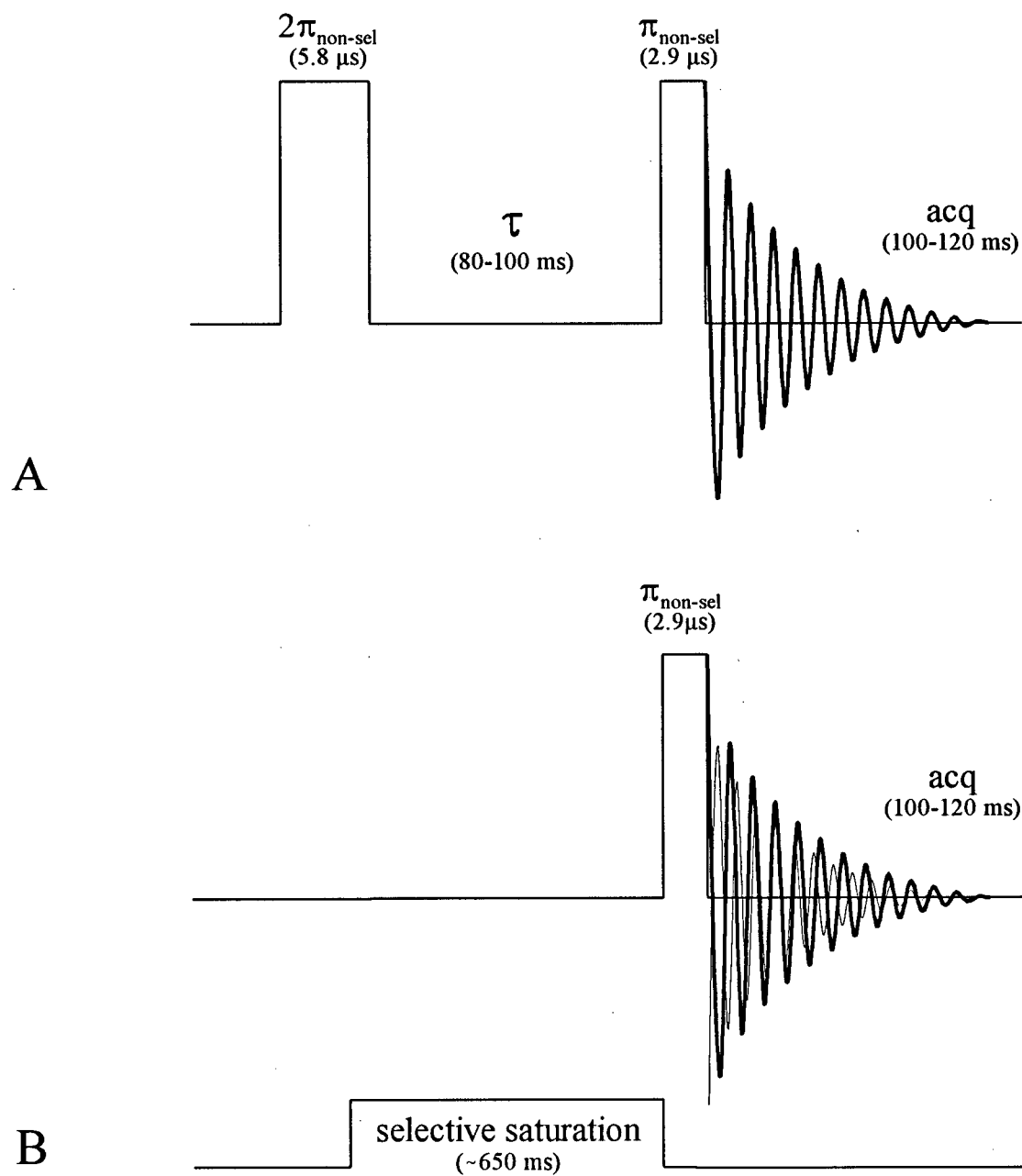
Figure 11. Schematic Diagrams of the superWeft (Inubushi & Becker, 1983) (A) and the inversion transfer pulse sequences used for the investigation of the yeast *iso*-1-ferricytochromes *c* in this work (B). The pulse durations quoted in these diagrams apply to the Bruker MSL 200 spectrometer.

performed using the routine of the program Grams386 (Galactic Software) to determine peak areas. For this procedure the algorithm optimized the proportion of Gaussian and Lorentzian peak character to minimize the χ^2 value for the fit.

To determine the thermodynamic parameters associated with the alkaline transition of each of the Lys→Ala variants, protein samples were prepared (~ 3 mM protein, 50 mM sodium phosphate buffer, pH* ~ 9.3), and the ^{1}H-NMR spectra were measured as a function of temperature. The pH of the samples was assumed to remain the same at all temperatures. The areas of the resonances corresponding to the heme 8-methyl group protons of the cytochrome in the alkaline and native states were calculated, and the ratio was used to estimate the equilibrium constants. These values were plotted as a function of temperature, and the entropic and enthalpic contributions associated with each alkaline isomerization were calculated from the resulting van't Hoff plots.

Magnetization transfer experiments were conducted to identify resonances that correspond to protons undergoing chemical exchange. These experiments were performed at elevated temperatures (~50°C) with selective presaturation (0.65 s) of known peaks applied through the decoupler channel (Figure 11b).

A variety of homonuclear, two-dimensional ^{1}H-NMR spectra of the variant Lys79Ala (50 mM sodium borate buffer, pH 10.4) were recorded by Dr. Paola Turano in the laboratory of Professor Ivano Bertini (Dipt. di Chimica, Universita degli Studi de Firenze, Italy) with a Bruker AMX600 spectrometer. The panel consisted of 2x1 kpoint NOE (100, 30 , and 15 ms mixing time) and TOC (90 and 30 ms spin lock) spectra measured at 295 and 303 K in normal and deuterated water (Banci et al., 1995). Spectral resolution was enhanced by multiplying the raw data in the $F1$ and $F2$ dimensions by a pure cosine squared function prior to Fourier transform and polynomial baseline correction. The resulting 2D maps were analyzed with the program XEASY (ETH, Zurich) (Eccles

et al., 1991).

All chemical shifts are referenced with respect to DSS using the residual water resonance as an internal standard.

2.2.2 EPR Spectroscopy

X-band frequency (~9.5 GHz) EPR spectra were obtained with a Bruker ESP 300E spectrometer equipped with an Oxford Instruments ESR900 continuous flow cryostat, an ITC4 temperature controller, and a Hewlett Packard 5352B microwave frequency counter. Data were typically collected at 10 K with microwave power of 0.63-2 mW and with modulation frequency and amplitude of 100 kHz and 1 mT respectively. Protein samples (1-2 mM, 200 µL) included 25 mM MES and/or 25 mM CAPS buffer, and glycerol (50% v/v) as a glassing agent. The pH was adjusted by titration with 1 M sodium hydroxide (*vide supra*) and all samples were frozen immediately in liquid nitrogen prior to loading in the sample cavity. All spectra were corrected by subtracting the cavity signature measured without a sample tube in place but using the same collection parameters. Some of these spectra were collected with the assistance of Dr. Ralf Bogumil.

2.2.3 Electronic Absorption Spectroscopy

UV/Visible absorption spectra were recorded at 25.0 °C with either a Cary 219 or a Cary 3 spectrophotometer. In general, spectra spanned the region between 700 and 260 nm with a minimum spectral resolution of 0.5 nm. Protein samples were prepared in 1.0 cm pathlength quartz cuvettes such that the absorption values were between 0.1 and 1.5 in the regions of interest.

2.2.4 Circular Dichroism and Magnetic Circular Dichroism Spectroscopies

Circular dichroism (CD) spectra were collected in the region between 190 and 720 nm with a Jasco Model J720 spectropolarimeter equipped with a computer-controlled Neslab RTE-111 water bath. Sample concentrations (~10 μM) and path length (0.1 or 1 cm) were selected to maximize the CD signal and to minimize the photomultiplier gain. Molar ellipticities $[\theta]_\lambda$ were determined according to Equation 6 (Bychkova, 1996) where θ_λ (mdeg) is the measured ellipticity, MRW is the mean residue molecular weight calculated from the protein sequence, and l (mm) and c (mg/ml) are the path length and protein concentration respectively.

$$[\theta]_\lambda = \frac{\theta_\lambda \cdot MRW}{l \cdot c} \qquad (6)$$

Magnetic circular dichroism (MCD) spectra were collected in the near infra-red region (800-2000 nm) with a Jasco Model J730 spectropolarimeter equipped with an InfraRed Associates Mercury-Cadmium-Telluride solid state detector Model IS7 that was cooled with liquid nitrogen. The magnet was an Oxford Instruments SM4 superconducting magnet capable of exerting a field of 5 T. Samples were thermostatted at 298 K with an Oxford Instruments ITC4 temperature controller. Protein samples (1.5-3 mM) were prepared in deuterated buffer as for ^{1}H-NMR and included glycerol 50 % v/v. A spectral band width of 10 nm was used together with a 1 nm data point interval, and spectra were collected at a rate of 100 nm/min between 1900 and 800 nm. All spectra are the average of at least three measurements and are corrected for the background CD signal prior to smoothing using the algorithm available in the Jasco software. The spectra are normalized with respect to protein concentration, magnetic field and path length to yield units of $M^{-1}T^{-1}cm^{-1}$. These spectra were collected with the help of Dr. Dean Hildebrand.

2.3 Physicochemical Properties of Cytochrome *c*

2.3.1 Electrochemistry

Cyclic voltammograms were obtained with a two compartment glass cell (Figure 12) that was thermostated at 25.0 °C. In all cases the reference and counter electrodes were saturated calomel (Radiometer, K401) and platinum mesh respectively. The calomel electrode was standardized relative to quinhydrone ($E^{\circ\,\prime}= 0.699$ mV *vs.* SHE; Hill, 1956; Landrum *et al.*, 1977), and potentials are referred to the SHE. Depending on the experiment, the working electrode was either a modified gold surface or edge-oriented pyrolytic graphite. The gold electrode was polished on Mastertex polishing cloth (Buehler) with slurries of increasingly finer grades of alumina to 0.05 microns. The excess alumina was removed by sonication in distilled water and thorough rinsing. The newly exposed gold surface was then electrochemically cleansed (deoxygenated 100 mM sodium perchlorate, 20 mM sodium phosphate buffer, pH 7.0) by repeated cycling between -1200 and 900 mV *vs.* SCE at a rate of 50 mV/sec. The surface was subsequently modified by dipping the electrode for 5 min in a saturated solution of 4,4'-dithiodipyridine [a few crystals in a 1 mL volume] (Eddows & Hill, 1977; Taniguchi *et al.*, 1984, 1985; Elliot *et al.*, 1986). The edge-oriented graphite electrode was polished with 0.3 micron alumina, sonicated and rinsed prior to each measurement without electrochemical cleansing or further surface modification (Panzer, 1975; Armstrong *et al.*, 1989).

The oxygen content in sample solutions (~0.3 mM protein, 0.5 ml) was reduced as much as possible by flushing the samples thoroughly with O_2-depleted N_2 or Ar. Because these gases were not "prepurified" grade, O_2 contamination was reduced by passing the N_2 or Ar gas through a 4×50 cm column packed with Catalyst R3-11 pellets (Chemalog) that had been thermally activated with a stream of H_2 gas. After passage through this catalyst the gases were bubbled through a thermostated solution of 0.5 M sodium phosphate buffer, pH 7.0 to neutralize and humidify the gas.
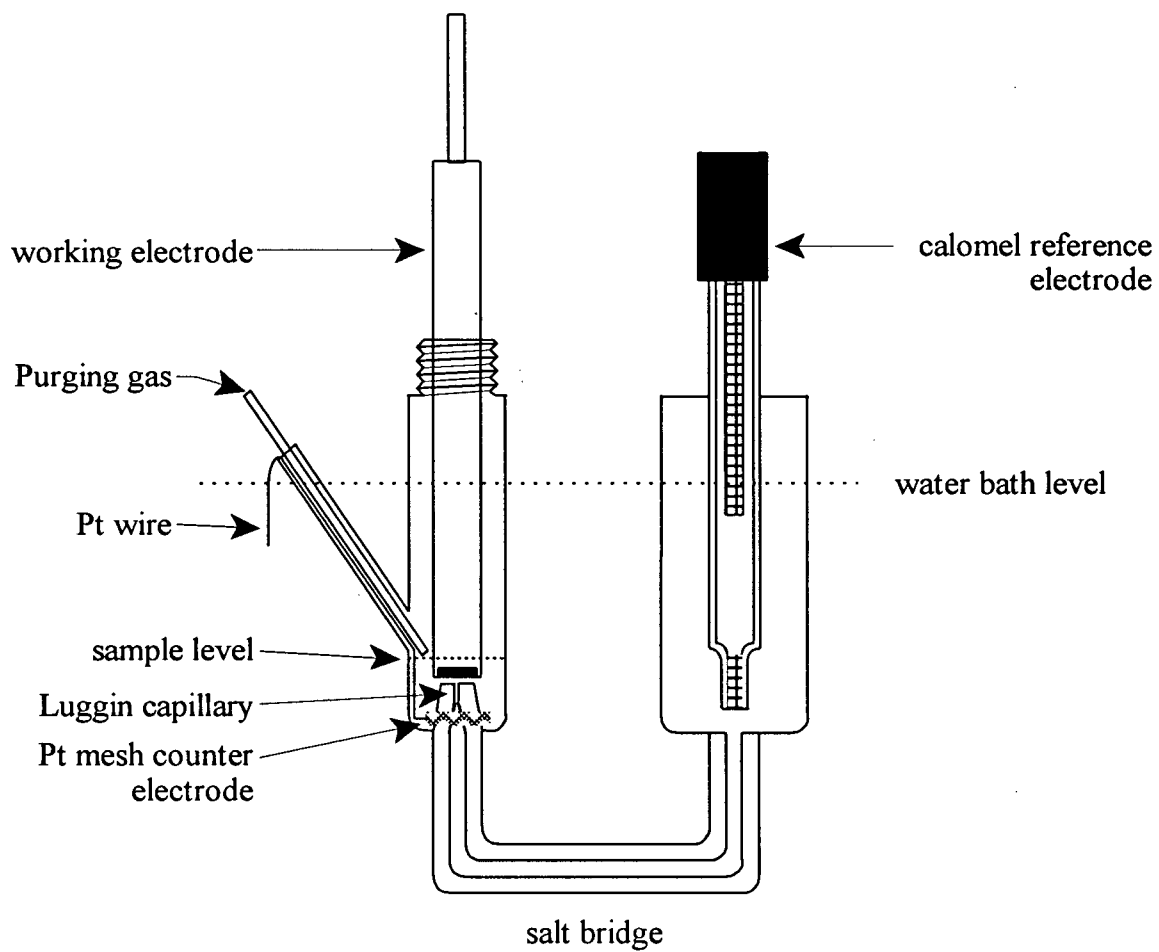
Figure 12. Schematic Diagram of the two compartment electrochemistry cell used for cyclic voltammetry experiments.

Potentials and sweep rates were controlled with an Ursar Electronics potentistat (Oxford, UK). Voltammograms were recorded directly with a Kipp and Zonen BD 90 X-Y flat bed recorder or with a Hitachi Model VC6050 digital storage oscilloscope. For later experiments, a microcomputer equipped with a National Instruments Model AT-MIO-16x analog-to-digital converter board was used to capture the output from the potentiostat.

For the analysis of the pH-dependence of the midpoint potentials of wild-type cytochrome c and its Lys73Ala and Lys79Ala variants the proteins were exchanged into 0.1 M sodium chloride. Protein solutions [~ 0.3 mM, 3 mL] were prepared, and the pH was adjusted to 5.0. Samples from this stock (~0.5 mL) were withdrawn for each measurement and pooled back with the remaining solution to adjust the pH to the next value. The voltammograms were collected on the second cycle at a sweep rate of 2 V/s as described by Barker and Mauk (1992).

2.3.2 Protein Stability

The thermal stability of the cytochromes was assessed under native and alkaline conditions by thermal titrations (Lloyd *et al.*, 1994; Hildebrand *et al.*, 1995). These measurements were carried out with the Jasco720 spectropolarimeter by monitoring the change in ellipticity at 222 nm as a function of temperature. The protein samples [~10 μM protein, ionic strength μ=5 mM, sodium phosphate buffer, pH 6.1 or μ=5 mM, sodium borate buffer, pH 9.3] in a cylindrical quartz cuvette (0.1 cm path length) were heated at a rate of 50 °C/hr from 25 to 70 °C. At least three measurements were averaged and smoothed with the Jasco software utility and the first derivative of the resulting trace was calculated to determine the inflection or midpoint (T_m) of the melting curves. The reversibility of this process was estimated by inverting the temperature gradient soon after the protein was unfolded and is expressed in terms of the percentage of ellipticity that was regained.

2.4 Alkaline Isomerization

2.4.1 pH Titrations

In general, the pK_{ap} value quoted for the alkaline transition of each cytochrome c is the value calculated from spectrophotometric titration of the 695 nm band. The standard conditions for these determinations were $\mu=0.1$ M sodium chloride, 25.0 °C.

Each variant was exchanged into 0.1 M sodium chloride through repeated ultrafiltration, and the resulting solution (~2.5 mL, 5-20 µM) was placed in a 3 mL cuvette equipped with a magnetic stirrer. The pH was measured with a Radiometer Model 84 pH meter fitted with a Radiometer combination electrode Model 2321C or pHC4406. The pH was adjusted to ~5.5 by addition of 0.1 M hydrochloric acid, and the spectrum was measured in the appropriate wavelength range after each micro-addition of 0.1 M sodium hydroxide. The resulting single-wavelength profiles were fitted to Equation 7:

$$Z_\lambda = \frac{B + A \cdot 10^{(pK_{ap}-pH)}}{1 + 10^{(pK_{ap}-pH)}} \qquad (7)$$

where Z_λ is the absorbance at a particular wavelength and B and A are the final and initial Z values, respectively. Note that this equation applies to the simple deprotonation of a titratable group. Under equilibrium conditions, however, Equation 7 also holds for the determination of the apparent pK for the more complicated pH-linked conformational reorganization of ferricytochrome c (see Appendix 1). In some instances, the resulting spectra from a pH titration of ferricytochromes c were also subjected to singular value decomposition analysis with the program Specfit (Spectrum Software Associates). These data were fitted to the model for a single deprotonation process and is applicable with the same assumptions as above.

The effect of ionic strength on the pK_{ap} of the alkaline transition of the wild-type, Lys73Ala,

and Lys79Ala proteins was investigated. Potassium chloride was selected to minimize any sodium-induced electrode artifact at higher pH. The resulting pK_{ap} values were analyzed with the Gouy-Chapman formalism (Koutalos *et al.*, 1990; see Appendix 2) (Equation 8):

$$Sinh[0.5 \cdot ln10 \cdot (pK_{true} - pK_{apparent})] = A \cdot \sigma \cdot \sqrt{C} \qquad (8)$$

In this relationship, $A = 8\epsilon\epsilon_0 N_A kT^{1/2} = 76.3 \text{ M}^{1/2}$ at 25.0 °C assuming that ϵ, the dielectric constant for yeast cytochrome c (25.0 °C) is 25 ± 10 (Simonson & Perahia, 1995), σ is the average surface charge density in the region of the titrating group which has an intrinsic $pK_a = pK_{true}$.

The influence of ionic strength on the distribution of native and alkaline conformers of wild-type cytochrome c was investigated by ^{1}H-NMR spectroscopy. The protein was exchanged into unbuffered, deuterated water, and the solution was divided into two equal portions (~300 μL each); the first was diluted with 0.5 ml D_2O (A) and the second with 0.5 ml 2.0 M potassium chloride in the same solvent (B). The pH of both solutions was adjusted to 10.0, and D_2O was added to A and B to a total volume of 1.0 mL. The ^{1}H-NMR spectrum of A was measured as described above and again after each successive additions of B to vary the concentration of potassium chloride from 0-0.5 M. The spectrum of B was measured in a similar fashion after mixing with increasing volumes of A. Attention was focused on the hyperfine-shifted region of the spectra between 10 and 25 ppm which is diagnostic of the state III ⇌ state IV equilibrium (Hong & Dixon, 1989; Ferrer *et al.*, 1992; Pollock *et al.*, 1998; Rosell *et al.*, 1998). To quantify the relative populations of the native and the two alkaline conformers, the resonances corresponding to the heme 8-methyl group protons were integrated as described in the ^{1}H-NMR section above.

2.4.2 Exogenous Ligand Replacement

Spectrophotometric titrations of the Lys73Ala/Lys79Ala variant of cytochrome c were carried out with methylamine hydrochloride (Sigma) that had been dried over phosphorus pentoxide. Two solutions were prepared which contained the same concentration of protein [~10 μM each] and buffer [238 mM sodium borate buffer, pH 9]. Whereas concentrated sodium chloride was added to solution A to a final ionic strength of 400 mM, concentrated methylamine hydrochloride was added to solution B [μ=400 mM]. Solutions A and B were mixed in varying proportions, and the A_{695} was monitored. The solution was allowed to reach an equilibrium (~5 min) prior to measuring the electronic absorption spectra between 720 and 260 nm. The resulting data were analyzed according to Connors (1987) to determine the apparent dissociation constant (K_d) for methylamine binding (Equation 9).

$$\text{Abs} = \frac{\text{Abs}_\infty \cdot [\text{NH}_3\text{CH}_3] + \text{Abs}_0 \cdot K_d}{[\text{NH}_3\text{CH}_3] + K_d} \qquad (9)$$

The EPR and ^{1}H-NMR spectra of the methylamine adduct of the Lys73Ala/Lys79Ala variant were measured at pH 9 to confirm that the protein binds methylamine. The ^{1}H-NMR spectrum of the methylamine adduct of the Met80Ala variant of cytochrome c and horse heart myoglobin were also recorded for comparison.

2.4.3 pH-Jump Kinetics

Unbuffered solutions of the wild-type, Lys73Ala, and Lys79Ala proteins [~9 μM] were prepared in 0.1 M sodium chloride and adjusted to pH 6.0. 40 mM buffer solutions [40 mM] of MES (pH 6.07), sodium phosphate (pH 7.07, 7.50, and 7.57), TAPS (pH 8.09, 8.19, 8.43, 8.76, and 8.94), CHES (pH 9.05, 9.54, and 9.80), sodium borate (pH 9.01, 9.28, 9.50, 9.70, and 9.89), and CAPS

(pH 10.17) were prepared with enough sodium chloride to a final ionic strength of 0.1 M. The pH-jump rapid mixing experiments were performed at 25.0 ± 0.2 °C with a Dionex Model S-100 stopped-flow spectrometer interfaced to a microcomputer. Absorbance changes were monitored at 390 nm which is reported to reflect the same event as that observed at 695 nm (Kihara *et al.*, 1976).

Kinetic data were fitted to a first-order exponential function, and the resulting rate constants (k_{obs}) were fitted to the minimal model of Davis *et al.* (1974) (Equation 10):

$$k_{obs} = k_b + \frac{k_f \cdot K_H}{K_H + [H^+]} \qquad (10)$$

where k_f and k_b are the forward and reverse rate constants respectively, K_H is the dissociation constant of the titrating group, and [H$^+$] is the proton concentration calculated from the pH of the buffer. In the kinetic analyses, the rate and dissociation constants were constrained to agree with the equilibrium pK_{ap} of the alkaline transition determined independently by titration of the 695 nm band. This constraint obeys the relation:

$$pK_{ap} = -\log_{10}(\frac{k_f \cdot K_H}{k_b}) = pK_C + pK_H \qquad (11)$$

where $K_C = k_f / k_b$.

The pH-jump kinetics of selected yeast *iso*-1-cytochrome *c* variants were also measured above pH 10 at 25.0 °C with an Olis RSM1000 rapid scanning stopped-flow spectrophotometer (On-Line Instrument Systems Inc.) which was equipped with a 2 cm pathlength cuvette. Spectra were collected between 400 and 630 nm with a period of 1 msec and a resolution of 0.7 nm. The results were fitted to two sequential monoexponential processes with the global fitting routine (Matheson, 1989) provided by Olis.

2.5   Numerical Analysis of Data

Quantitative experimental results were generally analyzed by fitting the data to the appropriate model(s) with the program Scientist version 2.0 (Micromath Scientific Software Inc.). This program uses a least-squares minimization procedure based on a modification of Powell's algorithm (1970). The statistical criteria used to accept the results from individual fitting analyses included a correlation coefficient > 0.99 and low standard deviations relative to the absolute value of each parameter, typically less than 10%. These standard deviations are indicated in parenthesis.

3 Results

3.1 Production of Yeast *iso*-1-Cytochrome *c* Variants

3.1.1 Construction of pBTR1

Ligation of the *Nco*I-*Hind*III fragments originating from pGYM and pBPCYC1(T-5A)/3 ΔN yielded the 5.6 kbp phagemid pBTR1. Digestion of this phasmid with *Cla*I results in two fragments of approximately 1.2 and 4.4 kbp. Digestion with *Sca*I, on the other hand, yields two fragments of 2 and 3.5 kbp. Both results are consistent with the expected map of pBTR1 as shown in Figure 13. In this phagemid, the f 1 origin of replication is oriented such that the coding strand of the *CYC*1 and *CYC*3 genes is packaged in the helper phage R408. Single-stranded DNA prepared using this helper phage was sequenced with primers that are complementary to the coding strand of *CYC*1. The 5' fusion region of pBTR1 was unaffected by the ligation of the fragments. More importantly, the *CYC*1 gene remains in frame for the correct transcription of cytochrome *c* using the *lacZ* promoter and the ribosome binding site that are exploited for myoglobin expression with pGYM (Guillemette *et al.*, 1991).

3.1.2 Expression and Purification of Cytochromes *c*

The source of the media used in yeast fermentation influences considerably the final yield of cytochrome *c*. Typically, yields of protein and semi-dry cell paste (3-4 mg/l and 20-30 g/l, respectively) are highest when the peptone and yeast extract are from either Merck or Difco. When Sigma yeast extract is used, the protein yield decreases by as much as 90 % even though the cell mass obtained is comparable to cultures which contained Merck or Difco yeast extract. This outcome varies with the lot of the yeast extract, and may result from contamination by glucose which is known to inhibit cytochrome *c* expression in *Saccharomyces cerevisiae* (Zitomer *et al.*, 1979; Laz, *et al.*,
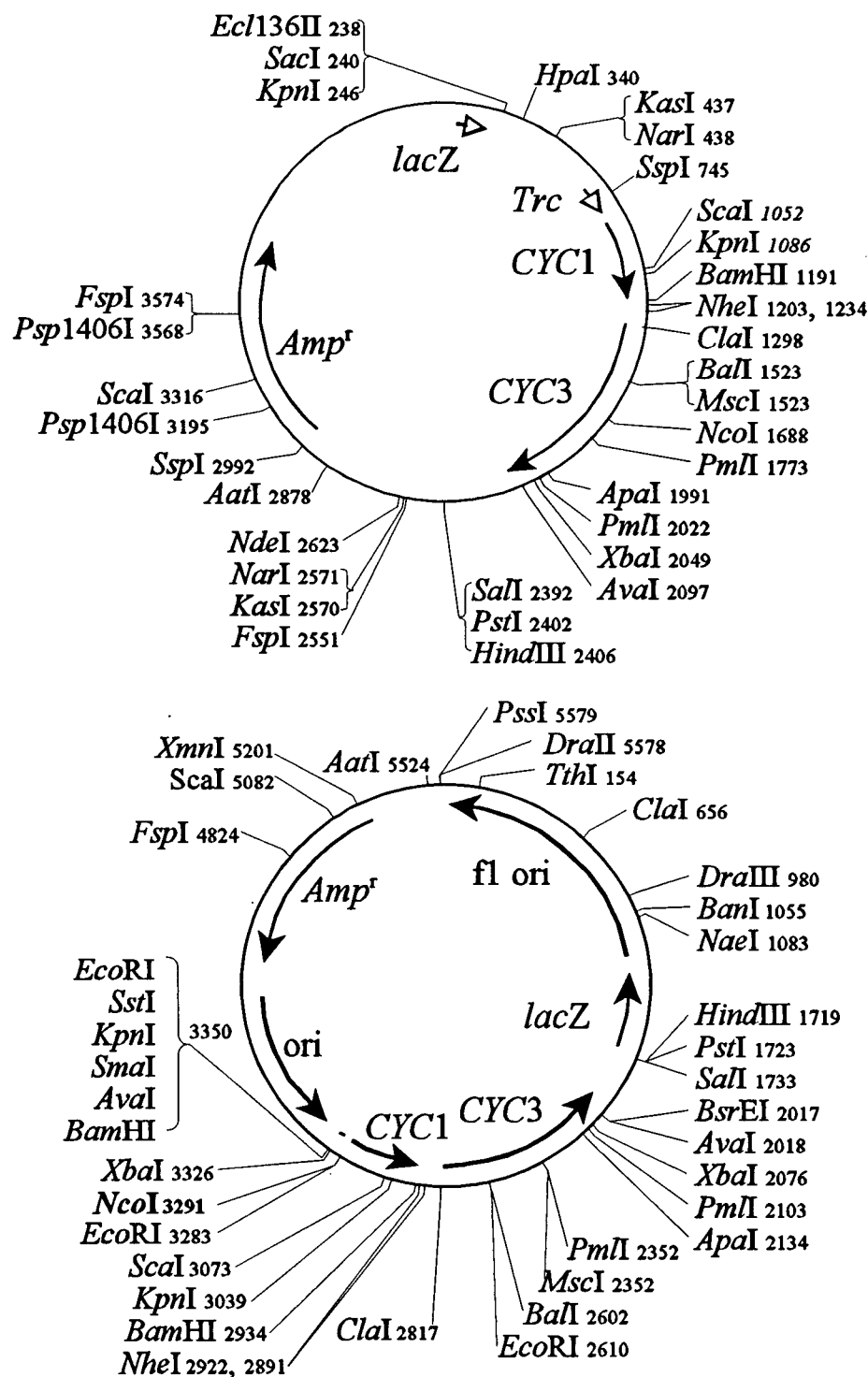
Figure 13. Functional map of (A) the 4.8 kbp plasmid pBPCYC1(wt)/3 and (B) the 5.6 kbp phagemid pBTR1. Selected restriction sites are shown as are the genes that encode β-lactamase (*Amp*ʳ), yeast *iso*-1-cytochrome *c* (*CYC1*), cytochrome *c* heme lyase (*CYC3*), *lacZ* and *Trc* promotors, and the origins of replication of bacteria (ori) and the phage (f1 ori). Vector distances are drawn approximately to scale. The *Nco*I site in pBTR1 is shown in bold to emphasize its use for mutagenesis by the protocol of unique site elimination (Deng & Nickoloff, 1990).

1984; Preznat *et al.*, 1987; Amegadzie *et al.*, 1990; Trumbly, 1992). Furthermore, visual estimation of the cell pellet colour suggested that the optimal culture schedule for cytochrome *c* production requires the lactate boost 48 h after inoculation and 72 h before harvesting as opposed to 72 and 48 hours respectively (Cutler *et al.*, 1987).

Fermentation of *E. coli* strain JM101 containing the phagemid pBTR results in the expression of ~15 mg of purified cytochrome *c per* litre of medium scale culture as defined by Pollock *et al.* (1998). These authors report a yield of approximately 7 mg/L of culture when bacteria containing the plasmid pBPCYC1(wt)/3 are also cultivated in 2L flasks.

Cytochrome *c* purification is achieved primarily through cation exchange chromatography. At the last chromatographic step the protein samples typically resolve into three bands. The bulk of the protein (> 90 %) elutes after a small fraction that is believed to be deamidated cytochrome *c* (Brautigan *et al*, 1978). Some protein batches also contain a third minor component which elutes after the main fraction and is a form of cytochrome *c* in which the *N*-terminal threonyl residue has been cleaved (Marcia Mauk, unpublished results). Neither the deamidated nor the cleaved protein were used in the present experiments.

3.2   Native Cytochromes *c*

Of the five Lys→Ala variants of cytochrome *c* included in this study (Lys73Ala, Lys79Ala, Lys73Ala/Lys79Ala, Lys86Ala and Lys87Ala), those modified at position 79 are the most susceptible to structural changes that could influence the alkaline transition characteristics of the protein. Replacement of Lys79 disrupts a limited hydrogen bond network involving the ϵ-amino group of Lys79, the carbonyl group of Ser47, and the ζ-hydroxyl group of Tyr46 (Figure 14). The Lys79-Ser47 hydrogen bond has been purported to play an important role in stabilizing the closed
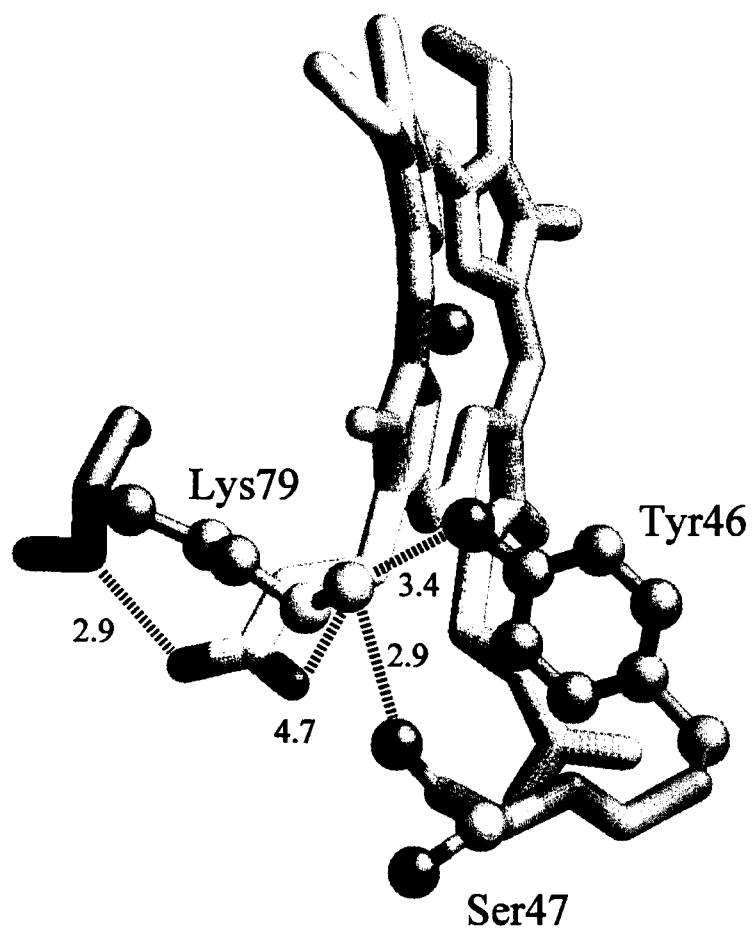
Figure 14. Structure of yeast *iso*-1-ferricytochrome *c* in the vicinity of Lys79. Potential hydrogen-bonding interactions of Lys79 with Tyr46, Ser47, and the heme 6-propionate group are shown, and the interatomic distances (Å) are noted.

conformation of the cytochrome (Osheroff *et al.*, 1980). The disruption of this so-called locking mechanism could weaken local structural elements to increase the mobility of the two halves of the protein. Nevertheless, spectroscopic and physicochemical scrutiny of the variants indicate that under native conditions (pH~6-7.0, 25 °C) the Lys→Ala replacements do not affect significantly the protein structure or its physical characteristics.

3.2.1 Spectrophotometry

Under native conditions (5 mM each, MES and CAPS buffers, pH 6, 25 °C), the electronic absorption spectra of the five Lys→Ala variants of ferricytochrome *c* are similar to that of the wild-type protein (Figure 15). Table 3 summarizes the relative intensities of the absorption maxima with respect to the Soret band (γ). Whereas the Soret band of all the proteins is centered at approximately 409 nm, the two cytochromes bearing the Lys79Ala replacement display a small blue shift (~1 nm) in the α/β band. The weak charge transfer band near 695 nm is present in the spectra of the five variants, indicating that the Met80-Fe^{3+} ligation is conserved. A higher γ:695 ratio suggests that the amino acid replacement at positions 73 and 79 may have weakened the bond. However, the γ:695 ratio and the position of the α/β band maxima are identical for all the spectra when measured in 20 mM sodium phosphate buffer, pH 7.2 (μ~50 mM).

Table 3. Ratios of electronic absorption maxima intensities of yeast *iso*-1-ferricytochromes *c* measured in 5 mM each, MES and CAPS buffers, pH 6.1, 25 °C.

Ratio	Wild-type	Lys73Ala	Lys79Ala	Lys73Ala/ Lys79Ala	Lys86Ala	Lys87Ala
γ : 695	119	131	130	136	125	127
γ : α/β	9.6	9.6	9.8	9.8	9.5	9.6
γ : 360	3.7	3.7	3.7	3.7	3.7	3.6
γ : 280	4.5	4.5	4.4	4.6	4.5	4.5
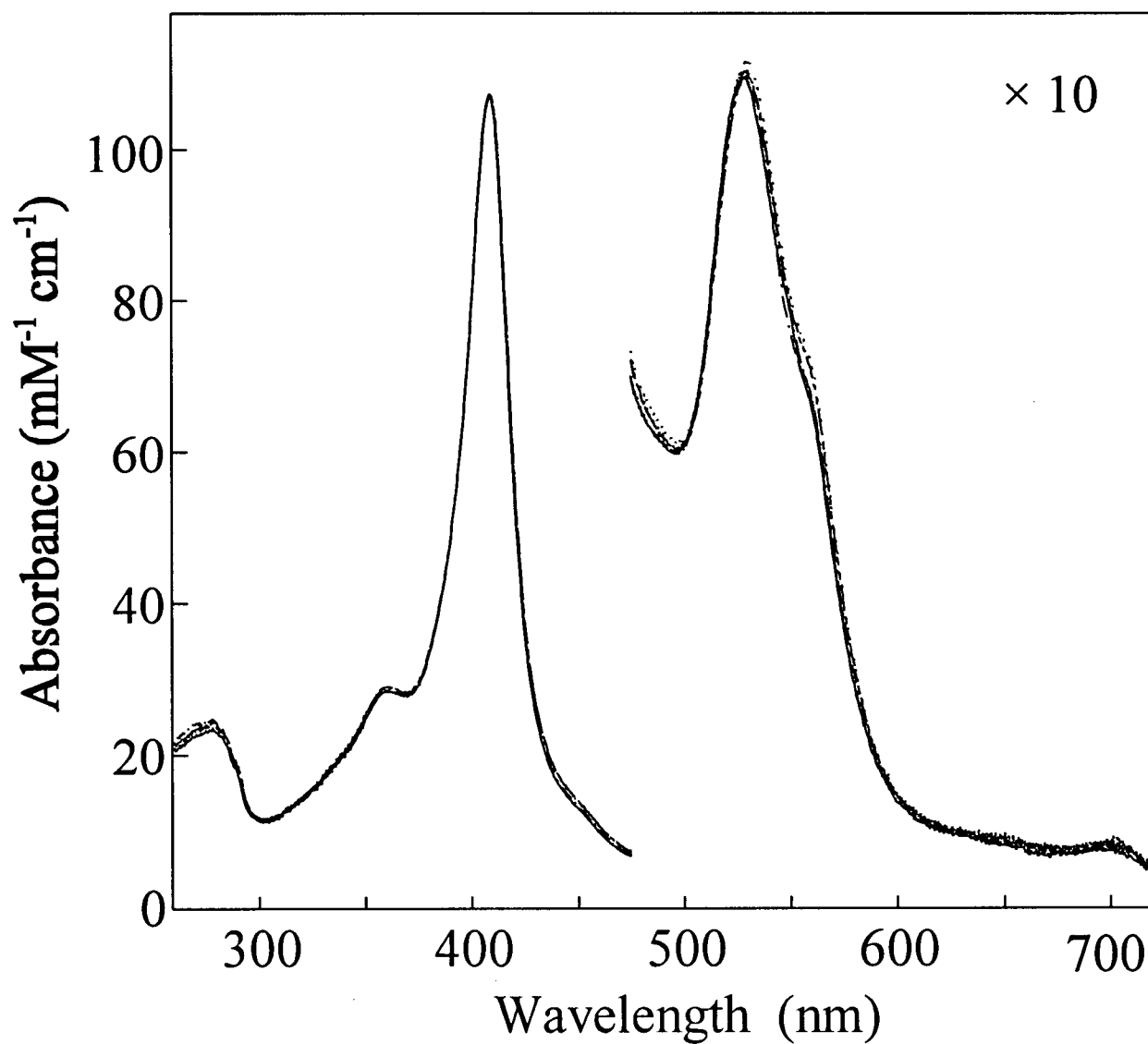
Figure 15. Electronic absorption spectra of yeast *iso*-1-ferricytochome *c*: wild-type (———), and the variants Lys73Ala (··········), Lys79Ala (– – – –), Lys73Ala/Lys79Ala (· – · – ·), Lys86Ala (··– –··), and Lys87Ala (···· ····) (12-16 μM protein in 5 mM each MES and CAPS buffers, pH 6.1, 25 °C, pathlength 1.0 cm).

3.2.2 Natural and Magnetic Circular Dichroism Spectroscopy

In the far-UV region, circular dichroism spectroscopy results indicate that the secondary structures of the Lys→Ala variants are similar to that of the wild-type protein (Figure 16, A). The minima at ~222 and 208 nm are diagnostic of alpha helical content (40-42 % for equine cytochrome c, Dong et al., 1992), and the molar ellipticities ([Θ]) of the variants at these wavelengths (~-10° ·cm²/dmol) are in close agreement with the values reported for other cytochromes c (Looze et al., 1976; Myer, 1985; Betz & Pielak, 1992). At longer wavelengths, only minor differences in the magnitude of the negative Cotton effects at 282 and 289 nm are encountered. These bands are associated with the single Trp residue at position 59 in yeast iso-1-cytochrome c (Davis et al., 1993). Because the intensities of these bands are associated with the mobility of the Trp side chain in particular (Bychkova et al., 1996), the small differences observed suggest that the protein environment in the vicinity of this tryptophanyl residue is not affected significantly by the mutations.

The positive and negative Cotton effects at 404 and 417 nm, respectively, are characteristic of an intact Met80-Fe^{3+} bond in cytochrome c (Looze et al., 1978; Santucci & Ascoli, 1997). Disruption of the metal-sulphur interaction causes these features to degrade into a single positive Cotton effect around 408 nm. The Soret region in the CD spectra of the Lys→Ala variants changes little relative to the spectrum of the wild-type protein (Figure 16, B), suggesting that the higher γ:695 ratios observed by electronic absorption spectrophotometry do not reflect a significant structural change.

The room-temperature, near-infrared MCD spectra of the Lys73Ala, Lys79Ala, and Lys73Ala/Lys79Ala variants of cytochrome c (Figure 17) provide further evidence that the Met80-Fe^{3+} ligation is maintained by these proteins at pH* 6.0. The variants display maxima at 1752 (Lys73Ala), 1761 (Lys79Ala), and 1762 nm (Lys73Ala/Lys79Ala) in good agreement with
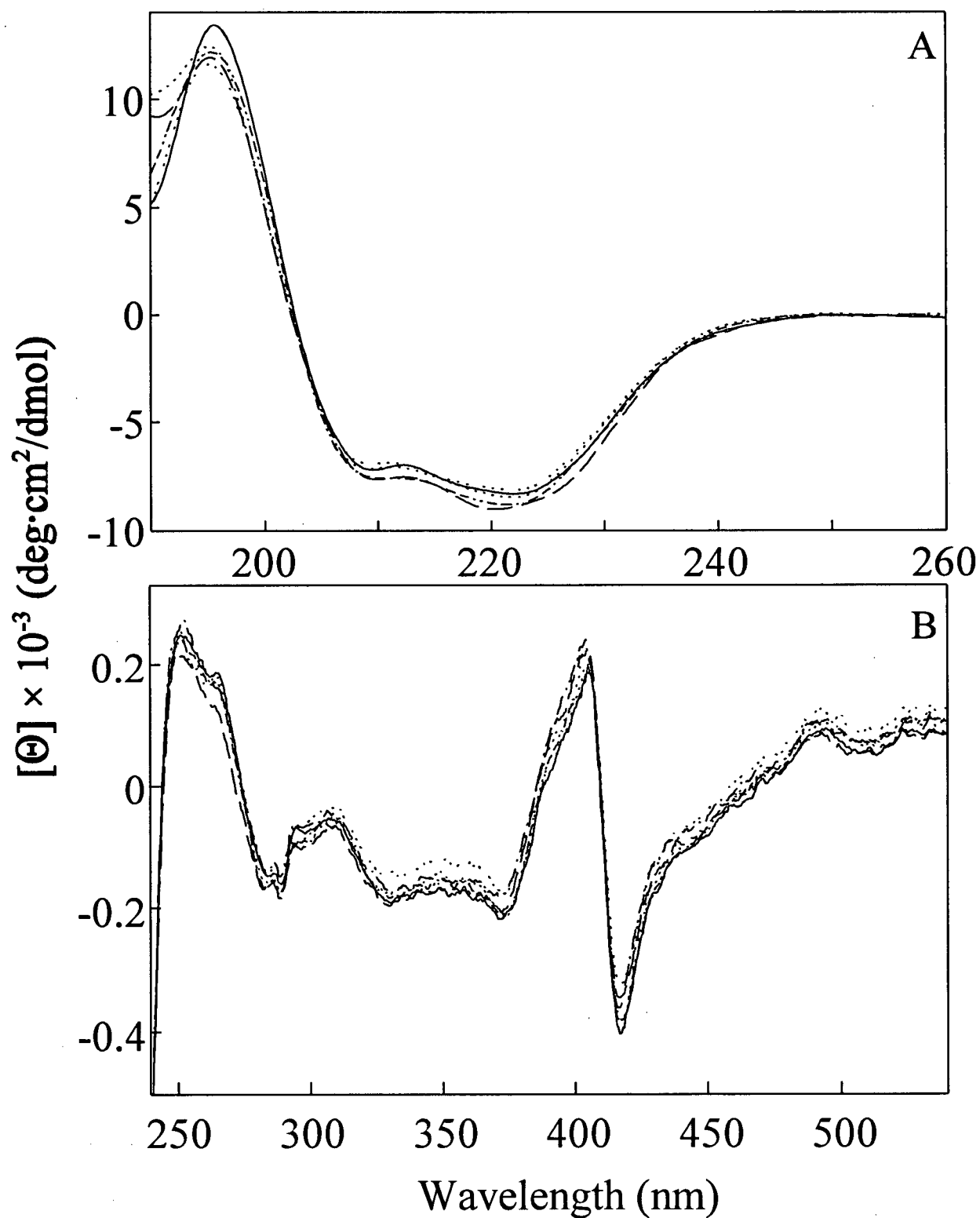
Figure 16. (A) Far-UV and (B) near-UV/visible circular dichroism spectra of yeast *iso*-1-ferri-cytochomes *c*: wild-type (————), and the variants Lys73Ala (·········), Lys79Ala (– – – –), Lys73Ala/Lys79Ala (·–·–·), Lys86Ala (··–––··), and Lys87Ala (··· ··· ···) (12-16 μM protein, in 5 mM each, MES and CAPS buffers, pH 6.1, 25 °C, measured with (A) 0.1 cm and (B) 1.0 cm pathlengths).
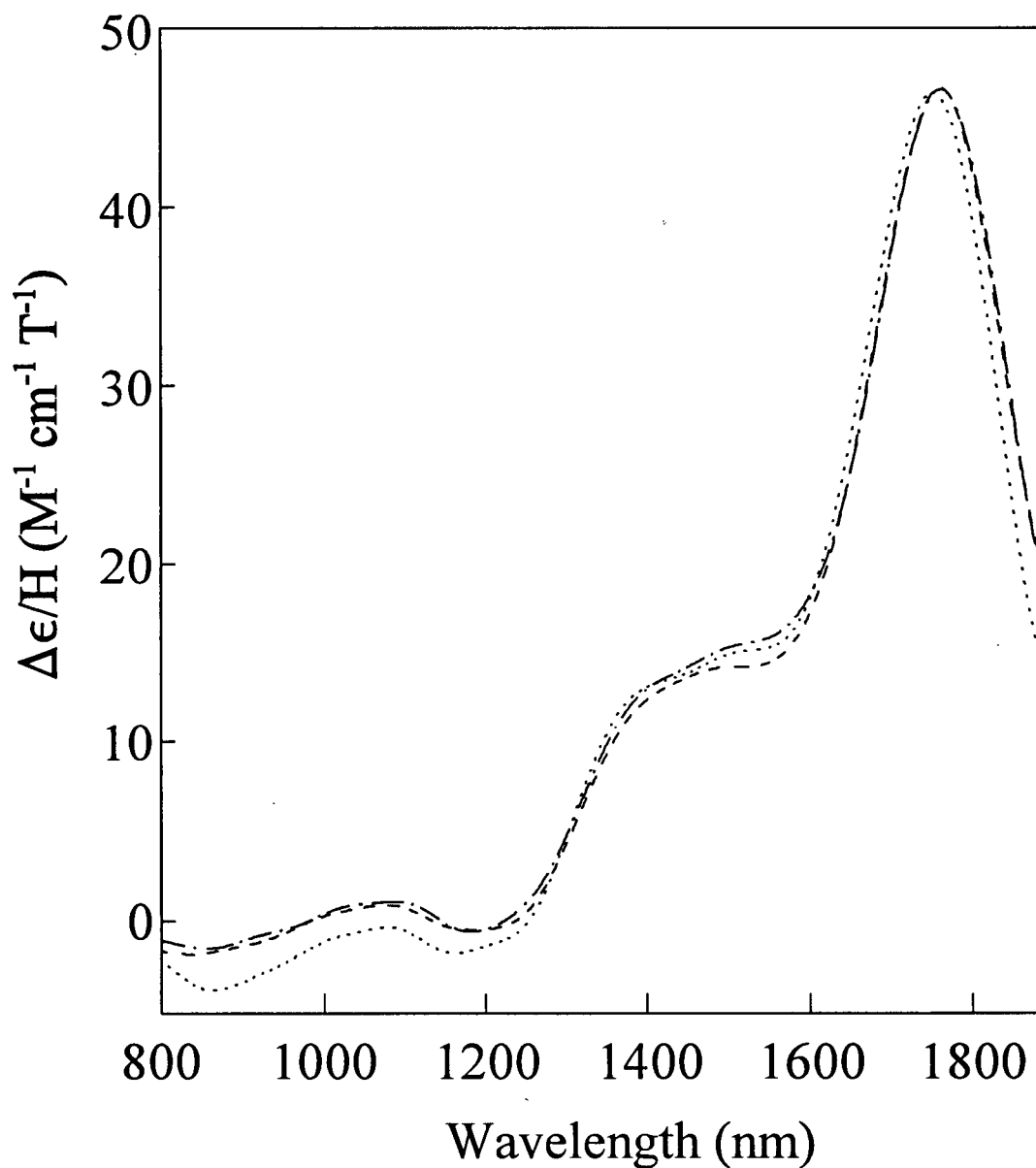
Figure 17. Near-IR MCD spectra of yeast *iso*-1-ferricytochromes *c*: variants Lys73Ala (········, λ_{max}=1752 nm), Lys79Ala (-----, λ_{max}=1761 nm), and Lys73Ala/Lys79Ala (-·-·-, λ_{max}= 1762 nm) (1.5-3 mM protein, 25 mM each, sodium phosphate and CAPS buffers, pH* 6.0, 50% v/v glycerol, 0.1 cm pathlength, 4.83 T, 25 °C).

previously published values for wild-type yeast cytochrome c measured under similar conditions (1756 nm; Simpkin *et al.*, 1989; 1750, Hawkins *et al.*, 1994). A maximum between 1740 and 1950 nm arises from a charge transfer from a porphyrin a_{1u} (π) orbital to the heme iron d_{yz} orbital in oxidized, low-spin heme proteins with His-Met ligation (Gadsby & Thomson, 1990; Cheesman *et al.*, 1991). Neither the relative intensities of the transitions, nor the small differences in the maximum wavelength are suggestive of significant structural perturbations.

3.2.3   EPR Spectroscopy

At pH 6.0-6.6 (50 mM MES, 50 % v/v glycerol, 10K), the EPR spectra of the Lys→Ala variants of yeast *iso*-1-ferricytochrome c are nearly the same as that of the wild-type protein (Figure 18). The g_z-values of these variants range from 3.07 to 3.10 whereas the g_y-values vary between 2.22 and 2.24 (Table 4). Note that when the g_x values could not be determined accurately from the spectra due to g-strain, these values were calculated assuming that the sum of the squared g-values equals 16 (Palmer, 1985). The observed and calculated g_x-values range from 1.15-1.26. The rhombicity (V/Δ) and tetragonal field (Δ/λ) calculated from these g-values are included in Table 4 and place the five variants and the wild-type protein within region C of Blumberg and Peisach's crystal field correlation (Figure 8; 1971a, b). In combination with the MCD results above, these EPR data confirm that the Met80-Fe^{3+} bond remains intact despite the Lys → Ala replacements.
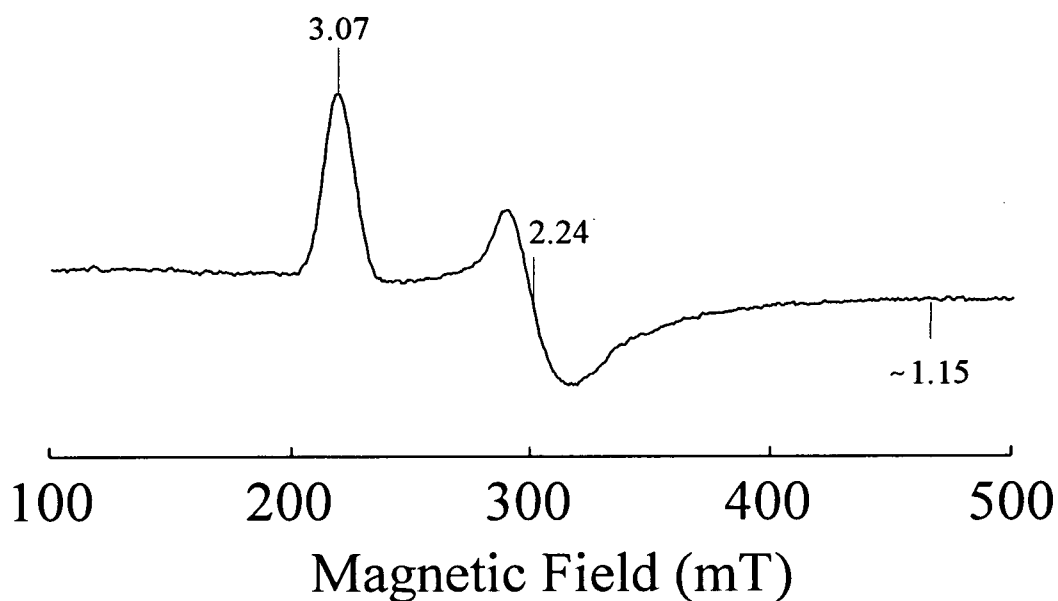
Figure 18. X-band EPR spectrum of wild-type yeast *iso*-1-ferricytochrome *c* (~ 1.2 mM protein in 20 mM MES buffer, pH 6.6, 50% glycerol, 10 K). This spectrum is representative of the spectra of the Lys→Ala variants measured near neutral pH. Calculation of the rhombicity and the tetragonal field from these *g*-values reveals that these cytochromes correspond to group C (solid circle) as shown in the "truth" diagram of Blumberg and Peisach (Figure 8; 1971).

Table 4. X-band EPR parameters of Lys→Ala variants of yeast *iso*-1-cytochrome *c* (~ 2 mM samples in 50 % glycerol plus 20 mM each, potassium phosphate and CAPS buffers, pH 6.6 or 20 mM each, MES and CAPS buffers, pH 6.0-6.6 (Lys86Ala and Lys87Ala), 10 K, ~9.45 GHz).

	wild-type	Lys73Ala	Lys79Ala	Lys73Ala/ Lys79Ala	Lys86Ala	Lys87Ala
g_z	3.07	3.07	3.09	3.10	3.08	3.09
g_y	2.24	2.24	2.22	2.22	2.24	2.23
g_x	~1.24	~1.26	~1.25	~1.26	~1.26	~1.25
V/Δ[a]	0.775	0.782	0.814	0.824	0.789	0.803
Δ/λ[a]	2.381	2.422	2.431	2.455	2.424	2.417

a. Note that the original axis system of Blumberg and Peisach was obtained by transforming the proper axis system according to Hall *et al.* (1974) (g_z-g_y, g_y-g_x, and g_x-g_z; see Palmer, 1979).

3.2.4 ¹H-NMR Spectroscopy

At neutral pH (50 mM sodium phosphate buffer, pH* 7.0, 20 °C), ¹H-NMR spectroscopy reveals that of the five variants Lys73Ala and Lys86Ala are the most similar to the wild-type protein in terms of the frequency of the hyperfine shifted resonances (Figure 19, a and b). The peaks corresponding to the heme methyl groups and the axial heme iron ligands are all within 0.2 ppm from the frequency at which the corresponding protons resonate in the spectrum of the wild-type protein (Table 5). However, the heme 3-methyl group resonance in the spectra of these two proteins is less intense than the neighboring resonance of the heme 8-methyl group. It is possible that these two proteins display the broadening phenomenon described by Burns and La Mar (1981). Cytochromes *c* from certain higher eukaryotes experience some localized structural heterogeneity in the vicinity of the heme 3-methyl group that results from Phe82 residing in two non-equivalent environments. At lower temperatures the exchange between these two conformations is sufficiently slow to be detected. However, the ¹H-NMR spectra of the Lys73Ala and Lys86Ala variants were not measured at
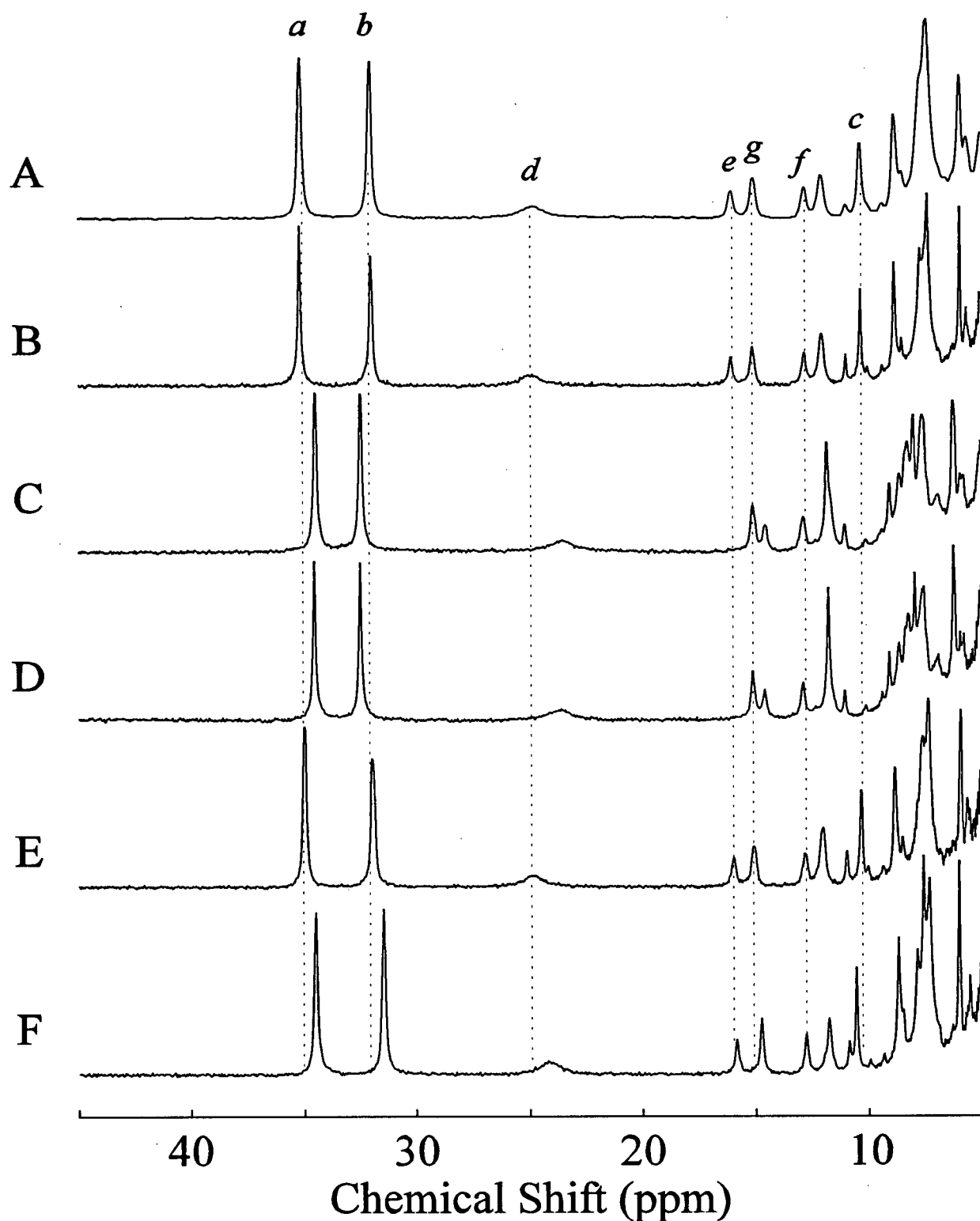
Figure 19a. Hyperfine shifted region of the 200 MHz ^{1}H-NMR spectra of native yeast *iso*-1-ferricytochromes c (2-3 mM protein, in 50 mM sodium phosphate buffer, pH* 7.0, 20 °C.): (A) wild-type; (B) Lys73Ala; (C) Lys79Ala; (D) Lys73Ala/Lys79Ala; (E) Lys86Ala; (F) Lys87Ala. The resonances labeled (a), (b) and (c) correspond to heme 8-, 3-, and 5-methyl groups respectively, (d) His18 ϵ1-H, (e) and (f) propionate 7α-CH$_2$, and (g) His18 β-CH.
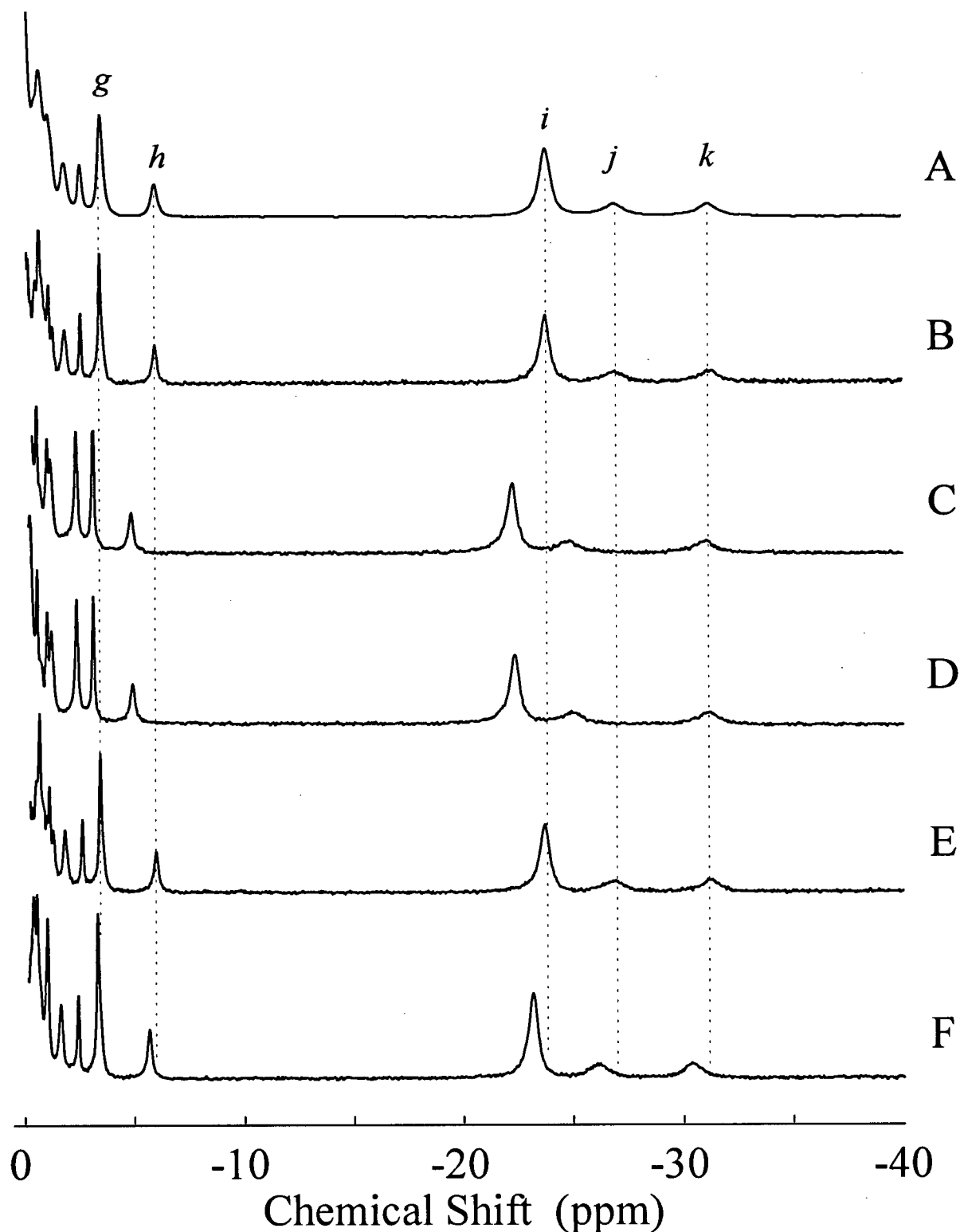
Figure 19b. Hyperfine shifted region of the 200 MHz ^{1}H-NMR spectra of native yeast *iso*-1-ferricytochromes c (2-3 mM protein, in 50 mM sodium phosphate buffer, pH* 7.0, 20 °C): (A) wild-type; (B) Lys73Ala; (C) Lys79Ala; (D) Lys73Ala/Lys79Ala; (E) Lys86Ala; (F) Lys87Ala. The labeled resonances correspond to (*g*) Leu68 δ-CH$_3$, (*h*) Pro30, (*i*) Met80 ε-CH$_3$, (*j*) His18 δ- CH, (*k*) Met80 γ-CH.

temperatures lower than 20 °C to confirm whether or not this broadening occurs for these two proteins.

Table 5. Hyperfine shifted resonances of the 200 MHz ^{1}H-NMR spectra of wild-type ferricytochrome c and five Lys→Ala variants (2-3 mM samples in 50 mM sodium phosphate pH[*] 7.0, 20°C).

^{1}H-NMR Shifts[a] (ppm)	WT	Lys73Ala	Lys79Ala	Lys73Ala/ Lys79Ala	Lys86Ala	Lys87Ala
8-CH$_3$	35.1	35.2	34.5	34.5	35.0	34.5
3-CH$_3$	32.0	32.0	32.5	32.5	32.0	31.5
His18, ε1-CH	24.8	25.0	23.5	23.6	24.8	24.2
Prop 7α-CH	16.0	16.0	15.1	15.1	16.0	15.9
His18, β-CH$_2$	15.1	15.1	14.6	14.6	15.1	14.8
Prop 7α'-CH	12.7	12.8	12.9	12.9	12.8	12.8
	12.1	12.1			12.1	11.8
	11.0	10.9			10.9	10.9
5-CH$_3$	10.3	10.3	11.9	11.8	10.3	10.6
	-1.9	-1.9			-1.8	-1.6
	-2.5	-2.6	-2.4	-2.4	-2.6	-2.4
Leu68 δ-CH$_3$	-3.5	-3.5	-3.1	-3.1	-3.5	-3.3
Pro30, δ-CH$_2$	-6.0	-6.0	-4.9	-4.9	-6.0	-5.7
Met80, ε-CH$_3$	-23.8	-23.8	-22.2	-22.2	-23.7	-23.2
His18, δ-CH	-26.9	-26.9	-24.9	-24.8	-26.9	-26.1
Met80, γ-CH	-31.2	-31.3	-31.1	-31.1	-31.2	-30.4

a. Chemical shift assignments are according to Gao and Pielak (1990), and Moench and Satterlee (1989).

The Lys79Ala and Lys73Ala/Lys79Ala variants exhibit more significant spectroscopic

differences from the wild-type protein. Some resonances in the downfield region are either absent from the spectrum of these variants, or they are shifted to a region where they are not sufficiently well resolved at 200 MHz. The aromatic region between 8 and 10 ppm in the spectra of these variants appears to be more crowded. Note also that while the resonance of heme 8-methyl group shifts upfield relative to its position in the spectrum of the wild-type protein, the signals of the heme 3- and 5-methyl group protons shift in the opposite direction. These observations could be a manifestation of the increased mobility of the protein as explained in the prologue to Section 3.2.

The replacement of Lys87 with an alanine also causes some changes in the hyperfine shifted resonances of cytochrome c. However, because Lys87 is more distant from the heme environment as well as significantly exposed to the solvent, it is unclear what causes these perturbations.

3.2.5 Spectrophotometric pH Titrations

One measure of the stability of the native conformation of ferricytochrome c is the pK_{ap} for the proton-linked isomerization of this species (state III) to its alkaline conformers (states IV). These values for wild-type yeast *iso*-1-ferricytochrome c and the Lys→Ala variants are listed in Table 6. The pK_{ap} values of the variants that contain a single Lys→Ala replacement are not too dissimilar from that of the wild-type protein. On the other hand, state III of the double variant is considerably more stable to alkaline pH and exhibits an estimated $pK_{ap} \sim 10.5$. The accuracy with which this pK_{ap} value may be determined is compromised because the variant undergoes a spectroscopic transition that does not occur in any of the other proteins until pH~12. Whereas the ferric heme in all the other proteins remains low-spin, the native state of the double variant turns into a high- or a mixed-spin species at pH greater than 10. Consequently, the titration data for this variant could not be fitted with a model that assumes involvement of a single ionization.

Table 6. pK_{ap} of the alkaline transition of wild-type yeast *iso*-1-ferricytochrome *c* and the Lys→Ala variants (0.10 M sodium chloride, 25 °C). The numbers in parenthesis are the standard deviations obtained from non-linear least-squares fitting of the data to the Henderson-Hasselbach equation. Representative titration curves are illustrated in Figure 20.

	Wild-type	Lys73Ala	Lys79Ala	Lys73Ala/ Lys79Ala	Lys86Ala	Lys87Ala
pK_{ap}	8.70(2)	8.82(2)	8.44(1)	~10.5	8.60(4)	8.47(2)

3.3 Identification of the Axial Ligands in Alkaline Ferricytochrome *c*

3.3.1 Electronic Absorption Spectrophotometry

At elevated pH (*e.g.*, 5 mM each, MES and CAPS buffers, pH 10.3, 25 °C), the four ferricytochrome *c* variants that bear a single Lys→Ala replacement display nearly the same electronic absorption spectrum as the wild-type protein (Figure 21). The Soret maxima of these proteins shift to ~ 405 nm and increase in intensity (~19 %). The α/β bands, centered at 528 nm, broaden and decrease in intensity (~12 %). The 695 nm band decreases in intensity and reflects the disruption of the Met80-Fe^{3+} bond (Moore & Pettigrew, 1990). The changes in the molar absorptivities of the Soret and the α/β band, though not exactly the same, are in good agreement with published results (Rosell *et al.*, 1998). The small discrepancy between these and the published values can be attributed to small difference in pH and other minor differences in buffer composition.

Only the spectrum of the Lys73Ala/Lys79Ala variant differs from that of wild-type cytochrome (Figure 21). Spectroscopic features of the native conformation (*e.g.*, the 695 nm band) persist even at high pH (~10) and only diminish to give rise to the spectrum of a high-spin species under more alkaline conditions. This high- or mixed-spin species displays a shoulder at ~600 nm and a very weak maximum at ~840 nm (inset). The band at ~600 nm corresponds to charge transfers between the porphyrin a_{1u} and a_{2u} π orbitals to the ferric d_{z^2}, d_{xz}, and d_{xy} orbitals. Although the Soret
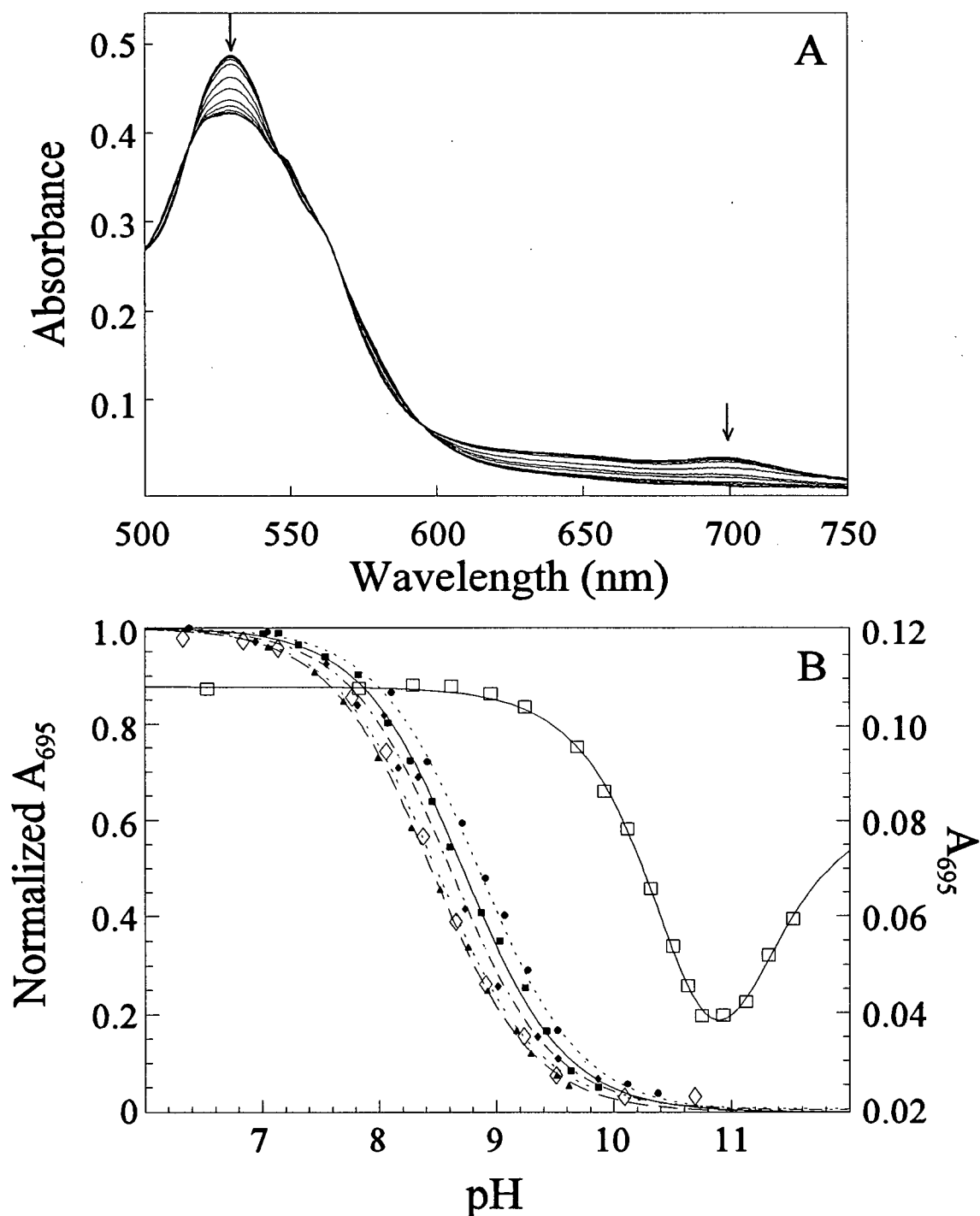
Figure 20. (A) Representative pH titration of wild-type yeast *iso*-1-ferricytochrome *c*. The arrows indicate the absorbance changes with increasing pH. (B) pH titration curves of yeast *iso*-1-ferricytochromes *c* monitored at 695 nm: wild-type (———■), Lys73Ala (······●), Lys79Ala (– – ▲), Lys86Ala (—–·◆), Lys87Ala (···· ····◇), and Lys73Ala/Lys79Ala (□). The scale on the right corresponds to the titration data for the Lys73Ala/Lys79Ala variant only. For all titrations, protein samples (~150 μM) were prepared in 100 mM sodium chloride, 25 °C, and the data were fitted to the Henderson-Hasselbach equation for 1 deprotonation (2 deprotonations in the case of the Lys73Ala/Lys79Ala variant).
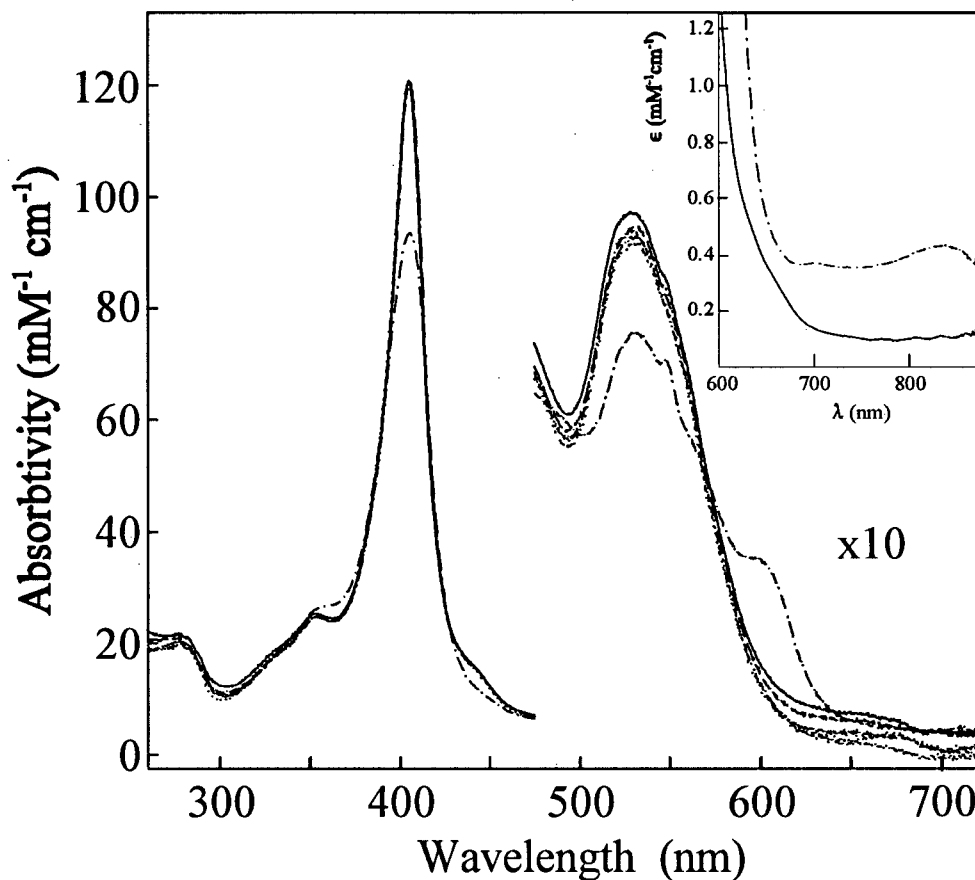
Figure 21. Electronic absorption spectra of yeast *iso*-1-ferricytochomes *c*: wild-type (—————), and the variants Lys73Ala (········), Lys79Ala (— — —), Lys73Ala/Lys79Ala (— · — · —), Lys86Ala (— ·· —), and Lys87Ala (···· ····). The spectra were measured in 5 mM each MES and CAPS buffers, pH 10.3, 25 °C with protein concentrations of 12-16 μM in a 1 cm cuvette. Note that the spectra were normalized with respect to the Soret maximum of the wild-type protein to allow for differences in pK_{ap}. The absorbtivity values of the variants are, therefore, only approximations. The spectrum of the Lys73Ala/Lys79Ala variant in the near infrared region is compared to that of the wild-type cytochrome (inset).

maximum also shifts to shorter wavelengths (~3.5 nm), its intensity, and that of the α/β band are attenuated (~25 %) relative to those of the other variants. The α/β region in the spectrum of the double variant broadens, and under some conditions, it also resolves into three maxima at 534.5, 523, and 550 nm. The maximum at 550 nm is most likely a consequence of protein reduction that occurs under the conditions of the measurement (Aviram, 1972).

3.3.2   Circular Dichroism Spectroscopy

Depending on the cytochrome, the far-UV circular dichroism spectra measured at pH 10.3 (5 mM each, MES and CAPS buffers, 25 °C) reveal that the variants undergo subtle changes in secondary structure. Figure 22 illustrates how the negative Cotton effects at 222 nm, and to a greater extent at 208 nm, increase in intensity. Similar changes have been reported to occur from methanol-induced denaturation of the cytochrome (Bychkova *et al.*, 1996; Kamatari *et al.*, 1996). Guanidinium hydrochloride and thermal denaturation, on the other hand, cause a reduction in optical activity at these wavelengths (Herrmann & Bowler, 1997). In the near-UV region, all the proteins retain optical activity at 289 and 282 nm. Methanol-induced protein unfolding or denaturation results in the reduction of these bands (Bychkova *et al.*, 1996; Kamatari *et al.*, 1996). In contrast, the alkaline transition of these cytochromes results in an increased CD signal, particularly in the Lys79Ala variant, suggesting that the structure around Trp59 becomes more rigid in the alkaline form of this variant. In the Soret region of this protein, the negative Cotton effect at 417 nm is lost entirely, and the positive optical activity at 404 nm increases as expected to follow scission of the Met80-Fe^{3+} bond (Looze *et al.*, 1978; Santucci & Ascoli, 1997).
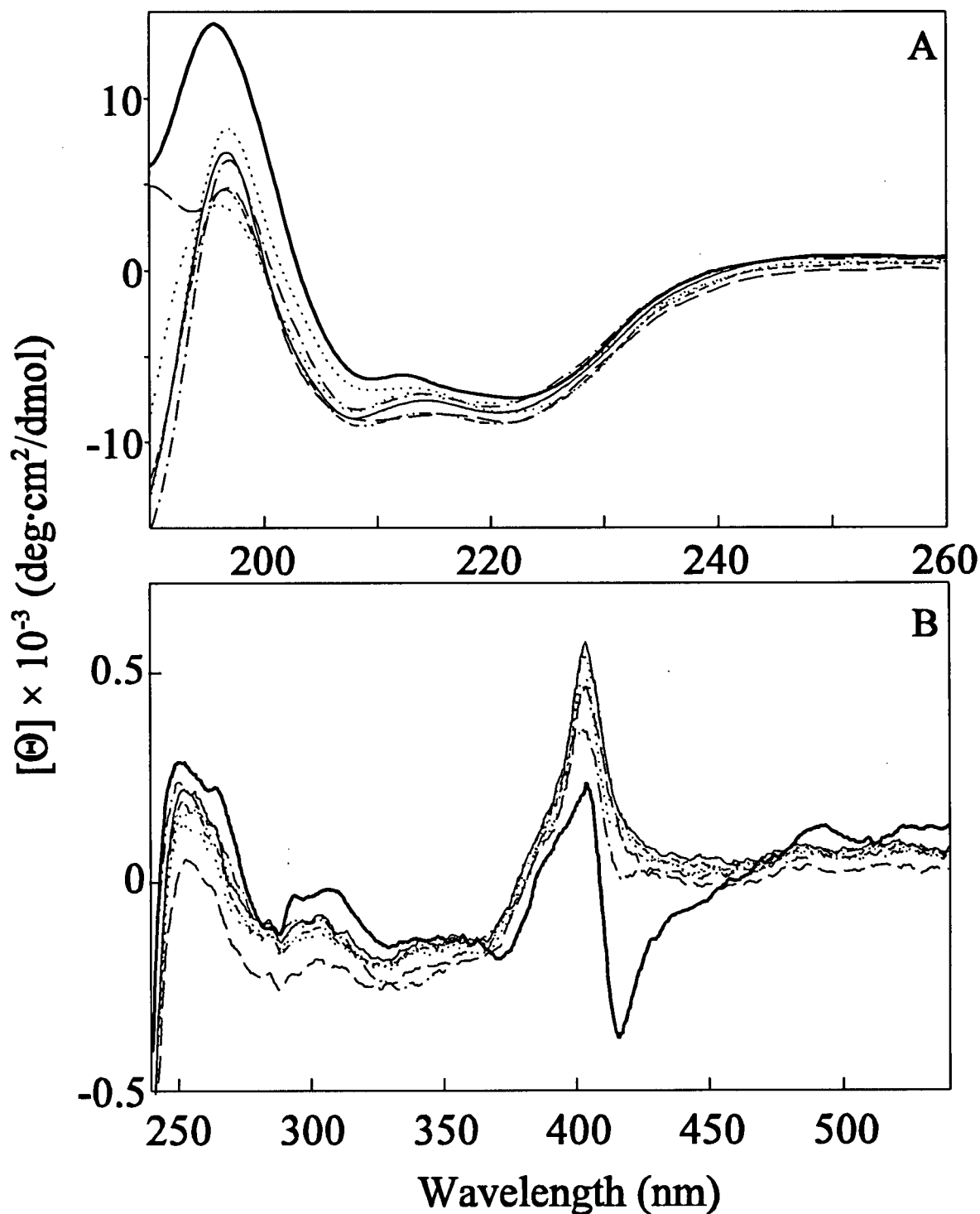
Figure 22. (A) Far-UV and (B) near-UV/visible circular dichroism spectra of yeast *iso*-1-ferri-cytochomes *c*: wild-type (————), and the variants Lys73Ala (············), Lys79Ala (— — —), Lys73Ala/Lys79Ala (—·—·), Lys86Ala (—··—··), and Lys87Ala (···· ····) (12-16 μM protein in 5 mM each, MES and CAPS buffers, pH 10.3, 25 °C, (A) 0.1 cm and (B)1.0 cm pathlengths). The spectrum of the wild-type protein measured at pH 6.1 is shown for reference (heavy solid line).

3.3.3 MCD Spectroscopy

The room temperature MCD spectra of the Lys73Ala, Lys79Ala, and Lys73Ala/Lys79Ala variants of yeast *iso*-1-ferricytochrome *c* measured at pH 10.5 are shown in Figure 23. These data illustrate that under these conditions the heme iron in the two single variants is bound by a nitrogenous ligand, consistent with the work of Gadsby and Thomson (1990). The Lys73Ala and Lys79Ala variants display maxima at 1477 (ϵ >65 M^{-1} cm^{-1} T^{-1}) and 1473 nm (ϵ ~58 M^{-1} cm^{-1} T^{-1}), respectively. The residual peak at ~1770 nm in the spectrum of the Lys73Ala variant reflects the higher pK_{ap} for the formation of the alkaline species of this protein. Note, therefore, that the intensity of the CT at 1477 nm in the spectrum of this variant is greater than that of the Lys79Ala cytochrome. The different intensities presumably reflect the different coordination geometry that results from ligation of Lys73, or Lys79 to the heme iron. As the angle formed by the coordinating amino group of the coordinating lysyl residue and the heme plane approaches 90°, the charge transfer associated with this band has a higher probability of occurring (Thomson & Gadsby, 1990). Hence, the lower intensity of the CT in the spectrum of the Lys79Ala variant relative to that of the Lys73Ala cytochrome suggests that the amino group of Lys73 coordinates the iron at a greater angle with respect to the normal to the heme plane.

At high pH, the near-IR MCD spectrum of the Lys73Ala/Lys79Ala variant differs from the corresponding spectra of the single variants. The band centered at 1766 nm is attributed to the residual Met80-bound heme which appears to comprise ~50 % of the sample while the remainder is likely in a high-spin state. Note that the feature near 850 nm, and perhaps that above 1000 nm, support this conclusion (Lloyd *et al.*, 1991).
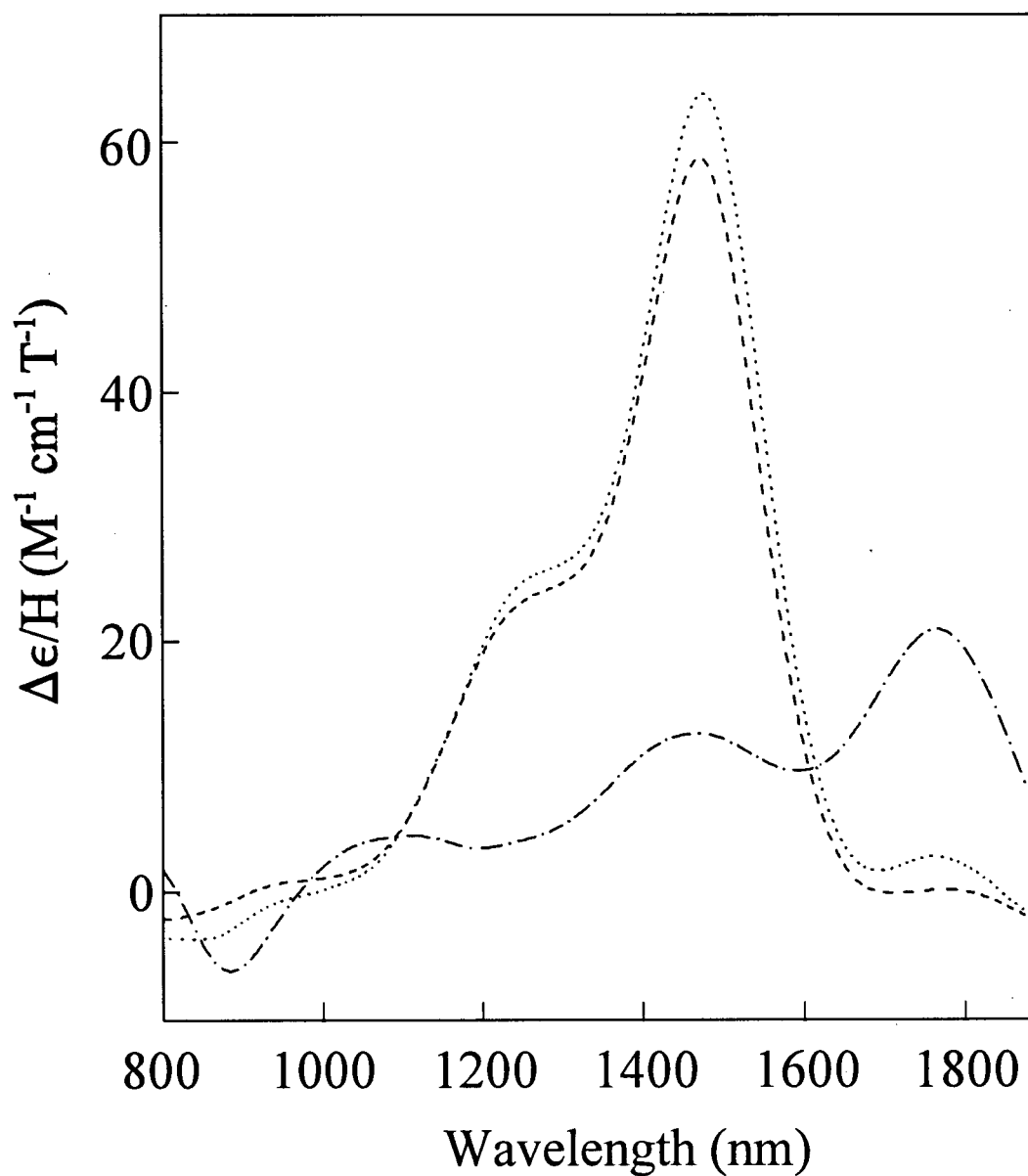
Figure 23. Near-IR MCD spectra of yeast *iso*-1-ferricytochrome *c* variants: Lys73Ala (·········; λ_{max}= 1477 nm), Lys79Ala (— — —; λ_{max}= 1473 nm), and Lys73Ala/Lys79Ala (— · —; λ_{max}= 1766 nm) (1.5-3 mM protein, 25 mM each, sodium phosphate and CAPS buffers, pH* ~10.5, 50% v/v glycerol, 0.1 cm pathlength, 4.83 T, 25 °C).

3.3.4 ¹H-NMR Spectroscopy

The downfield region of the ¹H-NMR spectrum between 10 and 25 ppm is diagnostic of the alkaline character of ferricytochrome c (Hong & Dixon, 1989; Ferrer *et al.*, 1993; Rosell *et al.*, 1998). Figure 24, b-d illustrate how at mildly alkaline pH the native isomer of yeast *iso*-1-ferricytochrome c (state III) is in equilibrium with two alkaline forms (states IV) reported by Hong and Dixon (1989). At 45 °C and pH* 9.3, the heme 8-methyl protons of the native state resonate at ~32 ppm. This group is in chemical exchange with two species (IV_a, 23.5 ppm and IV_b, 23 ppm) which increase in concentration with increasing pH or temperature and at the expense of the native protein. The remaining three heme methyl groups also display this conformational degeneracy which is consistent with the formation of two alkaline forms.

Unlike the Lys86Ala and Lys87Ala variants, which have essentially the same ¹H-NMR spectrum as the wild-type protein, the variants that contain Ala at position 73 or 79 display remarkably simplified spectra. Removal of either of these lysyl residues confines the protein to the formation of only one of the two possible alkaline conformers. Whereas one set of heme methyl group resonances is eradicated from the spectrum of the Lys73Ala protein (Figure 24 E), it is the other set of peaks that is absent from the spectrum of the Lys79Ala variant (Figure 24 F). These observations unquestionably identify Lys73 and Lys79 as the two endogenous ligands in yeast *iso*-1-ferricytochrome c that replace Met80 as the sixth ligand to the heme iron in response to an increase in pH. The appearance of a signal corresponding to a high-spin species at the expense of a persistent resonance of the native form in the spectrum of the Lys73Ala/Lys79Ala variant (Figure 24 G) is further evidence of the involvement of these lysyl residues in the alkaline transitions of the yeast protein. In this cytochrome, neither Lys73, nor Lys79 is available to replace Met80, resulting in a stabilized native state and a destabilized state V.
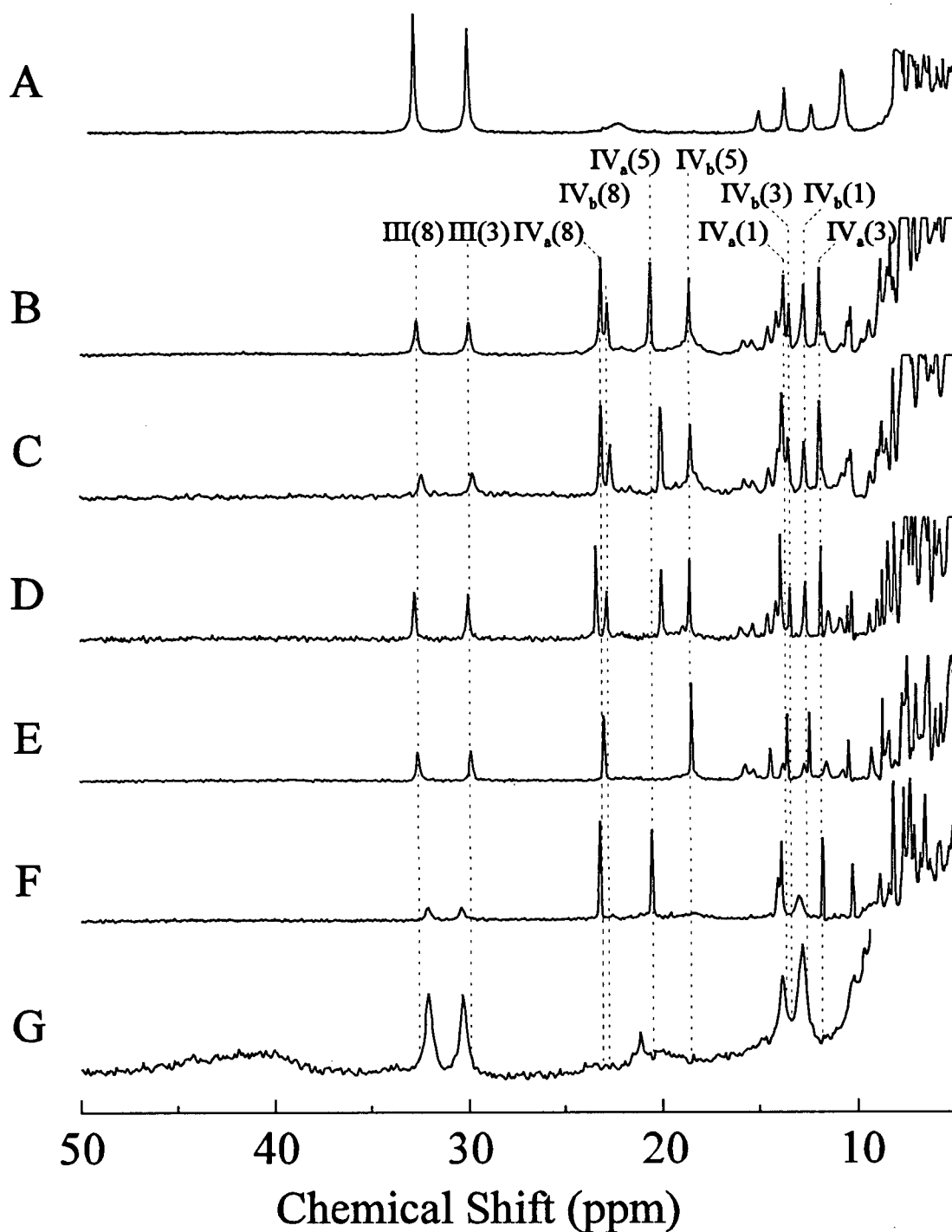
Figure 24. Hyperfine shifted region of the 200 MHz ^{1}H-NMR spectra of yeast *iso*-1-ferricytochrome *c*: wild-type pH* 7.0 (A) and pH* 9.3 (B), and the variants Lys86Ala (C); Lys87Ala (D); Lys73Ala (E); Lys79Ala (F); Lys73Ala/Lys79Ala (G). These spectra were measured at 45 °C with 2-3 mM protein in 50 mM sodium phosphate buffer, pH* 9.3 (B-F), and pH* 10.0 (G). The roman numerals refer to the native (III) or alkaline (IV) conformer of the protein as defined by Theorell and Åkesson (1941), the subscripts a and b specify the Lys73- or Lys79-bound alkaline conformer respectively, and the number in parenthesis refers to the heme methyl group that gives rise to the resonance.

3.3.5 EPR Spectroscopy

The EPR spectra of the Lys→Ala variants are consistent with the ^{1}H-NMR spectra. At alkaline pH wild-type ferricytochrome c consists of multiple low-spin species as shown by the EPR spectrum in Figure 25a. These low-spin species are characterized by g_z values of 3.04 (state III), 3.33 and 3.53 in agreement with published results (Brautigan *et al.*, 1977; Gadsby *et al.*, 1987). The two non-native forms exhibit EPR parameters that are similar to those of the N-butylamine adduct of leghemoglobin (Gadsby *et al.*, 1987) and to cytochrome f (Rigby *et al.*, 1988) which have g_z = 3.38 (pH 7.5) and 3.51, respectively. Raising the pH of the Lys86Ala and Lys87Ala variants results in essentially the same EPR spectrum observed for the wild-type cytochrome. On the other hand, replacement of Lys by Ala at positions 73 or 79 eliminates one of the two non-native low-spin species from the EPR spectrum of these proteins (Figure 25 b and c). Whereas the g_z = 3.33 component disappears from the spectrum by the removal of Lys73, removal of Lys79 eliminates the g_z = 3.53 component. Addition of the spectra of the Lys73Ala and Lys79Ala variants measured at alkaline pH results in a spectrum (Figure 25d) which closely resembles the spectrum of the wild-type protein measured at high pH. The shoulder that is observed at $g_z \sim$ 3.45 in the spectra of the Lys73Ala and Lys79Ala variants is attributed to less important subconformations or folding intermediates of the protein that are formed upon sample preparation. Further confirmation that Lys73 and Lys79 are involved in the formation of the two non-native low-spin species is found in the EPR spectrum of the double variant (Figure 25e). For this protein, the native conformation persists at higher pH as already described. Accordingly, the EPR spectrum of the Lys73Ala/ Lys79Ala variant is essentially that of the native cytochrome which coexists with a high-spin species that has a highly rhombic signature with g = 6.28.
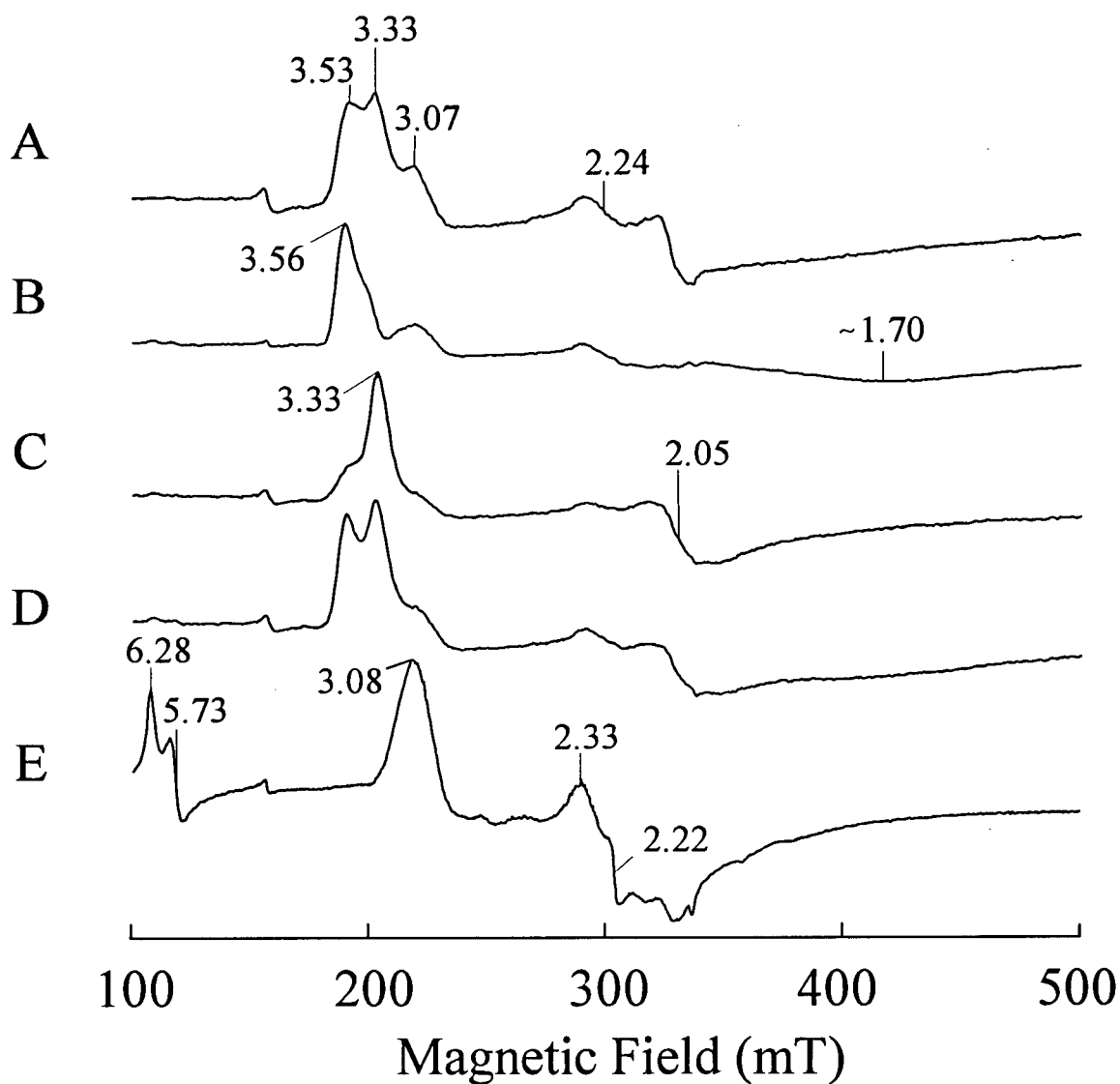
Figure 25. X-band EPR spectra of yeast *iso*-1-ferricytochromes *c*: wild-type (A); Lys73Ala (B); Lys79Ala (C); Lys73Ala/Lys79Ala (E) (~2 mM protein in 50 mM CAPS buffer, pH 10.5, 50% v/v glycerol, 10K). Spectrum D is the sum of spectra B and C.

3.3.6 Modeling the Spectroscopic Features of an Alkaline Conformer

The Lys73Ala/Lys79Ala variant of cytochrome c does not form a conventional alkaline conformer with an endogenous lysyl residue bound to the heme iron. However, under mildly alkaline conditions the native Met80 ligation is perturbed by the addition of exogenous amine compounds. Figure 26 illustrates the results of a spectrophotometric titration of the Lys73Ala/Lys79Ala variant with methylamine hydrochloride at pH 8.9 and 25 °C. The spectroscopic changes observed upon addition of the ligand are similar to those seen in the spectra of the other cytochromes. The Soret band shifts to higher energy (~405 nm), and it increases in intensity. The α/β band becomes less intense, and the 695 nm band disappears. Analysis of the titration data yields an apparent dissociation constant of 0.037(2) M^{-1} for binding of methylamine. Note that this K_d includes the binding equilibria involving the exogenous methylamine and Met80. Other amine-containing compounds such as ethanolamine and lysine were also tested. However, investigation of the affinity of the cytochrome for these ligands is complicated by sulphur-containing contaminants in the ethanolamine and the precipitation of the lysine at the elevated concentrations necessary for complex formation.

The ^{1}H-NMR spectra of the mixture of methylamine hydrochloride and the Lys73Ala/Lys79Ala variant of cytochrome c (Figure 27) are consistent with the formation of an alkaline-like species upon addition of the ligand to the variant. At concentrations as low as 30 mM methylamine (*i.e.*, ~ 10:1= ligand:protein), the intensities of the native heme 8- and 3-methyl groups decrease and give rise to new signals. New resonances at 26.9, 19.5, 10.5, and 9.2 ppm (20 °C) have intensities characteristic of heme methyl groups, and they increase with increasing methylamine concentrations. The resonance at 19.5 ppm is almost coincident with the heme 5-methyl group resonance of the Lys79-bound alkaline conformer. The signal at 26.9 ppm is believed to correspond to the heme 8-methyl resonance. However, the true assignment for these resonances have not been determined. The
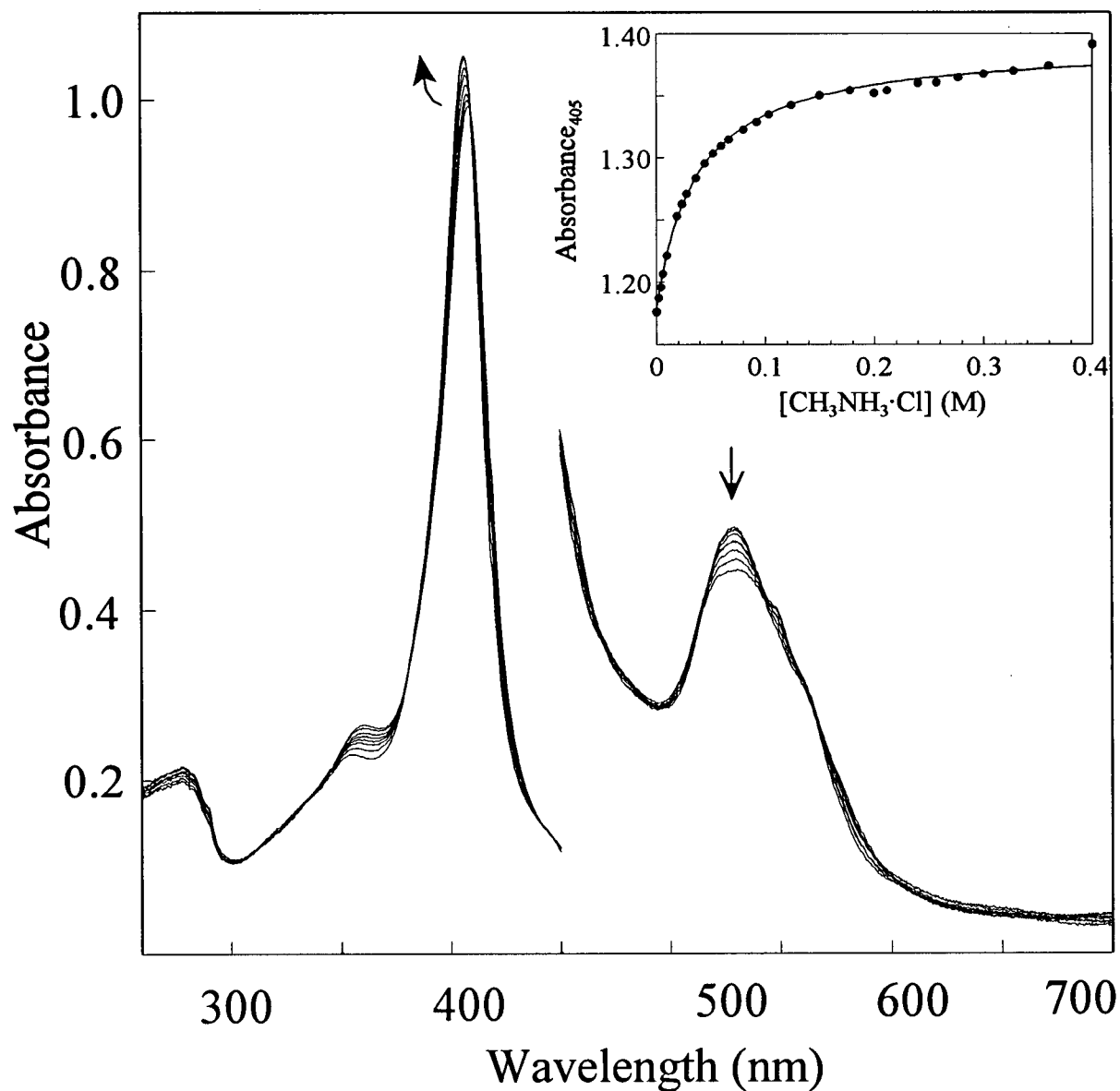
Figure 26. Spectrophotometric titration of yeast *iso*-1-ferricytochrome *c* Lys73Ala/Lys79Ala by methylamine hydrochloride (~10 μM protein, 240 mM sodium borate buffer, pH 8.9, μ = 0.5 M). The inset shows the change in absorbance at 405 nm as a function of ligand concentration. The dissociation constant calculated according to Connors (1987) for these data is 0.037(2) M^{-1}.
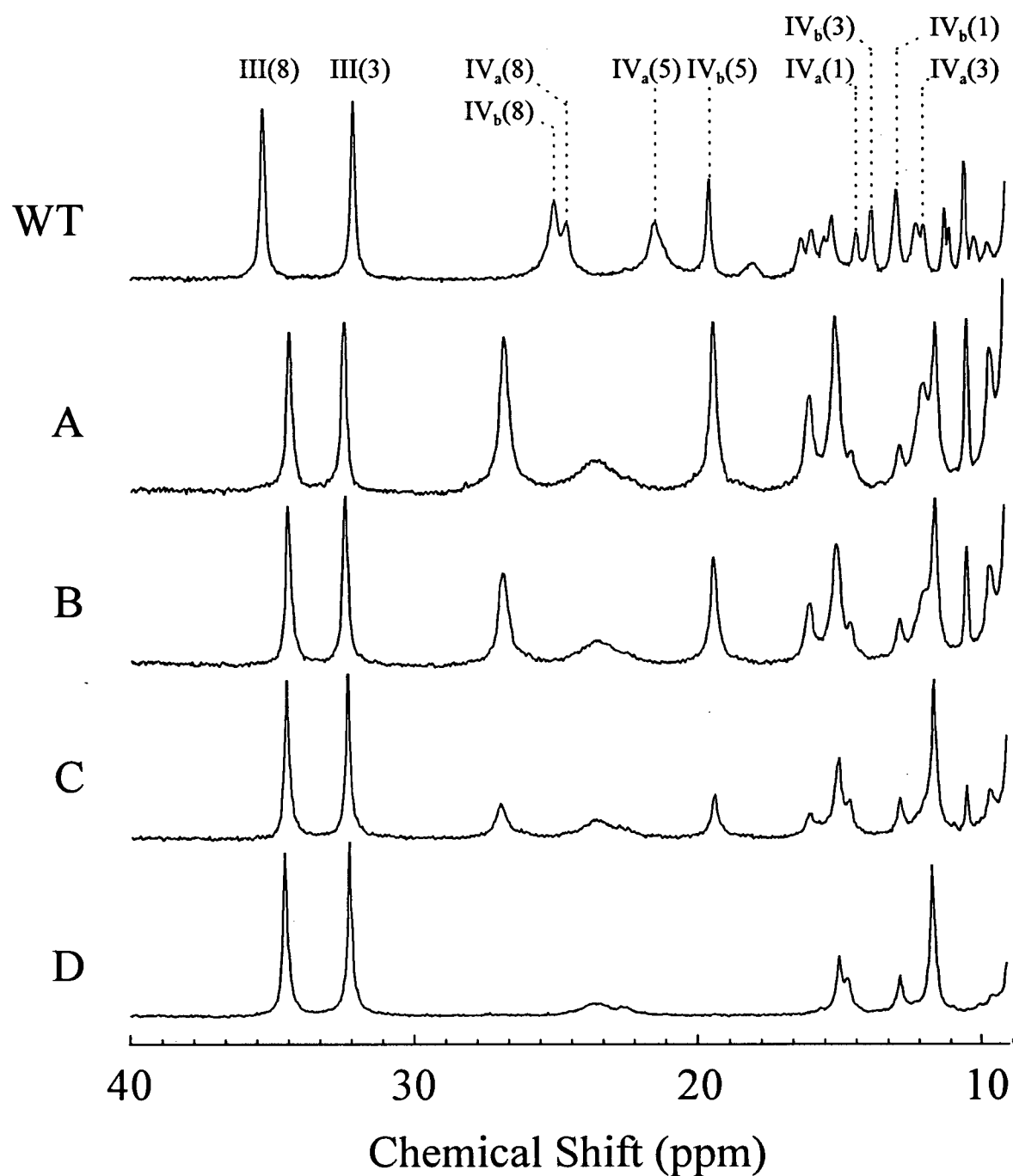
Figure 27. Hyperfine shifted 200 MHz ^{1}H-NMR spectra of yeast *iso*-1-ferricytochrome *c*: wild- type (WT: ~3 mM protein in 50 mM sodium phosphate buffer, pH* 9.3, 20 °C) and the Lys73Ala/ Lys79Ala variant (2-3 mM protein in 25 mM each sodium phosphate and sodium borate buffers, pH* 9.3, 20 °C plus (A) 300, (B) 200, (C) 70, and (D) 0 mM methylamine hydrochloride). Spectra A-D are normalized with respect to the intensity of the heme 8-methyl group resonance.

91

chemical exchange between the ligand-bound and the ligand-free species proceeds too slowly in the NMR time-scale to allow identification of these signals through magnetization transfer experiments.

The N-methylamine adduct of the Lys73Ala/Lys79Ala variant of cytochrome c results in a single species as demonstrated by the EPR spectrum of the complex (Figure 28). The complex has highly rhombic symmetry similar to the two alkaline conformers of ferricytochrome c. A sharp signal at $g_z=3.31$ dominates the spectrum and resembles a feature in spectrum of the Lys73-bound alkaline conformer [$g_z=3.33$]. Unlike the Lys73Ala and Lys79Ala variants, however, the N-methylamine adduct of the double variant does not display signs of the alkaline subconformations that form during the flash freezing process (*i.e.*, the shoulder at approximately $g=3.45$). At the concentration of methylamine used (~ 3 M), ~ 50 % of the protein retains the ligand even when the pH is reduced to 6.0.

3.4   Physical Properties of the Lys→Ala Variants of Cytochrome c

3.4.1   Direct Electrochemistry of Cytochromes c

Cyclic voltammetry at a 4,4'-dithiodipyridine-modified gold electrode indicates that the midpoint reduction potential of the five Lys→Ala variants of cytochrome c is unchanged from that of the wild-type protein [290 ±2 mV *vs.* SHE; $\mu=0.1$M sodium phosphate buffer, pH 6.0] (Table 7). The small differences in the potential of the variants are within the experimental uncertainty of these measurements. The peak-to-peak separations of 55-61 mV at 25 °C and the linear response of the peak cathodic currents with respect to the square root of the scanning rate also indicate that the electrochemical reaction of each variant at this electrode surface is reversible and diffusion-controlled (Rafferty, 1992, Barker & Mauk, 1992).

A pH titration of wild-type cytochrome c monitored by cyclic voltammetry reveals that a low
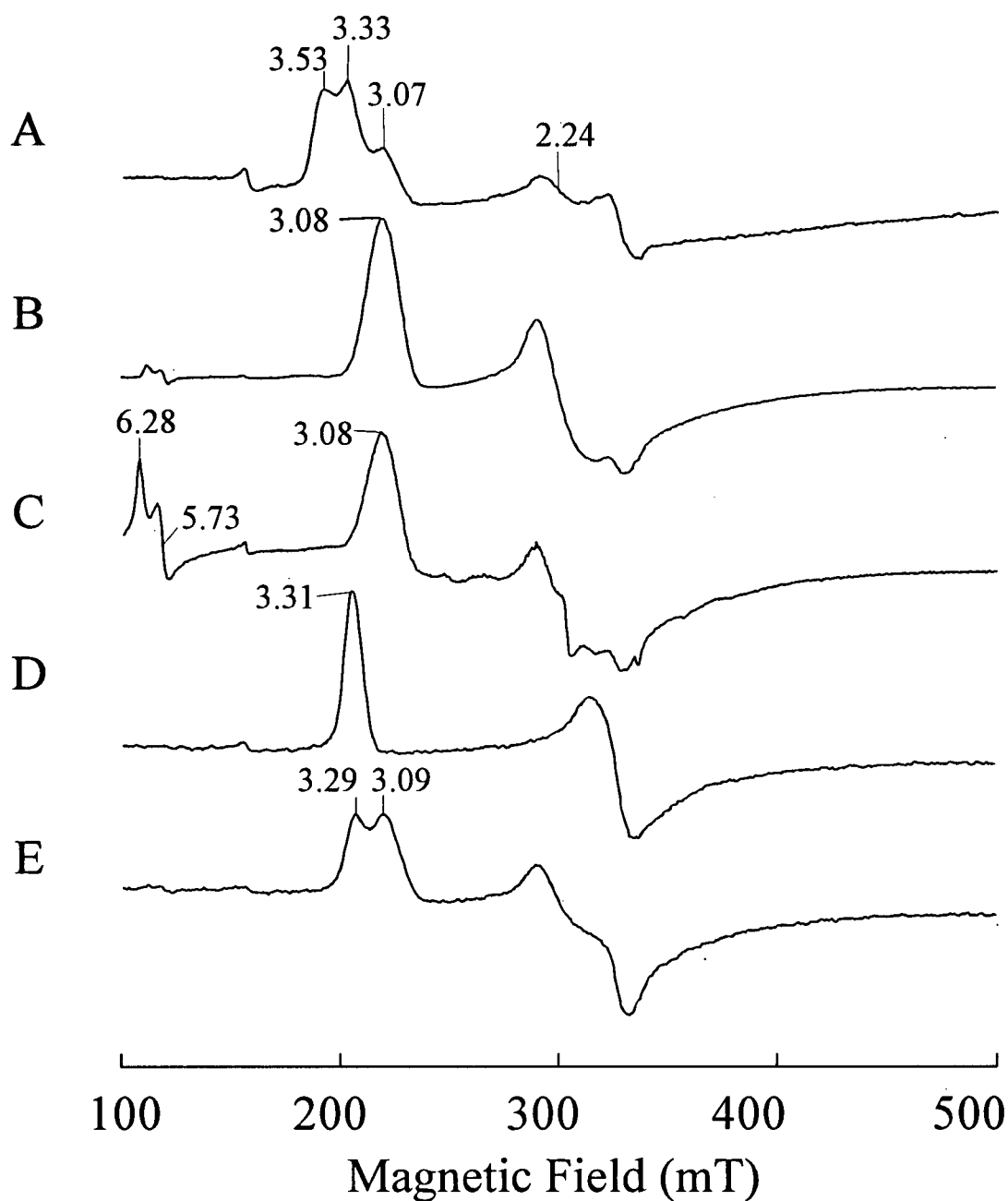
Figure 28. Comparison of the X-band EPR spectra of the *N*-methylamine adduct of the yeast *iso*-1-ferricytochrome *c* variant Lys73Ala/Lys79Ala and the wild-type protein (~2 mM protein, 50 mM CAPS, 10K): (A) wild-type (pH 10.5, 50% glycerol), and the Lys73Ala/Lys79Ala variant: (B) pH 7.2, (C) pH 10.5, (D) pH 9.7 with ~3 M methylamine, (E) pH 6.0 with ~3 M methylamine

93

potential wave attributable to non-native protein emerges at ~-200 mV *vs.* SHE at the expense of the native protein [~290 mV *vs.* SHE] (Barker & Mauk, 1992) (Figure 29). The results from titrations of the Lys73Ala (a and c) and Lys79Ala (b and d) variants are shown in Figure 30 and are summarized in Table 7. Panels a and b in the Figure reflect the typical pH dependence of the peak cathodic currents measured at an edge-oriented pyrolytic graphite electrode. The pK_{ap} determined by least squares fitting of these data to the Hendersson-Hasselbach relation corresponds to the equilibrium pK_{ap} of the alkaline transition of the ferricytochrome under investigation (Barker & Mauk, 1992). The values of 8.66(5) and 8.40(7) for the Lys73Ala and Lys79Ala variants, respectively, are in good agreement with the corresponding values determined by spectrophotometric titration (Table 6). Note that the data collected above pH 10 (represented with a cross) deviate sharply from the fitted titration curve. This result may reflect a pH threshold above which the edge-oriented pyrolytic graphite surface cannot interact favourably with the proteins (pI~9.5), thus eliciting a reduced current. These values were, therefore, excluded from the fitting routine.

Panels c and d illustrate the pH-dependencies of the midpoint reduction potentials of the variants. The scatter in the potential for a given pH is on the order of 10-15 mV. Because the conditions of the measurement (*i.e.*, 2 V/s, *pge* electrode, high pH, etc.) result in broad cathodic and anodic waves, the uncertainty in the determination of peak current potentials is estimated to be approximately the same magnitude as the scatter. This uncertainty accounts in part for the inconsistencies between the potentials calculated for the wild-type protein by Barker and Mauk (1992) and the values obtained for the alkaline species of the Lys73Ala and Lys79Ala variants under equivalent conditions (Table 7). These differences are largest at low pH (~6) where the reported reduction potential of the wild-type protein was estimated to be ~-170 mV *vs* SHE (Barker & Mauk, 1992). At this pH, a wave attributable to the non-native cytochrome is present in the voltammograms
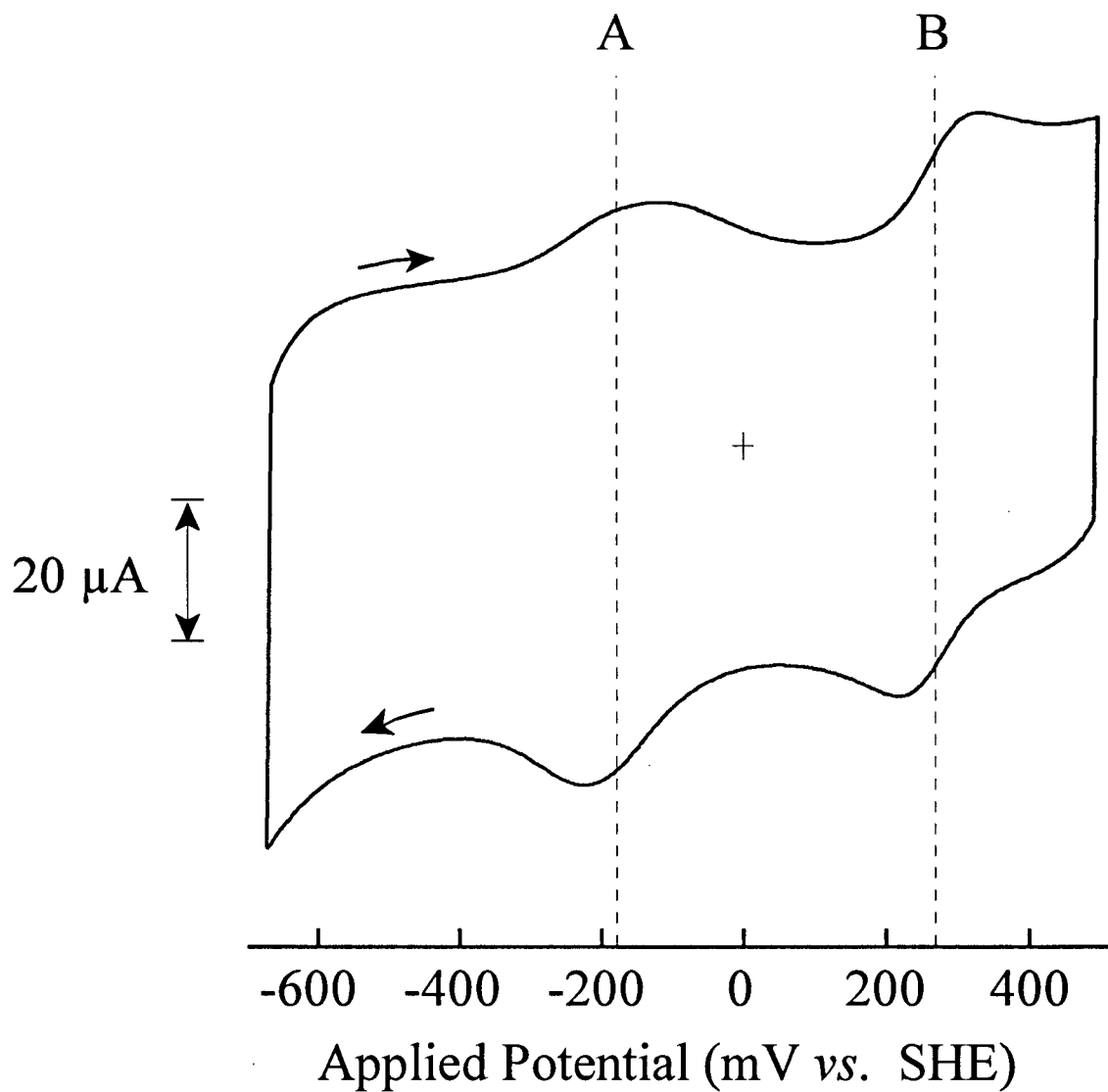
Figure 29. Representative cyclic voltammogram of the Lys79Ala variant of yeast *iso*-1-cytochrome *c* (320 µM protein, in 0.1 M sodium chloride, pH 8.43, 25 °C) measured at an edge-oriented pyrolytic graphite electrode on the second scan (2 V/sec). The arrows denote the direction of the scan while A and B indicate the midpoint reduction potentials of the alkaline and native conformers of the cytochrome respectively.
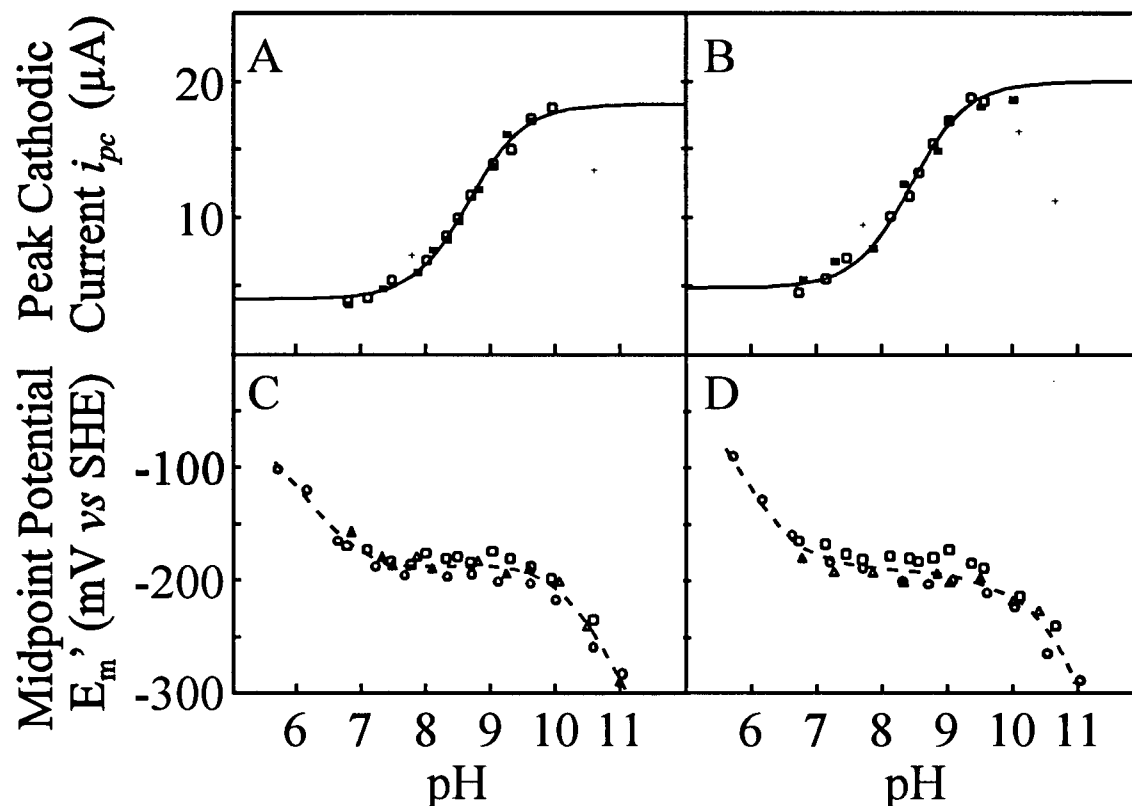
Figure 30. Titration of the yeast *iso*-1-cytochrome *c* variants Lys73Ala (A and C) and Lys79Ala (B and D) (~0.32 mM protein, in 0.1 M NaCl, 25 °C) monitored by cyclic voltammetry at an edge-oriented pyrolytic graphite electrode (2 V/sec). Panels A and B illustrate the peak cathodic current generated on the second scan, whereas panels C and D depict the midpoint reduction potentials of the low-potential wave. Data sets from 2 (A and B) or 3 (C and D) independent studies are differentiated by different symbols). The crosses in panels A and B represent points that were excluded from the fitting of the data to the Henderson-Hasselbach model for the deprotonation of a single titrating group (solid curves). The dashed curves in panels C and D have no theoretical basis.

Protein	Midpoint Potential (mV *vs* SHE)			
	Native (±2)	Alkaline[a] (±10)		
wild-type	290	-170 $^{6.0}$	-205 $^{8.45}$	-230 $^{10.4}$
Lys73Ala	287	-160 $^{\sim 6.7}$	-190 $^{\sim 8.9}$	-240 $^{\sim 10.6}$
Lys79Ala	289	-170 $^{\sim 6.7}$	-190 $^{\sim 8.4}$	-240 $^{\sim 10.4}$
Lys73Ala/Lys79Ala	291	n/m		
Lys86Ala	289	n/m		
Lys87Ala	290	n/m		

a. Measured in μ=0.1M sodium chloride, pH as indicated in the superscript, at an edge-oriented pyrolytic graphite electrode.

of the Lys73Ala and Lys79Ala variants which is consistent with a midpoint potential of ~-140 mV.

Although similar electrochemistry is observed for the two variants and the wild-type cytochrome, the results in the present work differ from those of Barker and Mauk (1992) in two ways. In the voltammograms of a solution of wild-type cytochrome *c* of comparable concentration only a high-potential cathodic wave (*i.e.*, ~260 mV) was measured below pH ~7. This wave had a magnitude of ~14 μA. On increasing the pH to ~10.2 a low-potential wave emerged (~-230 mV) at the expense of the native signal and reached a maximum current of ~10 μA. In contrast, the pH-dependence of the cyclic voltammograms of the Lys73Ala and Lys79Ala variants are characterized by a low- and a high-potential wave even at pH~6 (Figure 29). The magnitude of the cathodic peak, which corresponds to the alkaline form of the variants is never below 4 μA even though at pH~6, there is less than 0.5 % of the protein in the alkaline state. Furthermore, the maximum current achievable at high pH for 320 μM protein (between 18 and 20 μA) is greater than the current measured for the cathodic peak of the wild-type protein in the native state (~16 μA).

3.4.2 Influence of Temperature on the Alkaline Isomers of Ferricytochrome c

The stability of any organized structural element in a protein is invariably linked to temperature. In the case of cytochrome c, this interrelation has been observed to affect the strength of the Met80-Fe^{3+} bond (Wooten *et al.*, 1981; Santos & Turner, 1992; Taler *et al.*, 1995). Consistent with these reports, increasing temperature shifts the alkaline transition equilibrium of yeast *iso*-1-ferricytochrome c toward the alkaline conformers (Figures 31 and 32). Figure 31 illustrates the temperature dependence of the state III $\rightleftharpoons$ state IV equilibrium for each of the Lys→Ala variants and the wild-type protein at pH* 9.1-9.3. The equilibria were determined from the area ratio of equivalent heme methyl group resonances in the ^{1}H-NMR spectra. Table 8 summarizes the associated thermodynamic parameters of these processes.

Table 8. Thermodynamic characteristics of the state III $\rightleftharpoons$ state IV equilibrium of yeast *iso*-1-ferricytochromes c monitored by ^{1}H-NMR spectroscopy (50 mM sodium phosphate buffer, pH* 9.1-9.3). The equilibrium constants were calculated from the relative areas of the native and alkaline heme 8-methyl group resonances.

Protein	Wild-type[9.3]	Lys73Ala[9.3]	Lys79Ala[9.3]	Lys86Ala[9.2]	Lys87Ala[9.1]
$\Delta H°$ (kcal mol^{-1})	5.4(6)	5.9(9)	9.7(6)	6.6(4)	9.6(8)
$\Delta S°$ (e.u.)	19(2)	19(3)	32(2)	23(1)	32(3)
pK_{ap}	8.70(2)	8.82(2)	8.44(1)	8.60(4)	8.47(2)

pK_{ap} values were determined at 25 °C (Table 6). The pH at which each experiment was conducted is indicated with the superscript. (1 e.u. = 1 cal mol^{-1} K^{-1})

At this time it is unknown what role Lys87 may play in the alkaline transition of cytochrome c. The location of this residue at the surface of the molecule far from the heme center suggests that its influence is limited. However, the entropic and enthalpic changes associated with the structural reorganization of this protein are identical to those of the Lys79Ala variant. Not
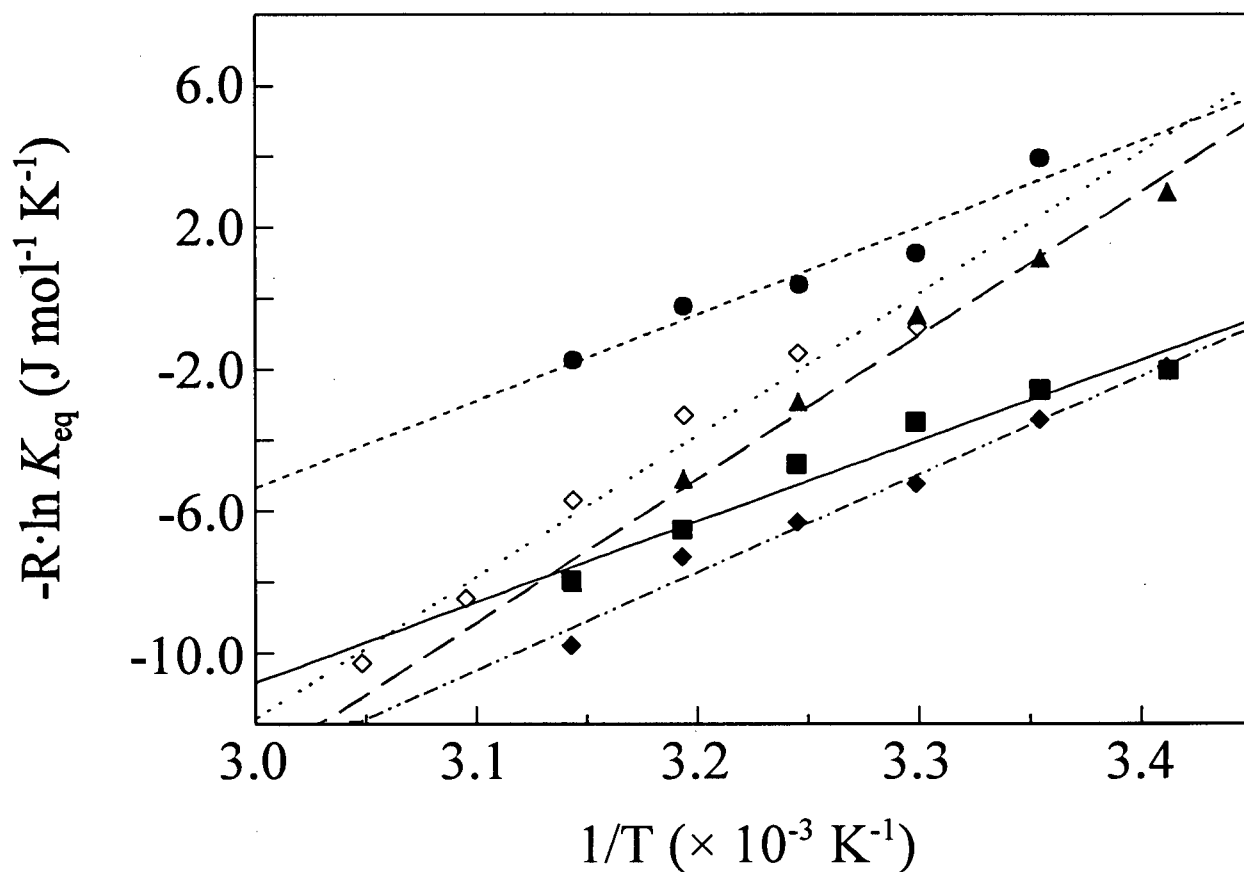
Figure 31. van't Hoff plot of the alkaline transition equilibrium of yeast *iso*-1-ferricytochromes *c*: wild-type(————■), Lys73Ala (⋯⋯●), Lys79Ala (— — —▲), Lys86Ala (– –⋯◆), and Lys87Ala (⋯ ⋯◇). ^{1}H-NMR spectra (~2-3 mM protein, in deuterated 50 mM sodium phosphate buffer) were measured at pH* 9.3 (wild-type cytochrome, and Lys73Ala, and Lys79Ala variants), pH* 9.2 (Lys86Ala variant), and pH* 9.1 (Lys87Ala variant). K_{eq} values were determined from the relative areas of the heme 8-methyl group resonances in the alkaline and native conformations.
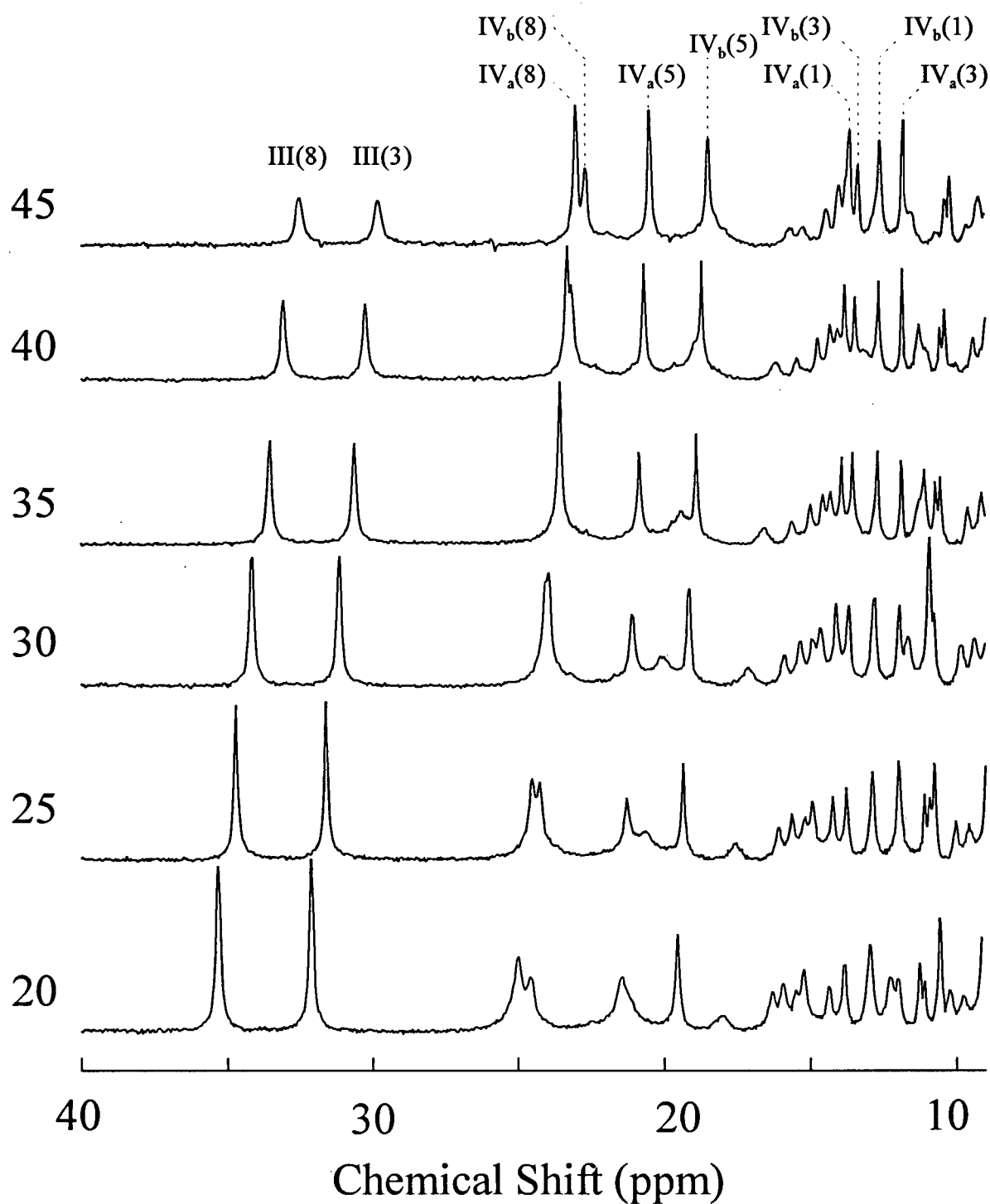
Figure 32. Temperature dependence of the downfield hyperfine shifted region of the 200 MHz ^{1}H-NMR spectra of wild-type yeast *iso*-1-ferricytochrome *c* (~3 mM protein in 50 mM sodium phosphate buffer, pH* 9.3). The number to the left of the spectrum indicates the temperature (°C) at which the data were collected. The peak assignment nomenclature is as in Figure 24.

surprisingly, these two proteins also have very similar pK_{ap}s, indicating that at mildly alkaline pH the Lys73-bound conformer is the preferred species formed by the Lys87Ala variant. Lys73Ala and Lys86Ala, on the other hand, more closely resemble the wild-type protein. The entropy and enthalpy of these three cytochromes are in good agreement with the values reported for the wild-type equine protein (ΔH° = 6.7(3) kcal mol^{-1} and ΔS° = 21.9 e.u.; Hong & Dixon, 1989).

Table 9. Thermal stability of the overall protein fold in the native and alkaline conformers of wild-type and variant forms of yeast *iso*-1-ferricytochrome c (μ=5 mM sodium phosphate or sodium borate buffer).

Protein	pH 6.15		pH 9.58	
	T_m (°C)	Reversibility (%)	T_m (°C)	Reversibility (%)
wild-type	52.7	78	52.0	68
Lys73Ala	53.7	86	48.2	47
Lys79Ala	51.4	89	52.3	25

The estimated uncertainty in the T_m values is on the order of 0.3 °C.

The thermal stabilities of wild-type ferricytochrome c and the Lys73Ala and Lys79Ala variants were evaluated by CD spectroscopy at pH 6.15 (μ = 0.01 M sodium phosphate buffer) and 9.58 (μ = 0.01 M sodium borate buffer). Whereas the ^{1}H-NMR analyses above focus primarily on the heme and its ligands, the thermal titrations monitored by optical activity at 222 nm focus on the protein secondary structure. The thermal stability of the Lys73Ala and Lys79Ala is compared to that of the wild-type protein in Table 9. The uncertainty in the T_m is estimated to be better than 0.3 °C, and that in the reversibility is ~10 %. These results indicate that the native Lys79Ala variant is less stable to thermal denaturation than the wild-type protein. The wild-type protein, in turn, is less stable than the Lys73Ala variant. The relatively lower stability of the Lys79Ala variant may be a consequence of the

removal of the hydrogen bond network in which Lys79 participates (Figure 14). On the other hand, the increased stability of the Lys73Ala protein is consistent with the results of Bowler and coworkers (Herrmann & Bowler, 1997). These authors have reported that replacing Lys73 with a neutral residue increases the stability of cytochrome c to guanidine hydrochloride denaturation. When the residue at position 73 is alanine, ΔG° associated with the folding of the protein decreases by ~1 kcal/mol relative to the wild-type protein.

At alkaline pH, the Lys73Ala variant is clearly less stable than the wild-type protein or the Lys79Ala variant. The ~5°C decrease in the T_m of the Lys73Ala variant is a surprising result considering that the structure of the alkaline conformer should not be too is dissimilar from the structure of the native isomer. By contrast, the alkaline isomer that involves the more significant structural rearrangements to accommodate Lys73 binding to the heme becomes more stable than the native structure. Although this variant appears more stable, it also displays the lowest reversibility with only 25% of the circular dichroism at 222 nm being restored upon cooling the sample. At present, the mechanistic origins of the behaviour described above cannot be determined from the information available, but a more rigorous calorimetric study of the cytochrome in the different alkaline states may provide more information regarding the isomerization.

3.4.3   Influence of Salt on Alkaline Ferricytochrome c

The stabilizing effect of some salts on the native conformer of ferricytochrome c has been known for some time (Osheroff et al., 1980; Andersson et al., 1980; Antalík et al., 1992). Figure 33 illustrates how increasing potassium chloride concentration stabilizes the native conformer of wild-type cytochrome c and of the Lys79Ala variant. In the case of the latter protein, the pK_{ap} increases by more than one pH unit over a range of 1 M potassium chloride. In contrast, the efficiency of this
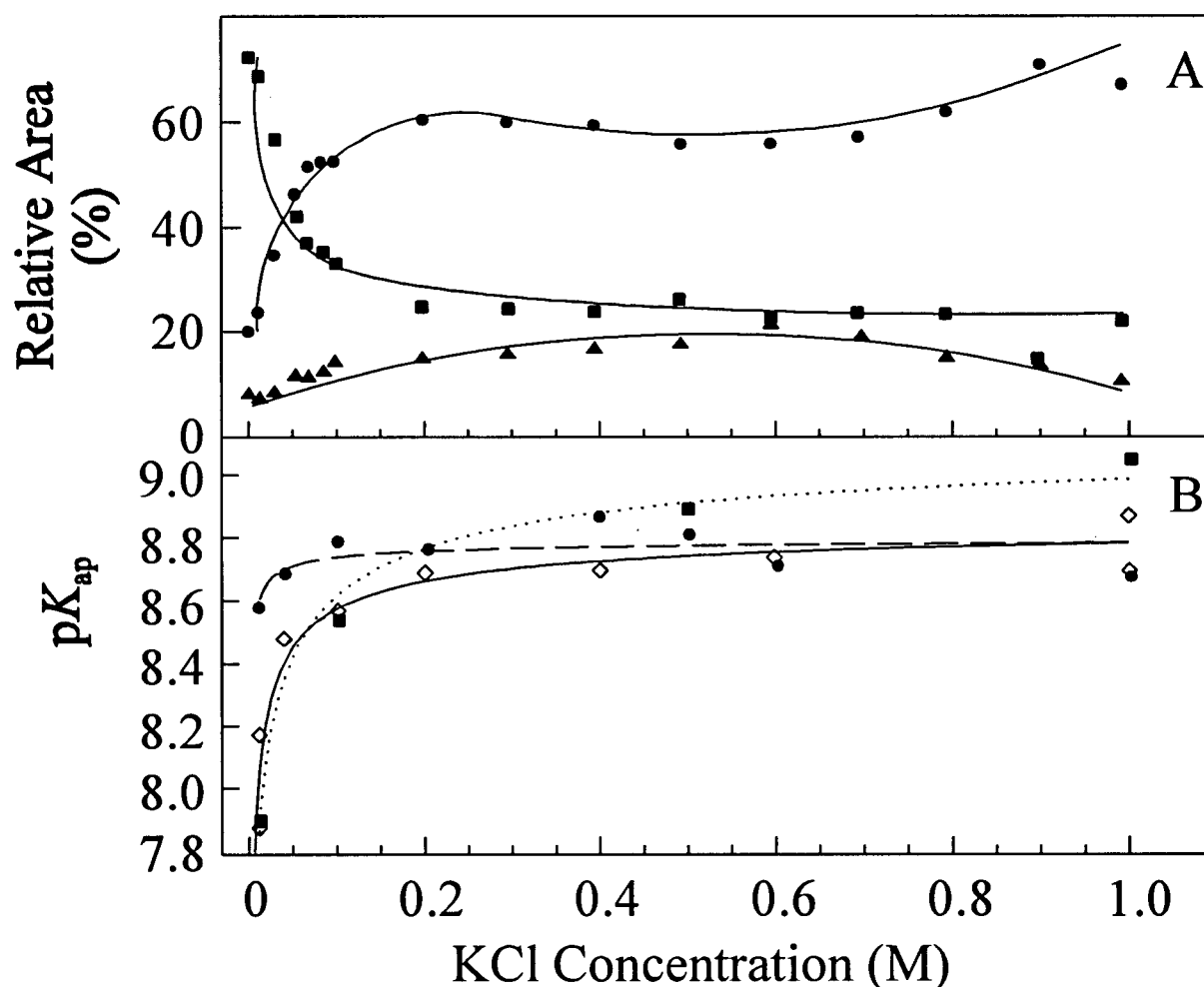
Figure 33. Influence of ionic strength on the alkaline transition of wild-type yeast *iso*-1-ferricytochrome *c* (25 °C). (A) Conformer distribution estimated on the basis of the relative peak areas of the native and alkaline heme 8-methyl group resonances (▲ Met80-, ● Lys79-, and ■ Lys73-bound; pH 10.0), and (B) salt dependence of the pK_{ap} for the alkaline transitions of the wild-type protein (——◊) and the variants Lys73Ala (— —●) and Lys79Ala (······■). The lines in (A) are drawn to illustrate the changes in isomer concentration with increasing ionic strength whereas the lines in (B) represent the non-linear least square fit of titration data to the Gouy-Chapman equation.

salt in the stabilization of the native Lys73Ala variant is marginal with the pK_{ap} only increasing ~0.2 pH units over the same range of potassium chloride concentration. However, it should be noted that this variant is already more stable (pK_{ap} = 8.7, 0.1 M potassium chloride) than the wild-type protein. Fitting the pK_{ap} values *vs*. potassium chloride concentration to the Gouy-Chapman relation yields the parameters shown in Table 10.

Table 10. Gouy-Chapman parameters of wild-type yeast *iso*-1-ferricytochrome *c*, and the Lys73Ala and Lys79Ala variants.

	pK_{true}	Average Surface Charge Density ($\mathrm{\mathring{A}^{-2}}$)
wild-type	8.87	1.3×10^{-2}
Lys73Ala	8.82	3.5×10^{-4}
Lys79Ala	9.17	2.8×10^{-3}

pK_{ap} values determined in varying concentrations of potassium chloride at 25.0±0.2 °C.

The effects of increasing the potassium chloride concentration on wild-type ferricytochrome *c* at pH 10.0 were monitored by ^{1}H-NMR spectroscopy as shown in Figure 34. The stabilization of the native conformer of the protein with higher salt concentrations is confirmed by the increasing intensities of the heme 8- and 3- methyl group resonances. This stabilization is maximal at approximately 0.6 M potassium chloride and then decreases. Concurrently, the Lys79-bound alkaline conformer, which represents only a small portion of the sample at low salt concentrations, becomes the major conformer at the expense of the Lys73-bound and the native forms at higher salt concentrations.

The population distribution and the pK_{ap} dependence of the proteins on ionic strength are interpreted in terms of charge shielding which exerts a stronger influence on Lys73 than on Lys79.
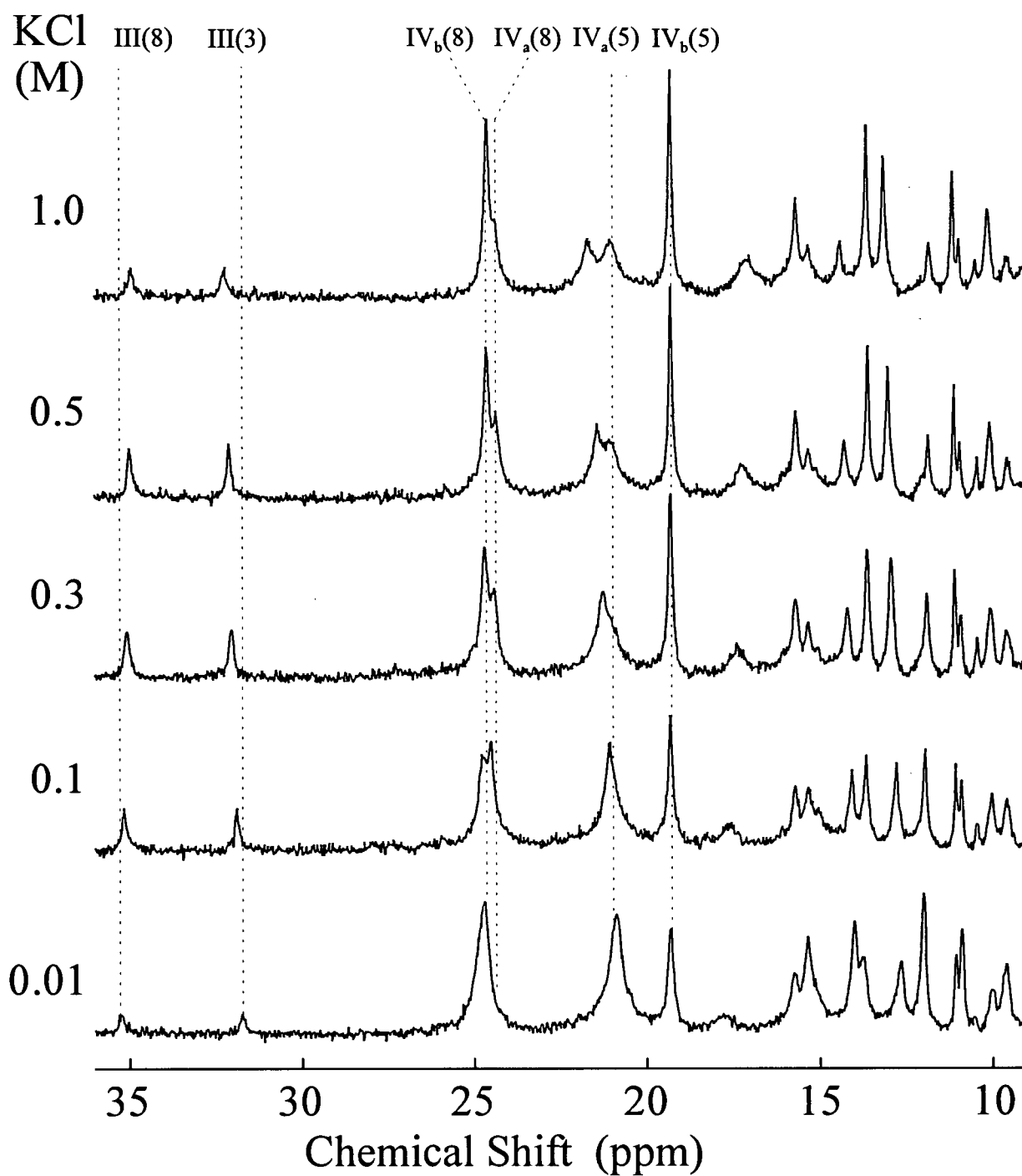
Figure 34. Hyperfine shifted region of the 200 MHz ^{1}H-NMR spectra of wild-type yeast *iso*-1-ferricytochrome *c* (~2 mM, pH* 10.0, 20 °C) as a function of ionic strength. The number to the left of each spectrum indicates the concentration of potassium chloride (M). Resonance assignments are as in Figure 24.

Because Lys73 is highly exposed to the solvent, it is also highly susceptible to ionic strength. At low salt concentrations, a deprotonated form of Lys73 is stabilized to minimize charge repulsions on the surface of the cytochrome. Interaction of chloride ions with the protonated ε-amino group of Lys73 reduces charge repulsion. The stabilization of a protonated Lys73, in turn, prevents this amino acid from replacing Met80 as an axial ligand to the heme. Consequently, with increasing potassium chloride concentrations, the native state of the cytochrome is stabilized. Lys79, on the other hand, is involved in a hydrogen bond network (Figure 14) which favours the protonated ε-amino group of this residue even at low salt concentrations. Increasing potassium chloride concentrations disrupt this hydrogen bond network to release Lys79. The abundance of salt therefore resembles mutation of Lys79 to Ala in that the protein exhibits more mobility. The migration of the native heme 8- and 3-methyl group resonances with increasing salt content (Figure 34) to resemble the ^{1}H-NMR spectrum of the Lys79Ala variant at pH 7.0 (Figure 19) is consistent with this observation. The effect of other salts was not investigated, but interaction of other salts with the cytochrome may influence the alkaline conformational equilibria in different ways.

3.5   Dynamics of the Alkaline Transition

3.5.1   pH-Jump Kinetics

The pH-jump reaction profiles corresponding to the Lys73Ala and the Lys79Ala variants (pH 6-10) are well described by a monophasic decay model (Figure 35). Similarly, the profiles of the wild-type protein can be fitted reasonably well to this model despite the two independent alkaline transitions that this protein can undergo. The pH-jump kinetics results for the wild-type and Lys73Ala and Lys79Ala variants are shown in Figure 36 together with the statistical fits to the model described by Davis *et al.* (1974). This model accounts for a ligand exchange that is associated with the
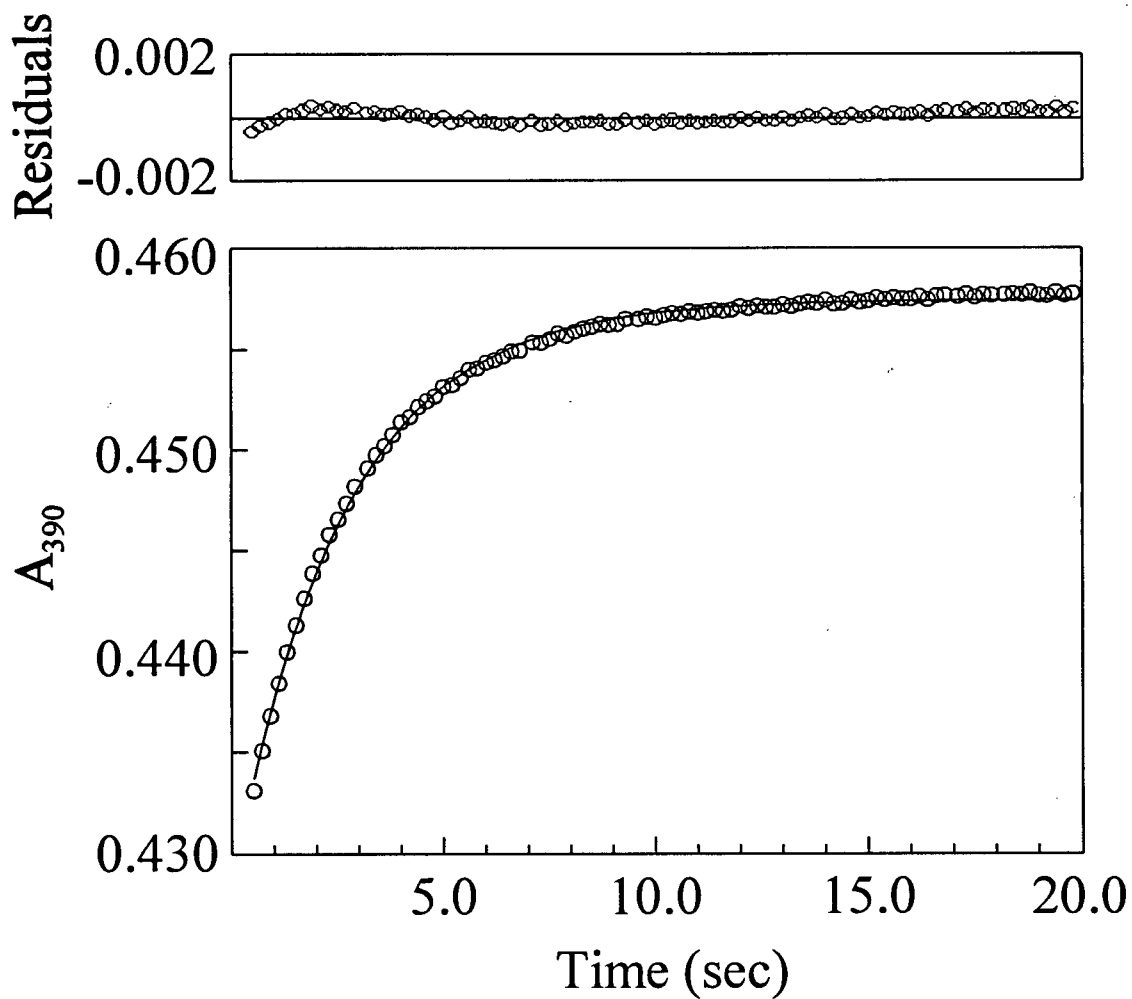
Figure 35. Representative pH-jump kinetics trace of the yeast *iso*-1-ferricytochrome *c* variant Lys79Ala (~9 μM protein in 0.1 M sodium chloride, pH 6.0 mixed with 40 mM sodium borate buffer, pH 9.45, ~80 mM sodium chloride, 25 °C). The data were fitted to a monoexponential rate equation which yielded k_{obs}=0.378(3) s^{-1}.

deprotonation of a titratable group. The kinetic parameters derived by fitting the data for the wild-type, Lys73Ala, and Lys79Ala proteins to the model are listed in Table 11 along with the parameters reported previously for wild-type yeast iso-1-ferricytochrome c (Pearce et al., 1989). Also listed in the table are the equilibrium pK_{ap} values determined by spectrophotometric titrations of the 695 nm band of each of the proteins. From the equilibrium pK_{ap} values, it appears that the wild-type protein behaves in a fashion that is intermediate between that of the two variants. All three parameters calculated (k_f, k_b, and pK_H) for the Lys79Ala variant are greater than those for the wild-type protein which are, in turn, greater than those for the Lys73Ala variant. This observation is also evident from Figure 36 in which the curve fitted to data obtained for the wild-type protein lies midway between the curves of the variants. This observation was explored further by reconstructing the k_{obs} versus [H$^+$] profile for the wild-type protein using a suitably weighted combination of the kinetic parameters of the single variants at positions 73 and 79 (Appendix 3). The inset in Figure 36 is the result of such a simulation for which the linear correlation coefficient is 0.91.

Table 11. Equilibrium and kinetic parameters for the alkaline transition of yeast ferricytochromes c.

Protein	k_f (s^{-1})	k_b x 10^2 (s^{-1})	K_c	pK_H	pK_c + pK_H	pK_{ap}[a]
wild-type	48 (2)	3.5 (1)	13.9 (8) x 10^2	11.7 (2)	8.6 (2)	8.70 (2)
wild-type [b]	8.5 (3)	3.5 (1)	244 (11)	11.0 (1)	8.6 (2)	8.5
Lys73Ala	1.51 (5)	1.6 (1)	94 (7)	10.8 (1)	8.8 (1)	8.82 (2)
Lys79Ala	160 (5)	4.0 (7)	4.0 (7) x 10^3	12.0 (3)	8.4 (4)	8.44 (1)

a. Apparent pK_{ap} determined by non-linear least squares analysis of pH titration data measured at 695 nm.
b. From Pearce et al., 1989. Note that in this reference, the values for wild type cytochrome c with Thr at position 102 and that with Cys at this position have been reversed (i.e., the line labeled "Cys-102 W.T." should bear the label "Thr-102" and vice versa).
The standard deviation in the last digit of the value determined by non-linear regression is quoted in parenthesis.
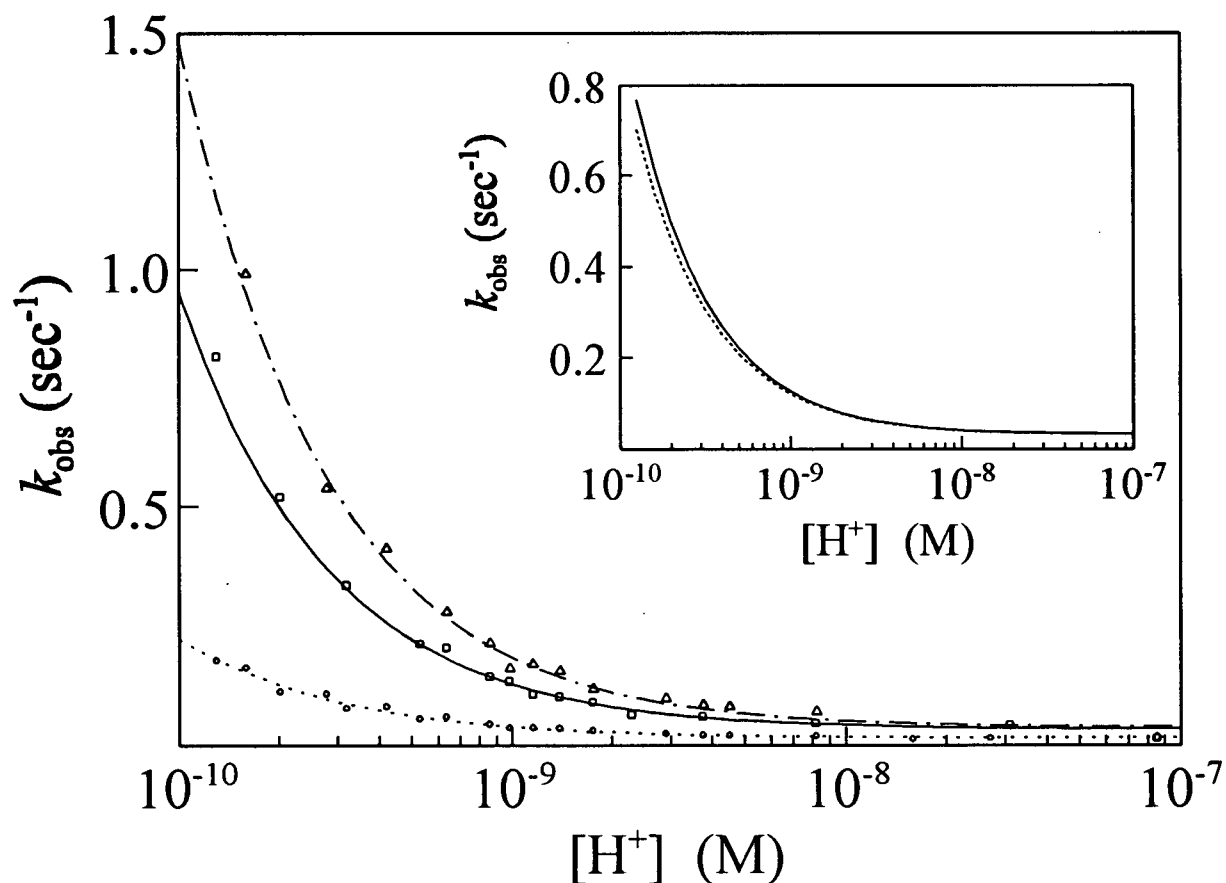
Figure 36. pH-dependence of the observed rate constants (k_{obs}) for the alkaline transitions of yeast *iso*-1-ferricytochromes *c*: wild-type (——— ,□), Lys73Ala (········ ,○), and Lys79Ala (— — — ,△). pH-jump kinetic experiments were carried out at 25 °C, with ~9 μM protein and a 2 cm pathlength cuvette. The curves shown are the non-linear least squares fits of the individual data sets to the model of Davis *et al.* (1974). The inset compares the pH-dependence of the kinetics of the wild-type protein (solid profile) to kinetics calculated from a weighted combination of the parameters determined for the Lys73Ala and Lys79Ala variants (dashed curve).

109

Despite the significant structural rearrangement that the Lys79Ala variant must undergo to introduce Lys73 into the coordination sphere of the heme iron, the stopped-flow kinetics data indicate that this isomerization is faster than the equivalent reaction involving Lys79. The pK_H associated with this faster structural reorganization is also greater, thus offsetting the faster structural reorganization to give an overall equilibrium value (*i.e.*, pK_{ap}) that is similar to that of the slower reaction observed for the Lys73Ala variant.

Although the model of Davis *et al.* adequately describes the kinetic properties of the alkaline transition of ferricytochrome c, it does not take into consideration either the transition to two alkaline conformers nor the structural intermediates that must form during the ligand exchange reaction. Specifically, the Davis model does not consider the formation and decay of a 5-coordinate species that must occur during the reaction. Several authors have observed the formation of an intermediate when the pH-jump exceeds pH 10 (Kihara *et al.*, 1976; Saigo, 1981; Rafferty, 1992). Wild-type yeast ferricytochrome c and the Lys73Ala and Lys79Ala variants also display this intermediate in stop-flow reactions above pH 10 (Figure 37). This transient is characterized by a band at ~600 nm that is characteristic of a high-spin heme iron and that may correspond to the mandatory 5-coordinate intermediate. This species also occurs in pH-jump experiments of the Lys73Ala/Lys79Ala variant but not in the Tyr67Phe cytochrome (*vide infra*). In the case of the Lys73Ala/Lys79Ala variant, however, the species with the 600 nm absorption is more stable and persists between pH~10-11.5 under equilibrium conditions (Figure 21).
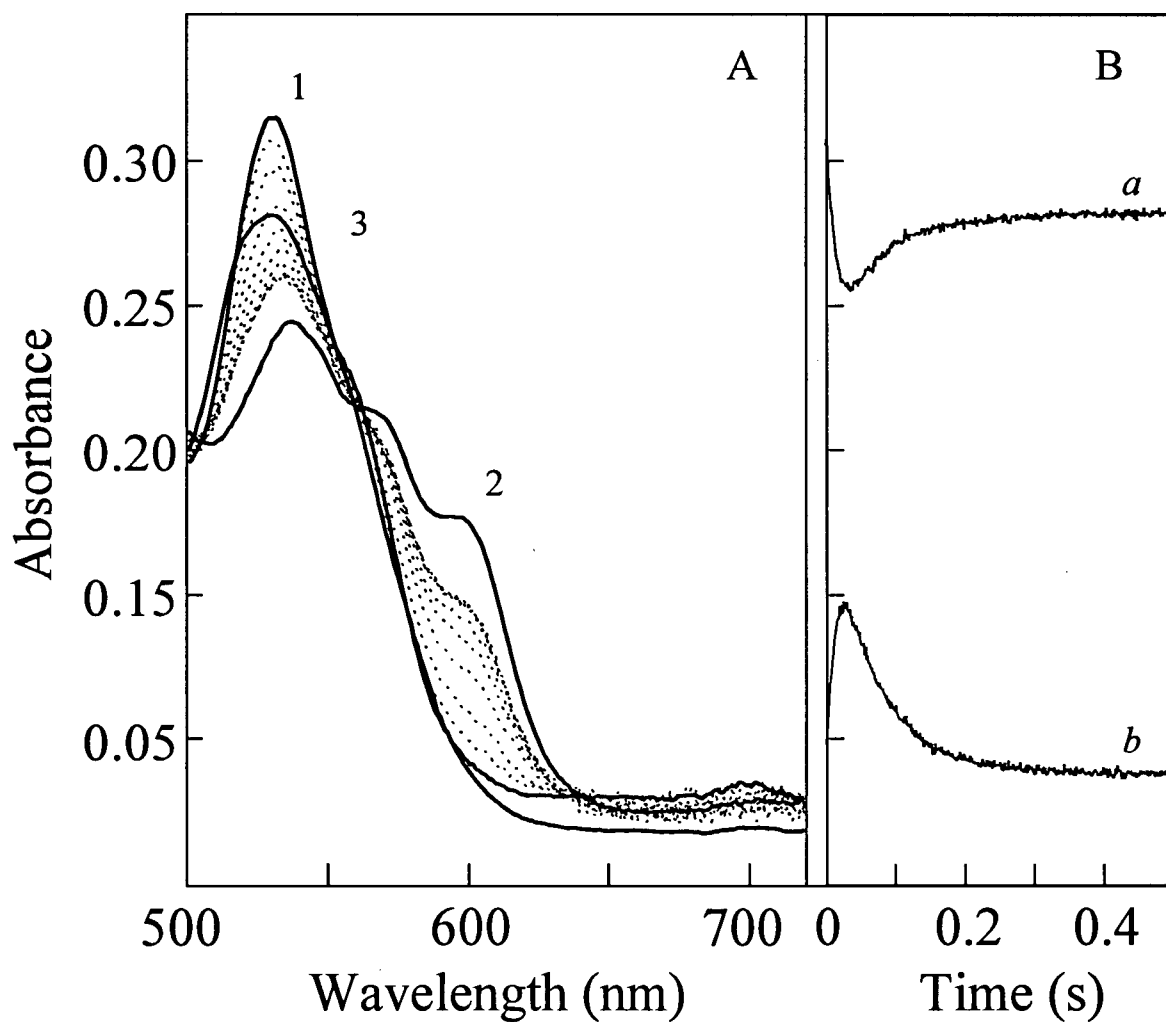
Figure 37. Sample pH-jump reaction progress (pH 6 to pH 11.5) of wild-type yeast *iso*-1-ferricytochrome *c*. (A) The dotted lines correspond to selected spectra extracted during the first 45 msec of the reaction, and the heavy solid lines are spectra derived from singular value decomposition analysis for a model where 1 → 2 → 3. (B) Experimental, single wavelength reaction profiles measured at (*a*) 530 and (*b*) 600 nm.

3.6 Yeast *iso*-1-Cytochrome *c* Expressed in *E. coli*

Yeast *iso*-1-cytochrome *c* was recently expressed in the cytoplasm of *E. coli* (Pollock *et al.*, 1998) together with the cytochrome *c* heme lyase that catalyzes the covalent attachment of the heme to the protein backbone (Dumont *et al.*, 1987). At neutral pH the electronic absorption, ^{1}H-NMR, and EPR spectra of the bacterially expressed yeast *iso*-1-ferricytochrome *c* (Figure 38) are indistinguishable from those of the yeast protein (Pollock *et al.*, 1998). The midpoint reduction potentials of the two proteins measured at a pyrolytic graphite electrode are also indistinguishable [wild-type: 282(2) mV *vs* SHE, n = 60.3 mV; Tml72Lys: 283(2) mV, n = 61.1 mV], as are the thermal stabilities of the two cytochromes. The only difference between the protein expressed in yeast and *E. coli* that can be detected near neutrality is the lack of trimethylation of Lys72 in the bacterially expressed protein (Pollock *et al.*, 1998). For this reason, the bacterially expressed protein is referred to from this point forward as the Tml72Lys variant of cytochrome *c*.

The lack of trimethylation of Lys72 exerts a strong influence on the protein under mildly alkaline conditions. The pK_{ap} of the alkaline transition of the Tml72Lys variant is 7.95(2) (μ=0.1 M sodium chloride, 25 °C) which is significantly lower than that of the trimethylated protein [pK_{ap}=8.70(2)]. Furthermore, the EPR spectra observed at high pH for the proteins isolated from the two hosts (Figure 39) indicate that the cytochrome from *E. coli* has an additional low-spin species with a g_z=3.20. Combined, these two results suggest that in the Tml72Lys variant, Lys72 can act as

Overleaf

Figure 38. Spectroscopic comparison of yeast *iso*-1-ferricytochrome *c* expressed in *Saccharomyces cerevisiae* (·········· Y), and *Escherichia coli* (——— B). (A) Electronic absorption spectra (~9 μM protein in 20 mM sodium phosphate pH 7.2, 25 °C); (B) X-band EPR spectra (~2 mM protein in 20 mM sodium phosphate pH 7.2, 50 % v/v glycerol, 10 K); and (C) downfield hyperfine-shifted 200 MHz ^{1}H-NMR spectra (~3 mM protein in 25 mM each sodium phosphate and sodium borate buffers pH* 7.2, 25 °C)

113
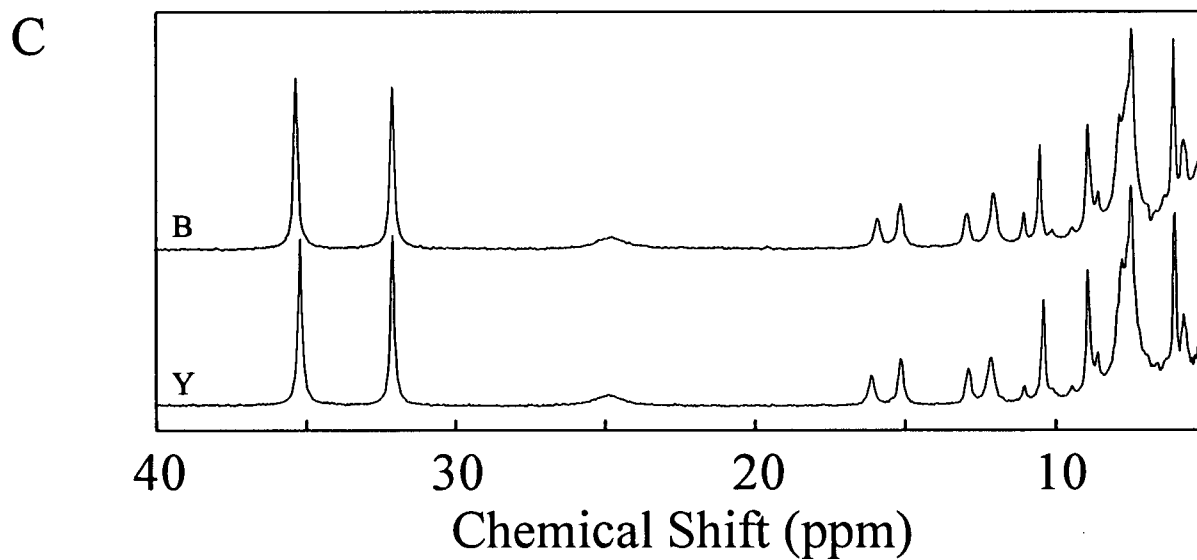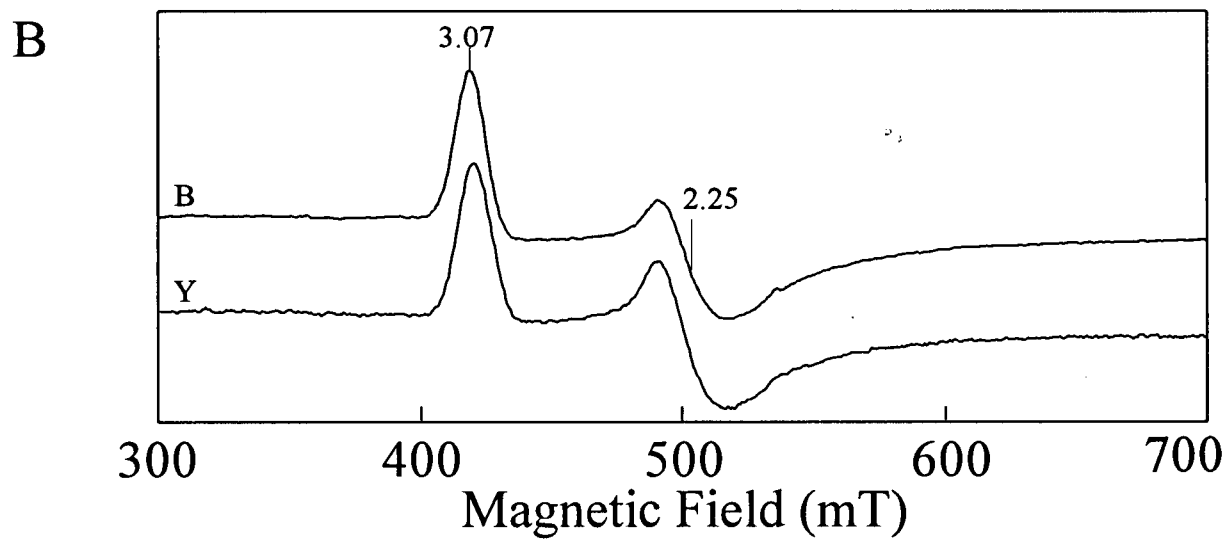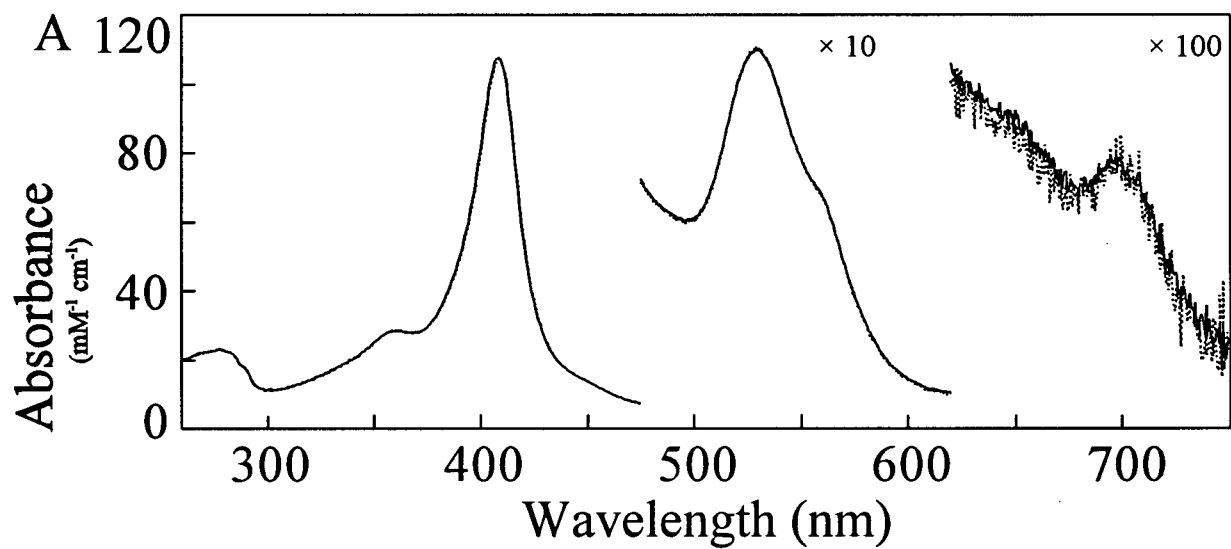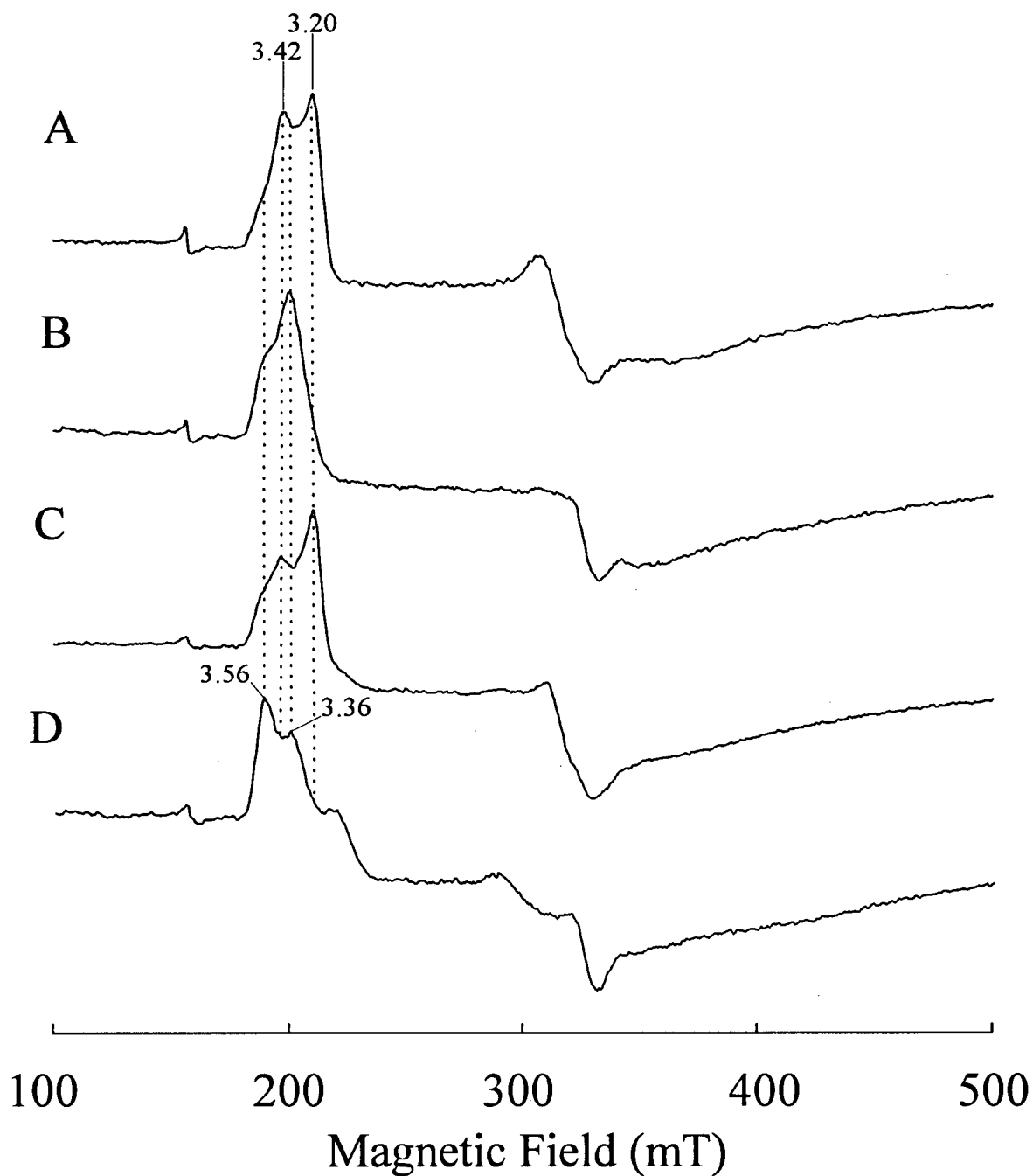
Figure 39. X-band EPR spectra of wild-type yeast *iso*-1-ferricytochromes *c* (~2 mM protein in 25 mM each, sodium borate and CAPS buffers, 50% v/v glycerol, 10 K): (A) cytochrome expressed in *E. coli*, pH 10.5; (B) cytochrome expressed in yeast, pH 10.5; (C) cytochrome expressed in *E. coli*, pH 9.5; (D) cytochrome expressed in yeast, pH 9.5.

a heme iron ligand at a lower pH than the Lys73 or Lys79. Because the pK_{ap} of the alkaline transition of cytochrome c is a weighted average of all possible alkaline isomerizations, the overall reduced stability of the native protein suggests that the pK_{ap} for the formation of this new Lys72-bound state is less than 7.9. Cytochromes c with an alkaline transition pK_{ap} even lower than 7 are known to exist (for $e.g.$, Phe82Gly, Pearce $et\ al.$, 1989; Barker & Mauk, 1992; Pro71Thr, Wood $et\ al.$,1987; Pro76Gly, Wood $et\ al.$, 1988 a and b).

The formation of a new alkaline conformer with Lys72 bound to the heme iron is confirmed by the ^{1}H-NMR spectrum of the Tml72Lys variant (Figure 40) which is significantly different from the spectrum of the trimethylated yeast cytochrome measured at alkaline pH. Magnetization transfer experiments reveal that the peaks at 22.4, 20.6, and 15.1 ppm correspond to protons that are in chemical exchange with the native heme 8-methyl group of the protein. The possibility exists that at least one of these peaks arises from a pure NOE interaction between the saturated protons and a nearby group; nevertheless, these peaks are tentatively assigned to heme 8-methyl groups of three alkaline isomers. Similarly, the resonance at 21.2 ppm is assigned to the heme 3-methyl group in one alkaline state based on the magnetization transfer observed upon inverting the corresponding resonance in the native conformer.

The identification of a new alkaline conformer in the Tml72Lys variant is further supported by the restoration of the pK_{ap} of the protein to 8.65(2) when Lys72 is replaced with an alanyl residue. Comparison of the neutral and alkaline ^{1}H-NMR spectra of the Lys72Ala variants expressed in bacteria and yeast reveals that these proteins are spectroscopically indistinguishable (Figure 40). Although these results support the formation of a Lys72-bound alkaline state conclusive evidence necessitates scrutiny of the Lys73Ala/Lys79Ala variant of cytochrome c expressed in $E.\ coli$.
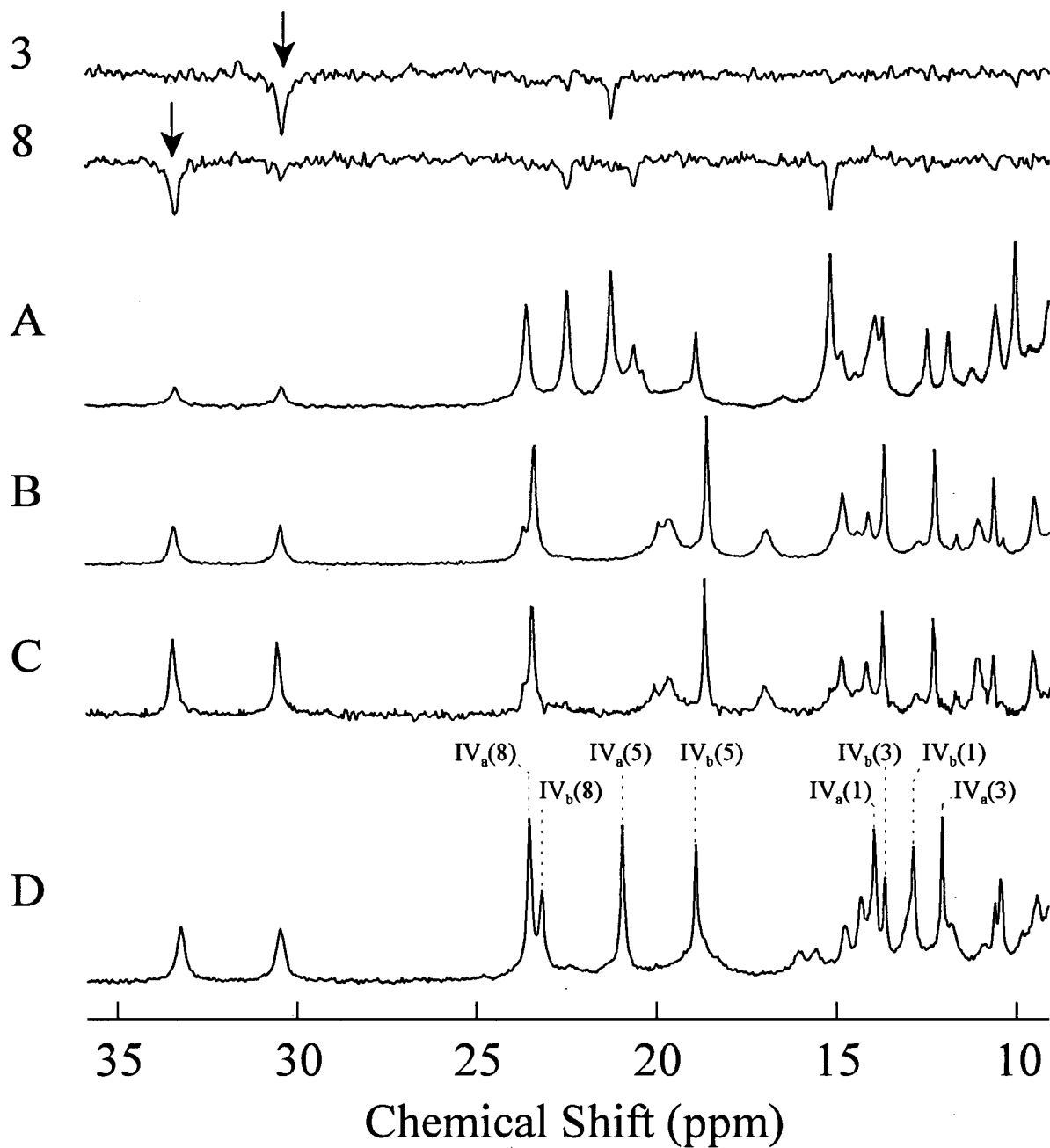
Figure 40. Downfield hyperfine shifted 200 MHz ^{1}H-NMR spectra of yeast *iso*-1- ferricytochromes *c* expressed in *E. coli* ((A) Tml72Lys ("wild-type"), (B) Lys72Ala)) and in yeast ((C) Tml72Ala variant, (D) wild-type). Protein samples (~3 mM) were prepared in 25 mM each, sodium phosphate and sodium borate buffers, pH* ~9.3, and spectra were measured at 45 °C. The difference spectra obtained from inversion transfer experiments in which the heme 8-methyl (8) or the heme 3-methyl (3) groups of the native conformer were selectively inverted (indicated with an arrow) are also shown. Peak assignments are as in Figure 24.

3.7   Effect of Other Point Mutations on the Alkaline Transition

3.7.1   Phe82Xxx

Phe82, a highly conserved residue in cytochrome c sequences, has been replaced with all naturally occurring amino acids (Pielak *et al.*, 1985; Inglis *et al.*, 1991). In the X-ray crystal structure of the wild-type yeast protein, the aromatic ring of Phe82 lies almost coplanar and adjacent to pyrrole rings B and C on the distal side of the heme (Figure 41), The alkaline transition of the variants with the Phe82→Gly, Lys, Ser, Asp, His, Met, Trp, and Ile replacements is characterized in this work. In all eight variants, the native state is destabilized significantly to alkaline pH (Table 12). The downfield hyperfine-shifted ^{1}H-NMR spectra of the native forms of these variants are shown in Figure 42. Distinctive spectroscopic features of the native protein can be recognized. However, under more alkaline conditions, the spectra of some of these proteins bear little resemblance to those of the wild-type protein or the Lys→Ala variants (Figures 24). Peak assignments were not attempted. The only criteria used for assessing what alkaline isomers are formed and their approximate distributions are (i) similarities to assigned spectra, (ii) confirmation from EPR analysis, (iii) the relative peak intensities of groups of resonances, and (iv) the dependence of signals on temperature or pH.

The ^{1}H-NMR spectra of the Phe82Gly and Phe82Ser variants measured at mildly alkaline pH are compared to spectra of wild-type cytochrome c in Figure 43 (Ferrer, unpublished). As for the wild-type protein, it appears that each of these variants have two alkaline conformers. Whereas in the wild-type cytochrome the two alkaline isomers are formed at about equal proportions, the smaller side chain at position 82 favours one alkaline transition over the other. This bias is more obvious at higher temperature where one conformer is 3-4 times more abundant (Table 12). On the basis of this temperature dependence, it appears that the Lys73-bound conformer is the preferred species at alkaline pH for these two variants. This assignment is consistent with the relatively low pK_{ap} for the
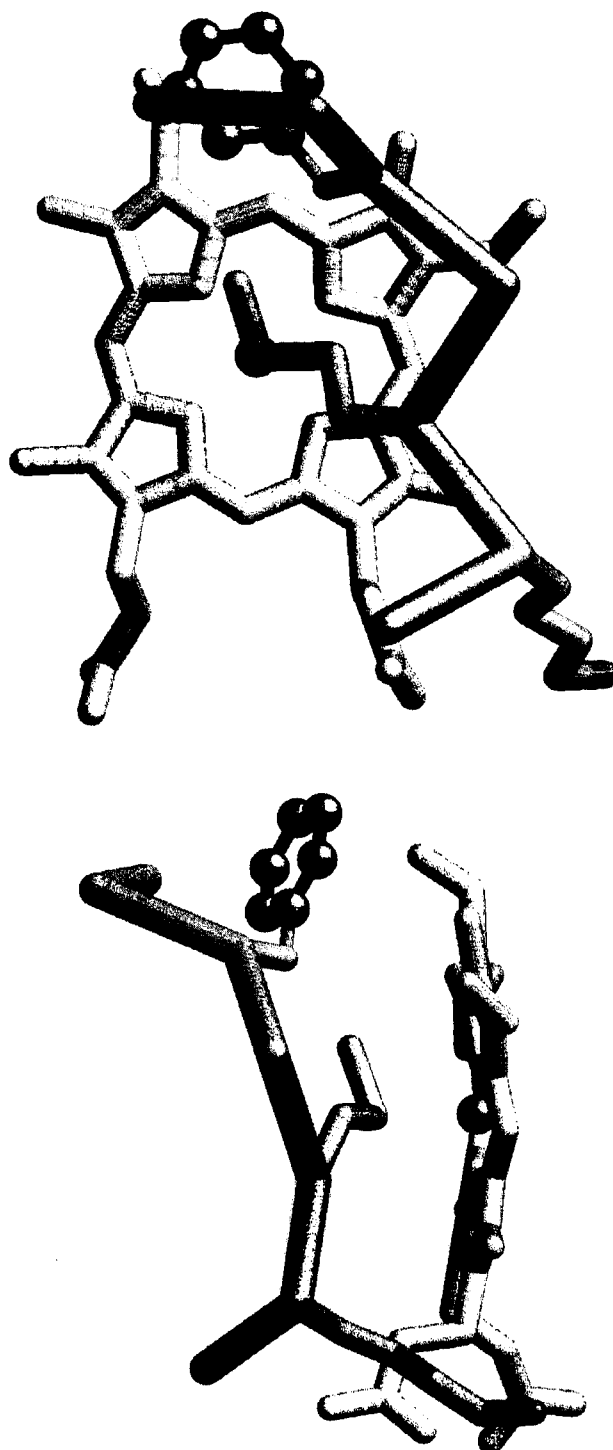
Figure 41. Detail of the native three-dimensional structure of yeast *iso*-1-ferricytochrome *c* showing the position of Phe82 (red) in relation to the heme prosthetic group (white). The iron is illustrated in orange. The native Met80 ligand and one of the alkaline ligands (Lys79) are also shown.
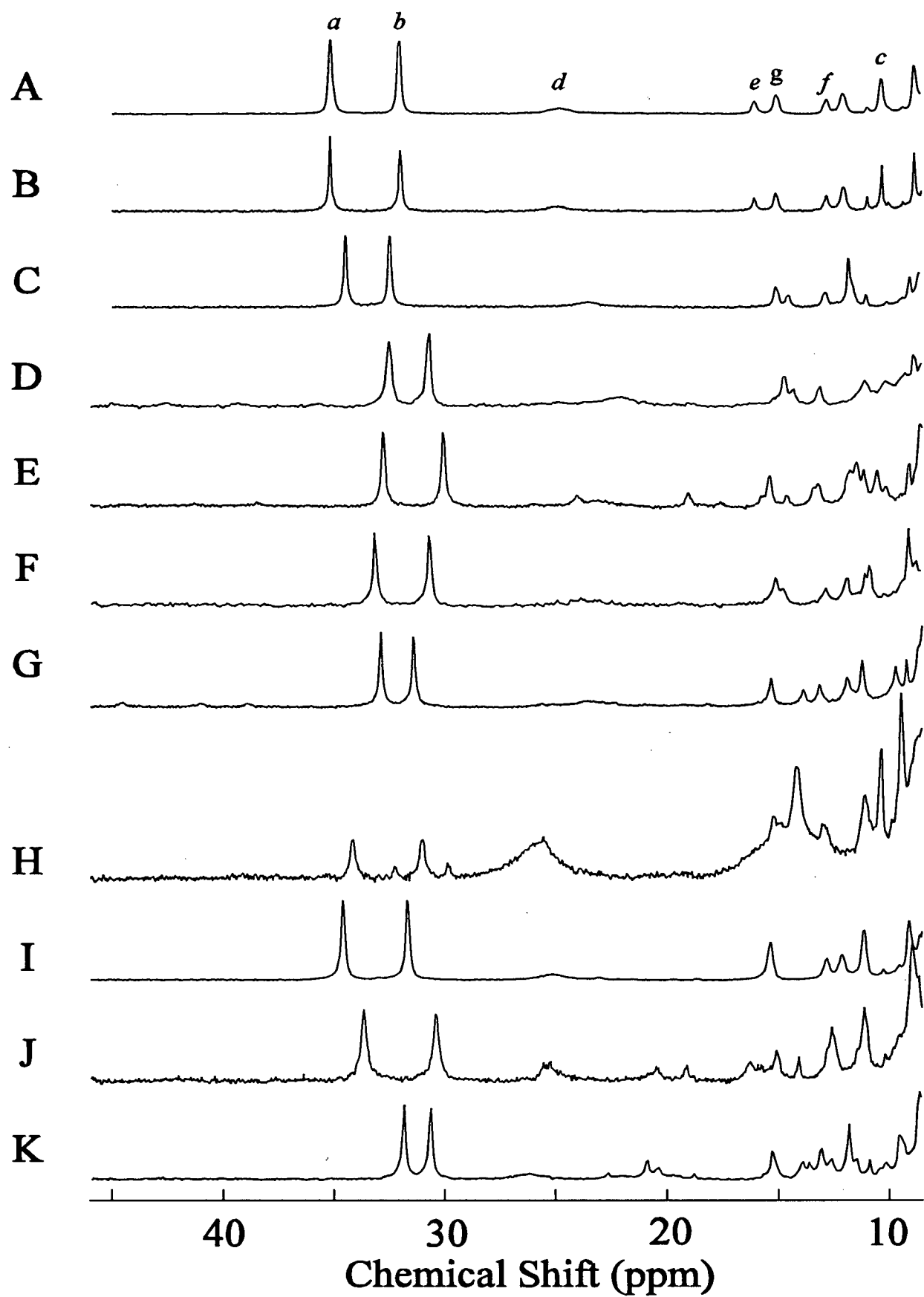
Figure 42. Downfield hyperfine ^{1}H-NMR spectra of yeast *iso*-1-ferricytochromes *c* measured at or near neutral pH (~2 mM protein 50 mM sodium phosphate buffer or 25 mM each sodium phosphate and sodium borate, 20 °C). (A) wild-type and the variants (B) Lys73Ala, (C) Lys79Ala, (D) Phe82Gly, (E) Phe82Lys, (F) Phe82Ser, (G) Phe82Asp, (H) Phe82His, (I) Phe82Met, (J) Phe82Trp, and (K) Phe82Ile. All spectra were measured at pH* 7.0 except for spectra E, G, and I which were recorded at pH* 6.5. The spectra are normalized with respect to the intensity of the heme 8-methyl group resonance except for the spectrum of the Phe82His variant for which the intensity of this peak is half that of the other spectra. The italicized labels denote the peaks that have been assigned in the wild-protein to (*a*), (*b*), and (*c*) heme 8-, 3-, and 5- methyl groups respectively, (*d*) His18 ϵ1-H, (*e*) and (*f*) propionate 7α-CH$_2$, and (*g*) His18 β-CH.

alkaline transitions of these proteins [~7.7; Pearce *et al.*, 1989].

Replacement of Phe82 by Asp, Met, or Ile also destabilizes the native conformation of cytochrome *c* considerably (Table 12). However, these variants differ from those above in that the native state is in equilibrium with one principal alkaline conformer. The EPR spectrum of the Phe82Asp variant measured at pH 8.9 (Figure 44) displays one major, non-native, low-spin species [g_z=3.29] and a minor component [g_z=3.46]. While the major peak at g_z=3.29 may correspond to Lys73 binding to the heme iron [g_z=3.33], the shoulder is more similar to the preparation-induced artifact that was encountered in the spectra of the Lys73Ala and Lys79Ala variants but still consistent with an amine-bound heme iron. The Lys72-bound alkaline conformer in the bacterially expressed cytochrome, and the *N*-methylamine adduct of the Lys73Ala/Lys79Ala variant also display similar signals [g_z~3.42 and 3.45, respectively].
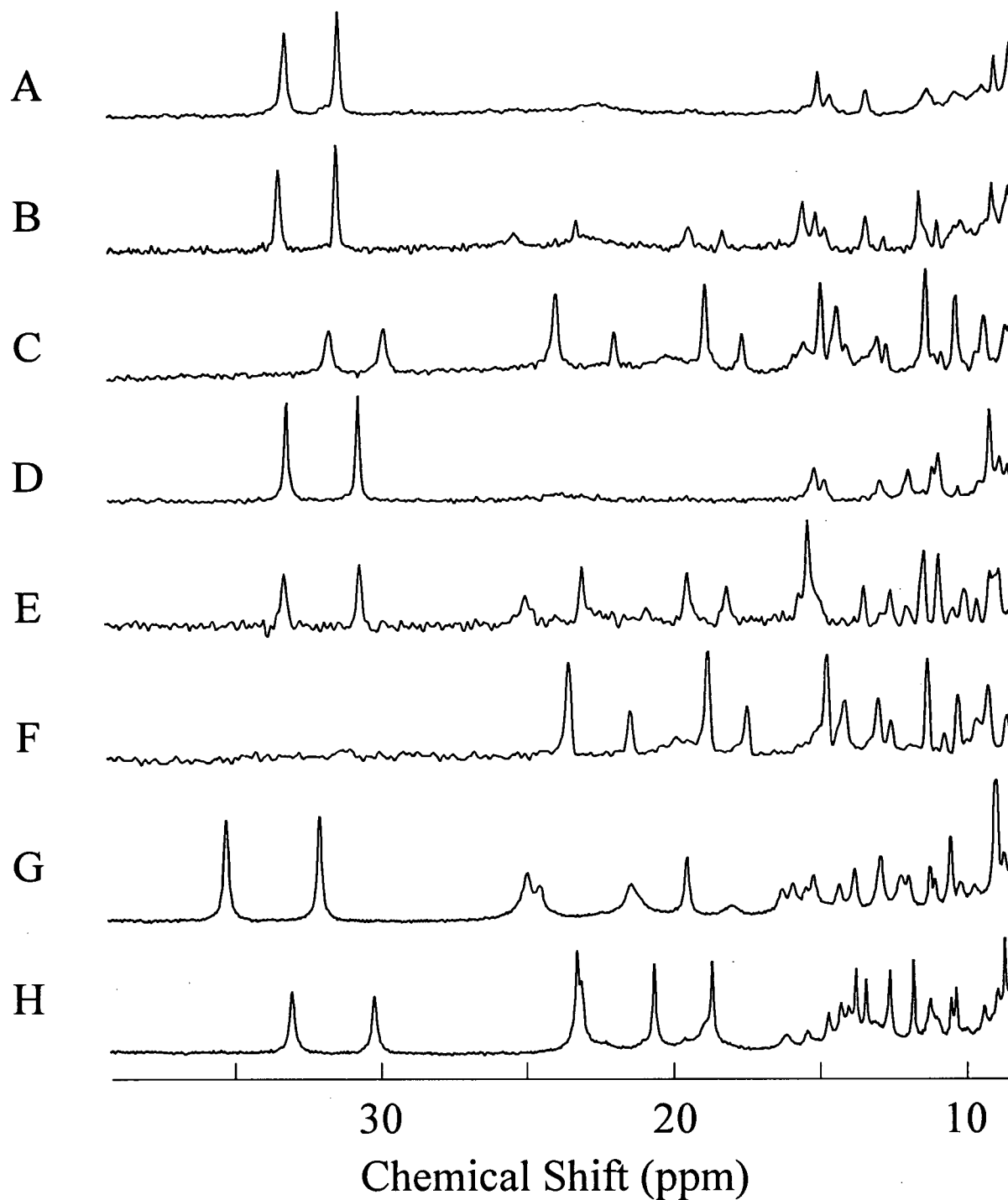
Figure 43. Comparison of the hyperfine shifted 200 MHz ^{1}H-NMR spectra of yeast *iso*-1-ferricytochromes *c*: variant Phe82Gly at (A) pH* 7.0, 20 °C; (B) pH* 8.0, 20 °C; (C) pH* 8.0, 40 °C; variant Phe82Ser at (D) pH* 7.0, 20 °C; (E) pH* 8.5, 20 °C; (F) pH* 8.5, 40 °C; wild-type cytochrome at pH* 9.3, (G) 20 °C; (H) 40 °C. Protein samples (~3 mM) were prepared in 50 mM sodium phosphate buffer.

121
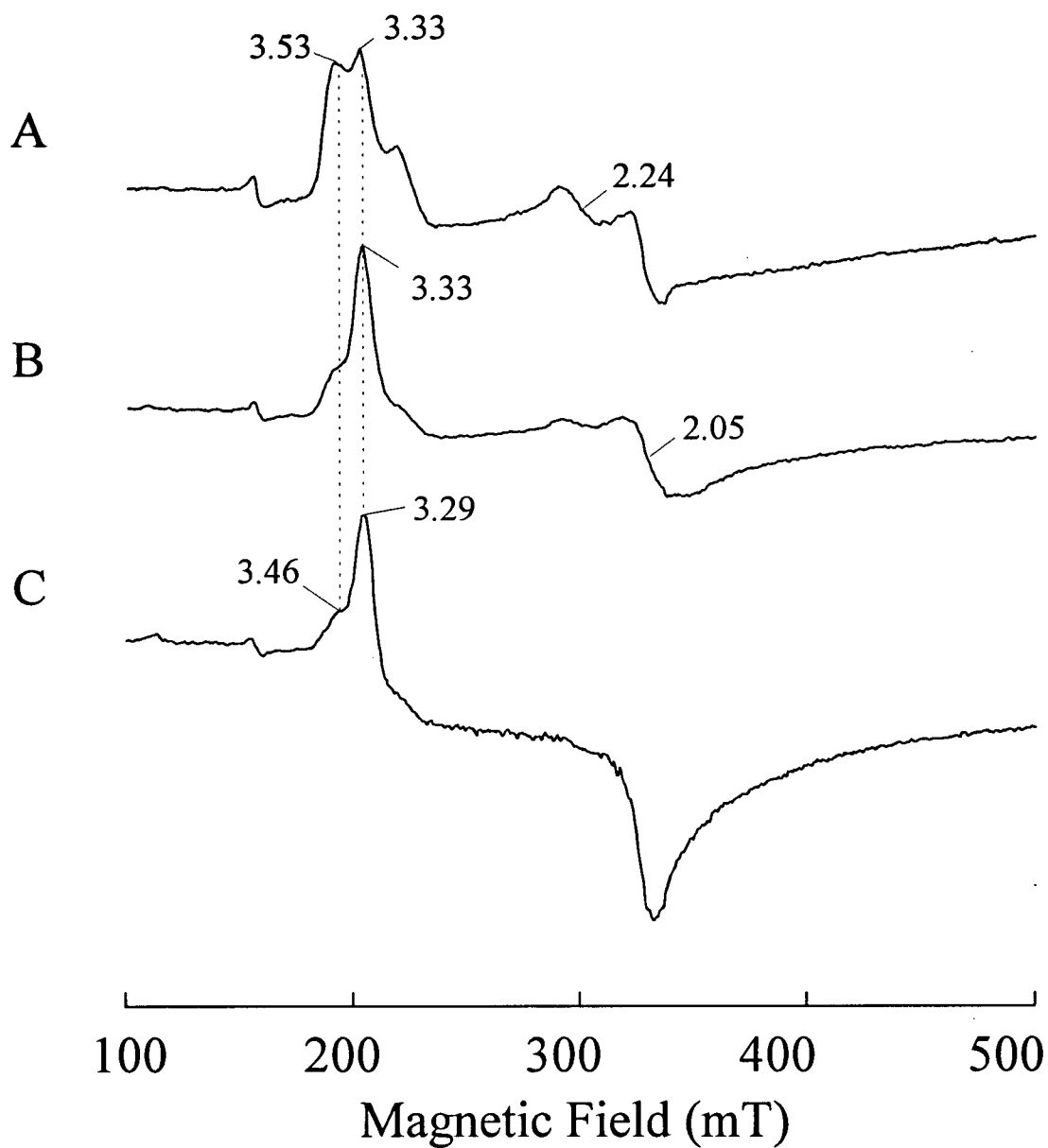
Figure 44. Comparison of the X-band EPR spectra of yeast *iso*-1-ferricytochrome *c*: (A) wild- type; and the variants (B) Lys79Ala and (C) Phe82Asp (~2 mM protein in 50 mM CAPS buffer, pH 8.9, 50% v/v glycerol, 10K(A and B), 4 K (C)).

Table 12. Alkaline transition of yeast *iso*-1-ferricytochrome *c* variants.

Variant	pK_{ap}	Major Alkaline Ligand(s)
wild-type	8.7	Lys73, Lys79
Lys73Ala	8.82	Lys79
Lys79Ala	8.44	Lys73
Phe82Gly	7.7[a]	Lys73
Phe82Lys	6.5	Lys73
Phe82Ser	7.7[a]	Lys73
Phe82Asp	7.4	Lys73
Phe82His	6.2, 9.9	His82, unknown
Phe82Met	7.1	Lys73
Phe82Trp	6.9; 10.0	RO⁻/OH⁻; Lys73, Lys79
Phe82Ile	7.2[a]	Lys73 ?
Tyr67Phe	10.7[b]	Lys79 ?
Thr78Ala	6.63	Lys73, Lys79
Met80Ala	na	Lys72

a Taken from Pearce *et al.* (1989).
b Taken from Luntz *et al.* (1989).

In the ^{1}H-NMR spectra of the Phe82Asp variant (Figure 45a), four peaks appear upon increasing the pH* that can be attributed to heme methyl group protons [22.4, 18.1, 15.6, and 13.1 ppm at 20 °C]. The smaller peaks that arise at higher pH* presumably correspond to the Lys79-bound conformer of this variant [25.6, 19.3, and 14.0 ppm at 20 °C]. Similarly, the ^{1}H-NMR spectra of the Phe82Met variant of cytochrome *c* (Figure 45b) are consistent with the formation of primarily one alkaline form. The four peaks at 23.2, 18.6, 13.0, and 11.6 ppm (20 °C) probably correspond to the heme methyl group protons. The peak at 13.0 ppm is coincident with that in the ^{1}H-NMR spectrum
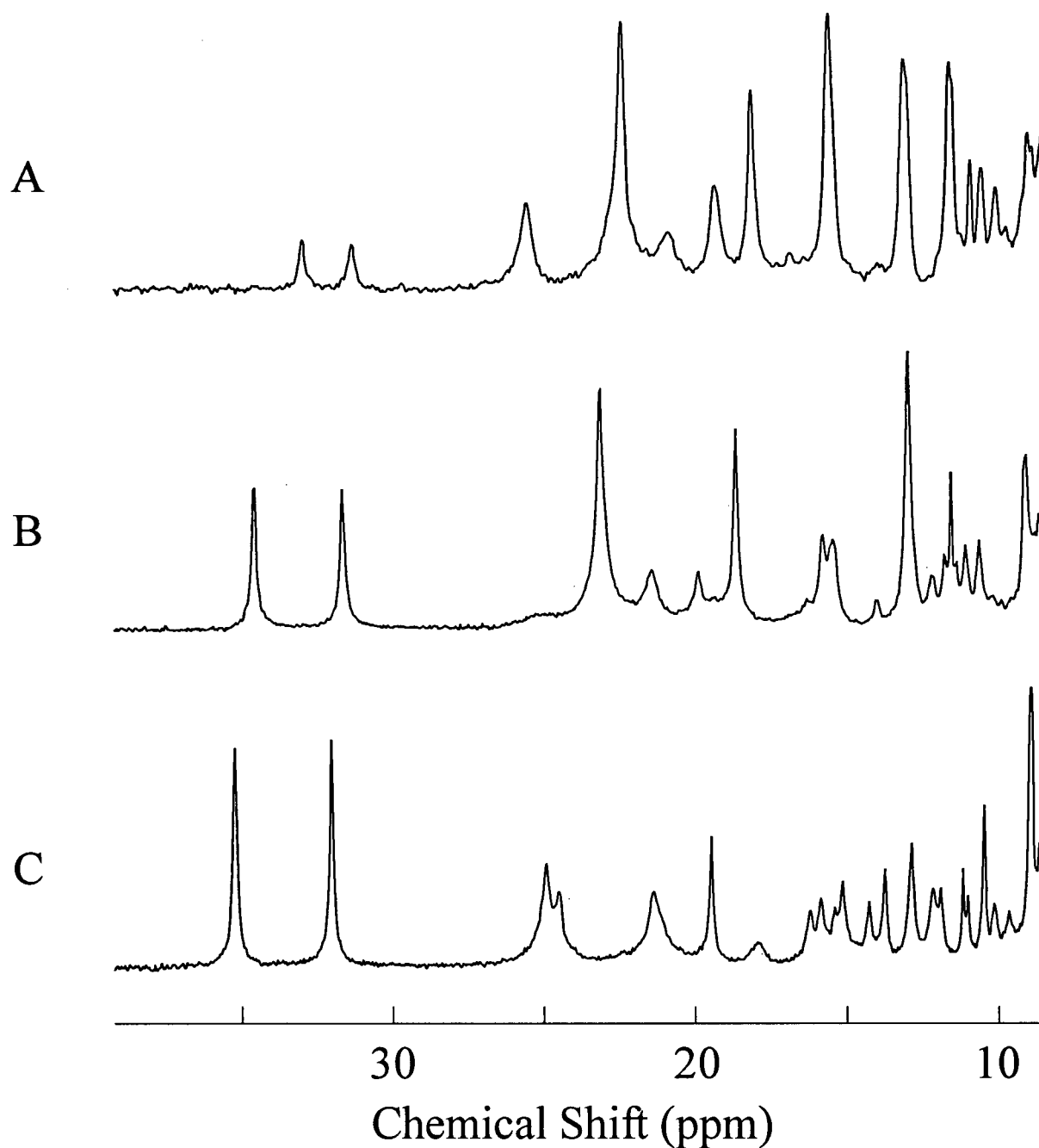
Figure 45. Comparison of the downfield hyperfine shifted 200 MHz ^{1}H-NMR spectra of yeast *iso*-1-ferricytochromes *c*: (A) Phe82Asp, pH* 8.9; (B) Phe82Met, pH* 8.2; and (C) wild-type, pH* 9.3. Proteins (~3 mM) were prepared in 25 mM each, sodium phosphate and sodium borate buffers (A and B) or 50 mM sodium phosphate buffer (C), and the spectra were measured at 20 °C.

of Phe82Asp; therefore, the major alkaline conformer of this protein is tentatively identified to have a Lys73-bound heme iron. This assignment is consistent with the observation that the less intense peak at 21.4 ppm (20 °C) is coincident with the peak corresponding to the heme 5-methyl group of the Lys79-bound alkaline conformer of the wild-type protein (Figure 24). The failure to align the remaining heme methyl group resonances in the spectra of the wild-type cytochrome or the Phe82Asp variant with other peaks in the spectra of alkaline Phe82Met, however, argues against this assignment.

The apparent deficit of peaks in the ^{1}H-NMR spectra of the Phe82Ile variant measured at high temperature and pH suggests that this protein undergoes the alkaline transition to a single alkaline conformer (Figure 46). Furthermore, the extremely low pK_{ap} of this protein [~7.2; Pearce *et al.*, 1989] also suggests that this alkaline conformer involves Lys73. Nevertheless, it is possible that the pair of peaks just above 20 ppm (20 °C; ~20 ppm at 45 °C) correspond to two species rather than to two functional groups of a single species. Both peaks shift upfield with increasing temperature, and the intensity of one species appears to vary at the expense of the other. Note that these peaks bear some remarkable similarities to those observed in the ^{1}H-NMR spectra of the Tyr67Phe variant (Figure 55) although the chemical shifts of the Tyr67Phe resonances exhibit a different temperature-dependence.

The introduction of a lysyl residue at position 82 could mimic the behaviour of the bacterially expressed cytochrome *c* in that this new amino acid is available to replace Met80 as an axial heme ligand and could thus potentially generate a third alkaline species. The low pK_{ap} of this protein (Table 12) supports the likelihood of the formation of this new alkaline form. However, EPR spectroscopy of the Phe82Lys variant of cytochrome *c* (Figure 47) reveals that below pH 10.7, only two species result from the alkaline transition of this protein. These species have g_z=3.47 and 3.28 [g_y~2.07, g_x~1.3]. The more abundant species [g_z=3.28] is that with Lys73 bound to the heme iron [g_z=3.33
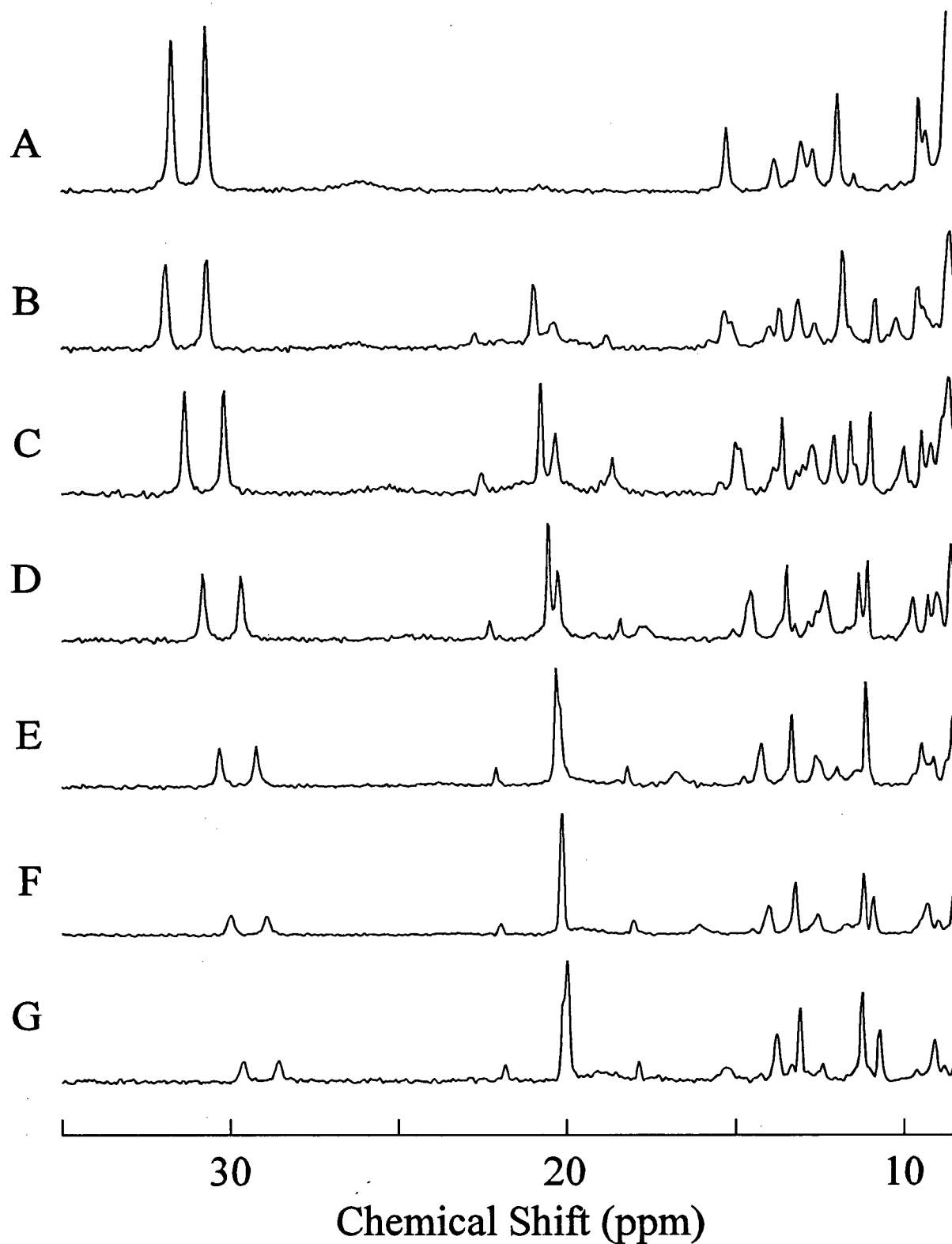
Figure 46. Downfield hyperfine shifted 200 MHz ^{1}H-NMR spectra of yeast *iso*-1-ferricytochrome *c* Phe82Ile (~3 mM protein in 50 mM sodium phosphate buffer) measured at (A) pH* 7.0, 20 °C; pH* 7.5 (B) 20 °C; (C) 25 °C; (D) 30 °C; (E) 35 °C; (F) 40 °C; (G) 45 °C.

126
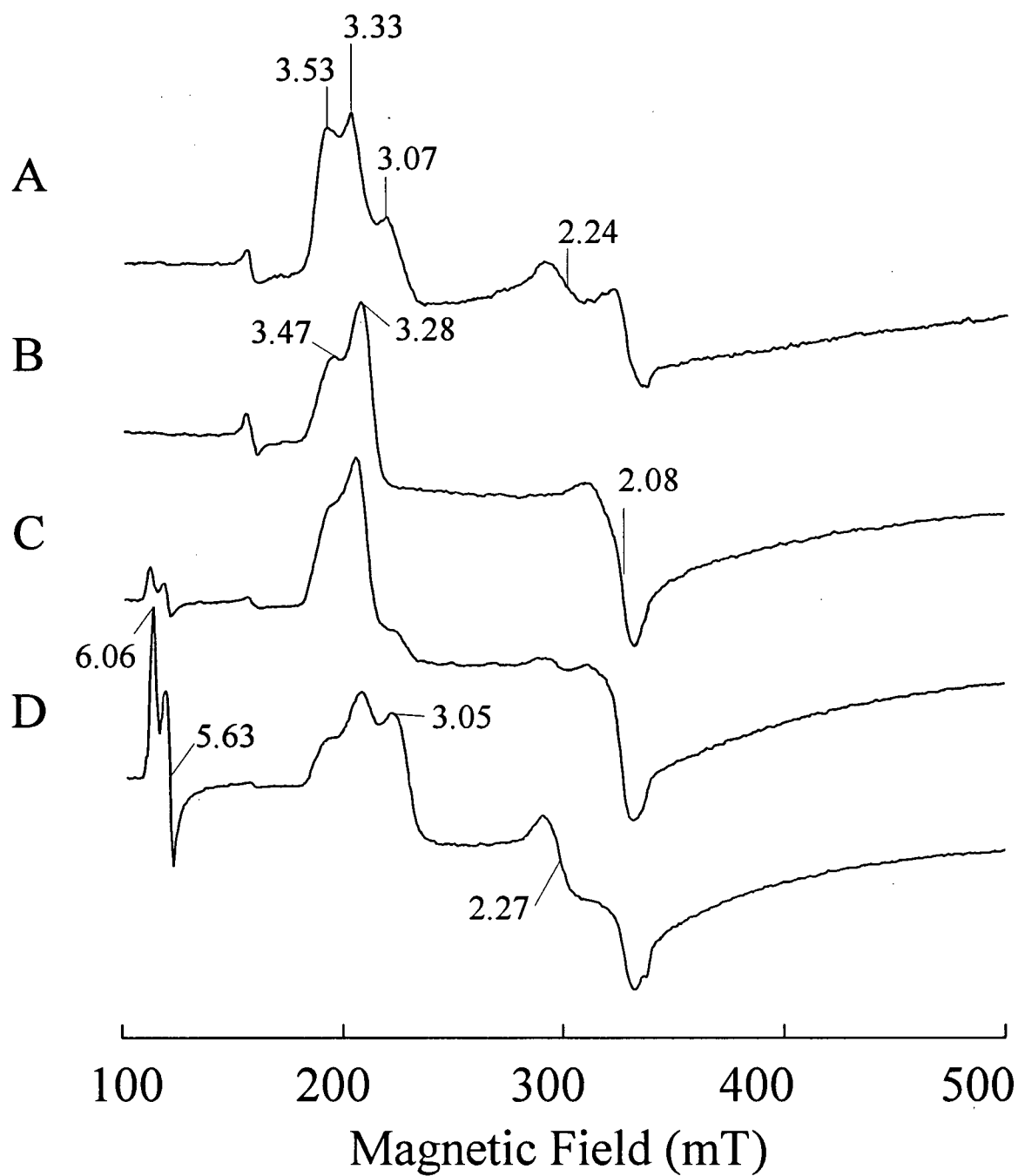
Figure 47. X-band EPR spectra of alkaline yeast *iso*-1-ferricytochrome *c*: (A) wild-type, pH 10.5; and the Phe82Lys variant (B) pH 10.7; (C) pH 7.9; (D) pH 6.4 (~2 mM protein, 50 mM CAPS buffer, 50% v/v glycerol, 10K).

in the wild-type protein] while the second species resembles the minor component of the Phe82Asp variant [g_z=3.46].

The ^{1}H-NMR spectrum of the Phe82Lys variant is consistent with the formation of only two alkaline species (Figure 48). The signals assigned to the heme 1, 3, and 8-methyl group protons of the Lys73-bound alkaline conformer in the wild-type protein spectra have close analogs in the spectra of the variant both in the high, and low temperature ranges. The larger peaks at 23.4, 14.0, and 12.3 ppm are thus in agreement with the EPR finding that Lys73 is the preferred alkaline conformer. Neither the EPR nor ^{1}H-NMR spectroscopy data suggest that Lys82 acts as a heme iron ligand. If a Lys82-bound alkaline conformer does form, the lower pK_{ap} of the protein implies that this would be the favoured conformer. However, the spectroscopic data do not support this. Therefore, the lower pK_{ap} of the Phe82Lys variant represents a true destabilization of the native structure rather than the formation of an energetically more favourable alkaline conformer as in the case of the bacterially expressed cytochrome.

In the oxidized state, the new histidyl residue in the Phe82His variant of cytochrome c is known to replace Met80 as a heme iron ligand even at neutral pH (Hawkins *et al.*, 1994; Schejter *et al.*, 1996; Feinberg *et al.*, 1998). The near-IR MCD and EPR spectra of this protein were reported to be characteristic of a bis-histidine coordinated, low-spin heme iron (Hawkins *et al.*, 1994). Although the alkaline transition properties of this variant were not reported, a pH titration of the protein (Figure 49) suggests that if a lysyl residue replaces the novel His ligand, the pK_{ap} for this transition is markedly higher (~10). Only minor spectroscopic changes are observed as the protein is titrated between pH 5.5 and 10. The data best satisfy a model consisting of four species and three deprotonations. This analysis yields values of pK_{ap}=6.2(3), 7.8(2) and 9.9(1) at 25 °C. While the first pK_{ap} would correspond to the replacement of Met80 by His82, the second may be linked to the
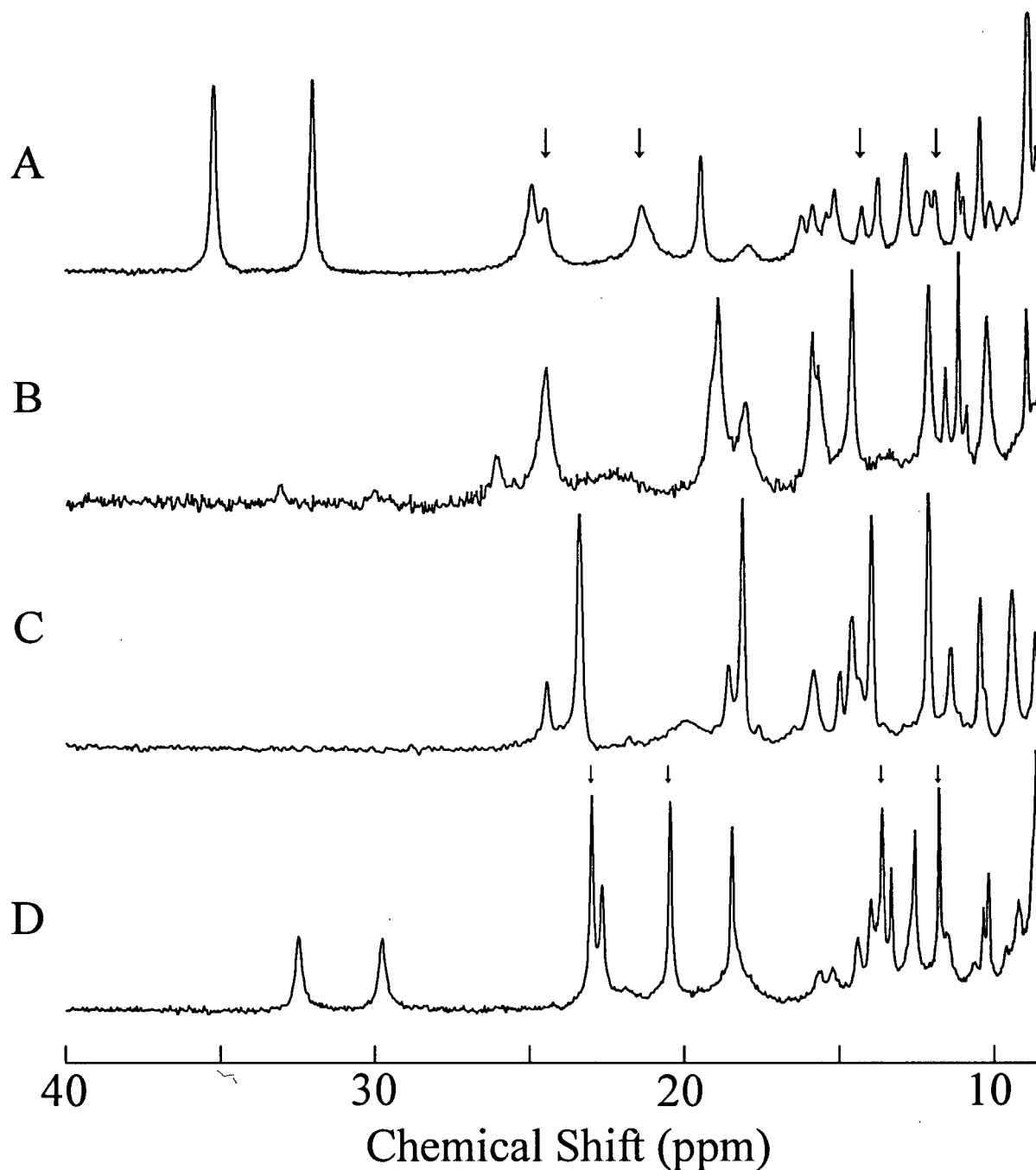
Figure 48. Comparison of the hyperfine shifted 200 MHz ^{1}H-NMR spectra of wild-type yeast *iso*-1-ferricytochrome *c* (A and D, pH* 9.3) and the Phe82Lys variant (B and C, pH* 8.4). Spectra (~3 mM protein in 25 mM each, sodium phosphate and sodium borate buffer) were measured at 20 (A and B) and 45 °C (B and C). The methyl group resonances corresponding to the Lys73-bound heme in the wild-type protein are indicated with arrows.
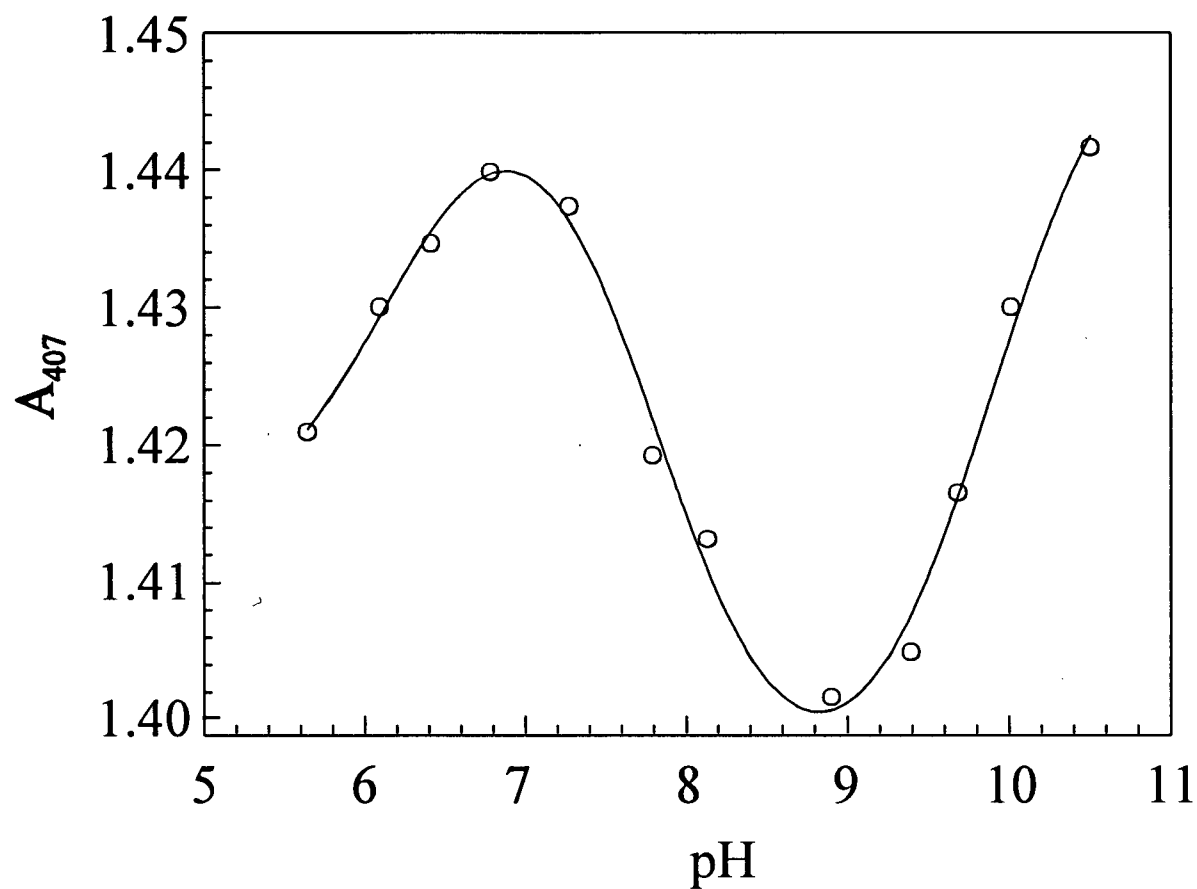
Figure 49. Single wavelength (A_{407}) titration analysis of the yeast *iso*-1-ferricytochrome c variant Phe82His. The curve represents the mathematical fit of the data to three pH-dependent processes with pK_{ap} values of 6.2(3), 7.8(2), and 9.9(1).

protonation state of the His82 ligand, and the third is probably associated with the formation of a Lys73- and/or Lys79-bound alkaline conformer(s).

^{1}H-NMR spectroscopy reveals that at least a small proportion of the Phe82His variant exhibits normal His-Met ligation even at pH* 7.5. The peaks at -21.0 and -29.9 ppm (Figure 50) may correspond to protons of Met80 that is bound to the heme iron (see Table 5) while the peaks at 34.2 and 31.0 ppm correspond to 8- and 3-heme methyl group protons. Assignment of the very broad features around 25 and 14 ppm to heme methyl group protons in the imidazole adduct are consistent with the work of Tang and coworkers (Shao *et al.*, 1995). The width of these features may imply that the histidine-bound species is experiencing rapid structural fluctuations. Furthermore, the peaks at 21 and 20 ppm are consistent with the 8- and 5-heme methyl group protons of a Lys-bound conformer as assigned in the equine, imidazole-bound cytochrome *c* (Liu *et al.*, 1996). The sharper peaks at 22.9 and 15.2 may correspond to the second Lys-bound form that is not observed in the imidazole adduct of the horse protein.

The Phe82Trp variant of cytochrome *c* undergoes two sequential heme-linked structural rearrangements between pH 5.5 and 10.5 (Table 12). Near neutral pH, the first process results in a high- or mixed-spin heme iron that is evident from the electronic spectra of the protein (Figure 51). An absorption maximum at ~600 nm reaches maximum intensity at pH 8.5, and it increases with temperature. Together with the blue-shifted Soret band, the spectrum of this stable intermediate is similar to that observed for the Lys73Ala/Lys79Ala variant of cytochrome *c* at pH~10.5. Increasing pH above 8.5 leads to the conventional spectrum of alkaline cytochrome *c* where the band at 600 nm is not present.

Inspection of the EPR spectra of the Phe82Trp variant (Figure 52) confirms that the protein is composed of multiple, pH-dependent species. At neutrality, two low-spin species [g_z=3.08 and
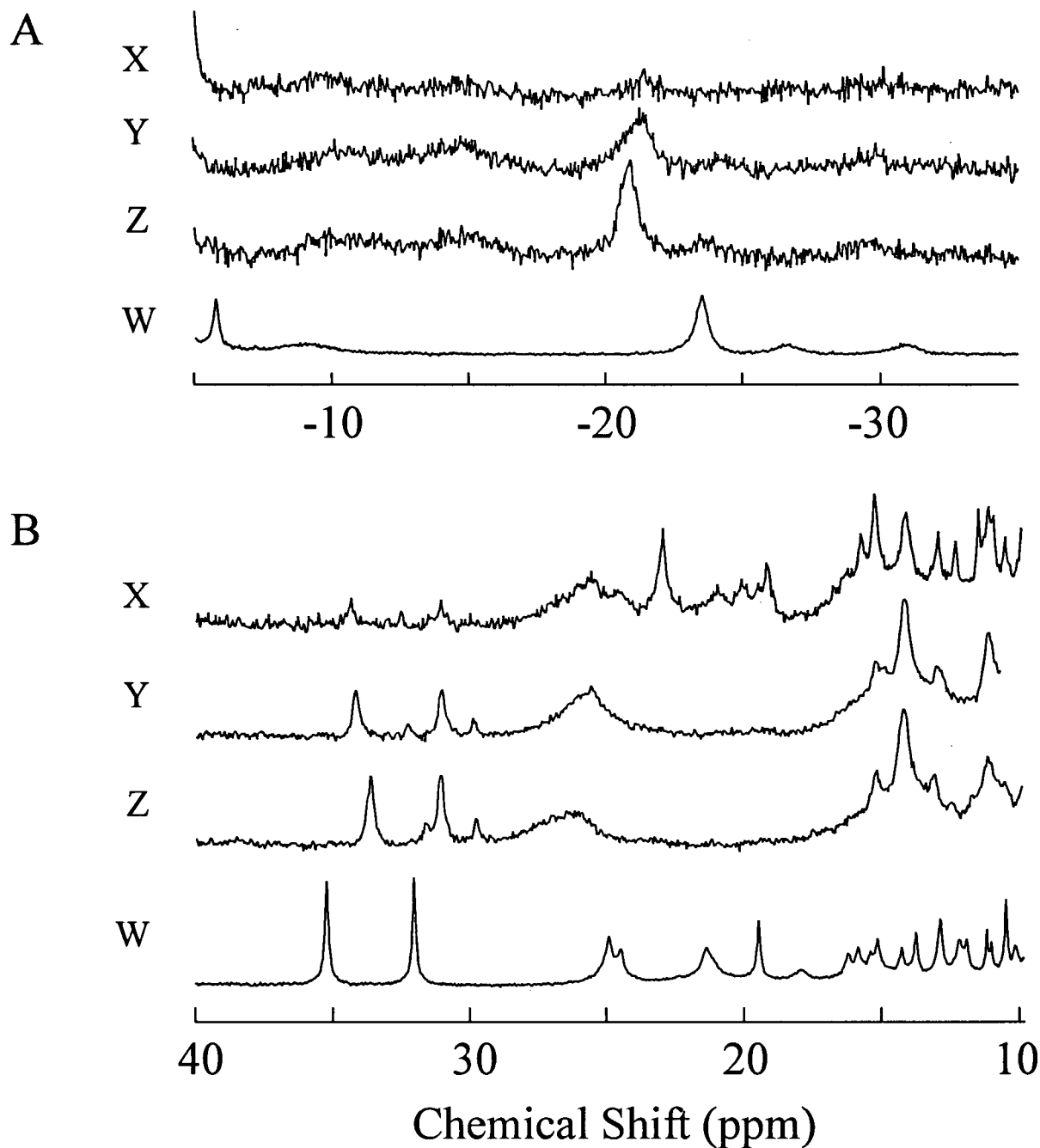
Figure 50. Comparison of the (A) upfield and (B) downfield hyperfine shifted ^{1}H-NMR spectra of (W) wild-type yeast *iso*-1-ferricytochrome *c* (~3mM in 50 mM sodium phosphate buffer pH* 9.3, 20 °C) and the Phe82His variant (~0.8 mM in 25 mM each, sodium phosphate and sodium borate buffers, 20 °C) at (X) pH*~8.4; (Y) pH* ~7.0; (Z) pH*~5.3.

132
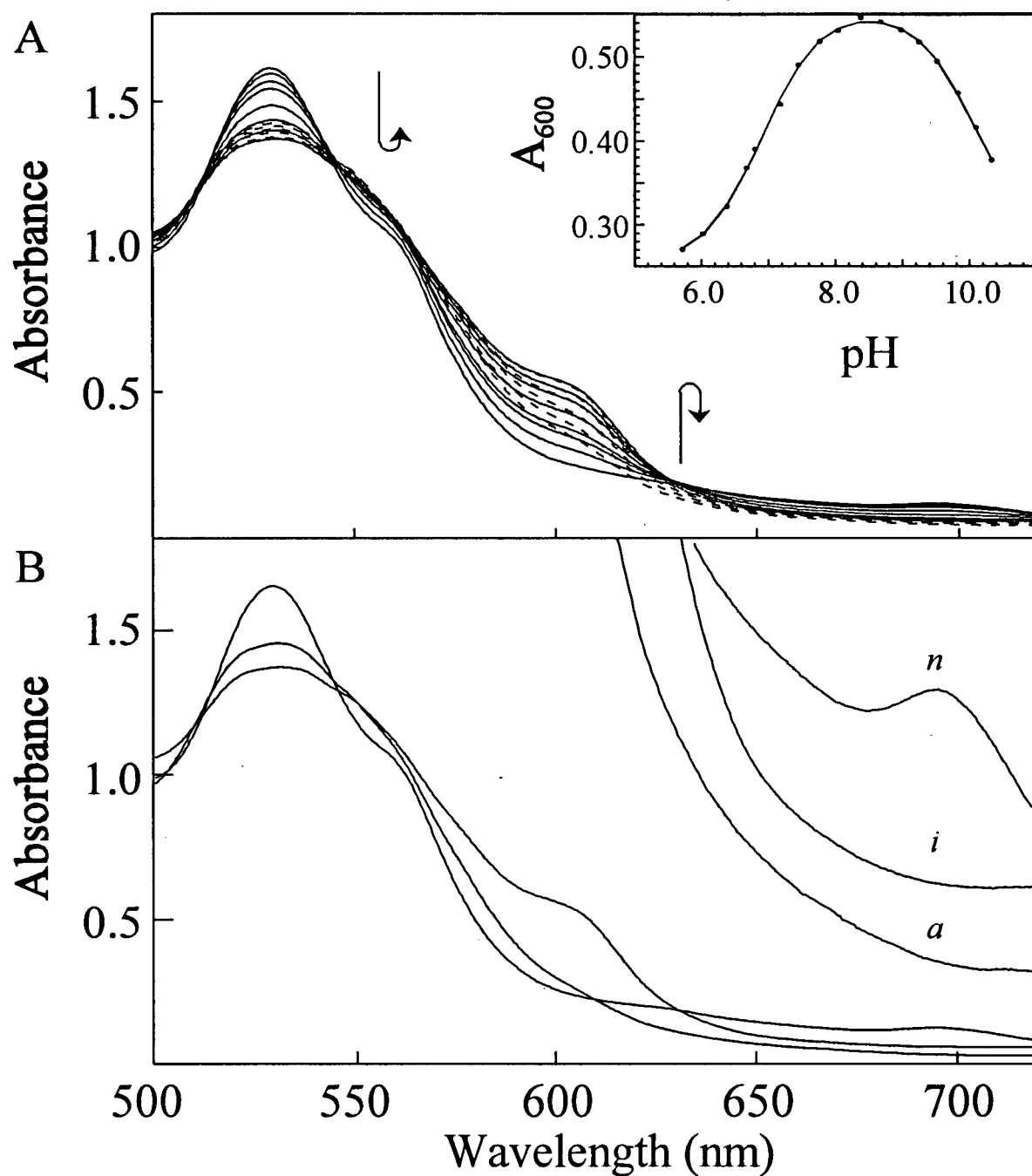
Figure 51. (A) Spectrophotometric titration of the yeast *iso*-1-ferricytochrome *c* variant Phe82Trp (~150 μM protein in 0.1 M sodium chloride, 25 °C) and (B) deconvoluted spectra derived from singular value decomposition analysis for a model were *n* (the native conformer) → *i* (a stable, high-spin intermediate) → *a* (the alkaline isomer(s)). In (A), the solid lines correspond to the spectra observed as the concentration of *i* increases, and the dashed lines correspond to the spectra observed as this intermediate decays

$g_z = 3.39$] coexist with a high-spin form of rhombic symmetry [$g = 6.02$ and 5.67]. The latter signals also appear in the EPR spectra of the Phe82Asp and Phe82Lys variants of cytochrome c, but these diminish with increasing pH such that at pH 9.1, they represent only a minor component. Increasing pH also results in the disappearance of the Met80-bound, native conformer [g_z=3.08] and the emergence of a second highly rhombic, high-spin species (S=5/2) [g_z=7.21 and g_y=4.67]. The latter spectroscopic characteristics are present even at pH 10.4 and are not unlike those observed in the spectrum of the His93Tyr variant of horse-heart myoglobin [g=7.13, g=4.89; 20 mM Tris, pH 8.0, 4K] (Hildebrand et $al.$, 1995). In this protein the proximal phenolate of Tyr93 binds to the oxidized heme iron to produce a 5-coordinate species that is spectroscopically similar to bovine liver catalase. This species also displays a 600 nm band in the electronic spectrum of the oxidized protein. For the Phe82Trp variant, the g_z=7.21 peak diminishes with increasing pH as a pair of low-spin species [g_z=3.38 and 3.27] emerge. The signal at g_z=3.39 probably corresponds to the Lys73-bound conformer of the protein, and that at g_z=3.27 may represent a subconformation of this alkaline conformer or alternatively, the Lys79-bound species.

^{1}H-NMR spectroscopy of the Phe82Trp variant above neutral pH also reveals the presence of a high-spin form. In the downfield region a set of three broad peaks [46, 42, and 36 ppm, 20 °C] is observed (Figure 53). This ^{1}H-NMR spectrum bears little resemblance to that of the His93Tyr variant of horse-heart myoglobin (Hildebrand, et $al.$ 1995). However, it has been suggested that in wild-type myoglobin, a similar profile corresponds to heme methyl groups of a hydroxide-bound, low-spin Fe^{3+} species that is in rapid exchange with a water-bound, high-spin heme (Iizuka & Morishima, 1975). The resonance frequencies of the broad ^{1}H-NMR peaks display a marked Bohr effect in myoglobin which results from the interaction of the water/hydroxide ligand and the distal His (E7) residue (Caughey, 1966). A six-coordinate, high-spin species is consistent with preliminary
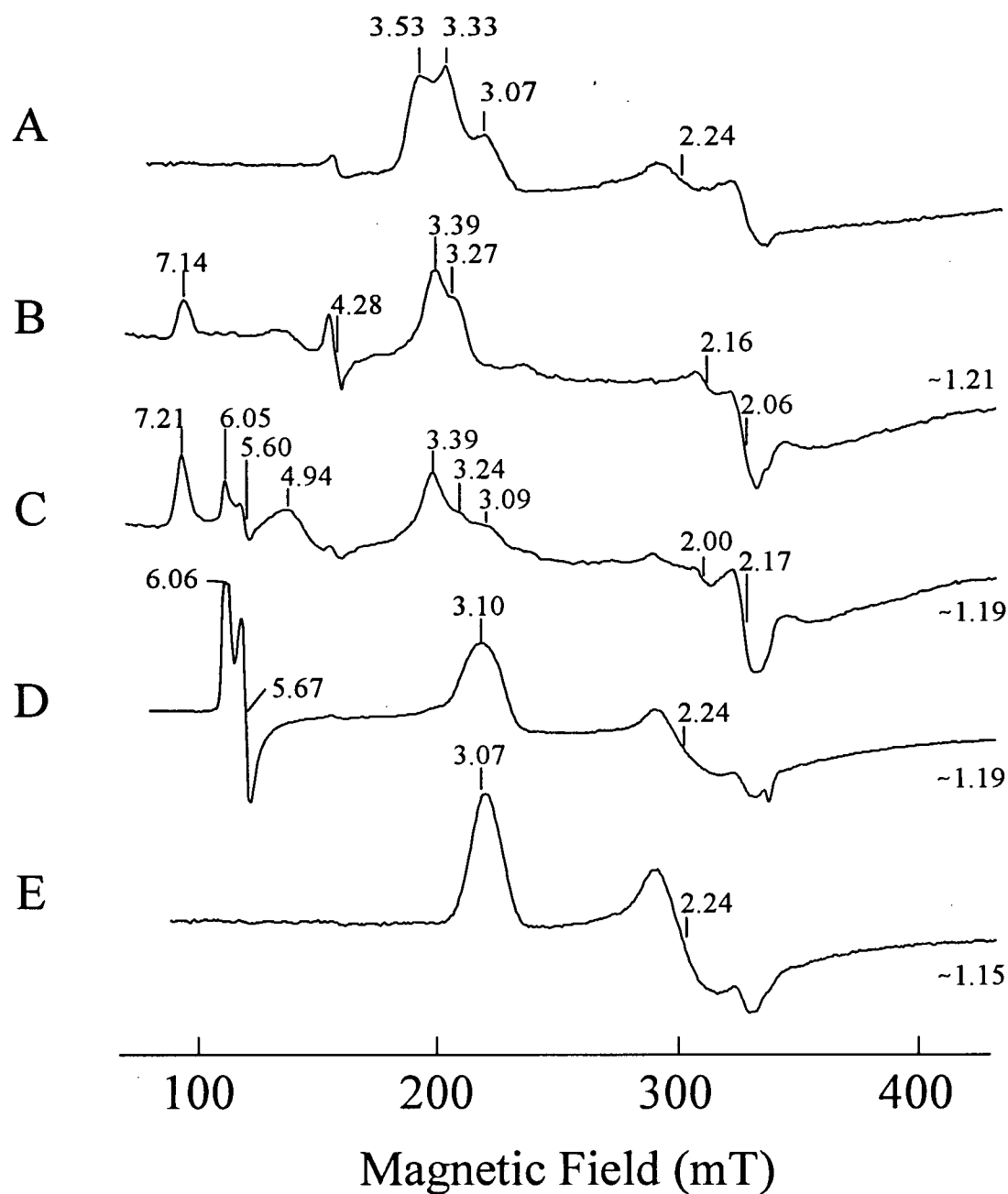
Figure 52. Comparison of the X-band EPR spectra of yeast *iso*-1-ferricytochromes *c*: wild-type ((A) 50 mM CAPS buffer, pH 10.5; (E) 50 mM MES buffer, pH 6.0), and the Phe82Trp variant (20 mM each, MES, TAPS, and CAPS buffers at (B) pH 10.8, (C) pH 8.3, and (D) pH 6.3). All samples (~2 mM protein) contained 50% v/v glycerol, and the spectra were measured at 10 K.

135
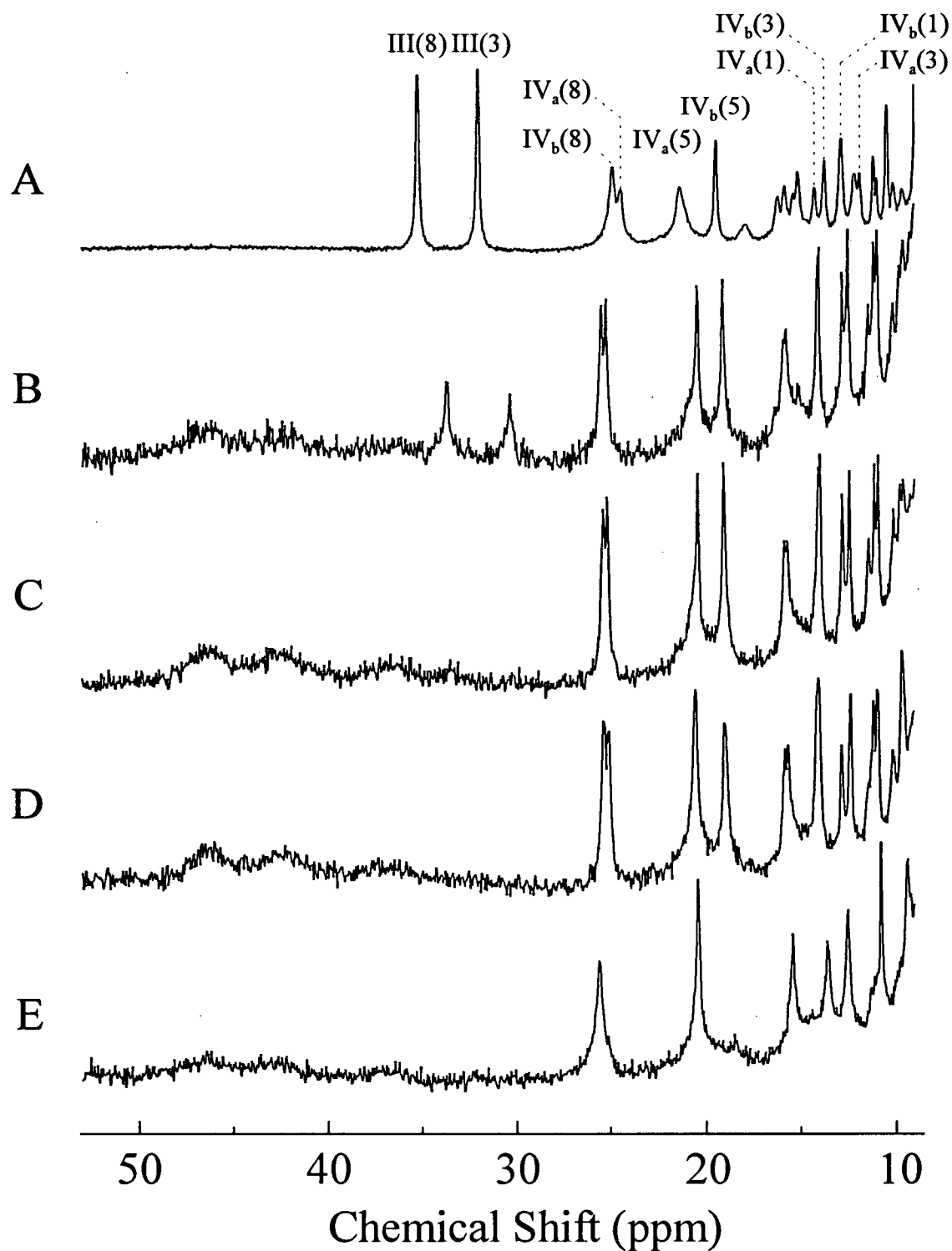
Figure 53. Downfield hyperfine shifted 200 MHz ^{1}H-NMR spectra of alkaline yeast *iso*-1-ferricytochrome *c*: (A) wild-type (50 mM sodium phosphate buffer, pH* 9.2), and the Phe82Trp variant (25 mM each, sodium phosphate and sodium borate buffer, (B) pH* 8.1; (C) pH* 9.1; (D) pH*; (E) pH* 10.9). Heme methyl group assignments are as in Figure 24.

resonance Raman analysis results of the Phe82Trp variant (Döpner & Hildebrandt, unpublished results). In contrast to myoglobin, however, the broad resonances in the spectra of the Phe82Trp variant of cytochrome c appear to be pH-independent. Presumably, the aqueous ligand may interact with the $\epsilon 1$ nitrogen of the Trp in a similar fashion, but this interaction is impervious to pH over the range studied here. Note that the binding of an endogenous hydroxyl group to the heme iron is an alternative to the H_2O/OH^--bridged Trp82-heme iron interaction. Tyr67 and Thr78 could, in principle, participate in such a structure. At this time, however, the identity of the sixth ligand to the heme iron is unknown.

A doublet at ~25.3 ppm that first appears at pH^* ~7 probably corresponds to alkaline heme 8-methyl group protons of two alkaline conformers while those at 20.5 and 21.2 ppm may be associated with the protons of the heme 5-methyl groups. More specifically, the peaks at 25.2 and 19.0 ppm (20 °C) are assigned to the Lys79-bound alkaline conformer of cytochrome c based on the similarity of the pattern of the resonant frequencies with corresponding peaks in the spectra of the wild-type protein. The presence of these alkaline features even at pH^* 7.0 conflicts with the global analysis of the spectrophotometric pH titration data. Supposedly, at pH 8.5 most of the sample consists of the stable high-spin intermediate while only a small proportion of the protein is present in either the native or alkaline states. At this pH^*, the total area subtended under the peaks that are tentatively assigned to heme 8-methyl group protons (native and alkaline) in the ^{1}H-NMR spectra is approximately one third the area bound by the corresponding peak of the native protein in the spectrum measured at pH^* 7.0. On this basis, it is estimated that the remaining 70 % of the protein is composed of the H_2O/OH^--bound species.

Above pH^* 10, the ^{1}H-NMR spectra of the Phe82Trp variant illustrate the persistence of the high-spin species. Interestingly, the distribution of alkaline conformers changes drastically from

apparently equal parts of Lys73- and Lys79-bound cytochrome c to almost entirely the Lys73-bound alkaline conformer by pH* 10.9. This result is in good agreement with the observation from EPR analysis and suggests that the low-spin species with $g_z=3.27$ (Figure 52) is indeed a strained subconformation of the Lys73-bound alkaline isomer.

3.7.2   Tyr67Phe

Tyr67 is another highly conserved residue in cytochromes c that is located in the distal side of the heme pocket (Figure 54). Together with Thr78, Tyr67 forms a hydrogen bond network via a bridging water molecule (H_2O166) (Berghuis & Brayer, 1992). In rat cytochrome c, mutation of Tyr67 to Phe enhances the stability of the native conformer of the molecule both at the acidic and alkaline extremes (Δ pK_{ap}=0.7 and 1.2 pH units respectively) (Luntz et $al.$, 1989). The increased stability of the Tyr67Phe variant of the yeast protein is evident in the ^{1}H-NMR spectra (Figure 55). Even at pH* 10, 25 °C, features of the native conformer predominate. What is not obvious is whether one or two alkaline isomers are formed at this high pH. Some spectroscopic features make this protein remarkably similar to the Phe82Ile variant, namely the pair of peaks at ~20.5 ppm which may correspond to heme 8-methyl group protons of two conformers. If speculation that Lys73 is the preferred ligand in the Phe82Ile variant at high pH is correct, then the opposite temperature dependence of the intensity of the peaks in spectra of Tyr67Phe indicate that Lys79 is the predominant ligand in this case.

pH-Jump experiments with the Tyr67Phe variant above pH 10 fail to detect a transient band at 600 nm, at variance with the behaviour exhibited by other cytochrome c variants described thus far. Assuming that the high-spin species in the Phe82Trp variant arises from a H_2O/OH^- or a phenolate-bound Fe^{3+}, the failure to observe the transient in the high pH-jump experiments of the
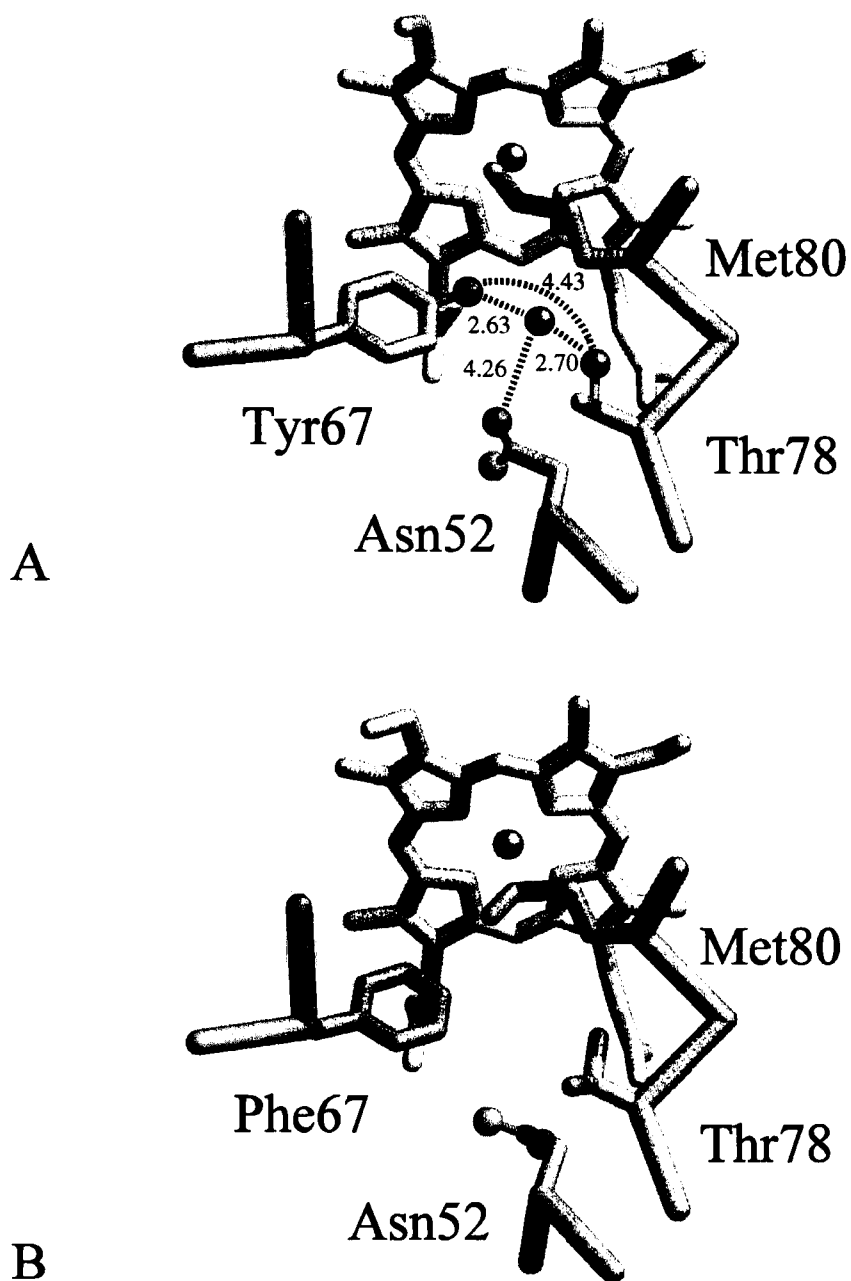
Figure 54. Comparison of the three-dimensional crystal structures of (A) wild-type yeast *iso*-1-ferricytochrome *c* showing the interatomic distances (Å) between Asn52, Tyr67, Thr78, and H₂O166, and (B) the Tyr67Phe variant. Note that in the crystal structure of the oxidized variant (1CTY.PDB), no water molecule equivalent to H₂O166 could be located in the electron density map. However, the presence of two water molecules at this site in the reduced form of the variant, suggests that these molecules are also present in the oxidized protein, but they are moving too rapidly for detection.
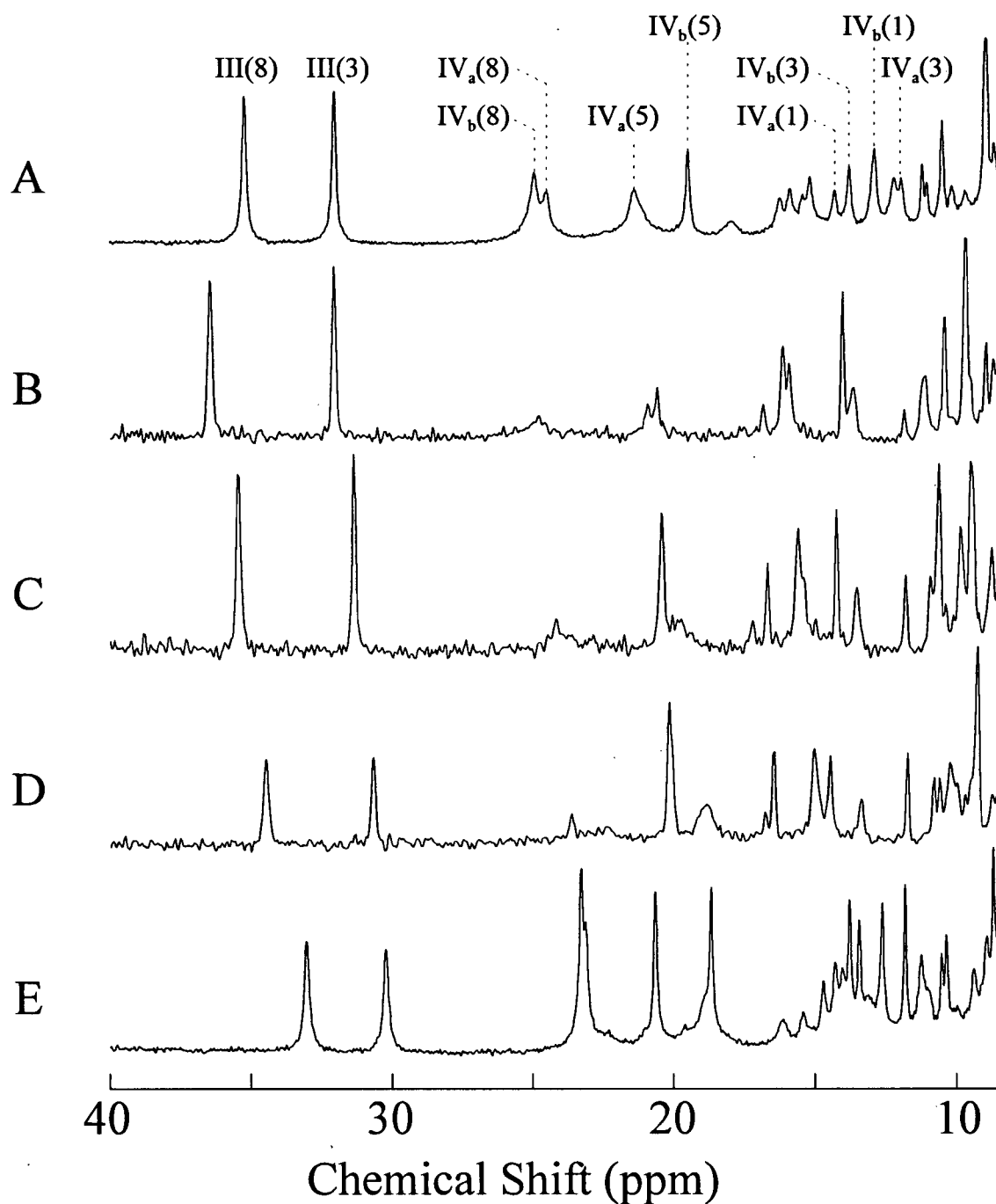
Figure 55. Hyperfine shifted region of the 200 MHz ^{1}H-NMR spectra of alkaline yeast *iso*-1-ferricytochrome *c* (A and E) wild-type, pH* 9.3 ((A) 20 °C and (E) 40 °C), and (B-D) the variant Tyr67Phe, pH* 10 ((B) 20 °C, (C) 30 °C, and (D) 40 °C) (~3 mM protein in 50 mM sodium phosphate buffer). The peak assignments are as in Figure 24.

Tyr67Phe cytochrome c is consistent with the involvement of the wild-type tyrosyl residue or its hydrogen-bonded water molecule in the alkaline transition of the wild-type protein.

3.7.3 Thr78Ala

In addition to its interaction with H_2O166 (Figure 54), Thr78 is hydrogen bonded to Lys79 and the heme 6-propionate group. A crystal structure of the Thr78Ala is presently unavailable to define the consequence of removing the gamma hydroxyl group of Thr78 on the positioning of H_2O166. However, this replacement is likely to weaken the native conformation of cytochrome c because the hydrogen bond to the propionate group does not exist, and the hydrogen bond network that includes H_2O166 is perturbed. Therefore, the properties of the heme prosthetic group should also be affected. The midpoint potential of the Thr78Gly variant at pH 6, for example, is 40 mV more negative than the wild-type protein (Rafferty, 1992). A decrease in potential is generally a consequence of increased solvent exposure of the heme which affects the dielectric constant of the environment around the prosthetic group. Also, the native structure of this variant is destabilized significantly under alkaline conditions (Δ pK_{ap}=-1.4) (Rafferty, 1992). Singular value decomposition analysis of the pH titration data for the Thr78Ala variant reveals that the transition between states II and III occurs with a pK_{ap}~4.2. Spectroscopic features of a high-spin species [λ_{max}=623 nm] are detectable in the electronic spectra of the protein at mildly acidic pH. Furthermore state III isomerizes into the alkaline conformers with a pK_{ap}=6.63(7), 0.5 pH units lower than what is observed for the Thr78Gly variant.

^{1}H-NMR spectroscopy illustrates that the Thr78Ala variant of cytochrome c undergoes two alkaline transitions (Figure 56). The downfield region of these spectra are not too dissimilar from that of the corresponding spectra of the wild-type protein measured under alkaline conditions (Figure 24).
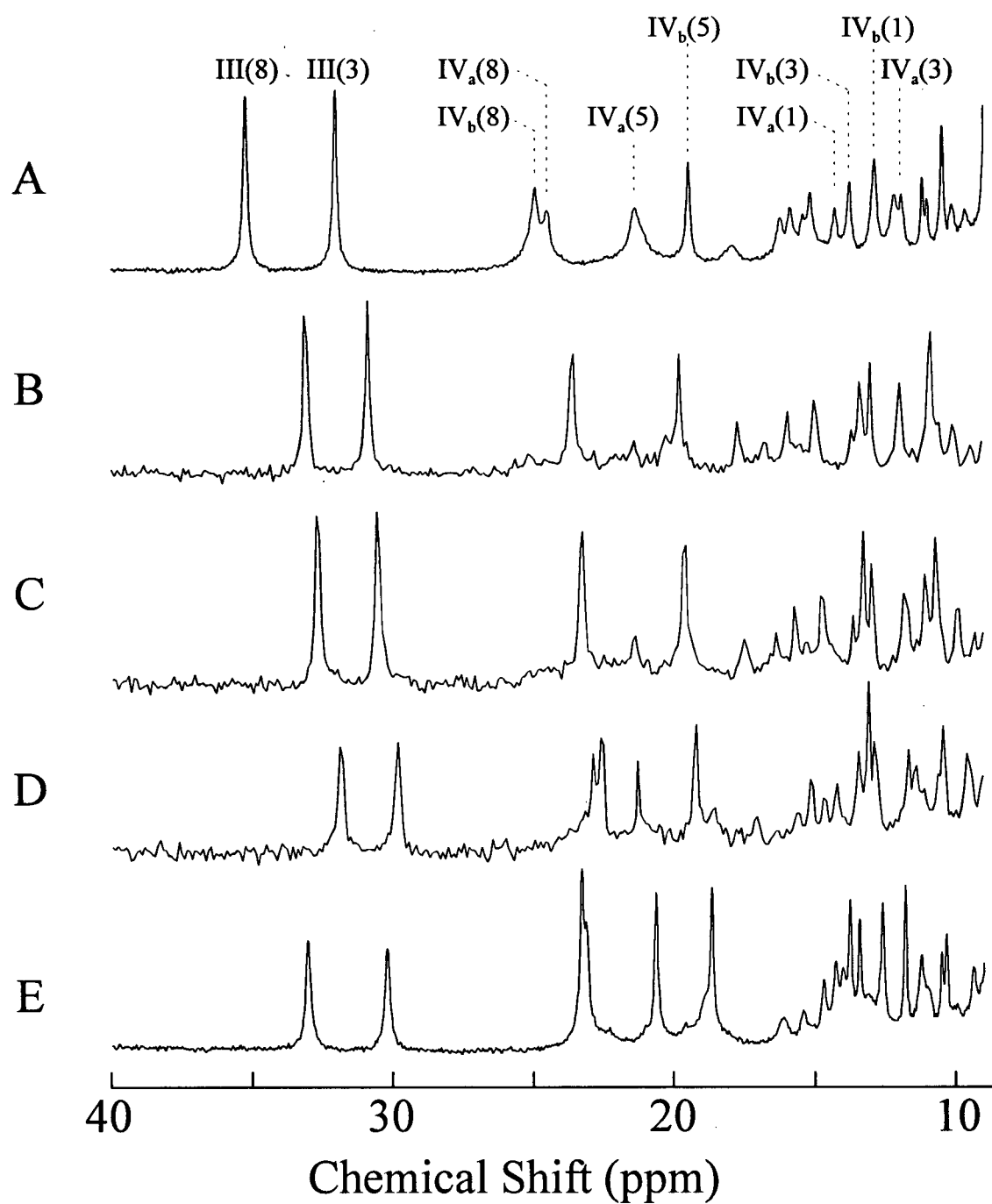
Figure 56. Downfield hyperfine shifted 200 MHz ^{1}H-NMR spectra of yeast *iso*-1- ferricytochromes *c*: wild-type, pH* 9.3 ((A) 20 °C; (E) 40 °C), and the Thr78Ala variant, pH* 7.2 ((B) 25 °C; (C) 30 °C; (D) 35 °C) (~3 mM protein in 50 mM sodium phosphate buffer). Peak assignments are as in Figure 24.

Furthermore, the spectra of the Thr78Ala variant also reveal that at pH^* 7.2, 25 °C, the preferred alkaline conformer is that with Lys79 bound to the heme iron. It is only at higher temperatures that the Lys73-bound conformer becomes apparent.

3.7.4 Tml72Lys/Met80Ala

Not surprisingly, the variant of yeast *iso*-1-cytochrome *c* with alanine at position 80 resembles myoglobin in that it can readily bind a variety of ligands in the oxidized and reduced states (Bren, 1996; Banci *et al.*, 1995; Twitchett, 1998). In the absence of exogenous ligands, this ferricytochrome variant possesses a water molecule as the sixth axial ligand. This molecule deprotonates with a pK_{ap} of 6.1(1) (Bren, 1996;Twitchett, 1998) thus causing a high- to low-spin state change. The results from a pH titration monitored by ^{1}H-NMR spectroscopy (25 mM each sodium phosphate and sodium borate buffer, 25 °C) are consistent with this finding (Figure 57). At pH^*~5.5 a multitude of broad resonances appears between 22 and 62 ppm. Presumably, these peaks correspond to the high-spin Fe^{3+} heme in the sample. As the pH is increased, the fast relaxing signals are replaced by those belonging to protons of low-spin forms of the protein. Coincidence of the peak at 19.5 ppm (20 °C) with that identified as corresponding to $IV_b(5)$ (nomenclature as in Figure 24) suggests that the Lys73-bound alkaline conformer is present in the sample at pH^* as low as 6.8. In addition, there are some spectroscopic similarities between the Tml72Lys/Met80Ala cytochrome and the wild-type protein expressed in bacteria. Based on these similarities, the peak at 22.5 ppm is assigned to the heme 8-methyl group of an alkaline conformer of the Tml72Lys/Met80Ala variant. Note that there are significant spectroscopic differences between the Met80Ala variant expressed in yeast (Banci *et al.*, 1995) and that expressed in bacteria much as there are in the case of the wild-type proteins measured at high pH. Whether these differences result from the lack of trimethylation of Lys72 in the
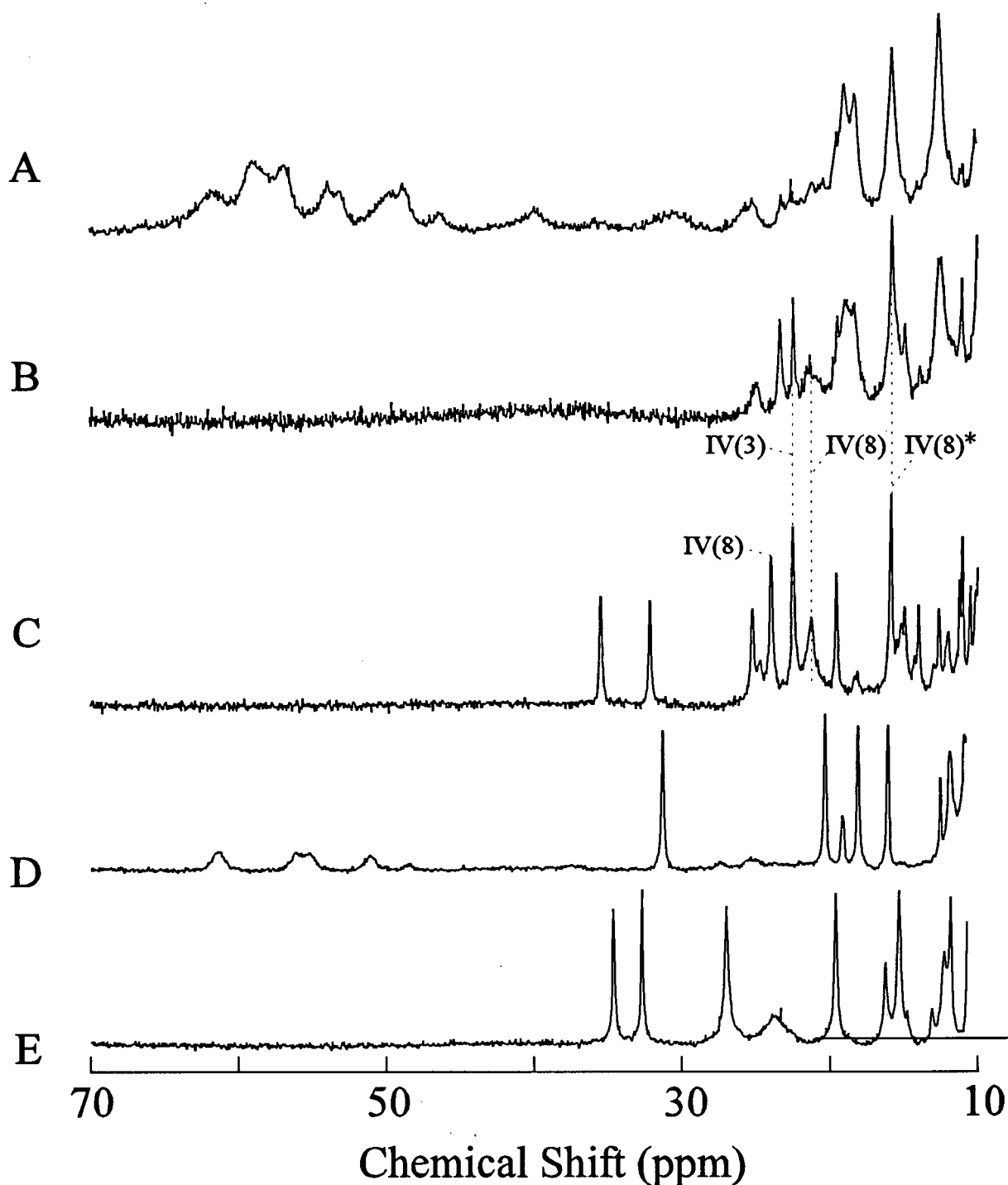
Figure 57. Downfield hyperfine shifted 200 MHz ^{1}H-NMR spectra of yeast *iso*-1- ferricytochromes *c*: Tml72Lys/ Met80Ala variant (A) pH* 5.5; (B) pH* 10.0; (D) pH* 7.0 plus 450 mM methylamine hydrochloride, and the Tml72Lys variant (C) pH* 9.3; (E) *N*-methylamine adduct of the variant Lys73Ala/Lys79Ala, pH* 8.9. The peaks labeled IV(X) correspond to heme 3-and 8-methyl group protons as in Figure 24. The peak indicated with an asterisk in (C) coincides with the resonance that has been assigned to a heme methyl group in the Lys72-bound alkaline conformer of the bacterial protein.

bacterially expressed cytochrome or to the difference in the generation of the proteins in the two expression hosts remains to be determined.

As for the Lys73Ala/Lys79Ala variant, the Tml72Lys/Met80Ala cytochrome binds methylamine near neutral pH (Figure 57 d and e). Note that in the presence of this exogenous ligand, nearly all of the high-spin species is abolished and the sample becomes more homogeneous. However, the ^{1}H-NMR spectrum of the resulting cytochrome adduct bears little resemblance to the spectrum of the N-methylamine adduct of the Lys73Ala/Lys79Ala variant of cytochrome c (Figure 27), or of any of the alkaline conformers (Figure 24).

4 Discussion

4.1 The Alkaline Conformational Transition of Cytochromes *c*

4.1.1 Yeast *iso*-1-Ferricytochrome *c*, State IV

A significant obstacle in the characterization of the alkaline conformational transition of ferricytochrome *c* has been the conclusive identification of the residues that coordinate the heme iron at elevated pH. Although the existance of multiple forms of cytochrome *c* at alkaline pH had been discussed before (Greenwood & Palmer, 1965; Brautigan *et al.*, 1977; Gadsby *et al.*, 1987), the demonstration by Hong and Dixon that the alkaline conformational transition of ferricytochrome *c* results in not one, but actually two alkaline isomers of the protein (1989), represents a major development in the characterization of this dynamic process. With knowledge of this key property of ferricytochrome *c*, Ferrer *et al.* were able to confirm earlier speculations that Lys79 is one residue that coordinates the heme iron at pH above neutrality (1993).Together with Lys72, Lys79 is cited most frequently in the literature as the amino acid that replaces Met80 as an iron ligand in the equine protein. The present work establishes that Lys73 is the residue in the yeast protein that is involved in the alternate conformational transition.

Lys79 is adjacent to the native heme axial ligand Met80. Near neutral pH, Lys79 forms part of a hydrogen bond network that closes the heme cavity and limits the "breathing" of the protein (*i.e.*, the expansion and contraction of the protein that involves the motions of the proximal and distal sides). By comparison, Lys73 is located at the surface, on the distal side of the protein. In the X-ray crystal structure of the yeast protein (Berghuis & Brayer, 1992) the side chain of this residue is almost co-aligned with a vector drawn by extending the bond from the heme iron past the δ-sulfur atom of Met80 and the ϵ-amino group is located ~19 Å from the iron atom. Therefore, whereas replacement of Met80 by Lys79 at alkaline pH can be described as a "frame-shift" of the polypeptide chain that

occurs as Lys79 rotates into coordination position, a 180° "swinging" motion of the side chain of Lys73 is required for the second isomerization process.

Comparison of a model of the Lys73-bound alkaline conformer to the X-ray crystal structure of the native cytochrome illustrates how the protein architecture might rearrange, particularly between residues 70 and 76, to give rise to this alkaline isomer (Figure 58). The swinging of Lys73 appears to extend the H3 α-helix (residues 62-69) by half a turn, while the 71-76 helix between two highly conserved proline residues (Pro71 and Pro76) is disrupted almost entirely. Although the loop containing Met80 is pushed away from the protein core so that the backbone protrudes at the exposed heme edge (~6Å), Lys79 remains engaged in a hydrogen bond network that is similar to that which favours the closed conformation of the native isomer. Ligation of Lys79 to the heme iron also extends the H3 α-helix, and the 71-76 helix relaxes but not to the same extent as in the Lys73-bound conformer. Met80 remains in the heme pocket with the side chain now occupying a position parallel to the heme plane adjacent to pyrrole rings B and C.

Note that the structural adjustments that occur to accommodate coordination of Lys79 appear less significant than those involving Lys73. Lys79 is in a loop region that is presumably more flexible and allows a wider range of motion without significantly disrupting other structural elements of the protein. Upon coordination of Lys79 to the heme iron, no other residue on the distal side of the protein appears to hydrogen bond any residues on the proximal side. Without such a locking mechanism, the Lys79-bound alkaline conformer may exhibit more "breathing" motions than the other alkaline isomer because the distal side of the protein is not anchored to the proximal side.

The three-dimensional structures of both alkaline conformers of ferricytochrome *c* remain to be elucidated. Presumably, part of the problem in determining these structures by NMR or X-ray diffraction techniques stems from the conformational heterogeneity observed for the wild-type protein
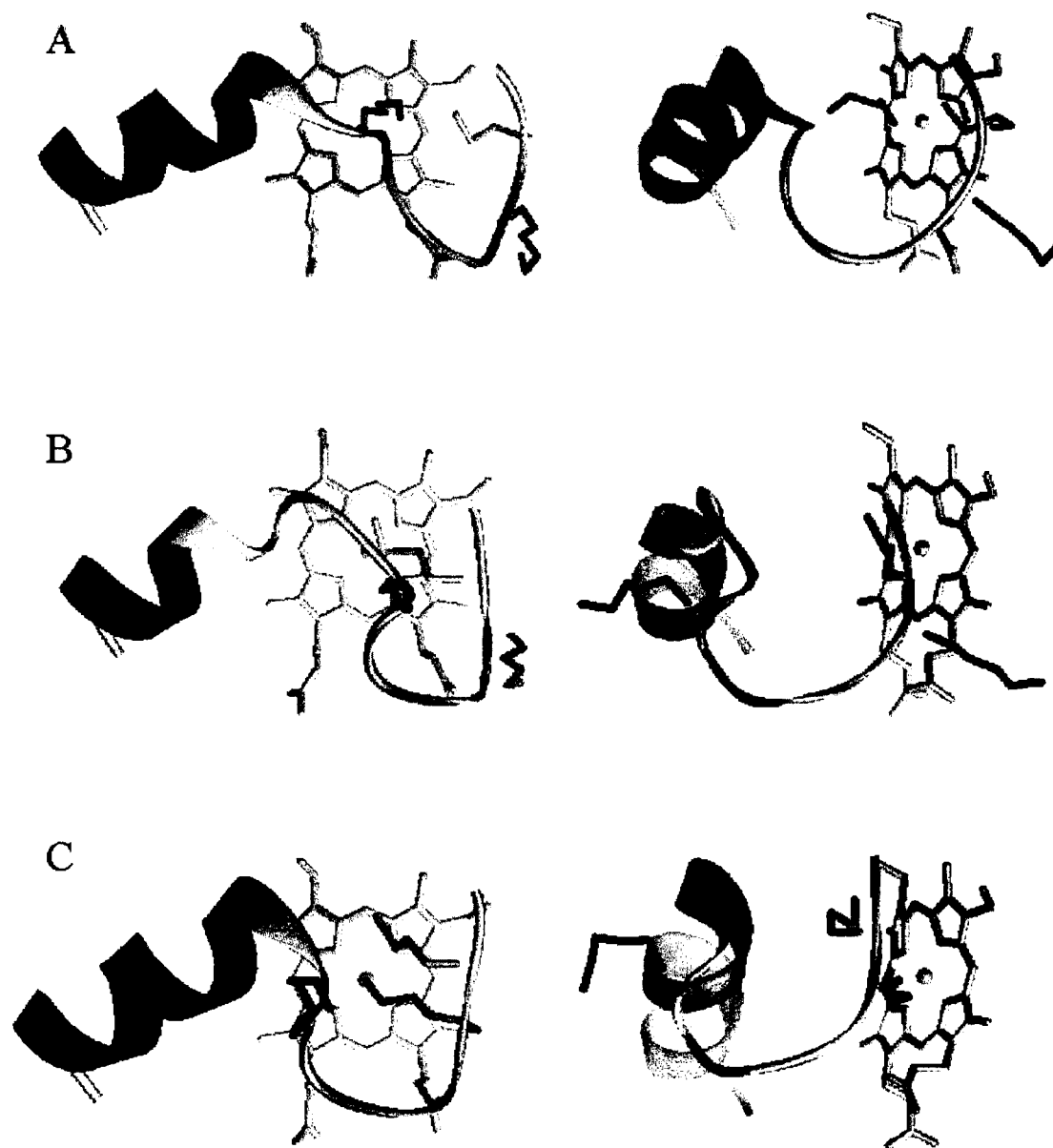
Figure 58. Comparison of the native structure of yeast *iso*-1-ferricytochrome *c* (B; 2YCC.PDB; Berghuis & Brayer, 1992) to models of the (A) Lys73- and (C) Lys79-bound alkaline conformers of the protein calculated by energy minimization of the structure in which the ϵ-amine-Fe^{3+} bond length was constrained to ~1.95 Å (energy-minimized structures courtesy of Dr. Terence P. Lo). Only residues 59-82 are included (secondary structure as indicated by the ribbon) with H3 helix shown in red. The side chains of residues Lys73, Lys79, and Met80 are shown in blue, green, and orange, respectively.

at high pH. Also, the optimum crystallization conditions at the elevated pH required to transform fully the native protein to either alkaline conformer remain to be defined. However, preliminary NMR results indicate that the structure on the proximal side of the protein of the Lys73-bound conformer of cytochrome c is very similar to that of the native protein. As noted earlier, fifty spin systems have been identified based almost exclusively on the similarity to reported assignments for the native protein (Gao *et al.*, 1991). These residues are located mainly on the proximal side which is predicted to undergo the least structural perturbation in both alkaline conformers. Also, a few residues have been located which are on the distal side (Figure 59). In the model of the Lys73-bound conformer, carbon atoms of Pro76 appear at almost the same coordinates as in the native protein despite the disruption of the 71-76 helix that precedes this residue. Interestingly, a spin system consistent with that of a proline residue was identified which has the same resonance frequencies as Pro76. Further work is required to elucidate the structure of the alkaline conformers of yeast ferricytochrome c completely, and before the properties of these isomers can be linked with confidence to specific structural features. This work is still in progress.

4.1.2   The Alkaline Isomers of Other Cytochromes c

Although cytochromes c exhibit a high degree of sequence and structural homology, it is premature to assume that Lys73 and Lys79 also participate in the alkaline conformational transition of all cytochromes. Selected surface lysyl residues in yeast, fungal, and some plant cytochromes c are post-translationally modified by a methyl-transferase which specifically methylates the ϵ-amino group of certain lysyl residues. In the yeast protein, the trimethylated Lys72 lacks the lone pair of electrons that is necessary to coordinate the heme iron. When expressed in *E. coli*, the yeast protein does not undergo trimethylation, and the native state is destabilized so that it forms a third alkaline conformer

149
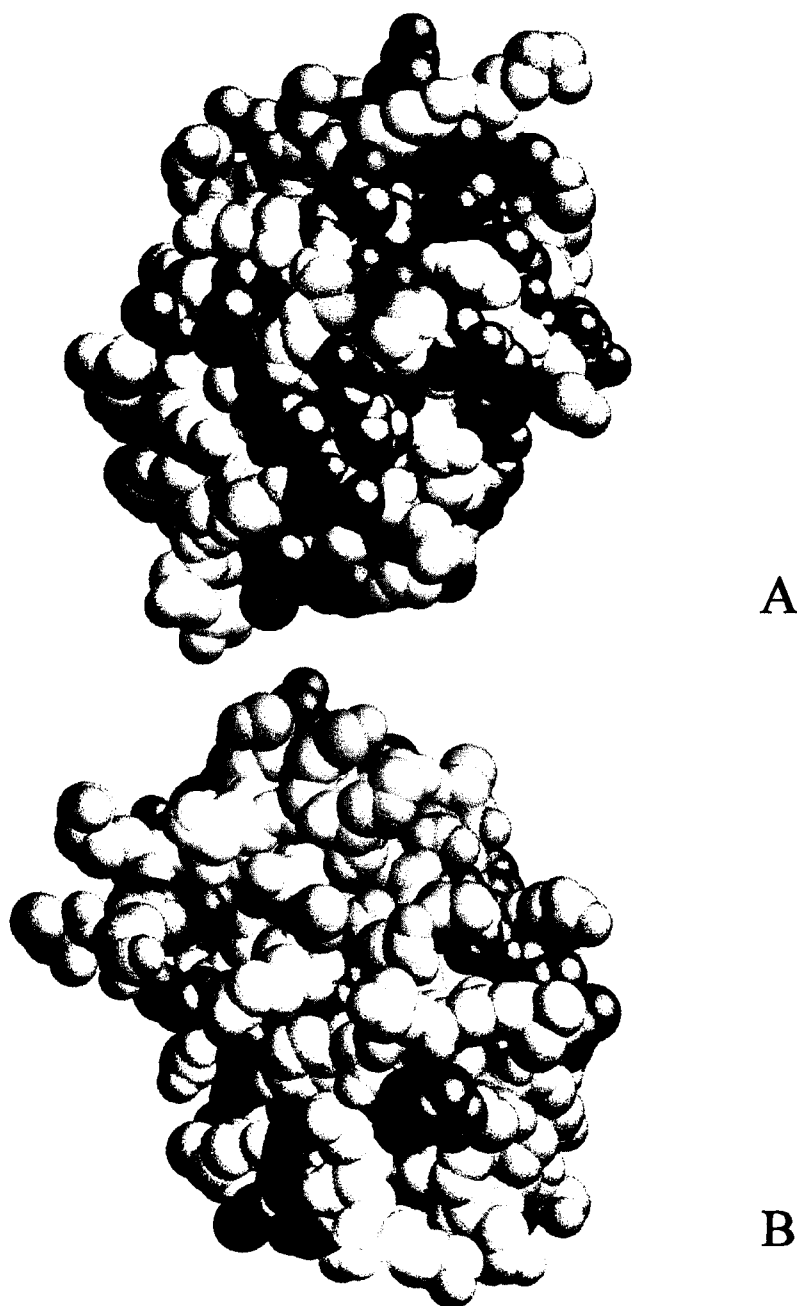
Figure 59. Space filling model of (A) the proximal, and (B) the distal faces of wild-type yeast *iso*-1-ferricytochrome *c* (2YCC.PDB; Berghuis and Brayer, 1992). The structures in green represent residues for which at least partial ¹H-NMR peak assignments have been made from spectra of the Lys79Ala variant collected at pH 10.8. These assignments are based on the similarity of the amino acid spin systems to the published assignments in the native wild-type protein (Gao, 1991; Paola Turano, personal communications).

at a lower pH than the protein that is expressed in yeast. Therefore, the decreased stability of the native conformer suggests that trimethylation in the yeast protein evolved to block Lys72 from coordinating the heme at high pH. If this function is indeed the purpose for trimethylation of this lysyl residue in yeast cytochromes c, then it is possible that in the rice protein, replacement of the Met axial ligand by Lys86 would occur were it not for trimethylation of this residue (Mori & Morita, 1980; Ochi *et al.*, 1983).

In horse cytochrome c, Lys72 is not trimethylated, yet this protein exhibits only two alkaline forms (Hong & Dixon, 1989). This observation leads one to question whether Lys73 or Lys79 are also the ligands involved in the alkaline conformational transitions of this and other cytochromes. The recent work by Banci and coworkers shows that spectroscopic features attributed to a third alkaline species of horse heart cytochrome c can be resolved with stronger magnetic fields (1998). However, the work of Ubbink *et al.* shows that the alkaline transitions of a cytochrome do not necessarily include Lys79 (1994). In cytochrome c_{550} from *Thiobacillus versutus*, Lys99, the residue at the position equivalent to Lys79, was mutated to glutamate with the expectation that this site replacement would eradicate the single alkaline transition of this protein. However, the Lys99Glu variant continues to undergo an alkaline conformational transition although at lower pH. The three-dimensional structure of cytochrome c_{550} from *Thiobacillus versutus* has not been elucidated, but assuming that this protein is similar to cytochrome c_{550} from *Paracoccus denitrificans*, then either Lys83 or Lys102 are the residues in these bacterial proteins that replace the axial Met ligand at high pH. This prediction is based on the residence of these lysyl residues in the equivalent region to that where Lys72 and Lys73 are located in the yeast protein. Note that in cytochrome c_{550}, Lys83 is flanked by prolyl residues at positions 82 and 84; therefore, if Lys83 is the heme axial ligand in this protein at high pH, then it is possible that the high degree of conservation of the prolyl residues in this area is a significant

structural component for the pH-dependent conformational dynamics of ferricytochromes c in general (*vide infra*).

4.1.3   Obstacles to the Identification of the Alkaline Ligands

Prior to the implementation of genetic techniques to produce cytochrome c variants, the most widely used approach to determine the lysyl residue that coordinates the heme iron at alkaline pH was chemical modification (Table 1b). Some of these protocols were highly sophisticated in terms of their ability to yield singly-modified proteins. However, even the most elegant of strategies suffered in that the binary nature of the alkaline transition was not considered. As it turns out, the failure to discriminate between the two different alkaline conformers is what hindered the identification. Although one of the appropriate residues may have been blocked by chemical modification, the alternate lysyl residue remained free to replace Met80 in the coordination sphere of the heme iron.

In general, spectrophotometric titration of the 695 nm was the preferred method to analyze the modified cytochromes (Table 1b). However, there are no detectable differences between the electronic spectra of the Lys73- and Lys79-bound alkaline conformers. EPR spectroscopy had also been used in the characterization of the isomerization products (Greenwood & Palmer, 1965; Gadsby *et al.*, 1987) and, although in retrospect these results are consistent with the formation of two protein conformers, the uncertainty associated with the collection of data under cryogenic conditions made such a conclusion speculative (Gadsby & Thomson, 1990). With the confirmation by ^{1}H-NMR spectroscopy that two distinct protein structures occur at elevated pH (Hong & Dixon, 1989), it is now clear that the heterogeneity observed in EPR spectra truly reflects the formation of two related protein structures rather than freezing artifacts. Consequently, ^{1}H-NMR spectroscopy should be used in assessing the conformational properties of other cytochromes c.

4.2 Mechanism of the Alkaline Conformational Transition

4.2.1 Intermediate Conformational States

In the simplified mechanism of the alkaline isomerization of ferricytochrome c, Davis et $al.$ envisioned the ionization of a titratable group (pK_H) which triggers a subsequent iron ligand exchange (pK_C) (1974). In general, this model describes satisfactorily the kinetics observed for the wild-type horse and yeast proteins as well as for several yeast cytochrome c variants bearing point mutations (Kihara et $al.$, 1976; Saigo, 1981; Pearce et $al.$, 1989; Nall et $al.$, 1989; Rafferty, 1992). However, a more complete description of the events leading to the alkaline conformers of the protein includes an intermediate in which the heme is probably 5-coordinate (Lambeth et $al.$, 1973; Saigo,1981) (Scheme 6; i is the intermediate and should not be confused with the acidic conformer of ferricytochrome c, state I). This species is a common precursor to both alkaline forms, and bifurcation of the isomerization mechanism at this point into two parallel branches, explains in part why the binary nature of the process has not been detected by pH-jump kinetics experiments. In the majority of these investigations, the decay of the 695 nm charge transfer band was monitored. As noted earlier, this absorbance is a manifestation of Met80-Fe^{3+} coordination (Schechter & Saludjian, 1967), so its decay reflects the generation of the common intermediate but not necessarily the alkaline conformers. If under the experimental conditions ($i.e.$, $\mu \sim 100$ mM, pH < 10), this step is rate limiting ($i.e.$, $k_1 <$ k_a, k_b) and insensitive to the nature of the final product, then a single monophasic process is detected (k_1).

$$\begin{array}{c} \mathbf{III} \\ k_{-1} \Big\Updownarrow k_1 \\ \mathbf{IV}_a \underset{k_{-a}}{\overset{k_a}{\rightleftharpoons}} \; i \; \underset{k_{-b}}{\overset{k_b}{\rightleftharpoons}} \mathbf{IV}_b \end{array} \qquad\qquad (6)$$
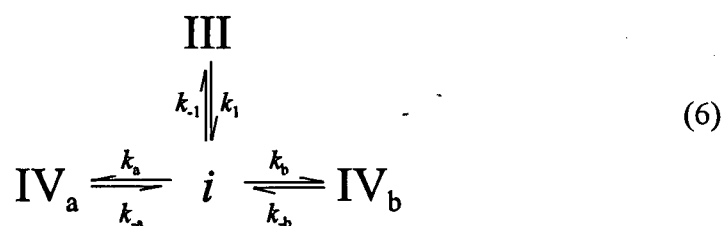
At pH >10.5, the intermediate in the isomerization process may also be the precursor to or the fifth conformer of ferricytochrome c (state V). However, within the pH range 8 to ~10.5, this common intermediate turns into the two stable, lysyl-bound conformers of ferricytochrome c that are distinguishable by NMR spectroscopy (Hong & Dixon, 198x; Ferrer *et al.*, 1993, Rosell *et al.*, 1998). Interestingly, there is no evidence from saturation transfer experiments that one alkaline conformer converts directly into the other. Presumably, the mechanism for the reversion from the two alkaline states to the native cytochrome is reversible as shown in Scheme 6. It is possible, therefore, that under the experimental conditions (50 mM sodium phosphate, pH~9.3, 55°C), the failure to detect saturation transfer between the two alkaline species results from a faster reversion to the native state than to the alternate alkaline conformer (*i.e.*, $k_{-1} > k_a, k_b$). Therefore, the bulk of the magnetization is transferred to the native species.

In revising the mechanism of Davis *et al.*, special emphasis has been placed on the experimental conditions. Below a certain pH threshold (~10), the 5-coordinate intermediate is not present at a sufficiently high concentration to be detected. However, evidence from pH-jump experiments above this threshold suggests that the situation changes under these conditions so that $k_1 > k_a, k_b$ or $k_{-1} < k_a, k_b, k_1$. The result is the transient formation of a high-spin species in appreciable amounts (*vide infra*). The relative variation of k_1, k_{-1}, k_a, or k_b with pH is consistent with the existence of a "trigger" group the protonation state of which controls the conformational transition of ferricytochromes. For example, a change in the deprotonation of a residue in the alkaline species following the conformational rearrangement could induce a shift in k_a or k_b. However, from the original analysis of Davis *et al.* (1974), such a scenario requires that the observed rate constant of the isomerization decreases with increasing pH. This is contrary to what is observed in all the pH-jump experiments. On the other hand, deprotonation of a group in the native cytochrome prior to the

conformational rearrangement would induce a shift in k_1 (or k_{-1}), and the observed rate constant would increase with pH. Conclusive identification of the group that triggers the alkaline conformational transition of ferricytochrome c would greatly enhance our understanding of the mechanism. This subject is considered further in the following section.

The electronic absorption spectrum of the transient species derived from singular value decomposition analysis of pH-jump kinetics data collected at pH > 10 resembles the spectra of two cytochrome c variants in which neither the native nor the alkaline heme ligation are in effect. In the Lys73Ala/Lys79Ala variant, Lys73 and Lys79 are unavailable to coordinate the heme. Therefore, at pH ~10.5 a stable high-spin species is formed when Met80 is expelled from the coordination sphere of the heme iron. In the Phe82Trp variant, the large tryptophanyl side chain represents a steric obstacle to the incoming lysyl residues and thus stabilizes a high-spin species that reaches maximum concentration at pH ~8.5. The spectroscopic similarities suggest that the alkaline transition intermediate is somehow trapped in the isomerization of the Lys73Ala/Lys79Ala and Phe82Trp variants. However, resonance Raman spectroscopy indicates that in both cases, the high-spin species consists of a 6-coordinate heme in which a hydroxide probably occupies the distal coordination site (Döpner, unpublished results). Notably, the spectrum of the Met80Ala variant at a pH where hydroxide occupies this site exhibits a maximum at ~625 nm rather than at ~600 nm (Bren, 1996; Twitchett, 1998).

4.2.2 The Identity of the Trigger Group

The identity of the functional group which, upon ionization, triggers the alkaline conformational reorganization of ferricytochrome c remains unknown. According to the pH-jump kinetics protocol of Davis *et al.* (1974), a key property that must be exhibited by the trigger group

is a relatively high pK_a for ionization (~10.5 to 12, depending on the cytochrome). Few amino acid side chains titrate in this pH range, and computational analysis of molecular dynamics and energy-minimized structures of cytochrome c (Zhou & Vijayakumar, 1997) identifies only lysyl, arginyl, and tyrosyl residues as potential trigger groups. The trigger residue may be located in an internal region of the protein that is pivotal for the stabilization of the native structure of the protein and which stabilizes the protonated form of this group. Alternatively, it may be located near the protein surface, but the intimate association of this residue with neighbouring amino acids results in an elevated pK_{ap}.

Among the functional groups that have been considered as the "trigger" (see section 1.3.4), the lysyl residues that coordinate the heme at high pH represent the simplest candidates, particularly because the ϵ-amino group of these amino acids must be neutralized before it can bind the iron and the stoichiometry of the isomerization consists of a single proton. Analysis of the pH-jump kinetics data collected for the Lys73Ala and Lys79Ala variants of the yeast protein yields pK_H values of 10.8 and 12.0, respectively. Assuming that the titration of these residues triggers the isomerization, these pK values correspond to Lys79 (10.8) and Lys73 (12.0). Although the former value is in reasonable agreement with the pK_a determined for this residue by Bosshard (~10.4; 1981), it is not clear why the pK for the latter is as high as 12.0. It is more likely, therefore, that the amino acid replacement at either position 73 or 79 results in the perturbation of the environment around the true trigger group. Consideration of the different environments around Lys73 and Lys79 in the wild-type protein structure (Berghuis & Brayer, 1992) reveals that mutation of Lys79 to Ala can potentially result in such a mutation-induced artifact because of its close association with Ser47, Tyr46, and the heme 6-propionate group. In contrast, Lys73 is highly exposed to the solvent, and mutation of this residue is unlikely to perturb the local structure of the protein significantly.

The role of the heme propionate groups in the alkaline conformational transition of

ferricytochrome c has been investigated by Moore and coworkers (Tonge *et al.*, 1989). This study argued that the heme 6-propionate group in the equine cytochrome has an unusually high pK_a (> 9), leading the authors to conclude tentatively that the ionization of this carboxylic acid could trigger the alkaline isomerization of the protein. Ser47 (Thr47 in the equine cytochrome) and Tyr46 are also in the proximity of the ϵ-amino group of Lys79, and the titration of these hydroxyl groups could also destabilize the cytochrome enough to cause the isomerization. Nevertheless, these residues have escaped scrutiny thus far. Inspection of the amino acid variability in this region of the protein reveals that Tyr46, Ser47, and Tyr48 are highly conserved and suggests that they are indeed significant for the structural stability if not the function of the native conformer of cytochromes c. Moreover, the calculated range of pK_a values calculated for the tyrosyl residues (Zhou & Vijayakumar, 1997) is consistent with the pK_as determined by pH-jump kinetics experiments. Upon ionization of either tyrosyl residue or the Ser47 γ-OH group, Lys79 could be released from the hydrogen bonds that anchor it, thus opening the heme cavity and facilitating the ligand exchange. In essence, mutation of Lys79 to Ala mimics this chain of events and results in a more open protein conformation that facilitates the isomerization to an alkaline form. Furthermore, Nall and coworkers have shown that interaction of horse heart cytochrome c with the antibody 2B5 significantly stabilizes the native conformation of this protein (ΔpK_{ap}~1; Raman *et al.*, 1992). In contrast, interaction of this cytochrome with antibody 5F8 barely affects the isomerization (ΔpK_{ap}~0.3; *Ibid*). The epitope of MAb 2B5 has been mapped to the immediate region surrounding residue 44, whereas that of MAb 5F8 is located on the opposite face of this cytochrome. Therefore, it may be that on binding to antibody 2B5, but not 2F8, the trigger group becomes isolated from the medium, and the protonated form of the isomerization trigger is stabilized to increase the pK_{ap} of the protein.

The occurrence of the trigger group on the surface of the cytochrome would resemble the

situation reported for rhodopsin by Koutalos *et al.* (1990). In metarhodopsin, a retinal moiety is linked to the protein backbone through a Schiff base. Deprotonation of this group triggers the isomerization of the retinal molecule from the 11-*cis*- to the all *trans*- conformation. This ionization is dependent on the surface charge density in the immediate surroundings of the Schiff base and, therefore, on the ionic strength of the medium. Consequently, Koutalos *et al.* analyzed the ionic strength dependence of the apparent pK_{ap} of this isomerization using the Gouy-Chapman formalism. This analysis parametrizes the average surface charge density in the vicinity of the titrating group, as well as the pK_a of the titrating group in isolation from the influences of the charged surface. Extension of this analytical approach to the alkaline isomerization of yeast ferricytochrome c results in a pK of ~8.9 for the wild-type and the Lys73Ala variant. In contrast, an equivalent analysis yields a value of ~9.2 for the Lys79Ala variant of the protein. These results suggest that replacement of Lys79 by an alanyl residue perturbs the environment around the trigger group and, therefore, the pK_a for its ionization. However, these pK values differ substantially from the corresponding pK_H for these variants determined by pH-jump kinetics suggesting that additional factors must be considered in the analysis of the ionic strength dependence of the alkaline conformational transition of ferricytochrome c. Alternatively, and assuming that the underlying premises of pH-jump kinetics analysis and the Gouy-Chapman theory apply to the conformational dynamics of cytochrome c, these pK values reflect different properties of the isomerization process.

4.3   Factors that Influence the Isomerization

4.3.1   The Driving Force of the Isomerization

An important issue raised by this work concerns the driving force for the alkaline conformational rearrangement of ferricytochrome c. It could be argued that coordination of a

nitrogenous ligand to the heme iron is a principal factor driving the isomerization reaction, in particular, the reaction which generates the Lys73-bound conformer. The increased stability of the native isomer in the Lys73Ala/Lys79Ala variant supports this argument. Despite the greater structural mobility that is expected in the distal half of the protein in the absence of Lys79 and the hydrogen bonds that stabilize the closed conformation of the protein, the Met80-Fe^{3+} bond is broken only at a pH (~10), well above the pK_{ap} of the alkaline transition in the wild-type cytochrome. However, addition of methylamine hydrochloride to the Lys73Ala/Lys79Ala variant, even at a pH closer to neutrality, results in a protein adduct with spectroscopic features that closely resemble those of the alkaline conformers of ferricytochrome c. Although the formation of this adduct could result from an ionic strength-induced destabilization of the native state of the variant, the observation of a bis-histidine coordinated species at neutral pH in the Phe82His variant (Hawkins et $al.$, 1994) confirms that the affinity of the ferric heme for a nitrogenous base is comparable, if not greater, than that for the methionyl δ-sulfur atom.

On the other hand, the apparent inability of Lys72, 73, and 79 to coordinate the iron in the Met80Ala variant near neutral pH suggests that loss of Met80 from the coordination environment of the heme iron is not sufficient to induce the conformational rearrangement. In this variant, the lysyl residues compete with water and hydroxide for this coordination site. Furthermore, azide (Sutin & Yandell, 1972; Saigo, 1986; Rafferty, 1992), cyanide (George & Tsou, 1952), and imidazole (Schejter & Aviram, 1969) are known to replace Met80 in the coordination sphere of the iron. A common feature of these relatively facile displacement reactions is the invariant rate for the rupture of the Met80-Fe^{3+} bond. Not surprisingly, there appears to be a correlation between the susceptibility of various cytochromes c to replacement of Met80 by a particular type of exogenous ligand and the pK_{ap} of the alkaline conformational transition associated with each protein (Saigo, 1986). Together,

these observations suggest that the expulsion of Met80 from the iron coordination sphere is another important determining factor of the alkaline isomerization.

The entropic and enthalpic changes associated with the alkaline conformational transition of the Lys73Ala variant of cytochrome c (Table 8: 19(2) e.u. and 5.4(6) kcal mol^{-1}, respectively) are comparable to those of the wild-type protein. In contrast, the entropy and enthalpy of the isomerization of the Lys79Ala variant are nearly doubled. The greater driving force for the isomerization associated with the Lys79Ala variant reflects the greater structural reorganization that the polypeptide must undergo to accommodate Lys73 in the coordination sphere of the heme iron.

4.3.2   Structural Elements

The manner in which the primary structure of a protein encodes the information for the proper folding of polypeptides into functional proteins/enzymes continues to demand much attention. Typically, this "problem" is addressed by studying the folding of a protein that is denatured by some means (*i.e.*, through the use of chemical agents or elevated temperatures), or by studying the reverse process. The alkaline conformational transition of ferricytochromes c exemplifies another facet of this so-called protein folding problem. Specifically, this isomerization illustrates how for some proteins, the amino acid sequence also includes essential instructions that permit multiple conformational states throughout the lifetime of the polypeptide.

Scrutiny of the effects of point mutations on the alkaline conformational transition of ferricytochrome c identifies components of the polypeptide chain that influence the ordered progression from the native protein to its alkaline conformers. For example, Phe82 is not only important for the electron transfer function of cytochromes c, but it is also a significant structural element involved in the pH-dependent dynamics of these proteins. Replacement of this conserved

residue with other amino acids generally destabilizes the native conformation of the yeast ferricytochrome, favouring in many cases the Lys73-bound alkaline conformer. The higher incidence of this species is consistent with the lower pK_{ap}s of variants like Phe82Gly and Phe82Ser. However, pH-jump kinetics experiments indicate that the reduced pK_{ap} for the alkaline transitions of these variants also results from a significant drop in the pK_H of the trigger group (Pearce *et al.*, 1989). Evidently, the structural changes induced by the replacement of Phe82 include a perturbation of the immediate environment around this trigger group. Comparison of the X-ray crystal structures of the Phe82Ser or Gly variants to that of the wild-type protein reveals that the most significant structural differences in these variants are the movement of a conserved water molecule (H_2O166) 0.7-1.4 Å closer to the heme iron (Figure 51), the collapse of the protein backbone between residues 82 and 84 into the heme cavity and closer to the porphyrin ring, and a general reorganization of the distal side of the protein that increases the solvent exposure of the heme (Louie, 1990).

Replacement of Thr78 by Ala also destabilizes the native conformation of the cytochrome significantly. The pK_{ap} of this variant is ~2 pH units lower than that of the wild type protein, but unlike the Phe82 variants discussed above, ^{1}H-NMR spectroscopy analysis indicates that the predominant alkaline conformer of this protein below 30 °C has Lys79 bound to the heme iron. Only at higher temperatures (~30°C) is the Lys73-bound conformer comparable in abundance to the Lys79-bound form. This marked temperature dependence of the alkaline conformer distribution makes the Thr78Ala variant unique among those described in this work. The structural basis for this property is not clear because the structure of the Thr78Ala variant has not been determined yet. Nevertheless, it is expected that removal of Thr78 will also perturb the protein in the region of the conserved, internal water molecule (H_2O166) because the hydrogen bond with the γ-OH group of the threonyl residue cannot be formed (Figure 54).

In contrast to the destabilization of the native conformer of ferricytochrome c induced by amino acid replacements at positions 78 and 82, replacement of Tyr67 with phenylalanine considerably stabilizes the native isomer. With a reported pK_{ap} of 10.7 (Lutz $et\,al.$, 1989), this protein is the most stable variant of cytochrome c. Without the Tyr67 OH group, the hydrogen bond between this oxygen and the Met80 δ-sulfur atom is severed, which evidently strengthens the Met80-Fe^{3+} bond (Berghuis $et\,al.$, 1994). Interestingly, there is no evidence that this variant exhibits a high-spin intermediate in pH-jump experiments above pH 10, or even as high as ~12. As indicated earlier, this observation suggests that the phenol group of Tyr67 is an integral part of the conformational transition and acts in one of at least three ways. The oxygen atom of this residue could coordinate the heme iron transiently, or it could hydrogen bond to an exogenous water/hydroxide ligand before coordination by a lysyl residue to the heme iron is established. Alternatively, the intermediate species detected in pH-jump experiments at high pH could result from a strengthened Tyr67-Met80 hydrogen bond and a concomitant weakening of the Met80-Fe^{3+} bond.

Other residues in the sequence of cytochrome c that have been have been shown to be relevant to the alkaline transition are the highly conserved prolyl residues which flank Lys73 and which delimit the 71-76 helix. Mutation of Pro71 to Thr, for example, depresses the pK_{ap} of yeast iso-2-ferricytochrome c from 8.45 to 6.63 (White $et\,al.$, 1987). Semisynthetic substitution of Pro71 by norvaline induces a greater shift in the conformational equilibria of the horse protein (Wallace & Clark-Lewis, 1997). In this protein, the pK_{ap} of the alkaline transition is ~4 pH units lower than in the wild-type protein. Although this dramatic change may be an artifactual result from the semisynthetic method ($i.e.$, through imperfect packing of the non heme-containing synthetic polypeptide to the heme-containing chain, $etc.$), it is clear that Pro71 plays a crucial role in the stabilization of the native conformer of ferricytochromes c. In the same manner, Pro76 appears to stabilize the native form of

cytochromes c. The pK_{ap} of the Pro76Gly variant is also shifted significantly (pK_{ap}~6.71; Wood *et al.*, 1988 a, and b), and pH-jump kinetics indicate that this destabilization is due almost exclusively to a 70-fold acceleration of the forward isomerization process (*i.e.*, $k_f = 3500$ s^{-1}), without affecting the pK of the trigger group (pK_H~12; Nall *et al.*, 1989). By comparison, the faster forward rate constant reported in the present work is that corresponding to the Lys79Ala variant (160 s^{-1}). Nall and coworkers attributed the marked increase in rate of the isomerization of the Pro76Gly variant to destabilization of the native conformer ($\Delta G°$~2.5 kcal/mol) rather than stabilization of the transition state or the alkaline species. Evidently, the function of Pro76, and perhaps Pro71, is to hinder the formation of the Lys73-bound alkaline conformer of cytochrome c much in the same manner that trimethylation hinders the formation of a Lys72-bound alkaline conformer in the yeast protein. However, this suggestion requires evaluation by ^{1}H-NMR spectroscopy.

4.3.3 Effects of Salts on the Conformational Transition of Cytochrome c

The pH-dependent conformational equilibria of wild-type ferricytochrome c clearly vary with temperature as well as with solution conditions. The pK_{ap} of the alkaline isomerization increases with potassium chloride concentration, and is maximal at ~600 mM. At the same time, one alkaline conformer (Lys79-bound) predominates at the expense of the other alkaline form (Lys73-bound). These observations were interpreted in section 3.4.3 to occur in response to an increasing shielding effect of charged residues by the electrolyte. This shielding would help to reduce potentially unfavourable electrostatic interactions which involve Lys73 and/or Lys79. This view is consistent with a substantial expansion of the oxidized protein at lower ionic strengths that is observed by small-angle X-ray scattering experiments (Trewhella *et al.*, 1988). However, it should also be noted that the cytochrome c surface has at least two chloride binding sites (Osheroff *et al.*, 1978; Andersson

et al., 1979, 1980). The first of these binding sites is associated with lysines 86, 87, 89 (Feng & Englander, 1990), and Lys13 (Morton & Breskvar, 1977), and the second site is associated with Lys60 (Stellwagen & Schulman, 1973). Although no significant structural differences were detected in the ^{1}H-NMR spectra of the protein measured in the absence or the presence of 200 mM sodium chloride at pH 7 (Feng & Englander, 1990), at higher salt concentration and pH (~500 mM, 7.3 respectively) local structural changes appear to cause the aromatic ring of Phe82 to approach the heme 3-methyl group of the porphyrin (Moench *et al.*, 1991). As shown above, perturbation of the protein structure in this region is closely associated with alterations to the alkaline conformational equilibria of ferricytochrome *c*.

A variety of other ions are also known to bind to cytochrome *c*, yet not all of these interactions have the same conformational influence as potassium chloride. Perchlorate, for example, is an efficient competitor for one of the chloride binding sites, particularly in the oxidized protein (Andersson *et al.*, 1980). Instead of stabilizing the native isomer, however, perchlorate depresses the pK_{ap} of the equine protein by as much as one pH unit (~200 mM sodium perchlorate). Andersson *et al.* reported the emergence of a second perchlorate binding site in the alkaline conformer of the protein. Presumably, this binding site is located in the distal side of the Lys73-bound conformer, and interaction with perchlorate serves to stabilize this structure. Closer to neutral pH, perchlorate destabilizes the Met80-Fe^{3+} bond as evidenced by a high-spin component that is detected by EPR spectroscopy (Andersson *et al.*, 1980).

Carbonate (Osheroff *et al.*, 1980), phosphate (Taborsky & McCollum, 1979), and various anionic and cationic coordination complexes (Otiko & Sadler, 1980; Arean *et al.*, 1988 and references therein; Moore *et al.*, 1995) also bind to ferricytochrome *c*. Every one of these interactions with charged species can be expected to influence different physicochemical and structural properties of

the protein depending on the site of interaction. Increasing salt concentrations, for example, depresses the reduction potential of various cytochromes c (Gopal *et al.*, 1988), and addition of Et₃PAuCl to protein solutions at neutral pH interferes with the heme core as evidenced by a spin-state change (Otiko & Sadler, 1980). Presumably, this gold compound binds ferricytochrome c at one of the ion binding sites and weakens the Met80-Fe^{3+} bond in a similar fashion as perchlorate. The result is a protein with spectroscopic features similar to those observed in the electronic spectrum of the Phe82Trp variant at pH 8.5. Furthermore, polyphosphates (Concar *et al.*, 1991) and other polyions have been of particular interest because these molecules are believed to mimic to some degree the surfaces of the electron transfer partners of cytochromes c (*vide infra*) (Hildebrandt, 1990; Antalík *et al.*, 1992; Sedlák, 1997; Sedlák & Antalík, 1998).

4.3.4 Cytochrome Conformational Equilibria at Charged Surfaces

Within the intermembranal space of mitochondria, cytochrome c is inevitably associated with the membrane surface. As much as 10% of the cytochrome is reported to remain attached to the inner mitochondrial membrane at a variety of ionic strengths (Cannon & Erman, 1980; Rytömaa & Kinnunen, 1994; Cortese *et al.*, 1995). In fact, cytochrome c has been reported to have at least two independent binding sites for acidic phospholipids (Rytömaa & Kinnunen, 1994). This association appears to increase the β-sheet character of the protein (~35%) at the expense of the α-helical component (Cortese *et al.*, 1998), it causes a localized conformational change in the vicinity of the heme 6-propionate group (Soussie *et al.*, 1990), and it disrupts the Met80-Fe^{3+} bond (Letellier & Schechter, 1973; Pinheiro & Watts, 1994). Although this destabilization of the native structure of ferricytochrome c yields a high-spin species, and thus should facilitate the alkaline conformational transitions, there are no indications that these isomers are formed. In one report, the interaction of

cytochrome c with cardiolipin is actually reported to increase the pK_{ap} of the alkaline isomerization (Soussi *et al.*, 1990). Note that the effect of lipid membranes on the conformation of ferricytochrome c may vary depending on the composition of the membrane. Consequently, the experimental results of the type described above must be considered carefully.

Investigations involving protein:protein interactions also indicate that the Met80-Fe^{3+} bond in ferricytochrome c is perturbed upon interaction of this protein with cytochrome c oxidase (Weber *et al.*, 1987; Michel *et al.*, 1989). The resonance Raman studies by Hildebrandt and coworkers confirm that cytochrome c undergoes structural changes upon interacting with charged surfaces that lead to a thermal equilibrium between two spectroscopic states (Hildebrandt & Stockburger, 1989). While state I is identical to the native protein, state II is composed of a mixture of species: a high-spin, 5-coordinate species, and high- and low-spin, 6-coordinate species (states I and II are the original terms used by Hildebrandt (1990), and should not be confused with the pH-linked conformers of ferricytochrome c as defined by Theorell & Åkesson, 1941). More recently, state II was redefined as state B2 which forms in both the Lys73Ala and Lys79Ala variants of the yeast protein at pH >10.5 and in the Lys73Ala/Lys79Ala variant at pH<10 (Döpner *et al*, 1998). State B2 does not correspond to either alkaline conformer but is a species observed at higher pH, state V. In this conformation, the heme iron is most likely coordinated by a hydroxide because spectroscopic features of B2 are also observed in the spectra of the Tyr67Phe and Thr78Ala variants.

Clearly, charged surfaces have the potential to alter the heme core of ferricytochrome c significantly. Whether or not the alkaline species of this protein play a metabolic role remains a matter of conjecture and requires further scrutiny.

4.4   pH-Linked Conformational Transitions in Other Proteins

Proteins are generally regarded to have an optimum pH range over which they have a folded structure and can function optimally. Outside of this range, the properties of the protein are largely ignored unless attempts to extend the pH limits through protein engineering are undertaken. However, other proteins that display pH-linked conformational equilibria similar to those of ferricytochrome c are becoming recognized (see for $e.g.$, Gerstein & Krebs 1997; http://bioinfo. mbb.yale.edu/MolMovDB/). A prime example of a family of proteins that undergo organized and reversible pH-linked conformational transitions as part of their physiological role are the serum transferrins (Aisen, 1989). Based on a structural analysis of ovotransferrin, Sacchettini and coworkers have proposed that the two domains of the N-terminal lobe of the protein exist in an open or closed conformation depending on the protonation state of Lys209 and 301 which are close together in three-dimensional space (Dewan et $al.$, 1993). In the closed conformation, one of these lysyl residues has an unusually low pK_{ap} so that near neutral pH the residue is deprotonated and hydrogen bonded to the neighbouring lysyl residue. Acidification of the solution results in the protonation of both lysines, the concomitant electrostatic repulsion between these residues, and the opening of the protein in a hinge-like fashion to release iron (Dewan et $al.$, 1993). Such a proton-assisted structural modification of the binding site is consistent with the observed rapid phase of iron release from holotransferrin (Chung & Raymond, 1993, Kretchmar-Ngyuen et $al.$, 1993; El Hage Chahine & Pakdaman, 1995).

Other examples of proteins that exhibit pH-linked conformational heterogeneity are phosphophoryn (Evans & Chan, 1994) and hemagglutinin (Tatulian & Tamm, 1996 and references therein). The former protein is isolated from tooth dentine and acts as an acidic template for biomineralization. According to a recent study by Evans and Chan, the calcium-depleted apo-protein

undergoes three distinct conformational reorganizations between pH 2 and 9. As the pH increases, the protein expands significantly in response to the electrostatic repulsion between an increasing number of Asp and phospho-Ser residues that are deprotonated. In the fully expanded form, the protein is believed to retain secondary structure elements as well as some of higher order, but it is an inefficient substrate for biomineralization. Hemagglutinin is a trimeric glycoprotein found in the protein coat of the influenza virus. At acidic pH, both the secondary and tertiary structures of the protein change (Wilson *et al.*, 1981; Bullough, *et al.*, 1994) so that the *N*-terminus of one of the subunits is inserted into the target membrane as a prelude to fusion of the viral and host membranes. Like the alkaline transition of ferricytochrome *c*, the acidic conformational transition of hemagglutinin is reversible in the absence of target membranes (Tatulian & Tamm, 1996).

Ligand shuttling is an elegant and efficient mechanism by which a metalloenzyme can carry out its metabolic function(s). In the case of cytochrome *c* oxidase, for example, labile coordination chemistry has been proposed to play a key role in the proton pumping activity of this enzyme. In one instance, Woodruff and coworkers envisioned a residue alternating as a ligand to the Cu_B centre and the heme a_3 iron (Woodruff, 1993). Binding of an exogenous ligand, such as dioxygen, to the Cu_B centre initiates a series of ligand exchanges which result in the transfer of the oxygen molecule to the heme a_3 for reduction, and the translocation of protons from one side of the membrane to the other. In a similar model proposed by Rousseau and coworkers, a histidyl and a tyrosyl residue alternately coordinate the heme a_3 iron from the same side (1993). In each phase of the axial ligand replacement cycle, protons are conveyed across the membrane and, at the same time, dioxygen is reduced via an oxyferryl heme intermediate. A third model favoured by Wikstrom and coworkers (1994; Morgan *et al*, 1994) involves the labile nature of a histidyl-Cu coordination bond. The oxidation and ligation states of the copper influence the pK_as of a histidyl residue so that the side chain cycles between three

protonation states and ligation to the copper atom and thus pumps protons across the membrane. Although other mechanisms have been proposed (for *e.g.*, Gelles *et al.*, 1986) and refuted based on details of the X-ray crystal structures of cytochrome *c* oxidase from *Paracoccus denitrificans* (Iwata *et al.*, 1995) and beef heart (Tsukihara *et al.*, 1996), the current opinion is that a ligand shuttle mechanism of some sort is included in the activity of cytochrome *c* oxidase.

4.5   Possible Roles of the Alkaline Conformers

The alkaline conformational transitions of ferricytochromes *c* are ligand shuttling processes that significantly alter the structural and functional properties of these proteins. A similar ligand shuttling event was shown recently to occur at the heme iron of the *c* domain of cytochrome cd_1 nitrite reductase from *Thiosphaera pantotropha* which converts nitrite to nitric oxide (Williams *et al.*, 1997). In this case, the ligand exchange from His/His to His/Met coordination upon reduction of the heme iron appears to protect the metal centre from the irreversible ligation by nitric oxide. Whether or not the alkaline transitions of ferricytochromes *c* occur for a specific metabolic function remains to be determined. The predominant view in the literature is that alkaline ferricytochromes *c* are inactive and rarely found *in vivo*. Part of this argument is that a Met-Fe^{3+} bond is required to maintain the midpoint reduction potential of cytochrome *c* at 250-320 mV *vs*. SHE despite its relative weakness, and the transition to an alkaline species is an "accidental" phenomenon. Nevertheless, several properties of these conformational transitions and of cytochrome *c* suggest that they are not merely chance events. (1) The isomerizations are highly reversible despite the significant structural reorganization that must occur to swing Lys73 into the coordination sphere of the iron. (2) The alkaline conformational transition is a common process in cytochromes *c* from a wide variety of species including bacteria and higher eukaryotes. (3) Amino acids shown here to influence these

conformational equilibria and rates of reactions are highly conserved. (4) Mechanisms appear to be in place to prevent the premature or unwanted formation of the Lys-coordinated species (*i.e.*, the prolyl residues that flank Lys73 severely restrict the spontaneous generation of the Lys73-bound alkaline conformer, and trimethylation of Lys72 in the yeast protein prevents this residue from replacing Met80 as a heme ligand) which argues for, and against the assumption that the alkaline isomerizations serve a metabolic function.

Clearly, the pH-linked structural dynamics of ferricytochromes *c* are strongly dependent on environmental factors including temperature, ionic strength, specific binding to ions, proteins and lipids. Therefore, it is imperative to define the nature of the milieu within the intermembranal space of mitochondria where cytochromes *c* reside. *In vivo*, interaction with phospholipids and hydration state may promote the formation of the alkaline conformers. The effects of phospholipids have been noted above. Early evidence that dehydration of ferricytochrome *c* (*i.e.*, lyophilization) destabilizes the Met80-Fe^{3+} bond to result in an alkaline-like species suggests a role for this consideration (Aviram & Schejter, 1972). Notably, upon rehydration at pH 7.0, the native conformation of the protein is reestablished over a period of a few minutes. Assuming that the water content in the intermembranal space of mitochondria is no greater than that of the cytoplasm (~70%; Alberts, 1994), the hydration state of the protein may be an under-appreciated physiological consideration.

If, as discussed above, the formation of the alkaline conformers of cytochrome *c in vivo* is possible under certain conditions, then hypotheses regarding the function of these alkaline species can be formulated on the bases of their known properties. For example, Nall and coworkers have demonstrated that ferricytochrome *c* denatures at a higher guanidine hydrochloride concentration at pH 9.1 (C_{50}~2.2 M guanidine hydrochloride) than at pH 7.2 (C_{50}~1.5 M guanidine hydrochloride) (Osterhout *et al.*, 1985). The ^{1}H-NMR spectra of the unfolded proteins at either pH are almost

indistinguishable. These observations suggest that at least one alkaline conformer of yeast *iso*-2-ferricytochrome *c* is less susceptible to chemical denaturation than the native protein and, therefore, that the alkaline transition of this hemeprotein may offer a degree of stabilization.

Whereas the dramatic decrease in the reduction potential upon isomerization (~450 mV; Barker & Mauk, 1993) reverses the thermodynamic driving force for the reduction of alkaline ferricytochrome *c* by cytochrome b_5, cytochrome *c* reductase, and sulfite oxidase, it enhances substantially the oxidation of the ferrous form by the peroxidase and the oxidase. Therefore, while the transfer of electrons to alkaline ferricytochrome *c* is essentially halted, the transfer from ferrocytochrome *c* to the peroxidase or the oxidase becomes more favourable if these interactions induce the alkaline transition in the ferrous form of the cytochrome. Although this isomerization of the reduced protein is not unprecedented *in vitro* (Barker & Mauk, 1992), it has not been documented *in vivo*. Nevertheless, resonance Raman evidence presently under review suggests that the Met80-Fe^{2+} bond in cytochrome *c* is disrupted by the interaction of the ferrocytochrome with charged surfaces in a similar fashion as the ferric protein (*vide supra*; Döpner *et al.*, submitted). On the other hand, if the conformational transition takes place immediately after the electron is transferred from the cytochrome to the oxidase/peroxidase, then the transition provides a conformational switch that gates the electron transfer.

As noted in the introduction, various lysyl residues are known to form an integral part in the docking surface of cytochrome *c* with its electron transfer partners. Lys73 and Lys79 figure prominently in the complexes of this heme protein with cytochrome *c* peroxidase, cytochrome b_5, and cytochrome *c* oxidase. Therefore, the role of the alkaline conformational transition may be to decrease the affinity of these proteins for the cytochrome, particularly if the "redox energy" is transformed into conformational energy as in the case of the cytochrome cd_1 nitrite reductase system

mentioned above (Williams *et al.*, 1997), or as in a model system based on the Phe82His variant of cytochrome *c* (Feinberg *et al.*, 1998). Such a mechanism is particularly useful for the decomposition of peroxides and the reduction of oxygen because these reactions are two electron processes that benefit from a low competition between ferri- and ferrocytochrome *c* for the binding site(s) in the partner protein. Therefore, isomerization to the alkaline conformers may facilitate the separation of the protein from the peroxidase/oxidase to promote docking of a second ferrocytochrome .

4.6   Concluding Remarks

The alkaline conformational transition of ferricytochromes *c* is an intriguing feature of this protein that remains only partially understood after decades of study. These isomerizations are highly organized processes that share some mechanistic features with the structural dynamics of other proteins. Therefore, the complete elucidation of the mechanisms by which these structural changes take place in ferricytochromes *c* should also contribute to a general understanding of the conformational dynamics of other proteins. The identification of the trigger group remains the most fundamental enigma of the process. However, it may turn out that this trigger is a collection of events rather than the deprotonation of a single titrating group that induces the alkaline transition of the protein. The elucidation of the three-dimensional structures of the alkaline conformers of ferricytochrome *c* is likely to be the next major milestone in the characterization of these conformational transitions. Fortunately, with the recent development of the bacterial expression system of mitochondrial cytochrome *c*, it is now feasible to prepare isotopically-enriched cytochrome *c* to facilitate the determination of these structures by nuclear magnetic resonance spectroscopy.

Bibliography

Aisen, F. (1989) *Iron Carriers and Iron Proteins* (Loehr, T.M. Ed.), VCH Publishers, New York, pp. 353-372.

Alberts, B. (1994) *Molecular Biology of the Cell*, John Wiley & Sons, New York.

Alleyne, T. & Wilson, M.T. (1987) *Cytochromes Systems, Molecular Biology and Bioenergetics* (Papa, S., Chance, B. & Ernster, L., Eds.), Plenum Press, New York, pp. 713-720.

Amegadzie, B.Y., Zitomer, R.S. & Hollenberg, C.P. (1990) *Yeast*, **6**, 429-440.

Andersson, T., Thulin, E. & Forsén, S. (1979) *J. Am. Chem. Soc.*, **18**, 2487-2493.

Andersson, T., Ångström, J., Falk, K.E. & Forsén, S. (1980) *Eur. J. Biochem.*, **110**, 363-369.

Antalík, M., Bona, M. & Jaroslava, B. (1992) *Biochem. Int.*, **28**, 675-682.

Arciero, D.M., Peng, Q., Peterson, J. & Hooper, A.B. (1994) *FEBS Lett.*, **342**, 217-220.

Arean, C.O., Moore, G.R., Williams, G. & Williams, R.J.P. (1988) *Eur. J. Biochem.*, **173**, 607-615.

Ångström, J., Moore, G.R. & Williams, R.J.P. (1982) *Biochim. Biophys. Acta*, **703**, 87-94.

Antalík, M., Bona, M. & Bágelová, J. (1992) *Biochem. Int.*, **28**, 675-682.

Armstrong, F.A., Bond, A.M., Hill, H.A.O., Psalti, I.S.M. & Zoshi, C.G. (1989) *J. Phys. Chem.*, **93**, 6485-6493.

Ashida, T., Tanaka, N., Yamane, T., Tsukihara, T. & Kakudo, M. (1973) *J. Biochem.*, **73**, 463-465.

Ausubel, F.M. (1993) **Current Protocols in Molecular Biology on CD ROM**, John Wiley & Sons, Inc., New York, NY.

Aviram. I. (1972) *Biochem. Biophys. Res. Commun.*, **47**, 1120-1125.

Aviram, I. & Schejter, A. (1972) *Biopolymers*, **11**, 2141-2145.

Aviram, I., Myer, Y.P. & Schejter, A. (1981) *J. Biol. Chem.*, **256**, 5540-5544.

Baistrocchi, P., Banci, L., Bertini, I., Turano, P., Bren, K.L. & Gray, H.B. (1996) *Biochemistry*, **35**, 13788-13796.

Baldari, C. & Cesarini, G. (1985) *Gene*, **35**, 27-32.

Banci, L., Bertini, I., Bren, K.L., Gray, H.B., Sompornpisut, P. & Turano, P. (1995) *Biochemistry* **34**, 11385-11398.

Banci, L., Bertini, I., Spyroulias, G.A. & Turano, P. (1998) *Eur. J. Inor. Chem.*, **5**, 583-591.

Barker, P.D. & Mauk, A.G. (1992) *J. Am. Chem. Soc.*, **114**, 3619-3624.

Berghuis, A.M. & Brayer, G.D. (1992) *J. Mol. Biol.*, **223**, 959-976.

Betz, S.F. & Pielak, G.J. (1992) *Biochemistry*, **31**, 12337-12344.

Blumberg, W.E. & Peisach, J. (1971) *Probes of Structure and Function of Macromolecules and Membranes*, **2**, (Chance, B., Yonetani, T., and Mildvan, A.S., Eds.), Academic Press, New York, pp. 215-227.

Blumberg, W.E. & Peisach, J. (1971a) *Adv. Chem. Ser.*, **100**, 271-291.

Blumberg, W.E. & Peisach, J. (1971b) *Magnetic Resonances in Biological Research* (Franconi, C., Ed.), Gordon and Breach, New York, pp. 65-73.

Bosshard, H.R. (1981) *J. Mol. Biol.*, **153**, 1125-1149.

Brautigan, D. L., Feinberg, B.A., Hoffman, B.M., Margoliash, E., Peisach, J. & Blumberg, W.E. (1977) *J. Biol. Chem.*, **252**, 574-582.

Brautigan, D. L., Ferguson-Miller, S. & Margoliash, E. (1978) *Methods in Enzymology*, **53**, 128-64.

Bren, K.L. (1996) Ph.D. Dissertation, California Institute of Technology, Pasadena CA.

Brittain, T. & Greenwood, C. (1975) *Biochem. J.*, **147**, 175-177.

Bullough, P.A., Hughson, F.M., Skehel, J.J. & Wiley, D.C. (1994) *Nature*, **371**, 37-43.

Burch, A.M., Rigby, S.E.J., Funk, W.D., MacGillivray, R.T.A., Mauk, M.R., Mauk, A.G. & Moore, G.R. (1990) *Science*, **247**, 831-833.

Burns, P.D. & La Mar G. (1981) *J. Biol. Chem.*, **256**, 4934-4939.

Bushnell, G.W., Louie, G.V. & Brayer, G.D. (1990) *J. Mol. Biol.*, **214**, 585-595.

Butt, W.D. & Keilin, D. (1962) *Proc. Royal Soc. Lond.*, **B152**, 429-458.

Bychkova, V.E., Dujsekina, A.E., Klenin, S.I., Tiktopulo, E.I., Uversky, V.N. & Ptitsyn, O.B. (1996) *Biochemistry*, **35**, 6058-6063.

Caughey, W.S. (1966) *Hemes and Hemoproteins* (Chance, B., Eastabrook, R.W. & Yonetani, T., Eds.), Academic Press, New York, pp. 276-277.

Cannon, J.B. & Erman, J.E. (1980) *Biochim. Biophys. Acta*, **600**, 19-26.

Cheesman, M.R., Greenwood, C. & Thomson, A.J. (1991) *Adv. Inorg. Chem.*, **36**, 201-255.

Chung, T.D.Y. & Raymond, K.N. (1993) *J. Am. Chem. Soc.*, **115**, 6765-6768.

Colon, W., Wakem, L.P., Sherman, F. & Roder, H. (1997) *Biochemistry*, **36**, 12535-12541

Concar, D.W., Whitford, D. & Williams, R.J.P. (1991) *Eur. J. Biochem.*, **199**, 569-574.

Connors, K.A. (1987) *Binding Constants*, John Wiley & Sons, New York.

Cortese, J.D., Voglino, A.L. & Hackenbrock, C.R. (1995) *Biochim. Biophys. Acta*, **1228**, 216-228.

Cortese, J.D., Voglino, A.L. & Hackenbrock, C.R. (1998) *Biochemistry*, **37**, 6402-6409.

Cutler, R.L., Pielak, G.J., Mauk, A.G. & Smith, M. (1987) *Protein Eng.*, *1*, 569-574.

Davies, A.M., Guillemette, J.G., Smith, M., Greenwood, C., Thurgood, A.G. P., Mauk, A.G. & Moore, G.R. (1993) *Biochemistry*, **32**, 5431-5435.

Davis, L.A., Schejter, A. & Hess, G.P. (1974) *J. Biol. Chem.*, **249**, 2624-2632.

Degtyarenko, K.N., North, A.C.T. & Findlay, J.B.C. (1997) *Protein Engineering*, **10**, 183-186.

Degtyarenko, K.N., North, A.C.T., Perkins, D.N. & Findlay, J.B.C. (1998) *Nucleic Acids Res.*, **26**, 376-381.

Deng, W.P. & Nickoloff, J.A. (1992) *Anal. Biochem.*, **200**, 81-88.

Dente, L., Cesarini, G. & Cortese, R. (1983) *Nucleic Acid Research*, **11**, 1645-1655.

Dente, L. & Cortese, R. (1987) *Methods in Emzymology*, **155**, 111-119.

Desbois, A. (1994) *Biochimie*, **76**, 693-707.

Dewan, J.C., Mikami, B., Hirose, M. & Sacchettini. J.C. (1993) *Biochemistry*, **32**, 11963-11968.

Dickerson, R.E., Takano, T., Eisenberg, D., Kallai, O.B., Samson, L., Cooper. A. & Margoliash, E. (1971) *J. Biol. Chem.*, **246**, 1511-1535.

Dickerson, R.E. & Timkovich, R. (1975) *The Enzymes* (Boyer, P.D. Ed..), Academic Press, New York, pp. 397-547.

Dixon, D.W., Hong. X. & Woehler, S.E. (1989) *Biophys. J.*, **56**, 339-351.

Dong, A., Huang, P. & Caughey, W.S. (1992) *Biochemistry*, **31**, 182-189.

Döpner, S., Hildebrandt, P., Rosell, F.I. & Mauk, A.G. (1998) *J. Am. Chem. Soc.*, **120**, 11246-11255.

Döpner, S., Hildebrandt, P., Rosell, F.I., Mauk, A.G., von Walter, M., Soulimane, T. & Buse, G. (1998) *Eur. J. Biochem.*, submitted.

Döpner, S. (1995) Ph.D. Dissertation, Max-Planck-Institut für Strahlenchemie, Mülheim an der Ruhr, Germany.

Dumont, M.E., Ernst, J.F., Hampsey, D.M. & Sherman, F. (1987) *EMBO J.*, **6**, 235-241.

Dumont, M.E., Corin, A.F. & Campbell, G.A. (1994) *Biochemistry*, **33**, 7368-7378.

Eaton, W.A. & Hochstrasser, R.J. (1967) *J. Chem. Phys.*, **46**, 2533-2539.

Eccles, C., Guntert, P., Billeter, M. & Wuthrich, K. (1991) *J. of Biomol. NMR*, **1**, 111-30.

Eddows, M.J. & Hill, H.A.O. (1977) *J. Chem. Soc. Chem. Commun.*, 771-772.

El Hage Chahine, J-M. & Pakdaman, R. (1995) *Eur. J. Biochem.*, **230**, 1102-1110.

Elliot, D., Hamnett, A., Lettington, O.C., Hill, H.A.O. &Watton, N.J. (1986) *J. Electroanal. Chem.*, **202**, 303-314.

Elöve, G.A., Bhuyan, A.K. & Roder, H. (1994) *Biochemistry*, **33**, 6925-6935.

Evans, J.S. & Chan, S.I. (1994) *Biopolymers*, **34**, 507-527.

Fanger, M.W. & Harbury, H.A. (1965) *Biochemistry*, **4**, 2541-2545.

Ferrer, J.C., Guillemette, J.G., Bogumil, R., Inglis, S.C., Smith, M. & Mauk, A.G. (1993) *J. Am. Chem. Soc.*, **115**, 7507-7508.

Feng, Y. & Englander, S.W. (1990) *Biochemistry*, **29**, 3505-3509.

Forsén, S. & Hoffman, R.A. (1963) *J. Chem. Phys.*, **39**, 2892-2901.

Frew, D.E. & Hill, H.A.O. (1988) *Eur. J. of Biochem.*, **172**, 261-269.

Fumo, G., Spitzer, J.S. & Fetrow, J.S. (1995) *Gene*, **164**, 33-39.

Gadsby, P. M. A., Peterson, J., Foote, N., Greenwood, C. & Thomson, A. J. (1987) *Biochem. J.*, **246**, 43-54.

Gadsby, P. M. A. & Thomson, A. J. (1990) *J. Am. Chem. Soc.* **112**, 5003–5011.

Gao, Y., Boyd, J., Pielak, G.J. & Williams, R.J.P. (1991) *Biochemistry*, **30**,7033-7040.

Gelles, J., Blair, D.F. & Chan, S.I. (1986) *Biochim. Biophys. Acta*, **853**, 205-236.

George, P. & Tsou, C.L. (1952) *Biochem. J.*, **50**, 440.

Gerstein, M. & Krebs, W.G. (1997) "A Database of Molecular Motions," submitted. (Database located at http://bioinfo.mbb.yale.edu/MolMovDB/).

Glasoe, P.K. & Long, F.A. (1960) *J. Phys. Chem.*, **64**, 188-191.

Gopal, D., Wilson, G.S., Earl, R.A. & Cusanovich, M.A. (1988) *J. Biol. Chem.*, **263**, 11652-11656.

Gouterman, M. (1959) *J. Chem. Phys.*, **30**, 1139.

Greenwood, C. & Palmer, G. (1965) *J. Biol. Chem.*, **240**, 3660-3663.

Guillemette, J.G., Matsushima-Hibiya, Y., Atkinson, T. & Smith, M. (1991) *Protein Eng.*, **4**, 585-592.

Guillemette, J.G., Barker, P.D., Eltis, L.D., Lo, T.P., Smith, M., Brayer, G.D. & Mauk, A.G. (1994) *Biochemie*, **76**, 592-604.

Hall, P.L., Angel, B.R. & Jones, J.P.E. (1974) *J. Mag. Res.*, **15**, 64-68.

Hampsey, D.M., Das, G. & Sherman, F. (1988) *FEBS Lett.*, **231**, 275-283.

Hampton, M.B., Zhivotovsky, B., Slater, A.F., Burgess, D.H. & Orrenius, S. (1998) *Biochem. J.*, **329**, 95-99.

Harbury (1965) *Proc. Natl. Acad. Sci. U.S.A.* **54**, 1658-1664.

Hasumi, H. (1980) *Biochim. Biophys. Acta*, **626**, 265-276.

Hawkins, B.K., Hilgen-Willis, S., Pielak, G.J. & Dawson, J.H. (1994) *J. Am. Chem. Soc.*, **116**, 3111-3112.

Herrmann, L.M. & Bowler, B.B. (1997) *Protein Science*, **6**, 657-665.

Hettinger, T.P. & Harbury, H.A. (1965) *Biochemistry*, **4**, 2585-2589.

Hildebrandt, P. (1990) *Biochim. Biophys. Acta.*, **1040**, 175-186.

Hildebrandt, P. & Stockburger, M. (1989) *Biochemistry*, **28**, 6710-6721.

Hildebrandt, P. & Stockburger, M. (1989) *Biochemistry*, **28**, 6722-6728.

Hildebrand, D.P., Burk, D.L., Maurus, R., Ferrer, J.C., Brayer, G.D. & Mauk, A.G. (1995) *Biochemistry*, **34**, 1997-2005.

Hill, R. (1956) *Modern Methods in Plant Analysis*, (Peich, I.K. & Tracey, M.V. Eds.), Springer-Verlag, New York.

Hodgson, D.R., Davis, R.E. & McConaghy (1995) *Brit. Vet. J.*, **150**, 219-235.

Hong, X.L. & Dixon, D.W. (1989) *FEBS Lett.*, **246**, 105-108

Inglis, S.C., Guillemette, J.G., Johnson, J.A. & Smith, M. (1991) *Protein Eng.* **4**, 569-574.

Inubishi, T. & Becker, E.D.J. (1983) *J. Magn. Reson.*, **51**, 128-133.

Iizuka, T. & Morishima, I. (1975) *Bioch. Biophys. Acta*, **400**, 143-153.

Iwata, S., Ostermeier, C., Ludwig, B. & Michel, H. (1995) *Nature*, **376**, 660-669.

Jeng, M.F. & Englander, S.W. (1991) *J. Mol. Biol.*, **221**, 1045-1061.

Kalinichenko, P. (1976), *Stud. Biophys.*, **58**, 235-240.

Kamatari, Y.O, Konno, T., Kataoka, M. & Akasaka, K. (1996) *J. Mol. Biol.*, **259**, 512-523.

Keilin, D. (1925) *Proc. Roy. Soc. (London)*, **B98**, 312.

Kihara, H., Saigo, S., Nakatani, H., Hiromi, K., Ikeda-Saito, M. & Iizuka, T. (1976) *Biochim. Biophys. Acta*, **430**, 225-243.

Kluck, R.M., Bossy-Wetzel, E., Green, D.R. & Newmeyer, D.D. (1997) *Science*, **275**, 1132-1136.

Kretchmar Ngyuen, S.A., Craig, A. & Raymond, K.N. (1993) *J. Am. Chem. Soc.*, **115**, 6758-6764.

Kroemer, G., Dallaporta, B. & Resche-Rigon, M. (1998) *Ann. Rev. Phys.*, **60**, 619-642.

Kunkel, T.A. (1985) *Proc. Natl. Acad. Sci. U.S.A.*, **82**, 488-492.

Kunkel, T.A., Roberts, J.D. & Zakour, R.A. (1987) *Meth. Enzymol.* **154**, 367-382.

Koutalos,Y., Ebrey, T.G., Gilson, H.R. & Honig B. (1990) *Biophys. J.*, **58**, 493-501.

La Mar, G. & Walker, F.A. (1979) *The Porphyrins*, **IV**, 61-157.

Lambeth, D.O., Campbell, K.L., Zand, R. & Palmer, G. (1973) *J. Biol. Chem.*, **248**, 8130-8136.

Landrum, H.L., Salmon, R.T. & Hawkridge, F.M. (1977) *J. Am. Chem. Soc.*, **99**, 3154-3158.

Laz, T.M., Pietras, D.F. & Sherman F. (1984) *Proc. Natl. Acad. Sci. U.S.A.*, **81**, 4475-4479.

Letellier, L. & Schechter, E. (1973) *Eur. J. Biochem.*, **40**, 507-512.

Li, F., Srinivasan, A., Wang, Y., Armstrong, R.C., Tomaselli, K.J. & Fritz, L.C. (1997) *J. Biol. Chem.*, **272,** 30299-30305.

Liu, G., Chen, Y. & Tang, W. (1996) *J. Chem. Soc.- Dalton Trans.*, **5,**795-801.

Liu, X., Kim, N.C., Yang, J., Jemmerson, R. & Wang, X. (1997) *Cell*, **86**, 147-157.

Lloyd, E., Ferrer, J.C., Funk, W.D., Mauk, M.R. & Mauk, A.G. (1994) *J. Am. Chem. Soc.*, **33**, 11432-11437.

Lloyd, E., Hildebrand, D.P., Tu, K.M. &.Mauk, A.G. (1995) *J. Am. Chem. Soc.*, **117**, 6434-6438.

Lo, T.P. (1995) Ph.D. Dissertation, Department of Biochemistry and Molecular Biology, The University of British Columbia.

Loew, G.H. (1982) *Iron Porphyrins, Part One* (Lever, A.B.P. & Gray, H.B., Eds.), Addison-Wesley Publishing Company, Don Mills, Ont, pp. 1-87.

Looze, Y., Polastro, E., Gielens, C. & Léonis, J. (1976) *Biochem. J.*, **157**, 773-775.

Looze, Y., Polastro, E., Deconinck M.C. & Léonis, J. (1978) *Intl. J.Pept. & Prot. Res.*, **12**, 233-236.

Louie, G.V., Hutcheon, W.L.B. & Brayer, G.D. (1988) *J. Mol. Biol.*, **199**, 295-314.

Louie, G.V. & Brayer, G.D. (1990) *J. Mol. Biol.*, **214**, 527-555.

Louie, G.V. (1990) Ph.D. Dissertation, Department of Biochemistry and Molecular Biology, The University of British Columbia.

Luntz, T.L., Schejter, A., Garber, E.A.E. & Margoliash, E. (1989) *Proc. Natl. Acad. Sci. U.S.A.*, **86**, 3524-3528.

Maltempo, M.M., Moss, T.H. & Cusanovich, M.A. (1974) *Biochim. Biophys. Acta*, **342,** 290-305.

Maltempo, M.M. (1976) *Q. Rev. Biophys.*, **9**, 181-215.

Maltempo, M.M. (1976) *Biochim. Biophys. Acta,* **434**, 513-518.

Margoliash, E. & Frohwirt, N (1959) *Biochem. J.,* **71**, 570-572.

Margoliash, E. & Schejter, (1995) *Cytochrome c. A Multidisciplinary Approach,* (Scott, R.A. & Mauk, A.G., Eds.) University Science Books, Sausalito, CA, pp.

Marion, D. (1994) *Biochemie,* **76**, 631-640.

Martinez, S.E., Huang, D., Szczepaniak, A., Cramer, W.A. & Smith, J.L. (1994) *Structure,* **2**, 95-105.

Matheson, I.B.C. (1989) *Computers Chem.,* **13**, 299-304.

Mauk, A. G., Coyle, C. L., Brodignon, E. & Gray, H. B. (1979) *J. Am. Chem. Soc.,* **101**, 5054–5056.

Meites, L. & Meites, T. (1948) *Anal. Chem.,* **20**, 984-985.

Meyer, T.E., Tollin, G. & Cusanovich, M.A. (1986) *Biochimie.,* **76**, 480-488.

Michel, B., Proudfoot, A.E.I., Wallace, C.J.A. & Bosshard, H.R. (1989) *Biochemistry,* **28**, 456-462.

Migita, C.T. & Iwaizumi, M. (1981) *J. Am. Chem. Soc.,* **103**, 4378-4381.

Mignotte, B. & Vayssiere, J.L. (1998) *Eur. J. Biochem.,* **252,** 1-15.

Mitchell, D.M., Adelroth, P., Hosler, J.P., Fetter, J.R, Brzezinski, P., Pressler, M.A., Aasa, R., Malmstrom, B.G., Alben, J.O., Babcock, G.T., Gennis, R.B. & Ferguson-Miller, S. (1996) *Biochemistry,* **35**, 824-828.

Moench, S.J. & Satterlee, J.D. (1989) *J. Biol. Chem.,* **264**, 9923-9931.

Moench, S.J., Shi, T-M. & Satterlee, J.D. (1991) *Eur. J. Biochem.,* **197**, 631-641.

Moore, G.R. & Pettigrew, G.W. (1990) *Cytochromes c. Evolutionary, Structural and Physichochemical Aspects,* Springer Verlag, New York.

Moore, G.R. (1983) *FEBS Lett.,* **161**, 171-175.

Moore, G.R., Cox, M.C., Crowe, D., Osborne, M.J., Mauk, A.G. & Wilson, J.T. (1995) *Nuclear Magnetic Resonance of Paramagnetic Macromolecules* (La Mar, G.N., Ed.), Kluwer Academic Publishers, Amsterdam, pp. 95-122.

Moore, G.R., Cox, M.C., Crowe, D., Osborne, M.J., Rosell, F.I., Bujons, J., Barker, P.D., Mauk, M.R., Mauk, A.G. (1998) *Biochem. J.,* **332**, 439-449.

Mori, E. & Morita, Y. (1980) *J Biochem.*, **87**, 249-266.

Morton, R.A. (1973) *Can. J. Biochem.*, **51**, 465-471.

Morton, R.A. & Breskvar, K. (1977) *Can. J. Biochem.*, **55**, 146-151.

Myer, Y.P. (1985) *Current Topics in Bioenergetics*, *14*, 149-188.

Nagendra, H.G., Sukumar, N.S. & Vijayan, M. (1998) *Proteins: Struc. Func. Gen.*, **32**, 229-240.

Nall, B.T. (1986) *Biochemistry*, **25**, 2974-2978.

Nall, B.T., Zuñiga, E.H., White, T.B., Wood, L.C. & Ramdas, L (1989) *Biochemistry*, **28**, 9834-9839.

Nall, B.T. (1995) *Cytochrome c. A Multidisciplinary Approach*, (Scott, R.A. & Mauk, A.G., Eds.), University Science Books, Sausalito, CA, pp. 167-201.

Nicholson, D.W., Hergersberg, C. & Neupert, W. (1988) *J. Biol. Chem.*, **263**, 19034-19042.

Nicholson, D.W. & Neupert, W. (1989) *Proc. Natl. Acad. Sci. U.S.A.*, **86**, 4340-4344.

Northrup, S.H., Thomasson, K.A., Miller, C.M., Barker, P.D., Eltis, L.D., Guillemette, J.G., Lo, T.P., Inglis, S.C. & Mauk, A.G. (1993) *Biochemistry*, **32**, 6613-6623.

Nozaki, M., Mutzushima, H., Horio, T. & Okunuki, K. (1958) *J. Biochem.*, **45**, 815-823.

Ochi, H., Hata, Y., Tanaka, N., Kakudo, M., Sakurai, T., Aihara, S. & Morita, Y. (1983) *J. Mol. Biol.*, **166**, 407-418.

Osheroff, N., Koppenol, W.H. & Margoliash, E. (1978) *Frontiers of Biological Energetics* (Dutton, P.L., Leigh, J. & Scarpa, A.), Academic Press, New York, pp. 439-449.

Osheroff, N., Borden, D., Koppenol, W.H. & Margoliash, E. (1980) *J. Biol. Chem.*, **255**, 1689-1697.

Osterhout, J.J.Jr., Muthukrishnan, K. & Nall, B.T. (1985) *Biochemistry*, **24**, 6680-6684.

Otiko, G. & Sadler, P.J. (1980) *FEBS Lett.*, **116**, 227-230.

Pal, P.K., Verma, B. & Myer, Y. (1975) *Biochemistry*, **14**, 4325-4334.

Palmer, G. (1979) *The Porphyrins*, vol. IV (Dolphin, D. Ed.), Academic Press, New York, pp. 313-353.

Palmer, G. (1985) *Biochem. Soc. Trans.*, **13**, 548-560.

Panzer, R.E. & Elving, P.J. (1975) *Electrochim. Acta,* **20,** 635-647.

Pearce, L.L., Gärtner, A.L., Smith, M. & Mauk, A.G. (1989) *Biochemistry,* **28,** 3152-3156.

Pettigrew, G.W. & Moore, G.R. (1987) *Cytochromes c: Biological Aspects,* Springer Verlag, New York.

Pettigrew, G.W., Aviram, I. & Schejter, A. (1976) *Biochem. Biophys. Res. Commun.,* **68,** 807-813.

Pfeil, W. (1981) *Mol. Cell. Biochem.,* **226,** 3-28.

Pielak, G.J., Mauk, A.G. & Smith, M. (1985) *Nature,* **313,** 152-154.

Pinheiro, T.J.T. & Watts, A. (1994) *Biochemistry,* **33,** 2451-2458.

Pollock, W.B.R., Rosell, F.I., Twitchett, M.B., Dumont, M.E. & Mauk, A.G. (1998) *Biochemistry,* **37,** 6124-6131.

Preznat, T., Pfeifer, K. & Guarente, L. (1987) *Mol. Cell Biol.,* **7,** 3252-3259.

Qi, P.X., Di Stefano, D.L. & Wand, A.J. (1994) *Biochemistry,* **33,** 6408-6417.

Qi, P.X., Beckman, R.A. & Wand, A.J. (1996) *Biochemistry,* **35,** 12275-12286.

Rafferty, S.P., Pearce, L.L., Barker, P.D., Guillemette, J.G., Kay, C.M., Smith, M. & Mauk, A.G. (1990) *Biochemistry* **29,** 9365-9369.

Rafferty, S.P. (1992) Ph.D. Dissertation, The University of British Columbia, Vancouver, B.C., Canada.

Raman, C.S., Jemmerson, R., Nall, B.T. & Allen, M.J. (1992) *Biochemistry,* **31,** 10370-10379.

Redfield, A.G. & Gupta, R.K. (1971) *Cold Spring Harb. Symp. Quant. Biol.,* **36,** 405-411.

Rigby, S.E., Moore, G.R., Gray, J.C., Gadsby, P.M.A., George, S.J. & Thomson, A. J. (1988) *Biochem. J.,* **256,** 571-577.

Roberts, G.C.K. (1993) *NMR of Macromolecules : A Practical Approach,* IRL Press at Oxford University Press, Oxford, U.K.

Rodgers, K.K., Pochapsky, T.C. & Sligar, S.G. (1988) *Science,* **240,** 1657-1659.

Rosell, F.I., Ferrer, J.C. & Mauk, A.G. (1998) *J. Am. Chem. Soc.,* **120,** 11234-11245.

Russel, M., Kidd, S. & Kelley, M.R. (1986) *Gene,* **45,** 333-338.

Rytömaa, M. & Kinnunen, P.K. (1994) *J. Biol. Chem.*, **269**, 1770-1774.

Saigo, S. (1981a) *Bioch. Biophys. Acta,* **669**, 13-20.

Saigo, S. (1981b) *J. Biochem.*, **89**, 1977-1980.

Saigo, S. (1986) *J. Biochem.*, **100**, 157-165.

Salemme, F.R. (1976) *J. Mol. Biol.*, **102**, 563-568.

Salerno, J.C. (1984) *J. Biol. Chem.*, **259**, 2331-2336.

Sambrook, J., Fritsch, E.F. & Maniatis, T. (1989) **Molecular Cloning: a Laboratory Manual,** Cold Spring Harbor Laboratory Press, Cold Spring Harbor, New York.

Sanishvili, R., Volz, K.W., Westbrook, E.M. & Margoliash, E. (1995) *Structure,* **3**, 707-716.

Santos, H. & Turner, D.L. (1992) *Eur. J. Biochem.*, **206**, 721-728.

Santucci, R. & Ascoli, F. (1997) *J. Inorg. Biochem.*, **68**, 211-214.

Satterlee, J.D. (1986) *Ann. Rep. NMR Spec.,* 17, 79-178.

Schechter, E. & Saludjian, P. (1967) *Biopolymers,* **5**, 788-790.

Schejter, A.& Aviram, I. (1969) *Biochemistry,* **8,** 149-153.

Schejter, A., Aviram, I. & Sokolovsky, M. (1970) *Biochemistry,* **9**, 5118-5122.

Schejter, A., Luntz, T.L., Koshy, T.I. & Margoliash, E. (1992) *Biochemistry,* **31**, 8336-8343.

Schejter, A., Taler, G., Navon, G., Liu, X.J. & Margoliash, E. (1996) *J. Am. Chem. Soc.,* **118**, 477-478.

Scott, R.A. & Mauk, A.G. (1995) *Cytochrome c. A Multidisciplinary Approach,* University Science Books, Sausalito, CA.

Sedlák, E. (1997) *Biochem. Molec. Biol. Int.,* **41**, 25-32.

Sedlák, E. & Antalík, M. (1998) *Biopolymers,* **46**, 145-154.

Shao, W., Sun, H., Yao, Y. & Tang, W. (1995) *Inorg. Chem.,* **34**, 680-687.

Sherman, F., Stewart, J.W., Parker, J.H., Inhaber, E., Shipman, N.H., Putterman, G.J., Gardisky, R.L. & Margoliash, E. (1968), *J. Biol. Chem.*, **243**, 5446-5456.

Simonson, T. & Perahia, D. (1995) *Proc. Natl. Acad. Sci. U.S.A.*, **92**, 1082-1086.

Simpkin, D., Palmer, G., Devlin, F.J., McKenna, M.C., Jensen, G.M. & Stephens, P.J. (1989) *Biochemistry*, **28**, 8033-8039.

Skov, K., Hofmann, T. & Williams, G.R. (1969) *Can. J. Biochem.*, **47**, 750-752.

Skulachev, V.P. (1998) *FEBS Lett.*, **423**, 275-280.

Smith, D.W. & Williams, R.J.P. (1970) *Struct. Bond.*, **7**, 1-45.

Smith, H.T. & Millet, F. (1980) *Biochemistry*, **19**, 1117-1120.

Somero, G.N. (1986) *Am. J. Phys. Soc.*, **25**, R197-R213.

Soussi, B., Bylund-Fellenius, A., Scherstén, T. & Ångström, J. (1990) *Biochem. J.*, **265**, 227-232.

Spiro, T.G. (1985) *Adv. Prot. Chem.*, **37**, 111-159.

Stellwagen, E. & Schulman, R.G. (1973) *J. Mol. Biol.*, **80**, 559-573.

Stellwagen, E., Babul, J. & Wilgus, H. (1975) *Biochim. Biophys. Acta*, **4**, 115-121.

Stuart, R.A., Nicholson, D.W. & Neupert, W. (1990) *Cell*, **60**, 31-43.

Sutin, N. & Yandell, J.K. (1972) *J. Biol. Chem.*, **247**, 6932-6936.

Swanson, R., Trus, B.L., Mandel, N., Mandel, G., Kallai, O.B. & Dickerson, R.E. (1977) *J. Biol. Chem.*, **252**, 759-775.

Taborsky, G. & McCollum, K. (1979) *J. Biol. Chem.*, **254**, 7069-7075.

Takano, T., Kallai, O.B., Swanson, R. & Dickerson, R.E. (1973) *J. Biol. Chem.*, **248**, 5234-5255.

Takano, T., Trus, B.L., Mandel, N., Mandel, G., Kallai, O.B., Swanson, R. & Dickerson, R.E. (1977) *J. Biol. Chem.*, **252**, 776-785.

Takano, T. & Dickerson, R.E. (1980) *Proc. Natl. Acad. Sci. U.S.A.* 77, 6371-6375.

Takano, T. & Dickerson, R.E. (1981a) *J. Mol. Biol.*, **153**, 79-94.

Takano, T. & Dickerson, R.E. (1981b) *J. Mol. Biol.*, **153**, 95-115.

Taler, G., Shejter, A., Navon, G., Vig, I. & Margoliash, E. (1995) *Biochemistry*, **34**, 14209-14212.

Tanaka, N., Yamane, T., Tsukihara, T., Ashida, T. & Kakudo, M. (1975) *J. Biochem.*, 77, 147-162.

Taniuchi, H., Basile, G., Taniuchi, M. & Veloso, D. (1983) *J. Biol. Chem.*, **258**, 10963-10966.

Taniguchi, I., Masahiro, I., Yamaguchi, I. & Yasukinicki, K. (1984) *J. Electroanal. Chem.*, **1975**, 341-348.

Taniguchi, I., Iseki, M., Yamaguchi, H & Yasuko-uchi, K. (1985) *J. Electroanal. Chem.*, **186**, 299-307.

Tatulian, S.A. & Tamm, L.K. (1996) *J. Mol. Biol.*, **260**, 312-316.

Teixeira, M., Campos, A.P., Aguiar, A.P., Costa, H.S., Santos, H., Turner, D.L. & Xavier, A.V. (1993) *FEBS Lett.*, **317**, 233-236.

Theodorakis, J.L., Garber, E.A., McCracken, J., Peisach, J., Schejter, A. & Margoliash, E. (1995) *Biochim. Biophys. Acta*, **1252**, 103-113.

Theorell, H. (1936) *Biochem. Z.*, **285**, 207-218.

Theorell, H. (1939) *Science*, **90**, 67.

Theorell, H. & Åkesson, A. (1941) *J. Am. Chem. Soc.*, **63**, 1804-1811.

Theorell, H. & Åkesson, A. (1941) *J. Am. Chem. Soc.*, **63**, 1812-1814.

Theorell, H. & Åkesson, A. (1941) *J. Am. Chem. Soc.*, **63**, 1815-1820.

Theorell, H. (1941) *J. Am. Chem. Soc.*, **63**, 1820-1827.

Thöny-Meyer, L. (1997) *Microbiol. Mol. Biol. Rev.*, **63**, 337-376.

Tollin, G., Hanson, L.K., Caffrey, M., Meyer, T.E. & Cusanovich, M.A. (1986) *Proc. Natl. Acad. Sci. U.S.A.*, **83**, 3693-3697.

Tonge, P., Moore, G.R. & Wharton, C.W. (1989) *Biochem. J.*, **258**, 599-605.

Trewhella, J., Carlson, V. & Curtis, E.H. (1988) *Biochemistry*, **27**, 1121-1125.

Trumbly, R.J. (1992) *Mol. Microbiol.*, **6**, 15-21.

Ubbink, M., Warmerdam, G.C., Campos, A.P., Teixeira, M. & Canters, G.W. (1994) *FEBS Lett.*, **351**, 100-104.

Uno, T., Nishimura, Y. & Tsuboi, M. (1984) *Biochemistry*, **23**, 6802-6806.

Walker, F.A., Huynh, B.H., Scheidt, W.R. & Osvath, S.R. (1986) *J. Am. Chem. Soc.*, **108**, 5288-5297.

Wallace, C.J.A. (1984) *Biochem. J.*, **217**, 604-604.

Wallace, C.J.A. & Clark-Lewis, I. (1992) *J. Biol. Chem.*, **267**, 3852-3861.

Wallace, C.J.A. & Clark-Lewis, I. (1997) *Biochemistry*, **36**, 14733-14740.

Weber, C., Michel, B. & Bosshard, H.R. (1987) *Proc. Natl. Acad. Sci. U.S.A.*, **84**, 6687-6691.

White, T.B., Berget, P.B. & Nall, B.T. (1987) *Biochemistry*, **26**, 4358-4366.

White-Dixon, D., Hong, X. & Woehler, S.E. (1989) *Biophys. J.*, **56**, 339-351.

Wilgus, H. & Stellwagen, E. (1974) *Proc. Natl. Acad. Sci. U.S.A.*, **71**, 2892-2894.

Williams, G., Moore, G.R., Porteus, E., Robinson, M.N., Soffe, N. & Williams, R.J.P. (1985) *J. Mol. Biol.*, **183**, 409-428.

Wilson, I.A., Skehel, J.J. & Wiley, D.C. (1981) *Nature*, **289**, 366-373.

Wilson, M.T. & Greenwood, C. (1995) *Cytochrome c. A Multidisciplinary Approach*, (Scott, R.A. & Mauk, A.G., Eds.) University Science Books, Sausalito, CA, pp. 611-635.

Wood, L.C., Muthukrishnan, K., White, T.B., Ramdas, L. & Nall, B.T. (1988) *Biochemistry*, **27**, 8554-8561.

Wood, L.C., White, T.B., Ramdas, L. & Nall, B.T. (1988) *Biochemistry*, **27**, 8562-8568.

Woodruff, W.H. (1993) *J. Bioenerg. Biomembr.*, **25**, 177-188.

Wooten, J.B., Cohen, J.S., Vig, I. & Shejter, A. (1981) *Biochemistry*, **20**, 5394-5402.

Wüthrich, K. (1986) *NMR of Proteins and Nucleic Acids*, John Wiley & Sons, New York.

Wyman, F. (1948) *Advances in Protein Chemistry*, IV, (Anson, M.L. & Edsall, J.T., Eds.) Academic Press Inc., New York, pp. 407-531.

Yamanaka, T., Mutzushima, H., Nozaki, M., Horio, T. & Okunuki, K. (1959) *J. Biochem.*, **46**, 121-132.

Yang, J., Liu, X., Bhalla, K., Kim, N.C., Ibrado, A.M., Cai, J., Peng, T., Jones, D.P. & Wang, X. (1997) *Science*, **275**, 1129-1132.

Zhivotovsky, B., Orrenius, S., Brustugun, O.T. & Doskeland, S.O. (1998) *Nature*, **391**, 449-450.

Zhou, H-X. & Vijayakumar, M. (1997) *J. Mol. Biol.*, **267**, 1002-1011.

Zitomer, R.S., Montgomery, D.L., Nichols, D.L. & Hall, B.D. (1979) *Proc. Natl. Acad. Sci. U.S.A.*, **76**, 3627-3631.

Zoller, M.J. & Smith, M. (1982a) *Nucleic Acids Res.* **10**, 6487-6500.

Zoller, M.J. & Smith, M. (1982b) *DNA* **3**, 479-488.

Zoller, M.J. & Smith, M. (1983) *Methods Enzymol.* **100**, 468-500.

Appendix 1. Definition of the model used to determine the K_{ap} of the alkaline conformational transition of yeast *iso*-1-ferricytochrome *c*.

$$\text{P-H} \underset{\text{H}^+}{\overset{K_a}{\rightleftharpoons}} \text{P} \qquad \text{1-1}$$
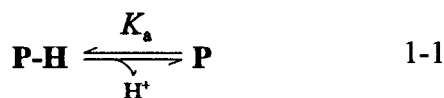
For the simple deprotonation of the molecule **P-H** as shown above, the Henderson-Hasselbach Relation is :

$$K_a = \frac{[P] \cdot [H^+]}{[P-H]} \qquad \text{1-2}$$

$$[P-H] = [P] \cdot 10^{(pK_a - pH)} \qquad \text{1-5}$$

$$pH = pK_a + \log(\frac{[P]}{[P-H]}) \qquad \text{1-3}$$

$$[P-H] = \frac{[T] \cdot 10^{(pK_a - pH)}}{(1 + 10^{(pK_a - pH)})} \qquad \text{1-6}$$

$$\log(\frac{[P-H]}{[P]}) = pK_a - pH \qquad \text{1-4}$$

where [T] is the total concentration of the molecule, therefore

$$[P] = [T] - [P-H] \qquad \text{1-7}$$

$$[P] = \frac{[T]}{(1 + 10^{(pK_a - pH)})} \qquad \text{1-9}$$

$$[P] = [T] - [P] \cdot 10^{(pK_a - pH)} \qquad \text{1-8}$$

The absorbance at a given wavelength, **Z**, reflects the contribution from all absorbing species

$$Z = \varepsilon_{(P-H)} \cdot [P-H] + \varepsilon_{(P)} \cdot [P] \qquad \text{1-10}$$

Substituting equations 1-6 and 1-9 into 1-10 yields

$$Z = \frac{[T] \cdot (\varepsilon_{(P-H)} \cdot 10^{(pK_a - pH)} + \varepsilon_{(P)})}{(1 + 10^{(pK_a - pH)})} \qquad \text{1-11}$$

$$Z = \frac{B + A \cdot 10^{(pK_a - pH)}}{(1 + 10^{(pK_a - pH)})} \qquad \text{1-12}$$

where

$$A = [T] \cdot \varepsilon_{(P-H)} \qquad \text{1-12a} \qquad\qquad B = [T] \cdot \varepsilon_{(P)} \qquad \text{1-12b}$$

However, the alkaline conformational transition of ferricytochromes c consists of a deprotonation that is coupled to a conformational reorganization of the protein. These linked equilibria are illustrated by the thermodynamic cycle shown in Relation 1-13.

$$
\begin{array}{ccc}
\text{N-H} & \overset{K_N}{\underset{\text{H}^+}{\rightleftharpoons}} & \text{N} \\
C_p \big\downarrow\big\uparrow & & \big\uparrow\big\downarrow C_d \\
\text{A-H} & \overset{\text{H}^+}{\underset{K_A}{\rightleftharpoons}} & \text{A}
\end{array}
\qquad 1\text{-}13
$$
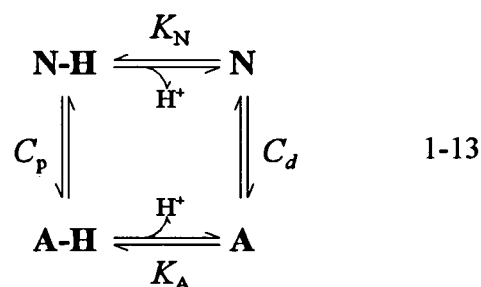
Spectrophotometrically, only the conformational states can be distinguished, not the protonation states. Consequently :

$$
K_{obs} = \frac{[NH] + [N]}{[AH] + [A]} \qquad 1\text{-}14
$$

or

$$
K_{obs} = C_d \cdot \left(\frac{1 + \dfrac{[H^+]}{K_A}}{1 + \dfrac{[H^+]}{K_N}} \right) \qquad 1\text{-}15
$$

because

$$
K_N \cdot C_d = K_A \cdot C_p \qquad 1\text{-}16
$$

At high pH :

$$
K_{obs} \rightarrow C_d
$$

and at low pH :

$$
K_{obs} \rightarrow C_p
$$

At equilibrium, the fraction of the sample in the native state is given by 1-17a while that of the alkaline species is given by 1-17b

$$
f(NH + N) = \frac{1}{1 + K_{obs}} \qquad 1\text{-}17a
$$

$$
f(AH + A) = \frac{K_{obs}}{1 + K_{obs}} \qquad 1\text{-}17b
$$

$$
Z = \varepsilon_N \cdot \left(\frac{1}{1 + K_{obs}} \right) + \varepsilon_A \cdot \left(\frac{K_{obs}}{1 + K_{obs}} \right) \qquad 1\text{-}18a
$$

$$
Z = \frac{\varepsilon_N + \varepsilon_A \cdot K_{obs}}{1 + K_{obs}} \qquad 1\text{-}18b
$$

At any given wavelength, the measured absorbance is the sum of the contribution of all absorbing species as shown in Equations 1-18 and 1-19.

$$
Z = \frac{\varepsilon_N \cdot \left(1 + \dfrac{[H^+]}{K_N} \right) + \varepsilon_A \cdot C_d}{C_d + \left(1 + \dfrac{[H^+]}{K_N} \right)} \qquad 1\text{-}19
$$

As $C_p \to 0$ (*i.e.*, the ligand exchange is strongly disfavoured prior to deprotonation), $K_A \gg 1$ so that

$$Z \to \frac{\varepsilon_N \cdot (1 + \frac{[H^+]}{K_N}) + \varepsilon_A \cdot C_d}{C_d + (1 + \frac{[H^+]}{K_N})} \qquad 1\text{-}20$$

At low pH, $[H^+] \gg K_N$, therefore

$$Z \to \frac{\varepsilon_N \cdot (\frac{[H^+]}{K_N}) + \varepsilon_A \cdot C_d}{C_d + \frac{[H^+]}{K_N}} \qquad 1\text{-}21$$

At $C_d \ll 1$:

$$Z \to \varepsilon_N$$

at $C_d = 1$

$$Z \to \frac{\varepsilon_N \cdot (\frac{[H^+]}{K_N}) + \varepsilon_A}{1 + \frac{[H^+]}{K_N}}$$

and at $C_d \gg 1$

$$Z \to \varepsilon_A$$

At high pH, $[H^+] \ll K_N$, therefore

$$Z = \frac{\varepsilon_N + \varepsilon_A \cdot C_d}{C_d + 1} \qquad 1\text{-}22$$

At $C_d \ll 1$:

$$Z \to \varepsilon_N$$

at $C_d = 1$

$$Z \to \frac{\varepsilon_N + \varepsilon_A}{2}$$

and at $C_d \gg 1$

$$Z \to \varepsilon_A$$

Equation 1-20 can be rearranged to 1-23 where $K_{ap} = K_N \cdot C_d$. Note that Equation 1-23 is analogous to 1-12 when $C_d \gg 1$. In this case A and B, from Equation 1-12 are ϵ_N and ϵ_A, respectively. This assumption is justified considering that the measured values of C_d of the yeast *iso*-1-ferricytochromes *c* studied here range from 94-4000 (=K_c in Table 11).

$$Z = \frac{(\varepsilon_A + \frac{\varepsilon_N}{C_d}) + \varepsilon_N \cdot (\frac{[H^+]}{K_{ap}})}{(1 + \frac{1}{C_d}) + \frac{[H^+]}{K_{ap}}} \qquad 1\text{-}23a$$

$$Z = \frac{(\varepsilon_A + \frac{\varepsilon_N}{C_d}) + \varepsilon_N \cdot 10^{pK_{ap} - pH}}{(1 + \frac{1}{C_d}) + 10^{pK_{ap} - pH}} \qquad 1\text{-}23b$$

190

Applying the same assumption ($K_{ap} = K_N \cdot C_d$) to the thermodynamic cycle (Equation 1-13) leads to the same conclusion as above.

$$K_{ap} = K_N \cdot C_d = K_A \cdot C_p \qquad \text{1-24}$$

$$K_{ap} = \frac{[N] \cdot [H^+]}{[NH]} \cdot \frac{[A]}{[N]} = \frac{[A - H] \cdot [H^+]}{[NH]} \cdot \frac{[A]}{[A - H]} \qquad \text{1-25}$$

$$K_{ap} = \frac{[A] \cdot [H^+]}{[NH]} \qquad \text{1-26}$$

This form of the apparent equilibrium constant is the same as that shown in Equation 1-2. Therefore, titration data can be fitted to the Henderson-Hasselbach model for the simple deprotonation of a group using Equation 1-12 provided that the protonation state of the native and alkaline species does not influence the corresponding extinction coefficients.

Appendix 2. Using the Gouy-Chapman equation to investigate the ionic strength dependence of the alkaline conformational equilibrium of cytochromes c.

According to the Boltzmann equation, the local pH at a surface depends on the bulk pH of the solution and on the electrostatic potential of the surface, ϕ_0.

$$[H^+]_{local} = [H^+]_{bulk} \cdot \exp(\frac{-e\phi_0}{kT}) \quad (2\text{-}1)$$

where e is the charge of the proton, ϕ_0 is the electrostatic potential of the surface, k is the Boltzmann constant, and T is the temperature (K). Because $pK_{true} = pH_{local}$ at the midpoint of the titration, the $pH_{bulk} = pK_{apparent}$ (Koutalos et al., 1990). Therefore, Equation 2-1 can be redefined as

$$pK_{true} - pK_{apparent} = \log[\exp(\frac{-e\phi_0}{kT})] \quad (2\text{-}2)$$

$$\frac{e\phi_0}{kT} = 2.30 \cdot (pK_{true} - pK_{apparent}) \quad (2\text{-}3)$$

According to the Gouy-Chapman equation, the surface potential ϕ_0 is a function of the surface charge density and the ionic strength.

$$A \cdot \frac{\sigma}{\sqrt{C}} = \sinh(\frac{z \cdot e \cdot \phi_0}{2kT}) \quad (2\text{-}4)$$

where σ is the surface charge density, C is the salt concentration, z is the valence of the electrolyte (i.e., $z = 1$ for KCl), and A a the constant :

$$A = (8 \cdot \epsilon \cdot \epsilon_0 \cdot N_A k \cdot T)^{\frac{1}{2}} \quad (2\text{-}5)$$

In Equation 2-5, ϵ is the dielectric constant of the protein ($\epsilon = 25 \pm 10$; reported by Simonson and Perahia (1995) assuming that the radius of cytochrome c, including all protein atoms in 2YCC.PDB and 20 bound water molecules is 16.5 Å), ϵ_0 is the permittivity of free space, and N_A is Avogadro's number. At 25 °C, $A = 76.3\ M^{\frac{1}{2}}$ for cytochrome c.

Substitution of this constant and Equation 2-3 into the Gouy-Chapman Equation (2-4) yields the expression :

$$\frac{76.3 \cdot \sigma}{\sqrt{C}} = \sinh[1.15 \cdot (pK_{true} - pK_{apparent})] \quad (2\text{-}6)$$

$$\sinh(x) = [\frac{e^x - e^{-x}}{2}]$$

The $pK_{apparent}$ values are determined according to Appendix 1 and at a variety of salt concentrations.

These values are then be fitted to Equation 2-6 to estimate the true pK_a of the titrating group and the average surface charge density in the immediate region around this titrating group.

Appendix 3. Simulation of the alkaline transition kinetics of wild-type yeast *iso-1-*
ferricytochrome*c*.

At a given pH, the percentage of the total ferricytochrome c in the alkaline state (**A**) can be determined from the experimentally determined pK_{ap} using the Henderson-Hasselbach equation (3-1)

$$\frac{A}{1-A} = 10^{(pH - pK_{ap})} \quad (3-1)$$

Assuming that in the wild-type protein the alkaline conformational rearrangement to each of the two Lys-bound states (A_{73} and A_{79}) occurs independently from the other, these ratios can be used as weighing factors to reconstruct the k_{obs} for the wild-type protein using the k_{obs} obtained for the Lys73Ala and Lys79Ala variants. The fraction of the wild-type protein that is in the LysX-bound alkaline state is :

$$WT^X\% = \frac{A_{wt} \cdot A_X}{A_{73} + A_{79}} \quad (3-2)$$

Therefore

$$k_{obs}^{WT} = k_{obs}^{73} \cdot WT^{73}\% + k_{obs}^{79} \cdot WT^{79}\% \quad (3-3)$$

where k^X_{obs} is the observed rate constant observed in pH-jump experiments of cytochrome c X at a given pH.

194

Appendix 4. Preliminary residue-specific proton assignments for the yeast *iso*-1-ferricytochrome *c* variant Lys79Ala/Cys102Thr. These assignments were compiled from NOE and TOC spectra collected at pH* 10.8, 298 K in H_2O and D_2O.

Residue		Proton	(ppm)	Residue		Proton	(ppm)	Residue		Proton	(ppm)
Phe	-3	HD1	7.062	Leu	15	HB2	2.415		36	CE1	6.711
	-3	CE1	7.227		15	HB3	2.106		36	HZ	7.248
	-3	HZ	7.137		15	HG	2.337	Gly	37	HA1	3.673
Ala	-1	HN	7.936		15	QD1	1.446		37	HA2	4.188
	-1	HA	3.634		15	QD2	2.051	His	39	HD2	6.974
	-1	QB	1.125	Cys	17	HA	5.981		39	HE1	8.495
Gly	1	HA1	3.553		17	HB2	0.635	Ser	40	HA	4.467
	1	HA2	4.400		17	HB3	-0.880		40	HB2	4.201
Ser	2	HA	4.823	Thr	19	HA	6.542		40	HB3	3.768
	2	HB2	3.724		19	HB	5.692	Ala	43	HA	4.315
	2	HB3	3.182		19	QG2	2.495		43	QB	1.361
Ala	3	HA	4.036	His	18	HN	11.395	Gly	45	HA1	3.623
	3	QB	1.515		18	HB3	15.033		45	HA2	4.247
Lys	5	HN	7.706		18	HB2	9.467	Tyr	46	HD1	6.434
	5	HA	4.067		18	HA	10.743		46	HE1	7.077
	5	HB3	1.762		18	HD2	6.222		46	HD2	6.040
	5	HG2	2.276		18	HE1	6.882		46	HE2	6.730
	5	HG3	2.719	Val	20	HA	4.199	Tyr	48	HA	4.111
	5	HD2	2.008		20	HB	2.301		48	HB2	6.299
	5	HD3	1.687		20	QG1	1.075		48	HB3	3.232
	5	HE2	1.002		20	QG2	0.928		48	HD1	6.932
Gly	6	HA2	3.296	Gly	23	HA1	3.133		48	HE1	6.563
	6	HA1	3.992		23	HA2	4.160	Asn	52	HN	8.445
Ala	7	HA	2.398	Gly	24	HA2	3.894		52	HA	4.594
	7	QB	1.238		24	HA1	4.399		52	HB2	2.891
Thr	8	HA	3.948	His	26	HD2	6.952		52	HB3	3.161
	8	HB	4.186		26	HE1	7.764		52	HD1	7.031
	8	QG2	1.226	Val	28	HA	3.388	Ile	53	HA	3.405
Leu	9	HA	3.824		28	HB	1.133		53	HB	2.851
	9	HB3	1.877		28	QG1	-0.861		53	QG2	1.370
	9	QD1	0.649		28	QG2	0.616		53	HG12	0.730
	9	QD2	0.895	Asn	31	HA	5.724		53	HG13	1.167
Phe	10	HA	3.425		31	HB2	3.475		53	QD1	1.031
	10	HB2	2.964		31	HB3	2.492	Asn	56	HA	4.317
	10	HB3	2.659		31	HD1	8.550		56	HB2	2.314
	10	CD1	7.011	His	33	HE1	8.060		56	HB3	3.146
	10	CE1	7.470		33	HD2	7.250		56	HD1	6.788
	10	HZ	8.568	Gly	34	HA2	3.700	Val	57	HA	3.821
	10	HE2	7.530		34	HA2	3.840		57	HB	1.128
Leu	15	HA	6.026	Phe	36	CD1	7.618		57	QG1	0.471

Residue		Proton	(ppm)
Val	57	QG2	-0.158
Trp	59	HA	5.161
	59	HB2	3.932
	59	HB3	3.284
	59	HE3	7.121
	59	HZ3	6.533
Trp	59	HZ2	6.736
	59	HH2	6.365
Asn	62	HA	4.558
	62	HB2	2.858
	62	HB3	2.918
Asn	63	HA	4.415
	63	HB2	2.942
	63	HB3	3.229
	63	HD21	7.054
Tyr	67	HE1	6.318
	67	HD1	7.226
Leu	68	HA	4.408
	68	HB2	1.527
	68	HB3	1.963
Leu	68	HG	1.088
	68	QD1	-1.550
	68	QD2	-0.500
Ile	75	HA	4.974
	75	HB	3.463
	75	QG2	2.068
	75	HG12	2.741
	75	HG13	2.861
	75	QD1	2.381
P	76	HA	5.426
	76	HB2	2.194
	76	HB3	2.494
	76	HG2	2.304
	76	HG3	2.939
	76	HD2	3.892

Residue		Proton	(ppm)
	76	HD3	3.045
Ala	81	HA	5.275
	81	QB	1.448
Phe	82	HA	4.826
	82	HB2	3.174
	82	HB3	3.711
	82	HD1	7.560
	82	HE1	7.020
	82	HZ	8.620
Leu	94	HN	8.152
	94	HA	3.799
	94	HB2	1.270
	94	HB3	1.323
	94	HG	0.907
	94	QD1	0.370
	94	QD2	0.039
Ile	95	HN	8.550
	95	HA	2.940
	95	HB	1.738
	95	QG2	0.292
	95	HG12	0.224
	95	QD1	0.536
Thr	96	HA	3.622
Thr	96	HB	4.253
	96	QG2	1.075
Tyr	97	HD1	6.712
	97	HE1	7.676
	97	HE2	7.185
	97	HD2	5.738
Leu	98	HA	3.193
	98	HB2	1.218
	98	HB3	1.312
	98	HG	0.897
	98	QD1	-0.431
	98	QD2	-0.283

Residue		Proton	(ppm)
Ala	101	HA	4.042
	101	QB	0.622
Thr	102	HA	4.607
	102	HB	1.420
	102	QG2	0.976
Glu	103	HN	6.795
	103	HA	4.093
	103	HB2	1.952
	103	HB3	2.057
	103	HG2	3.140
	103	HG3	2.299
Hem	104	QM1	13.834
	104	QM3	12.271
	104	QM5	20.566
	104	QM8	24.828
	104	HAM	5.301
	104	HBM	-3.320
	104	HGM	4.897
Hem	104	HDM	-4.771
	104	QT2	-0.440
	104	QT4	0.139
	104	HT4	-0.040
	104	HAP61	0.593
	104	HAP62	-0.887
	104	HBP63	1.123
	104	HBP64	3.364
	104	HAP71	-0.343
	104	HAP72	-0.611
	104	HBP73	1.359
	104	HBP74	-0.255

Note that these assignment are preliminary and require further confirmation by assigning the remaining protons.

Appendix 5. Electrochemistry of yeast *iso*-1-ferricytochromes *c* as a function of pH.

	Lys79Ala					
pH	ΔE (mV)	E (mV *vs* SHE)	i_{pc} (µA)	ΔE (mV)	E (mV *vs* SHE)	i_{pc} (µA)
6.73	59.8	-165.4	4.6	81.2	278.0	13.3
7.14	58.6	-168.1	5.6	80.2	275.4	11.6
7.46	74.6	-177.0	7.1	75.6	274.6	13.2
7.71	63.9	-181.8	9.5	77.8	272.4	11.4
8.13	62.1	-179.2	10.1	75.4	272.6	10.6
8.43	66.2	-180.9	11.6	80.4	271.2	9.4
8.57	62.8	-184.0	13.3	86.8	273.0	7.1
8.79	79.0	-180.1	15.4	86.1	272.6	6.0
9.04	105.3	-173.4	17.1	81.3	274.0	4.1
9.37	77.5	-185.3	18.8	82.9	280.9	3.4
9.57	101.6	-189.2	18.6	88.5	277.9	2.3
10.11	80.7	-214.6	16.3	64.1	287.9	0.6
10.66	70.4	-240.1	11.3			
6.78	44.3	-179.8	4.8			
7.27	46.5	-191.8	5.8			
7.86	48.6	-192.8	6.5			
8.33	55.9	-201.2	10.1			
8.85	61.1	-193.4	11.9			
9.04	58.7	-201.6	13.5			
9.51	62.7	-197.3	14.4			
10.01	62.0	-217.9	14.8			
10.41	68.4	-226.7	13.0			
4.39	44.8	-15.6				
5.07	40.4	-60.4				
5.72	43.9	-89.9				
6.16	59.6	-128.2				
6.62	54.5	-159.3				
7.20	50.8	-183.3				
7.70	61.9	-188.9				
8.31	47.4	-200.5				
8.71	54.1	-202.9				
9.09	72.0	-199.4				
9.61	64.5	-211.4				
10.03	65.8	-223.0				
10.53	61.0	-264.0				
11.04	48.4	-288.1				

			Lys73Ala			
pH	ΔE (mV)	E (mV vs SHE)	i_{pc} (μA)	ΔE (mV)	E (mV vs SHE)	i_{pc} (μA)
6.79	59.6	-169.5	4.0	79.5	271.0	13.6
7.10	77.9	-172.2	4.2	86.7	266.9	16.0
7.47	54.3	-182.7	5.5	82.5	270.0	15.4
7.78	54.4	-185.9	7.3	82.2	262.8	16.4
8.01	72.7	-175.4	6.9	81.5	263.9	14.6
8.32	61.4	-180.6	8.7	81	263.9	12.9
8.50	71.1	-179.0	10.0	92.4	264.5	13.2
8.70	59.5	-184.1	11.7	91.2	264.6	12.9
9.04	87.2	-174.3	14.0	83.4	262.8	9.2
9.32	87.2	-180.5	15.0	90	263.9	5.8
9.63	93.1	-187.6	17.3	97.9	268.2	3.5
9.95	89.2	-198.1	18.1	100.8	265.0	2.7
10.60	68.8	-234.4	13.5			
6.85	56.5	-156.0	3.5			
7.32	53.2	-178.6	4.1			
7.86	61.2	-178.1	5.0			
8.10	58.1	-188.8	6.2			
8.49	63.9	-185.9	8.0			
8.81	58.0	-182.3	9.5			
9.25	67.8	-193.6	12.5			
9.60	78.0	-189.7	13.4			
10.07	71.6	-200.7	12.0			
10.50	54.8	-239.4	12.5			
11.00	141.9	-288.8				
4.38	54.5	-31.6				
5.06	66.4	-66.0				
5.72	72.5	-100.7				
6.16	95.5	-119.0				
6.64	46.7	-164.2				
7.22	37.4	-187.0				
7.67	44.8	-195.2				
8.33	71.8	-195.6				
8.71	77.2	-193.8				
9.12	90.5	-200.5				
9.62	98.5	-202.2				
10.01	73.2	-217.1				
10.59	70.0	-258.4				
11.04	65.2	-281.9				

Appendix 6. Temperature dependence of the equilibrium constants for the alkaline conformational transition of wild-type yeast *iso*-1-ferricytochrome *c* and the variants Lys73Ala, Lys79Ala, Lys86Ala, and Lys87Ala.

$$K_{eq} = \frac{[\text{alkaline}]}{[\text{native}]} \approx \frac{\text{area}[IV_a(8) + IV_b(8)]}{\text{area}[III(8)]}$$

T	1/T	$-R \cdot \ln(K_{eq})$ $(J \cdot mol^{-1} \cdot K^{-1})$				
(°C)	(K⁻¹)	Lys87Ala	Lys86Ala	Wild-type	Lys79Ala	Lys73Ala
20	0.00341		-1.9833	-2.0383	2.9940	0.6617
25	0.00335		-3.4858	-2.6655	1.1059	3.9336
30	0.00330	-0.8655	-5.2858	-3.5367	-0.4723	1.2424
35	0.00325	-1.6003	-6.3730	-4.6838	-2.9387	0.3864
40	0.00319	-3.3671	-7.3561	-6.5599	-5.0945	-0.2290
45	0.00314	-5.7476	-9.8393	-8.0356	-8.0199	
50	0.00309	-8.5278				
55	0.00305	-10.3496				

Appendix 7a. Distribution of conformational states of wild-type ferricytochrome c measured at pH[*] 10.0, 25 °C, as a function of potassium chloride concentration.

[KCl] (mM)	III(8)			III(3)		
	δ (ppm)	Peak Area	Peak Height	δ (ppm)	Peak Area	Peak Height
0	35.23	22.40	46.61	31.71	18.85	50.17
12	35.24	21.28	67.32	31.74	18.61	68.12
30	35.24	22.80	64.75	31.80	17.82	83.06
53	35.21	30.68	98.49	31.83	27.18	103.07
69	35.20	32.24	109.02	31.88	26.69	112.67
85	35.18	35.93	119.63	31.89	32.20	135.61
98	35.15	42.21	139.26	31.90	35.69	141.52
199	35.11	44.80	147.09	32.00	36.60	156.87
296	35.07	46.88	171.31	32.05	43.33	181.78
395	35.02	49.84	159.80	32.09	43.20	184.12
494	34.97	53.55	181.39	32.11	58.88	200.75
597	35.00	68.01	268.33	32.17	67.42	289.31
697	34.97	59.16	237.14	32.19	57.94	251.72
797	34.96	42.24	172.81	32.22	41.51	170.61
903	34.97	38.93	146.92	32.25	33.40	135.89
996	34.96	30.42	102.22	32.26	30.37	101.21
	$IV_a(8)$			$IV_b(8)$		
0	24.97	56.73	125.09	24.75	203.08	447.64
12	24.94	68.31	150.60	24.71	196.79	434.00
30	24.93	94.04	207.32	24.69	151.88	373.46
53	24.82	123.70	217.68	24.59	112.07	303.86
69	24.81	146.02	252.00	24.58	104.75	274.85
85	24.80	149.74	271.76	24.55	100.41	276.25
98	24.77	152.26	289.08	24.52	95.34	281.53
199	24.72	183.50	377.55	24.45	74.46	257.91
296	24.69	181.53	429.58	24.41	73.36	240.40
395	24.66	176.94	460.53	24.38	71.49	222.16
494	24.64	170.48	516.38	24.34	80.37	231.04
597	24.63	168.71	571.95	24.33	65.29	179.87
697	24.62	177.85	602.85	24.33	73.70	193.92
797	24.62	176.06	608.69	24.34	66.09	185.30
903	24.62	191.20	612.09	24.35	40.09	165.91
996	24.63	192.08	625.03	24.37	62.70	187.39
	$IV_a(5)$			$IV_b(5)$		
0	20.91	230.18	128.33	19.32	97.63	316.09
12	20.98	223.86	112.86	19.31	101.73	362.01
30	na	na	na	19.32	96.98	364.95
53	na	na	na	19.31	105.45	397.71
69	na	na	na	19.33	111.02	426.07
85	20.92	10.34	20.92	19.32	112.49	456.86
98	20.79	39.06	55.09	19.31	118.49	470.70
199	20.85	10.85	38.24	19.31	129.32	583.35
296	20.96	47.75	87.25	19.30	138.40	667.92
395	20.98	57.71	115.91	19.29	142.02	699.98
494	21.01	102.31	157.95	19.29	155.07	767.49
597	21.04	95.87	152.07	19.30	157.96	793.36
697	21.03	111.26	169.29	19.29	163.70	855.19
797	21.03	111.61	161.35	19.30	162.24	824.16
903	21.05	99.86	153.45	19.30	158.13	781.36
996	21.04	117.28	168.29	19.30	166.48	812.36

Appendix 7b. Influence of ionic strength on the pK_{ap} of wild-type yeast *iso*-1-ferricytochrome *c* and the variants Lys73Ala and Lys79Ala.

[KCl] (M)	pK_{ap} Wild-type	pK_{ap} Lys73Ala	pK_{ap} Lys79Ala
0.01	8.17 (4)	8.59(3)	7.89(4)
	7.87(1)		
0.04	8.49(9)	8.69(2)	
0.1	8.57(1)	8.80(1)	8.54(1)
0.2	8.72(2)	8.77(2)	
0.4	8.70(2)	8.87(2)	
0.5		8.82(2)	8.89(3)
0.6	8.74(3)	8.72(2)	
1.0	8.71(2)	8.69(1)	9.05(2)
	8.86(3)		

Appendix 8. pH-Jump kinetics data of wild-type yeast *iso*-1-ferricytochrome *c* and the variants Lys73Ala and Lys79Ala.

Wild-type		Lys73Ala		Lys79Ala	
pH	k_{obs} (s⁻¹)	pH	k_{obs} (s⁻¹)	pH	k_{obs} (s⁻¹)
6.07	0.038(2)	6.07	0.0128(7)	6.07	0.04(2)
6.13	0.0083(1)	6.20	0.0076(8)	7.57	0.0403(7)
7.07	0.0152(6)	7.07	0.0103(5)	8.09	0.0709(3)
7.57	0.043(5)	7.57	0.0158(2)	8.35	0.081(2)
8.09	0.0472(2)	7.80	0.014(1)	8.43	0.0852(3)
8.43	0.0617(3)	8.09	0.0206(1)	8.54	0.099(2)
8.54	0.0651(2)	8.35	0.02196(7)	8.76	0.1185(4)
8.76	0.0909(4)	8.43	0.0223(2)	8.86	0.1552(4)
8.86	0.1014(6)	8.54	0.02546(7)	8.94	0.170(4)
8.94	0.1075(6)	8.76	0.0323(1)	9.01	0.1615(6)
9.01	0.1337(5)	8.86	0.0366(1)	9.07	0.2148(7)
9.07	0.1434(7)	8.94	0.03804(9)	9.20	0.28(1)
9.20	0.2041(9)	9.01	0.0372(2)	9.28	0.244(1)
9.28	0.2122(1)	9.07	0.0451(1)	9.38	0.41(1)
9.38	0.3133(9)	9.20	0.0603(1)	9.50	0.379(2)
9.50	0.335(1)	9.28	0.0567(1)	9.56	0.541(1)
9.56	0.474(1)	9.38	0.0817(1)	9.70	0.552(3)
9.70	0.52(2)	9.50	0.0781(2)	9.80	0.99(2)
9.80	0.802(3)	9.56	0.1084(1)	9.89	0.860(5)
9.89	0.814(4)	9.70	0.1135(3)		
		9.80	0.1630(3)		
		9.89	0.1781(3)		